THE EXTRUSIVE AND INTRUSIVE BASALTIC ROCKS OF THE MOLTENO-JAMESTOWN AREA

by

A.A. MITCHELL, B.Sc. (Hons)

Thesis presented for the degree of Master of Science in the Department of Geology, Rhodes University, Grahamstown.

January, 1980

DECLARATION

All work in this thesis is the original work of the author except where specific acknowledgement is made to the work of others.

SIGNED : 

A.A. Mitchell,
Department of Geology,
Rhodes University,
Grahamstown.

January, 1980.

ABSTRACT

The Karoo basalt outliers between Molteno and Jamestown in the north-eastern Cape Province are associated with two central volcanic vent complexes, referred to in the text as the Brosterlea and the Modderfontein complexes.

The basalts, particularly those associated with the Brosterlea complex, show geochemical variations throughout the sequence, a factor which has facilitated the subdivision of the Brosterlea basalts into a series of discrete units, each having its own chemical characteristics. Most of the basalt units at Brosterlea can be correlated with units identified in the Barkly East basalt suite.

As is the case around Barkly East, the Brosterlea basalt units cannot be related to one another by any simple crystal fractionation or partial melting process, and the most feasible alternative explanation lies in the existence of inhomogeneities in the upper mantle at the time of generation of the magmas.

New electron microprobe data are presented for the silicate phases in the Karoo basalts. Analyses of augites from a limited number of slides indicate that pyroxenes from different basalt units define different trends on the Ca - Mg - Fe triangular diagram. The plagioclases in the Brosterlea basalts are fairly Ca-rich (average 70% An), and the K-content of the plagioclases is shown to vary with the K-content of the parent basalt.

A comparison of the Karoo Central Province with the younger Columbia River and Deccan Trap Provinces shows many similarities in the evolutionary history of the three provinces. The Karoo Province, however, is distinct from the other two provinces in some aspects of the geochemistry. Broadly speaking, the Karoo basalts are depleted in the incompatible elements relative to the Columbia River and Deccan basalts, and often enriched in the transition metals, most specifically Cr.

CONTENTS

1. INTRODUCTION

The outliers of Karoo-age basalt between the towns of Molteno and Jamestown in the north-eastern Cape Province, together with their associated network of dolerite intrusions, were first described by Du Toit (1911) and Gevers (1928). This dissertation, supplemented by data from the work of Rumble (1979), constitutes the first detailed geochemical work to be done in the area.

Whilst Rumble's work deals specifically with an isolated intrusion of andesitic material on the farm Roodehoek, the intention of the present study is to gain some understanding of the relationships, both physical and chemical, between the dolerites and the basalts, and between the various geochemically distinct units within the basalt succession. In addition to bulk-rock geochemical data, a number of electron microprobe analyses of the silicate phases of the basalts are presented.

The new geochemical data presented here supplement and, in many ways, compliment data already presented by Robey (1976) and Pemberton (1978), and the project is an extension of the work of WORKING GROUP 4 " GEODYNAMICS OF CONTINENTAL AND OCEANIC RIFTS" within the framework of the International Geodynamics Project.

2. PREVIOUS WORK

The existence of outliers of Karoo-age basalt west of Jamestown was first noted by Du Toit (1904). In a later study, Du Toit (1911) reported the results of detailed mapping and petrographic work in the vicinity of the Telemachus Kop and Modderfontein vent structures, which constitute the northern extremities of the area of present interest (Fig. 1 and Fig. 2).

The first work dealing with the volcanic field centred on the present site of the Brosterlea railway siding, some 15 to 20 km south of Telemachus Kop and Modderfontein (Fig. 2), was that of Gevers (1928). He was primarily concerned with the nature of the volcanic vents in the area, rather than the overlying basalt lavas. Using a modified form of the vent classification scheme proposed by Du Toit (1904), Gevers identified five distinct varieties of vent in the Molteno area, based on the nature of the vent-filling material. The vents, which Gevers believes to be unrelated to "pre-existing tectonic lines", are linked in the present study to the collapse of the Brosterlea caldera.

The volcanic episode at Brosterlea started before the end of the deposition of the Clarens Formation. Gevers gives the following account : "The volcanic activity in this area began towards the end of the Cave Sandstone[1] period, while this rock was still in the process of formation. The tuffaceous nature of the upper part of the Cave Sandstone in places, as for instance in the northern portion of Wolwefontein, and the layers of volcanic ash not infrequently to be found in it, testify to this. On the other hand, before the basal lavas were erupted the Cave Sandstone was already being actively denuded in places, and was sometimes completely removed". On the farm Noodhoek, the very irregular contact between the Clarens Formation Sandstone and the overlying pyroclastics, found during the present study, is clear evidence of an erosional episode towards the close of Clarens Formation times.

---

[1] *The "Cave Sandstone" is now known as the Clarens Formation.*

Of particular interest to Gevers was the "area of eruption around Roodepoort[2] and Zwartfontein", i.e. the central part of the Brosterlea complex. He identifies and describes areas of "shattering and dislocation" on the farms Klein Hoek, Roodehoek and Klipfontein, these being related to an area of "considerable subsidence". The zone of shattering and dislocation described above is the edge of the Brosterlea caldera (present study). The area of subsidence is filled with a variety of fragmental rocks, the nature of which Gevers discusses in some detail. The irregular outline of the centre of eruption on Zwartfontein and Roodekloof prompted Gevers to postulate that there were originally "several closely neighbouring vents, which ultimately merged into one". The existence of more than one vent in the central complex is confirmed in the present study (see Fig. 2).

As the Karoo volcanic episode developed, central complexes like the one at Brosterlea were effectively extinguished as eruptive centres by the encroachment of great thicknesses of basalt. Gevers subscribes to Du Toit's (1911) belief that the basalts were derived from fissure eruptions. In a more recent work, Lock et al. (1974) discuss the evolution of the Drakensberg subgroup in the Barkly East district. They believe that volcanic activity began at discrete centres, this period being characterized by more explosive activity than was experienced in later phases of development, and giving rise to abundant pyroclastic material. The central eruptions ultimately gave way to fissure-type eruptions, which produced the greater part of the basalt sequence in the form of "quiet effusions of highly mobile lava" (Lock et al., op. cit.).

The geochemical investigation of the Brosterlea area was begun only very recently, and the whole-rock analyses of 38 basalts and dolerites from the Brosterlea complex presented in this thesis, together with the seven analyses of the Roodehoek andesite from Rumble (1979), are presented

---

[2] *The farm referred to as Roodepoort by Gevers is listed as Roode Kloof on the most recent trigonometrical survey maps, from which Map 2 (this study) was drawn.*

and discussed. Results of the present study are in agreement with Pemberton's (1978) conclusion that the mantle below Southern Africa was chemically heterogeneous during Karoo times, in that successive basalt sequences cannot be related to one another, or to a common mantle source, by any known low pressure igneous process.

3. FIELD WORK AND SAMPLING PROCEDURE

Field work was carried out in the course of five excursions in the period February, 1978, to March, 1979. The purpose of the field work was, firstly, to complete a reconnaissance mapping project of the Karoo basalt outliers between Molteno and Jamestown. This mapping, combined with aerial photograph interpretations, formed the basis for the structural interpretation of the Brosterlea Volcanic Complex, as illustrated in Fig. 2. The second aim of the field work was to measure sections through the lava pile at various points spaced throughout the area of interest, measuring the thickness of individual lava flows by means of an aneroid barometer.

Where possible, a sample was taken from each lava flow identified, for the purpose of petrographic and geochemical analysis. The problem of weathering is, however, a very real one in this area, and many flows were considered too weathered to merit sampling.

In addition to the analysis of thirty-three basalts from the Brosterlea and Modderfontein complexes, whole rock geochemical analyses were also performed on five dolerite samples. These samples were collected from :

a) The Brosterlea outer ring dyke complex.

b) The Brosterlea radial dyke swarm.

c) The "Dragon's Back" dyke.

d) The Modderfontein ring dyke (two samples).

The location of the eight sections measured and sampled through the basalt pile are indicated on Fig. 2, and the sample sites together with their respective sample numbers are listed in Appendix 1.

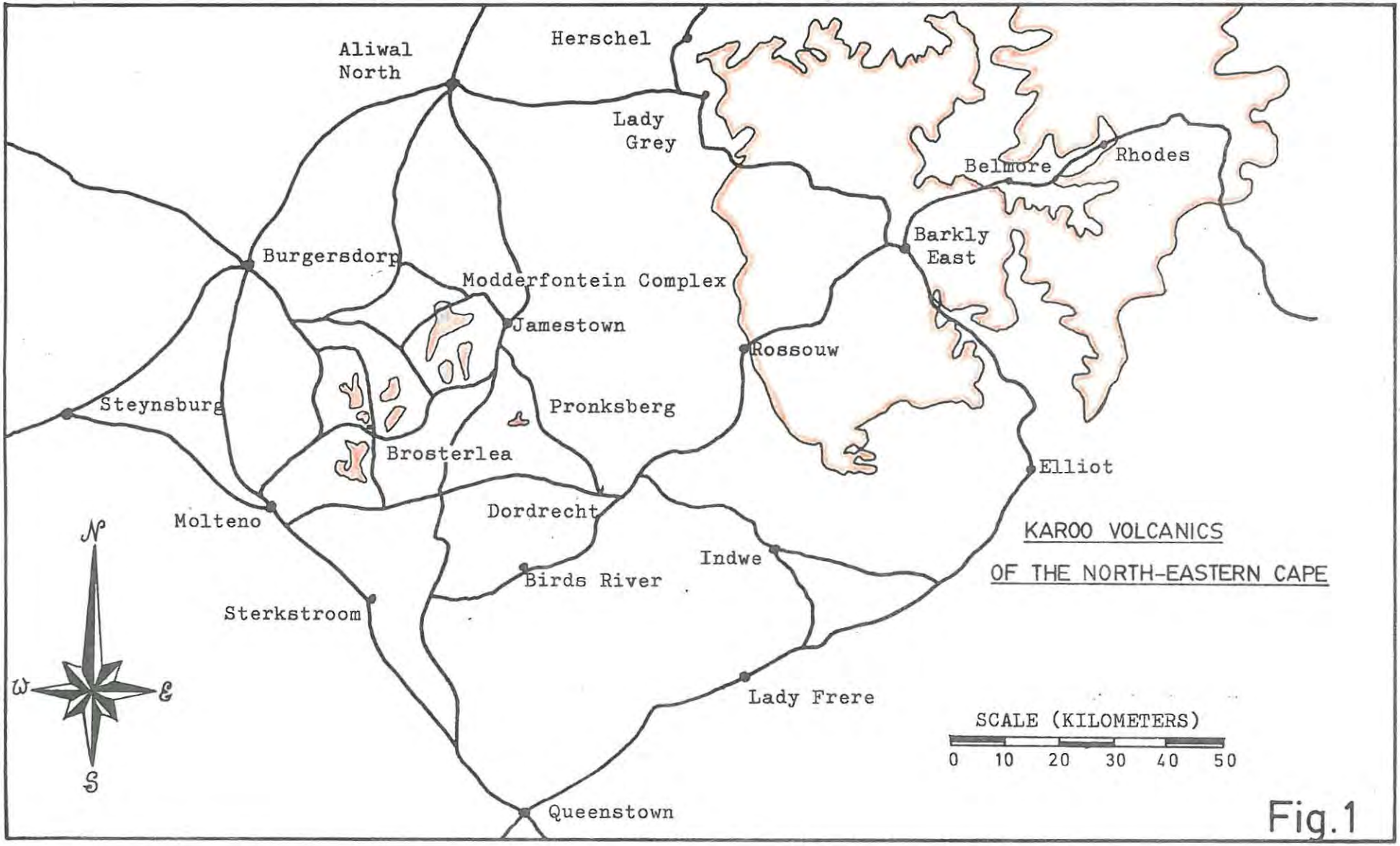
Aliwal North
Herschel
Lady Grey
Belmore
Rhodes
Barkly East
Burgersdorp
Modderfontein Complex
Jamestown
Rossouw
Steynsburg
Pronksberg
Brosterlea
Elliot
Molteno
Dordrecht
Indwe
Birds River
Sterkstroom
Lady Frere
Queenstown
N
W
E
S
KAROO VOLCANICS
OF THE NORTH-EASTERN CAPE
SCALE (KILOMETERS)
0 10 20 30 40 50

Fig.1

Fig. 2 : THE BROSTERLEA AND MODDERFONTEIN VOLCANIC COMPLEXES

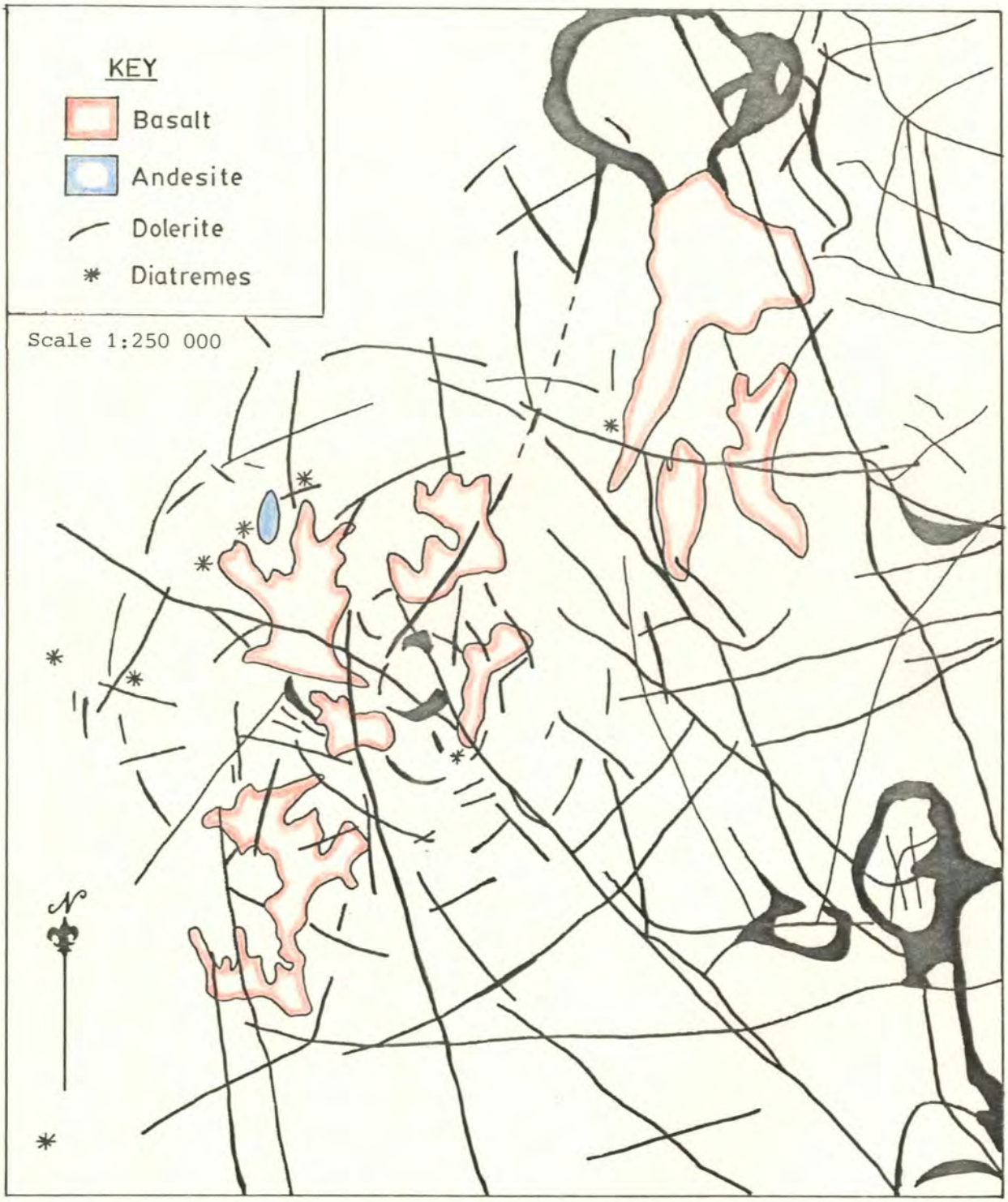

Fig. 2 : THE BROSTERLEA AND MODDERFONTEIN VOLCANIC COMPLEXES

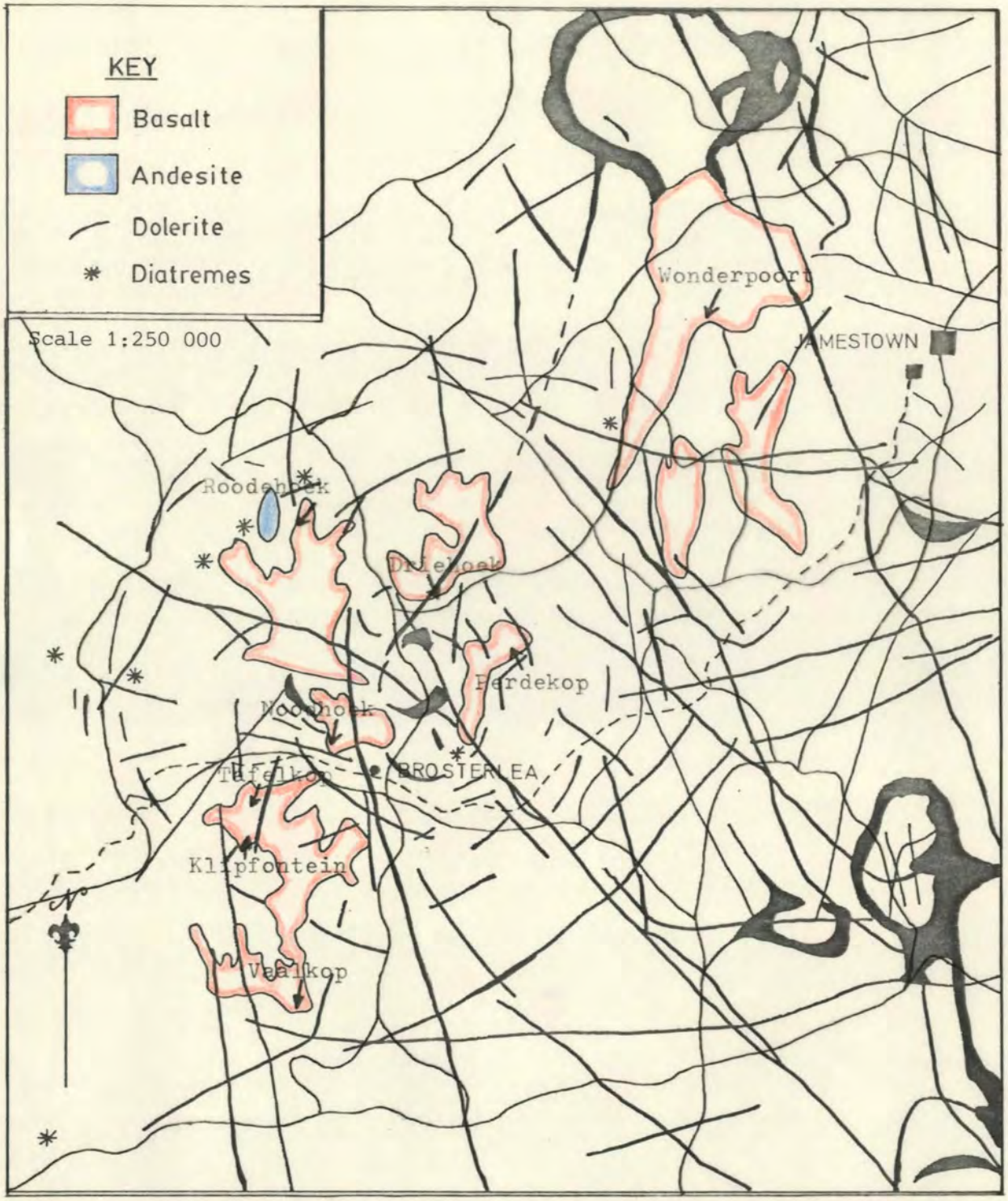

Fig. 2 : THE BROSTERLEA AND MODDERFONTEIN VOLCANIC COMPLEXES

4. GEOLOGICAL SETTING

4.1 Stratigraphy and stratigraphic nomenclature

South African stratigraphic nomenclature is at present in a state of flux, pending the final report of the South African Council for Stratigraphy (S.A.C.S.). In the absence of any formal nomenclature, the author has followed the recommendations of the preliminary report of S.A.C.S. (Johnson et al., 1975). According to this report, the Karoo sequence may be subdivided as follows :

Karoo Supergroup
- Drakensberg Group
- Clarens Formation (old Cave Sandstone)
- Elliot Formation (old Red Beds)
- Molteno Formation
- Beaufort Group
- Ecca Group
- Dwyka Formation

The Drakensberg Group comprises the volcanic material overlying the Clarens Formation, and its boundaries and conceptual framework remain essentially unchanged from those laid down by Du Toit (1954).

Lock et al. (1974) have subdivided the Drakensberg Group in the Barkly East area into a number of mappable units, to which they have assigned formation names. Robey (1976) and Pemberton (1978) have characterised the various formations at Barkly East in terms of geochemistry, and it is the aim of the present work to carry out a similar program on the basalts of the Brosterlea and Modderfontein complexes. The stratigraphic columns for each of the sampling localities in the Brosterlea area are presented in Fig. 3, and a brief discussion of the characteristics and stratigraphic position of the various basalt units is set forth in the following section.

4.1.a The Tafelkop Lavas

The lavas at the base of the Tafelkop sequence are probably some of the earliest to be erupted in the Brosterlea area. The various flows within this grouping of lavas are geochemically distinct from one another, but have been grouped together because they are considered to be the exception, rather than the rule, within the overall succession at Brosterlea. The collective thickness of the Tafelkop lavas at Tafelkop is 160 meters, thinning southward to just over 70 meters at Klipfontein. These two sites are the only localities at which the Tafelkop lavas outcrop, a feature which points to the possibility that these early lavas were extruded from a small vent peripheral to the main central complex. The lowermost of the Tafelkop lavas are coarse-textured. There was apparently an hiatus, represented by sandstone lenses within the sequence, between the early, coarser-grained material and the uppermost layers of the Tafelkop sequence. The uppermost of the Tafelkop type lavas are highly amygdaloidal, and weather easily, thus forming negative topographic features, in contrast to the lower Tafelkop lavas, which tend to form prominent ridges. The nature of the Tafelkop lavas confirms the observation by Gevers (1928) that "At various places around its (the vent's) edge there is proof that the lowermost basalts crowning the plateaus in the vicinity were directly poured out from this vent". Gevers' reference to the "vent" implies the entire complex of vents which goes to make up the Brosterlea complex. Gevers notes, in accord with the findings of the present study, that the lowermost basalts are "... either of a doleritic or a highly vesicular, even pumiceous, type of basalt", and that "... all types very often occur over a small range (of distance)".

4.1.b The Strypoort (Drumbo Type) Unit

The basal layer of basalt at the Perdekop sampling locality is considered to be the first of the layers of laterally extensive lava flows which ultimately smothered

the vent-type eruptions of the early phases of Karoo volcanism. This early lava flow has been named the Strypoort Unit in the Brosterlea area, but it has very definite geochemical affinities with the Drumbo Basalt Member, which is the lowermost of the basalt units in the Barkly East area (Lock et al., 1974; Pemberton, 1978). The Strypoort Unit outcrops only at Perdekop, where it attains a thickness of some 30 meters. In hand specimen, the Strypoort Unit is fine-grained, and grey-green in colour.

4.1.c The Chaotic Pyroclastics

Although the pyroclastics do not reach as far as Perdekop, they are assumed, on the rather tenuous basis of the similarities between Brosterlea and the Barkly East stratigraphies, to be the product of a later phase of eruption than are the basalts of the Strypoort Unit. The pyroclastics are unbedded and poorly sorted, containing fragments of dolerite and of green and red shales. At most localities in the Brosterlea area, the pyroclastics are badly weathered, and any volcanic glass which might have been present is by now completely altered. If the interpretation of Lock et al. (op. cit.) is to be accepted, these pyroclastics, which blanket most of the central vent complex at Brosterlea, are lahars, erupted during caldera collapse. In contrast to the Barkly East stratigraphic sequence, the Brosterlea chaotic pyroclastics are not overlain by reworked, bedded pyroclastics. This fact, combined with the absence of pillow lavas within the Brosterlea sequence, may be taken as an indication that there was not as much surface water present at Brosterlea as there must have been in the vicinity of Barkly East at the time of these eruptions. The pyroclastics are exposed at Noodhoek, Tafelkop and Klipfontein, as well as within the central vent complex itself. The thickness of the pyroclastics is highly variable, and is controlled by the post-collapse morphology of the caldera structure, as well as by the pre-eruption topography of the Clarens Formation sandstone. The measured thickness of the pyroclastics is about 70 meters at Noodhoek,

decreasing southward to 45 meters at Tafelkop, and 30 meters at Klipfontein.

4.1.d The Roodehoek (Omega Type) Unit

The Roodehoek Unit overlies the chaotic pyroclastics at Noodhoek, Tafelkop and Klipfontein, and oversteps onto Clarens Formation sandstone at Vaalkop and Roodehoek. This unit weathers more easily than the overlying Vaalkop Unit, and is often reduced almost to topsoil. The lavas of the Roodehoek Unit are either compact or highly amygdaloidal in appearance. Sandstone lenses occur at intervals throughout the unit, and are especially prevalent at Roodehoek and Noodhoek. The presence of sandstone lenses within the lavas is evidence of hiatuses in the eruptive history of the lavas.

4.1.e The Vaalkop Unit

The Roodehoek Unit is overlain, in most parts of the Brosterlea complex, by the compact, fine-grained basalts of the Vaalkop Unit. This unit has no equivalent in the Barkly East district. The Vaalkop Unit reaches a thickness of slightly over 60 meters at Noodhoek, the only sampling locality at which the full, uneroded sequence of the Vaalkop lavas is exposed. The lavas of this unit are more resistant to weathering than are the underlying Roodehoek lavas, and form positive topographic features. This effect is well illustrated at the Vaalkop sampling locality, where the Vaalkop lavas form prominent ridges along the top of the mountain (Fig. 5a).

4.1.f The Perdekop Unit

The Perdekop Unit is the uppermost of the units at Brosterlea, and is represented by only two samples, AM40 from Noodhoek and AM28 from Perdekop. The two rocks are very similar to each other in hand specimen, being fine-to medium-grained and doleritic in texture. Both the Perdekop and the Noodhoek representatives of the unit are highly fractured in outcrop, which makes selection of unweathered

sample material difficult. The Perdekop Unit is correlated with the Lesotho Formation of the Barkly East district (Lock et al., 1974) on the basis of close chemical similarities.

4.1.g The Sequence at Modderfontein

Although no detailed work has been undertaken during this study of the lavas associated with the Modderfontein vent, a representative sequence of samples was taken through the lavas on the farm Wonderpoort.

The basal lava from the Wonderpoort sequence is a vesicular basalt, but was considered too weathered to warrant analysis. Overlying the basal lava is a sequence of lava flows which are geochemically related to the Vaalkop Unit of the Brosterlea sequence. These lavas have a collective thickness of just over 30 meters, and display collumnar jointing in places. Overlying the Vaalkop-type lavas is a fine-grained basalt which is a dark blue-grey colour in hand specimen. This lava has affinities, both petrologically and geochemically, with the Kraai River Formation of the Barkly East succession. The uppermost lava layer at Wonderpoort is a crumbly, doleritic rock with geochemical similarities to the Lesotho Formation.

4.2 Geological History

The Brosterlea volcanic complex forms, together with the Modderfontein complex (Du Toit, 1911), a series of isolated outliers of Karoo-age basaltic material, some sixty kilometers to the west of the major outcrop of Karoo volcanics which constitutes the Drakensberg and Lesotho highlands (see Fig. 1).

A structural interpretation of the Brosterlea complex is presented in Fig. 2. The Brosterlea central complex is a mass of coalescing vents and diatremes (Fig. 2). This complex

is an expression of the earliest phase of volcanic activity in the area, and the eroded valley in which it is exposed at the present time is filled with pyroclastics, interlayered with, and intruded by, volcanic material. The complex interrelations of the volcanics and pyroclastics indicates that they are both products of the eruptions of the central vents.

The eruptions in the central complex led to collapse along an outer ring fracture, along which further diatremes and volcanic plugs penetrated. An example of the latter is the Tafelkop vent, lavas from which form the basal layers of the volcanic stratigraphy in the vicinity of Tafelkop and Klipfontein.

The caldera collapse of the Brosterlea complex appears to have been hinged, with no vertical displacement in the south and a fairly substantial displacement in the northern part of the ring fracture (Fig. 4). The maximum vertical displacement along the ring fracture has a magnitude of some 300 meters, and involves a shear zone some 100 to 200 meters wide, along which a series of small dolerite dykes have intruded. The shear zone, which brings Molteno Formation sediments into juxtaposition with the basalts, was first identified by Gevers (1928), and has been traced across the farms Roodehoek, Eyzerfontein and Klipfontein (Fig. 2).

The subsidence of the central part of the Brosterlea complex heralded a period of violent explosive eruptions, and the collapse structure filled with a thick blanket of chaotic pyroclastics, the nature of which is discussed in Section 4.1.c. The pyroclastics probably attained a thickness of some 400 to 500 meters in the central part of the caldera, thinning southward. The preserved thickness of the pyroclastics at Noodhoek is 200 meters, thinning southward to 135 meters at Tafelkop, and 95 meters at Klipfontein. The Roodehoek andesite (Rumble, 1979) presumably intruded at some stage during the caldera collapse (Fig. 4). This

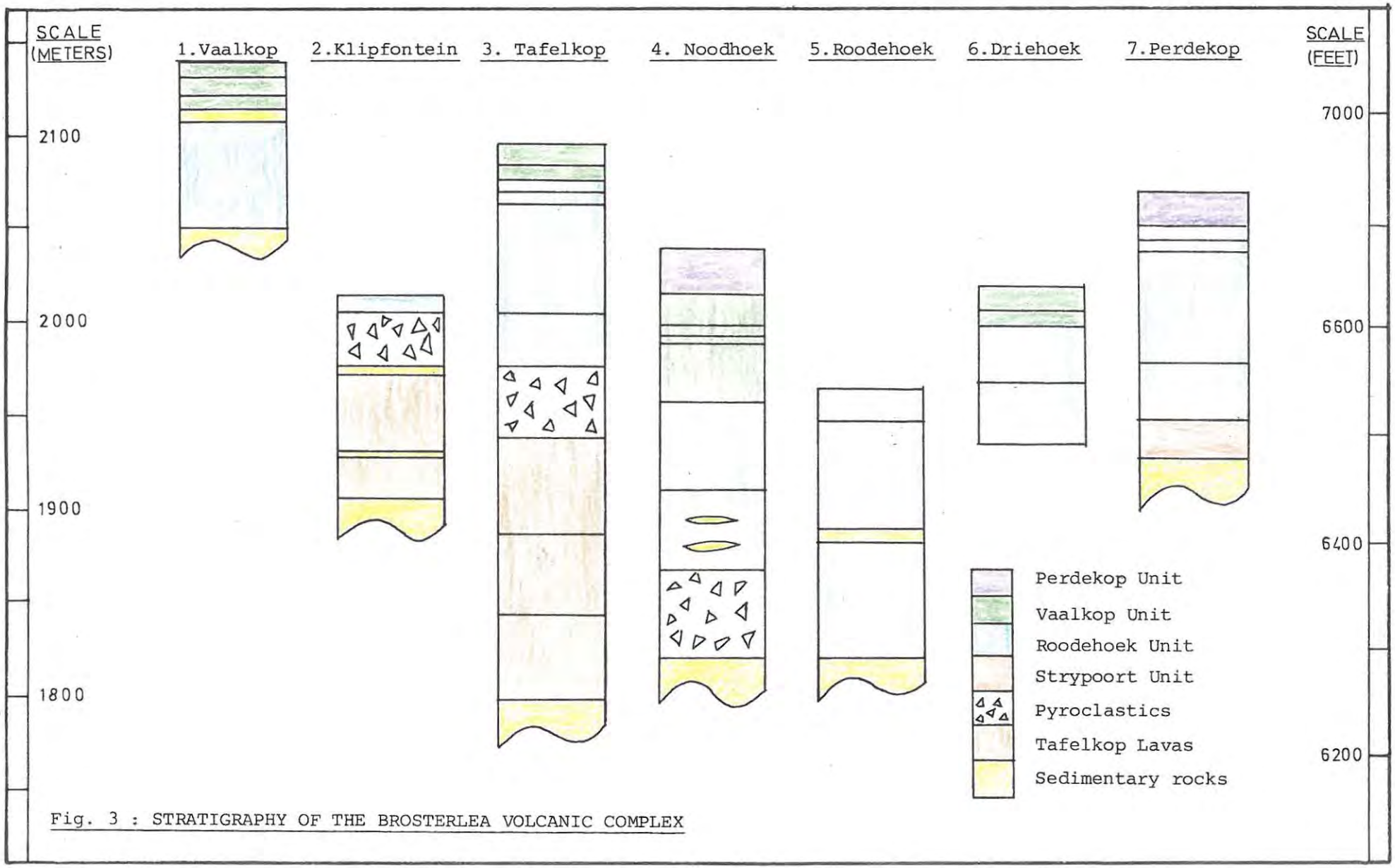

Fig. 3 : STRATIGRAPHY OF THE BROSTERLEA VOLCANIC COMPLEX

intrusion is situated close to the shear zone, mentioned earlier, on the farm Roodehoek (Fig. 2).

The central vent phase of eruption was brought to an end by the onset of a long period of quiet fissure-type eruptions, lavas from which ultimately smothered the vents. Lavas of this later phase of volcanicity were highly mobile, and laterally extensive flows can be traced over many miles. As is the case in the Barkly East district (Pemberton, 1978), the basalts of the Brosterlea and Modderfontein complexes may be divided into a sequence of distinct units, chiefly on the basis of their chemistries.

The radial dyke swarm at Brosterlea is interpreted as a response to the tensions resulting from caldera collapse. Some of the radial dykes must be presumed to be parental to the overlying layers of basalt, but many bear a cross-cutting relationship to the lavas. When traced through the basalts, the dolerite dykes are seen to form negative topographic features i.e., they tend to weather far more rapidly than the basalts.

A final phase of igneous activity at Brosterlea was the intrusion of the "Dragon's Back" dyke, which constitutes a prominent feature of the present-day topography. This dyke, which cuts through all other intrusives and extrusives at Brosterlea, extends from Brosterlea some 40 kilometers south-eastward, eventually cutting across the Birds River Gabbro Complex (Eales and Booth, 1974). The proposed geological evolution of the Brosterlea complex is outlined diagrammatically in Fig. 4.

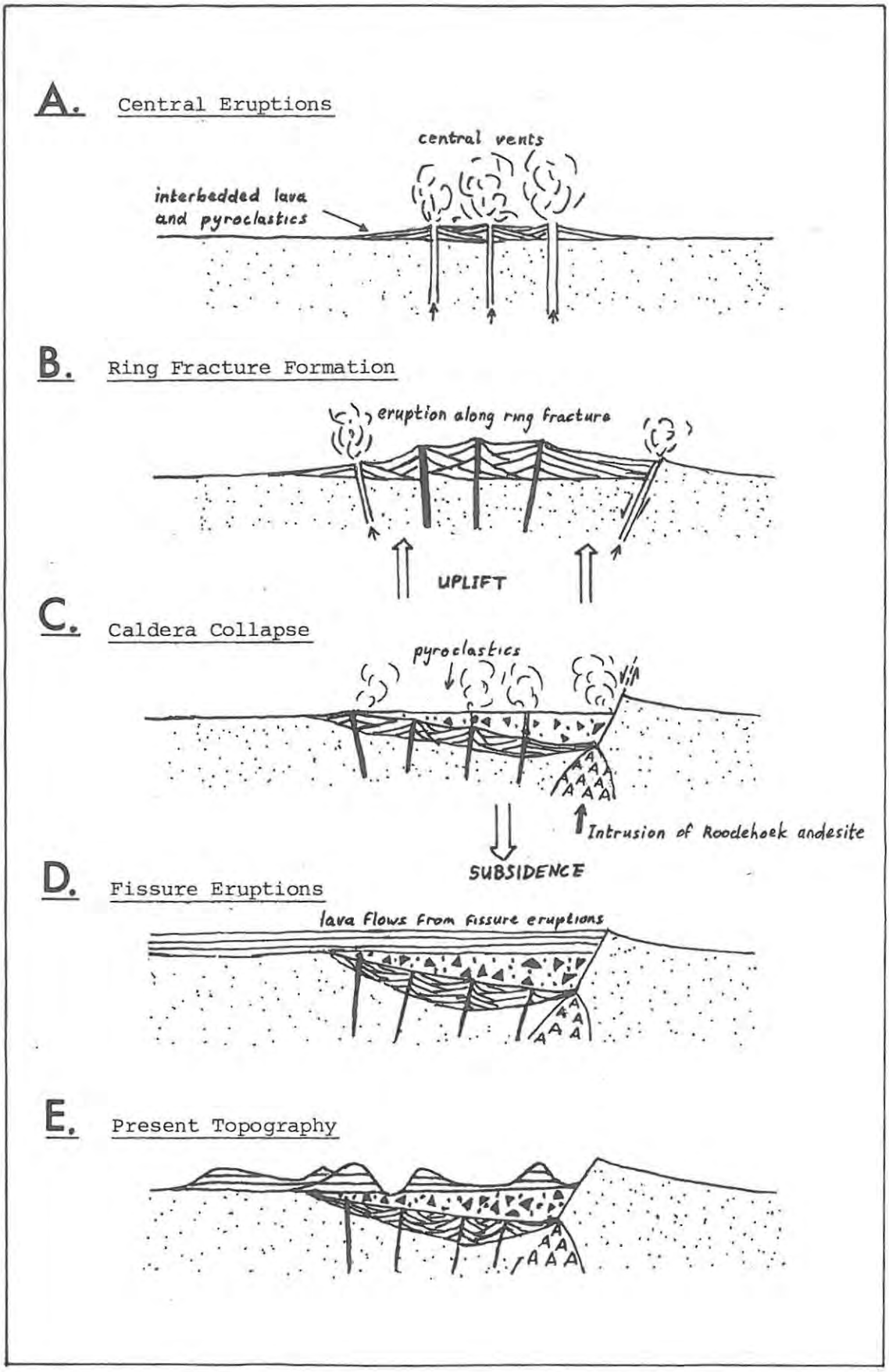

Fig. 4 : POSTULATED HISTORY OF THE BROSTERLEA COMPLEX

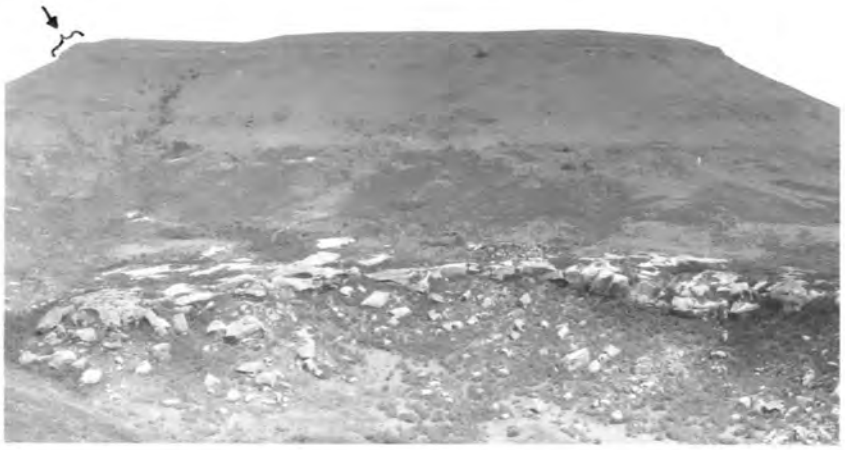

Fig. 5(a) : Vaalkop, illustrating the prominent ridges formed by the Vaalkop Unit lavas.

Fig. 5(b) : View north from Vaalkop, showing eroded remnants of basalts overlying Clarens Formation sandstones.

Fig. 5(c) : Perdekop, showing the sedimentary layer separating the Roodehoek Unit from the Perdekop Unit.

Fig. 5(d) : Wonderfontein, the type section for the Modderfontein lavas.

5. PETROGRAPHY

5.1 Introduction

The petrography of the main basalt units at Brosterlea, as defined in the previous section, is described below. Included in the discussion are the lavas associated with the Modderfontein vent complex to the north of the Brosterlea complex, as well as various dolerites from both Brosterlea and Modderfontein.

5.2 The Roodehoek (Omega Type) Unit

The basalts of the Roodehoek Unit, although geochemically relatively uniform, occur as two distinct petrographic types, designated type (a) and type (b).

Type (a) : This type is represented by samples AM15, AM23, AM26, AM27, AM31, AM36T, AM36M, AM36B and AM46, and is hypocrystalline phaneritic, with a seriate texture. Grains of augite, 0,5 to 3 mm in diameter, make up 30% to 40% of the rock. Pigeonite has been identified as cores to the augite in most of the rocks, and the characteristic "hourglass" zoning is displayed by some of the augite grains (see Fig. 6(h)). Ophitically penetrating the large pyroxene grains are laths of plagioclase up to 1,5 mm in length. The plagioclases show normal compositional zoning in the range An_{50} to An_{80}, and earlier-formed plagioclase grains are poikilitically to ophitically included in larger, later-formed plagioclases. Pseudomorphs after olivine make up less than 5% of the rock in the general case, a notable exception being AM36M, which contains 10% to 15% olivine. The possibility that the AM36M olivines are a cumulus phase is discussed in the chapter on mineralogy, in which microprobe analyses of the olivines are presented. Interstitial spaces in the type (a) rocks are filled with devitrified glassy mesostasis, with which is associated anhedral grains of opaque oxide. The Roodehoek type (a) rocks are the products of rapid cooling, as indicated by the highly zoned nature of the mineral grains, especially plagioclase, and by the presence of a glassy mesostasis.

Type (b) : As represented by samples AM14, AM21 and AM22, this petrographic type is glomeroporphyritic, with labradorite phenocrysts making up 15% to 20% of the rock. The plagioclase laths average 0,5 mm in length. Pseudomorphs after olivine constitute about 5% of the rock, and occur in clusters of small grains, the grains being somewhat less than 0,5 mm in diameter. The groundmass is an intersertal network of microcrystalline plagioclase and clinopyroxene.

5.3 The Vaalkop Unit

The basalts of the Vaalkop Unit are petrographically, as well as chemically, uniform from one outcrop to another. The rocks are hypocrystalline and porphyritic, tending towards glomeroporphyritic in most cases. Phenocryst phases are labradorite and augite, occuring in a ratio of about 9:1. Pseudomorphs after olivine do occur in some of the rocks, but make up less than 2% of the phenocryst assemblage. The proportion of phenocrysts varies from rock to rock within the unit, ranging between 20% and 30%.

Augite phenocrysts usually occur as discrete grains up to 0,5 mm in diameter, subhedral in outline and equant of habit, often optically penetrated by small laths of plagioclase. Labradorite phenocrysts occur in glomeroporphyritic aggregates, often forming radial clusters of laths, the laths being 0,5 to 1 mm in length. Olivine pseudomorphs, where present, are subhedral in outline, and seldom reach 0,5 mm in diameter.

The groundmass is a microcrystalline intersertal network of plagioclase, clinopyroxene and acicular opaque oxides. There is a tendency, especially apparent in AM30, for patches of glassy mesostasis to accumulate around phenocryst clusters. Small amounts of opaque oxide, associated with the mesostasis, tend to partially enclose phenocrysts of labrodorite.

5.4 The Perdekop (Lesotho Type) Unit

The Perdekop Unit outcrops at only two of the sampled sections within the Brosterlea complex, namely Perdekop and Noodhoek, and is the uppermost unit of the Brosterlea sequence. The unit is represented by only two samples, AM28 from Perdekop and AM40 from Noodhoek.

The Perdekop Unit rocks are hypocrystalline and phaneritic fine-grained, with laths of labrodorite 0,5 to 1 mm in length sub-ophitically to ophitically related to anhedral augite grains of comparable size. Pyroxene and plagioclase occur in more or less equal proportions. Plagioclase, which constitutes 55% of the rock, is sub-ophitically related to the anhedral augite. Mesostasis glass and oxides together constitute about 10% of the rock.

The "Dragon's Back" dyke, a late-stage doleritic intrusion, extending some 40 km from Brosterlea southeastward as far as the Bird's River complex, is represented in this study by sample AA23. This rock, although fresh in hand-specimen, has undergone extensive deuteric alteration. Granularity is phaneritic fine-grained, tending towards microcrystalline, with plagioclase laths 0,5 to 1 mm in length subophitically related to clinopyroxene. Plagioclase probably makes up 55% of the rock, clinopyroxene 30%, and mesostasis and opaques 15%, although proportions are difficult to determine due to the highly altered state of the rock.

The Modderfontein ring dyke is represented by samples AA30 and AA31. These dolerites are very similar to one another, and are hypocrystalline and phaneritic fine- to medium-grained, with a seriate array of labradorite, from somewhat less than 0,5 mm up to 1,5 mm, ophitically related to large, anhedral grains of augite, some of which exceed 5 mm in diameter. Small, subhedral pseudomorphs after olivine constitute less than 5% of the rock, while interstitial glass makes up about 10%, plagioclase and clinopyroxene, in more or less equal proportions, making up the balance.

5.5 The Tafelkop Lavas

The Tafelkop lavas, with a collective thickness of 170 meters, represent the basal part of the sequence at the Tafelkop locality.

Sample AM38, lying immediately on Clarens Formation sandstone, is hypocrystalline and phaneritic fine-grained, with plagioclase sub-ophitically related to the clinopyroxene. The rock appears to have cooled rapidly; the glassy mesostasis makes up 20% of the rock, and the plagioclase laths are strongly zoned. Acicular and anhedral opaque oxides occur in association with the mesostasis.

AM38T overlies AM38, and the two rocks are texturally similar, except that AM38T contains only about 5% mesostasis. AM37, from the flow overlying AM38T, is petrographically equivalent to the latter. AA05, a sample representing the Klipfontein equivalent of the Tafelkop lavas, is petrographically comparable with AM38T and AM37.

5.6 The Strypoort (Drumbo Type) Unit

AM24 is the basal layer of the sequence of basalts at Perdekop. It is set apart from the other rocks in the sequence by its chemistry, and is the only representative of the Strypoort Unit.

AM24 is hypocrystalline phaneritic and equigranular, with both clinopyroxene and plagioclase reaching maximum diameters of 0,5 mm, olivine pseudomorphs being somewhat smaller. Plagioclase makes up 55% of the rock, clinopyroxene 30%, olivine pseudomorphs approximately 10%, and accessory minerals and glass 5%.

5.7 The Modderfontein Lavas

The Modderfontein lavas, although not strictly part of the Brosterlea sequence, are included in this study for the sake of comparison.

AM53, the basal lava of the Modderfontein sequence, is hypocrystalline and glomeroporphyritic, with phenocrysts of labrodorite up to 1 mm in length set in a microcrystalline intersertal groundmass of clinopyroxene and plagioclase. The phenocryst assemblage accounts for approximately 15% of the rock.

AM52, the next flow up in the sequence, is similar in texture to AM53, to which it is also related geochemically. In contrast to the basal flow, AM52 has undergone extensive alteration, and the plagioclase is highly sericitized.

Sample AM51 is hypocrystalline and porphyritic, with phenocrysts of plagioclase and highly altered pyroxene making up approximately 10% of the rock. These phenocrysts reach a maximum diameter of 0,5 mm and are set in a cryptocrystalline groundmass of pyroxene, plagioclase and glass. A curious feature of the groundmass is that, although generally cryptocrystalline, it contains isolated patches of microcrystalline pyroxene and feldspar.

AM50 is hypocrystalline and seriate, with labradorite making up 55% of the rock, augite 30%, olivine 5% and the mesostasis and accessory minerals 10%. Plagioclase reaches a maximum length of 1 mm, while clinopyroxene and olivine are somewhat smaller.

5.8 The Brosterlea and Modderfontein Dolerites

Three dolerites from the Brosterlea complex are discussed below, together with two samples of the great ring dyke at Modderfontein (see Du Toit, 1911).

Sample AA21 is representative of the outer ring dyke structure of the Brosterlea complex. This rock is highly altered, and many of the labradorite laths are almost completely sericitized. A seriate array of plagioclase phenocrysts, ranging from somewhat less than 0,5 mm to approximately 1 mm in length, is set in an intersertal

microcrystalline groundmass of clinopyroxene and saussuritized plagioclase. Phenocrysts account for approximately 40% of the rock.

AA22, representing the radial dyke system at Brosterlea, is hypocrystalline and phaneritic fine grained, with an average grain size of 0,5 mm, although some plagioclase laths reach 2 mm in length.

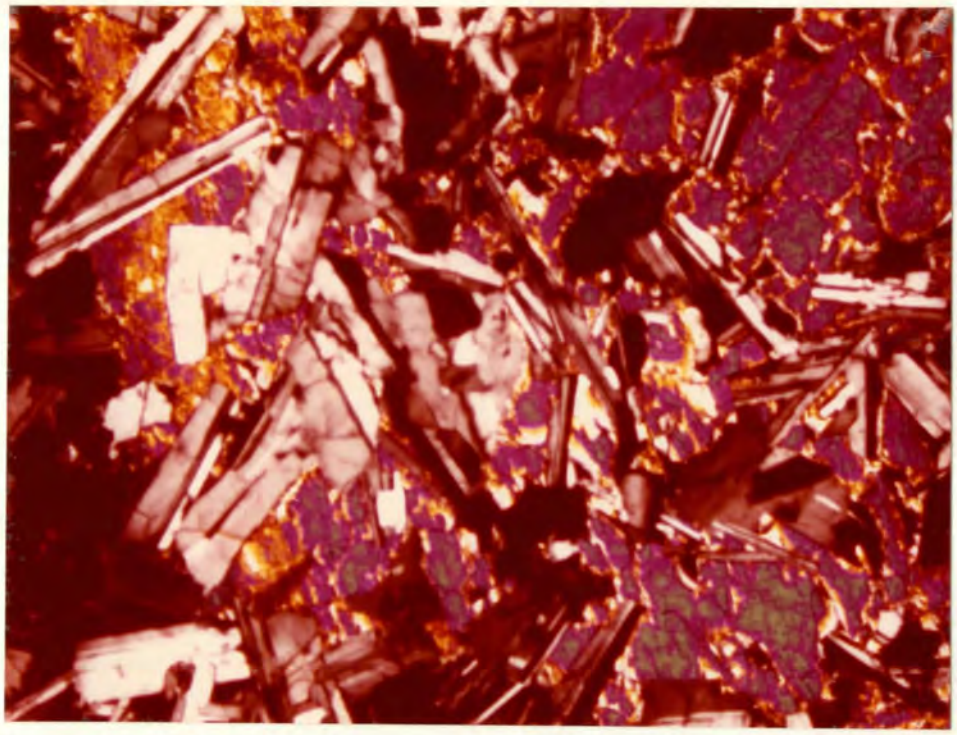

Fig. 6(a) : AM31 : Roodehoek Unit petrographic type (a) (crossed nicols). Large clinopyroxene grain and ophitically related plagioclase.

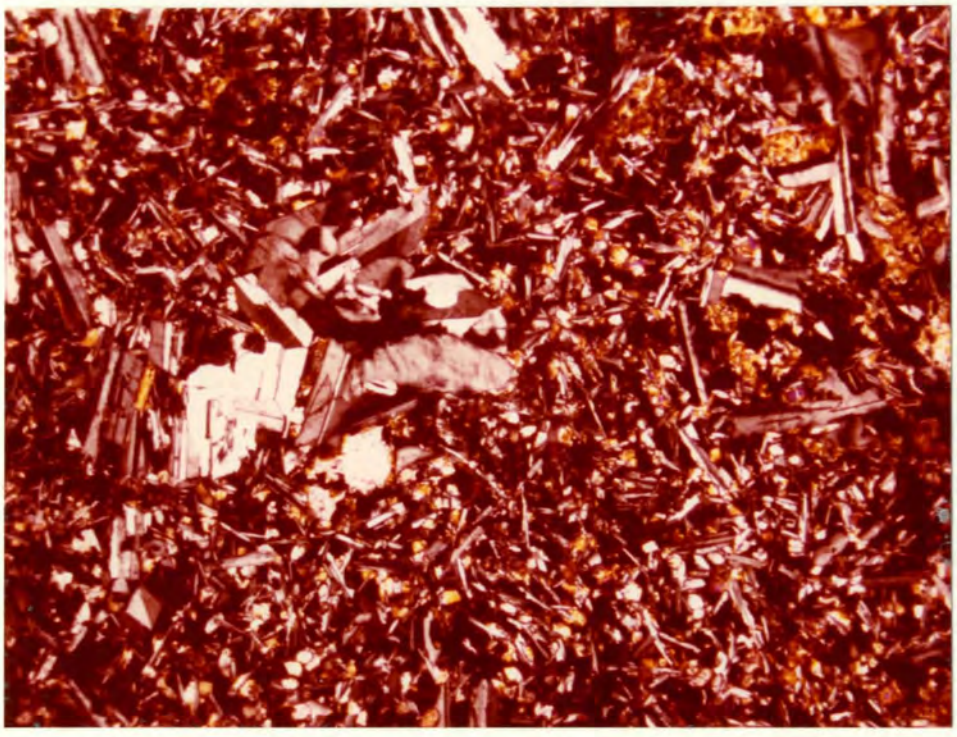

Fig. 6(b) : AM22 : Roodehoek Unit petrographic type (b) (crossed nicols). Glomeroporphyritic plagioclase.

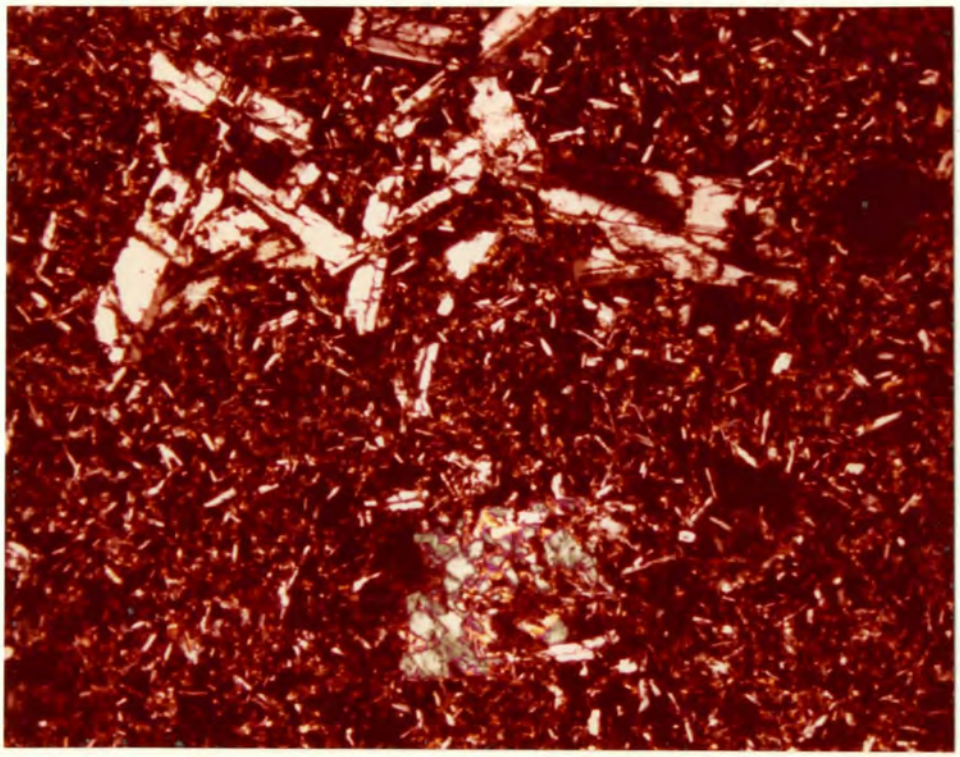

Fig. 6(c) : AM13 : Vaalkop Unit. Plagioclase and Clinopyroxene phenocrysts (crossed nicols).

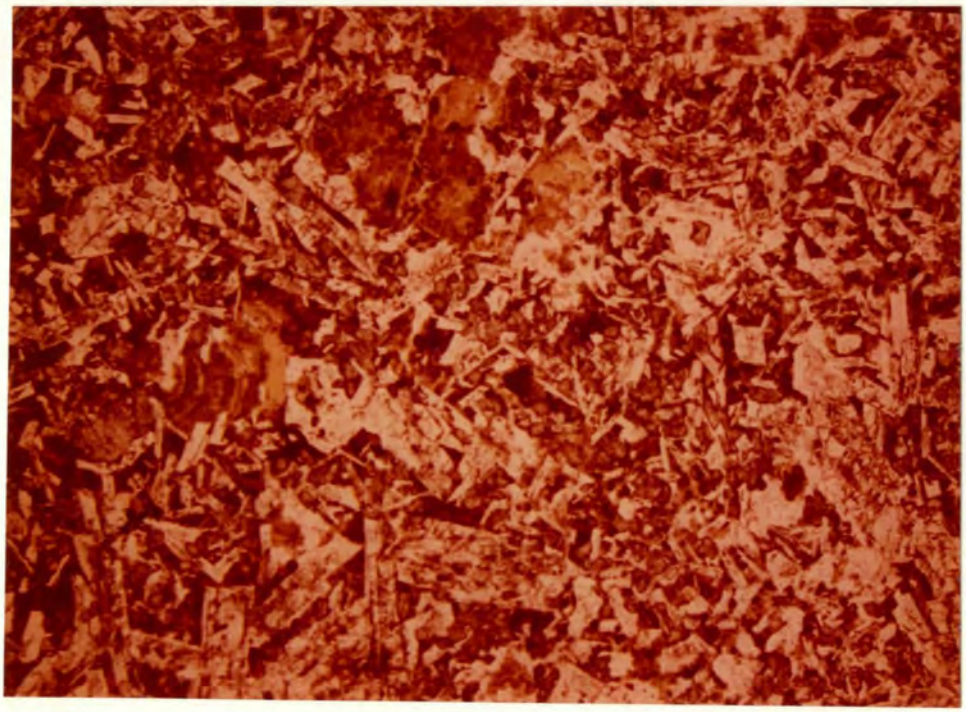

Fig. 6(d) : AM40 : Perdekop Unit. Intersertal plagioclase (white) and clinopyroxene (grey). Brown patches of alteration are possibly olivine pseudomorphs (Plane polarised light).

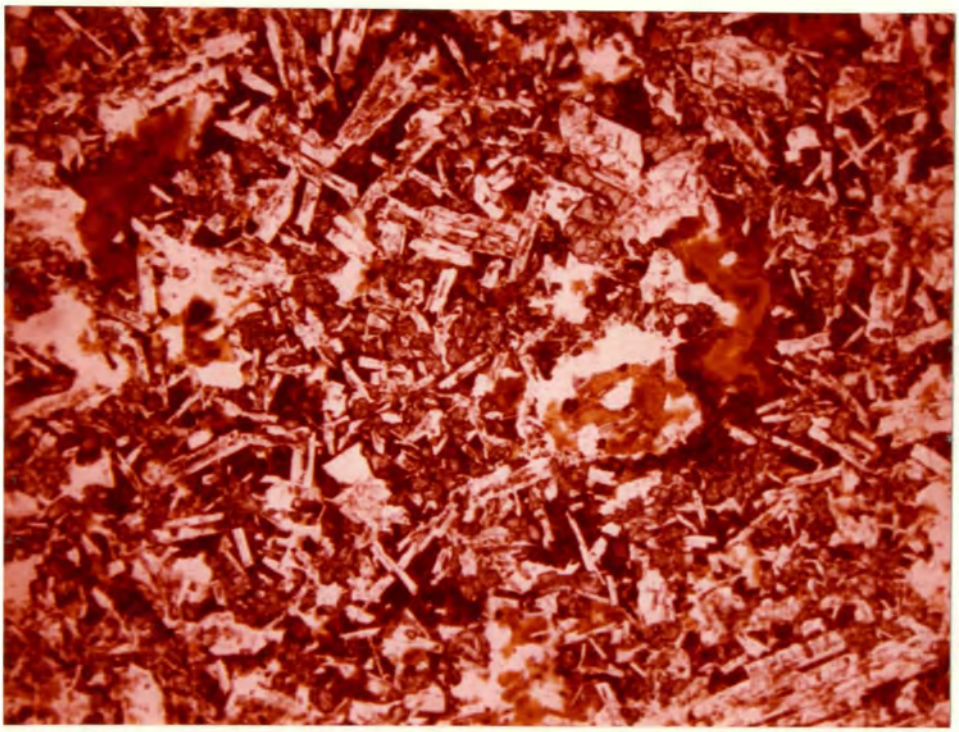

Fig. 6(e) : AM24 : Strypoort Unit. Clinopyroxene (grey) and plagioclase (white). Brown patches are altered olivine or glass. (Plane polarised light).

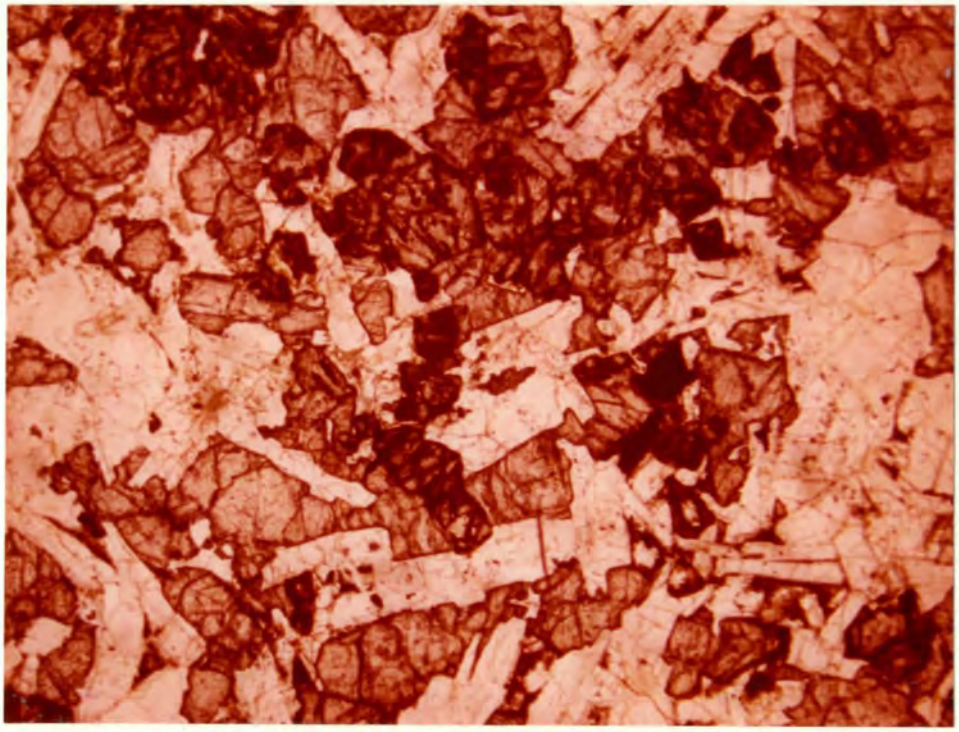

Fig. 6(f) : AM36M : Roodehoek Unit. Plagioclase (white) ophitically related to clinopyroxene (grey). Clusters of small, subhedral grains (dark grey to black) are olivines. (Plane polarised light).

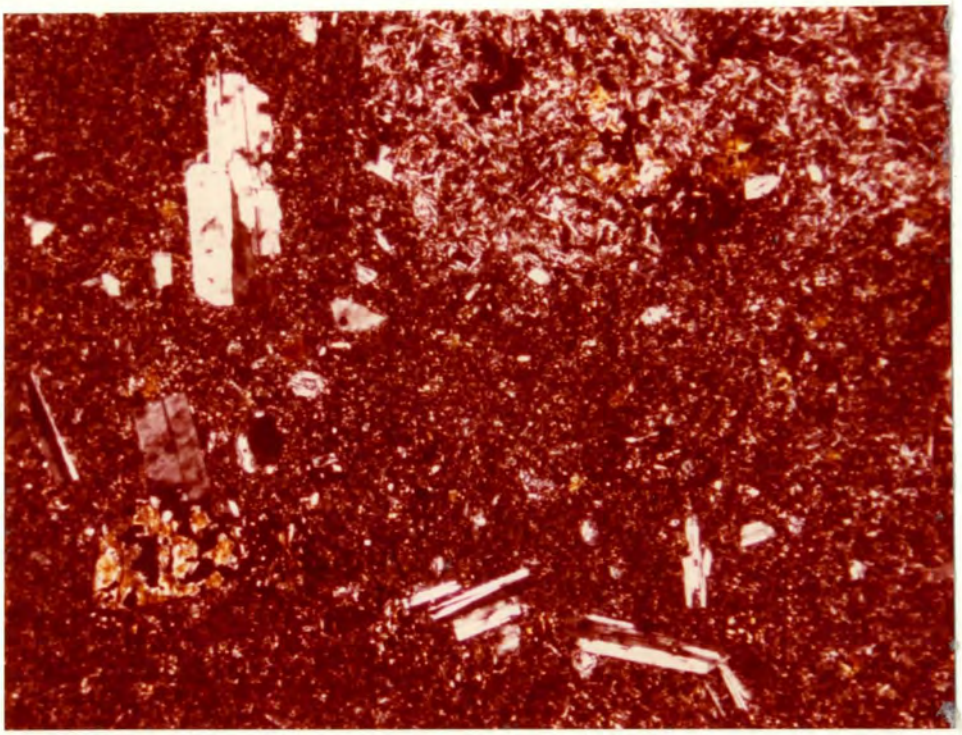

Fig. 6(g) : AM51 : Phenocrysts of plagioclase (white and grey) and altered pyroxene (yellow) in fine-grained groundmass. Note variability of groundmass grain-size. (Crossed nicols).

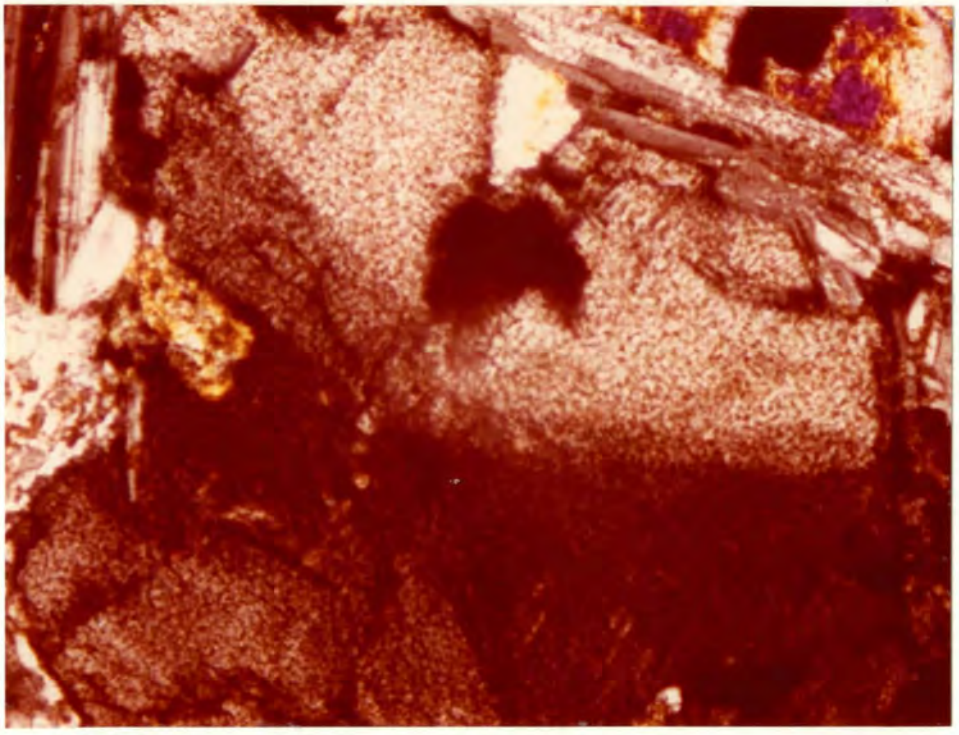

Fig. 6(h) : AM36T : Roodehoek Unit. Hourglass zoning in augite (Crossed nicols).

6. MINERALOGY

6.1 Introduction

Representative microprobe analyses of the main silicate phases of the basaltic assemblage (i.e. olivine, pyroxene and feldspar) are presented in this chapter for ten rocks of the Brosterlea area, and also for two rocks from the Barkly East area (Pemberton, 1978), although the latter have been analysed for olivine only.

Each of the mineral phases analysed is discussed separately below. Details of microprobe analytical conditions are provided in appendix 3.

6.2 Olivine

The olivine structure consists of independent SiO_4 tetrahedra, linked by divalent cations in six-fold co-ordination. There are two non-equivalent six-fold co-ordinated sites in the olivine structure (M_1 and M_2). The most predominant cations in the M sites are Mg and Fe, which approach random distribution between M_1 and M_2 (Birle et al., 1968). The almost complete disordering of Fe and Mg between M_1 and M_2 is explained by Burns (1970a) in terms of Crystal Field Theory.

The common ferromagnesian olivines form a solid solution series between forsterite (Mg_2SiO_4) and fayalite (Fe_2SiO_4). Within this basic framework, there is minor substitution by Ni, Cr, Mn and Ca for Fe and Mg. The partitioning of nickel into olivine, in particular, has received considerable attention over the past few years (Sato, 1977; Hart and Davis, 1978; Leeman and Lindstrom, 1978), and there is a wealth of information available on estimated olivine/liquid distribution co-efficients, these ranging between 4,8 and 34 (Leeman and Lindstrom, op. cit.).

In Fig. 7, Ni contents (in parts per million : ppm) are plotted against weight percent MgO for a variety of Karoo-

age igneous environments. The cumulus nature of the Elephant's Head olivines, and their effect on MgO content of the host rock, are discussed in a recent paper by Eales and Marsh (1979a). These olivines fall at the high-Mg, high-Ni end of the trend in Fig. 7. The trend is hyperbolic, with Ni content of the olivines decreasing rapidly from the Elephant's Head values to the low-Ni olivines of the Drumbo Basalt Member. This type of relationship is an expression of the high distribution coefficient of Ni for olivine, which results in a rapid depletion of Ni in residual melts, and consequently in a lower Ni-content for olivines from more fractionated rocks.

The strong zoning in the Drumbo olivines (Fig. 7) in terms of both Ni and Mg is indicative of non-equilibrium crystallisation, with each successive zone being in equilibrium with a more fractionated residual liquid.

The only rock from the Brosterlea complex which contains olivines fresh enough for microprobe analysis is AM36M, a sample from the Tafelkop sampling locality. Sample AM36M is classified as a member of the Roodehoek Unit on the basis of stratigraphic relationships and trace element geochemistry, but differs from its congeners in having higher contents of MgO (10,32%) and Ni (182 ppm). These latter data suggest a component of cumulus olivine in the rock.

Weathering has rendered the field relationships of AM36M too indistinct for any definite conclusions to be drawn as to its origin, but certain assumptions can be made on the basis of the chemistry and petrography of the rock. The olivine content of sample AM36M, as determined by modal analysis, is 15%, which would presumably be sufficient to raise the MgO and Ni contents of the rock to the observed levels. Indeed, an MgO/Ni mixing line, using the average Roodehoek basalt as the hypothetical parent melt (Fig. 8), indicates by lever rule calculations that approximately 15% olivine enrichment would be required to derive AM36M from the parent.

The olivine enrichment model breaks down, however, when an attempt is made to derive mixing lines for other elements. Most of these plots indicate a stronger element of pyroxene control than olivine control on the bulk composition of AM36M. Probably the most conspicuous amongst the evidence against olivine enrichment is the plot of MgO vs. FeO, which indicates that the AM36M olivines are far too iron-rich to fall on the hypothetical mixing line (Fig. 9).

Of particular interest to the present problem is the work by Moore and Evans (1967) on olivine in the prehistoric Makaopuhi lava lake in Hawaii. Differentiation at Makaopuhi cannot be modelled in terms of simple "olivine control" lines. One of the reasons for this, and probably the most important in the context of the AM36M olivines, is the clear evidence that the olivines in the Makaopuhi lake changed after crystallisation to more Fe-rich compositions. Moore and Evans (op. cit.) estimate that this transformation must have occurred within the temperature range 1100^{o}C to 800^{o}C i.e., very close to the solidus temperature of the basalts. This change, it is pointed out, was not simply a case of homogenisation of the Mg-rich cores and the Fe-rich rims of the olivines, but was a "substantial enrichment of the whole olivine phenocryst at the expense of the surrounding phases" (Moore and Evans, op. cit.). This certainly seems a plausible explanation of the AM36M situation, where an initially Mg-rich cumulus olivine phase, transformed by reaction with its host rock to a more Fe-rich composition, releases Mg to the rock, this having the effect of inhibiting the iron enrichment of other mineral phases in the rock, e.g. pyroxene, and at the same time increasing the bulk MgO content of the rock.

Sub-solidus iron enrichment of the olivines would be expected to produce an effect like that seen in the AM36M olivines (Fig. 7), where all the olivines are brought to a more or less constant Fe/Mg ratio, this ratio, however, being much higher than the calculated equilibrium Fe/Mg ratio. Nickel, by virtue of its very high distribution coefficient

for olivine, is not affected by any cation-exchange reactions, and zoning in terms of this element is effectively "frozen in" the olivines (Fig. 7). The post-crystallisation alteration of the Fe/Mg ratio of the olivines excludes the possibility of any attempts at quantitative or semi-quantitative modelling of the history of crystallisation of the olivines e.g., by the methods of Roeder and Emslie (1970) or Hart and Davis (1978).

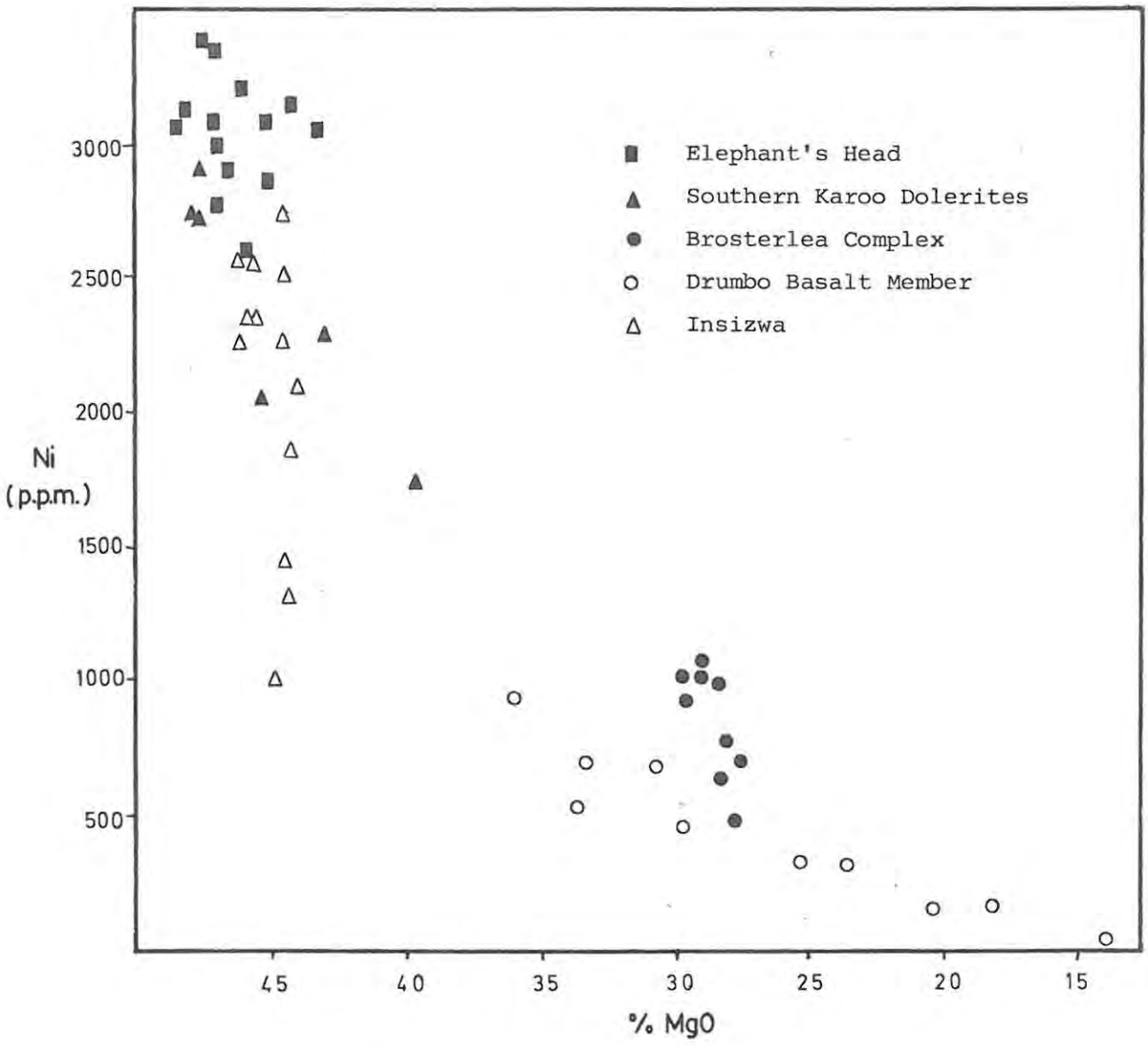

Fig. 7 : Plot of Ni (ppm) vs. weight % MgO for olivines from the Karoo igneous province.

Sources of information : H.V. Eales (Elephant's Head, Insizwa); J.S. Marsh (Southern Karoo Dolerites); This study (Brosterlea, Drumbo).

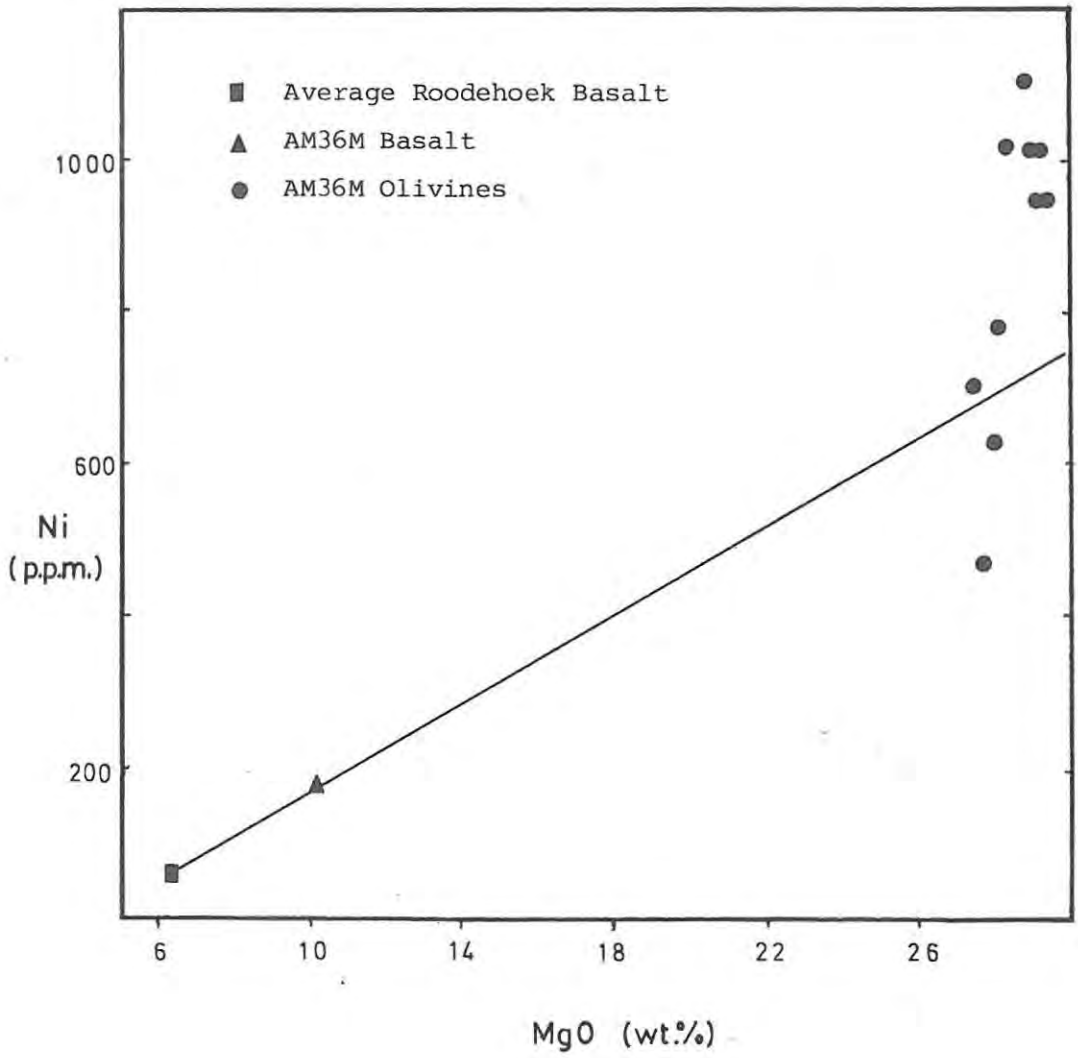
Average Roodehoek Basalt
AM36M Basalt
AM36M Olivines
1000
600
200
Ni
(p.p.m.)
6
10
14
18
22
26
MgO (wt.%)

Fig. 8

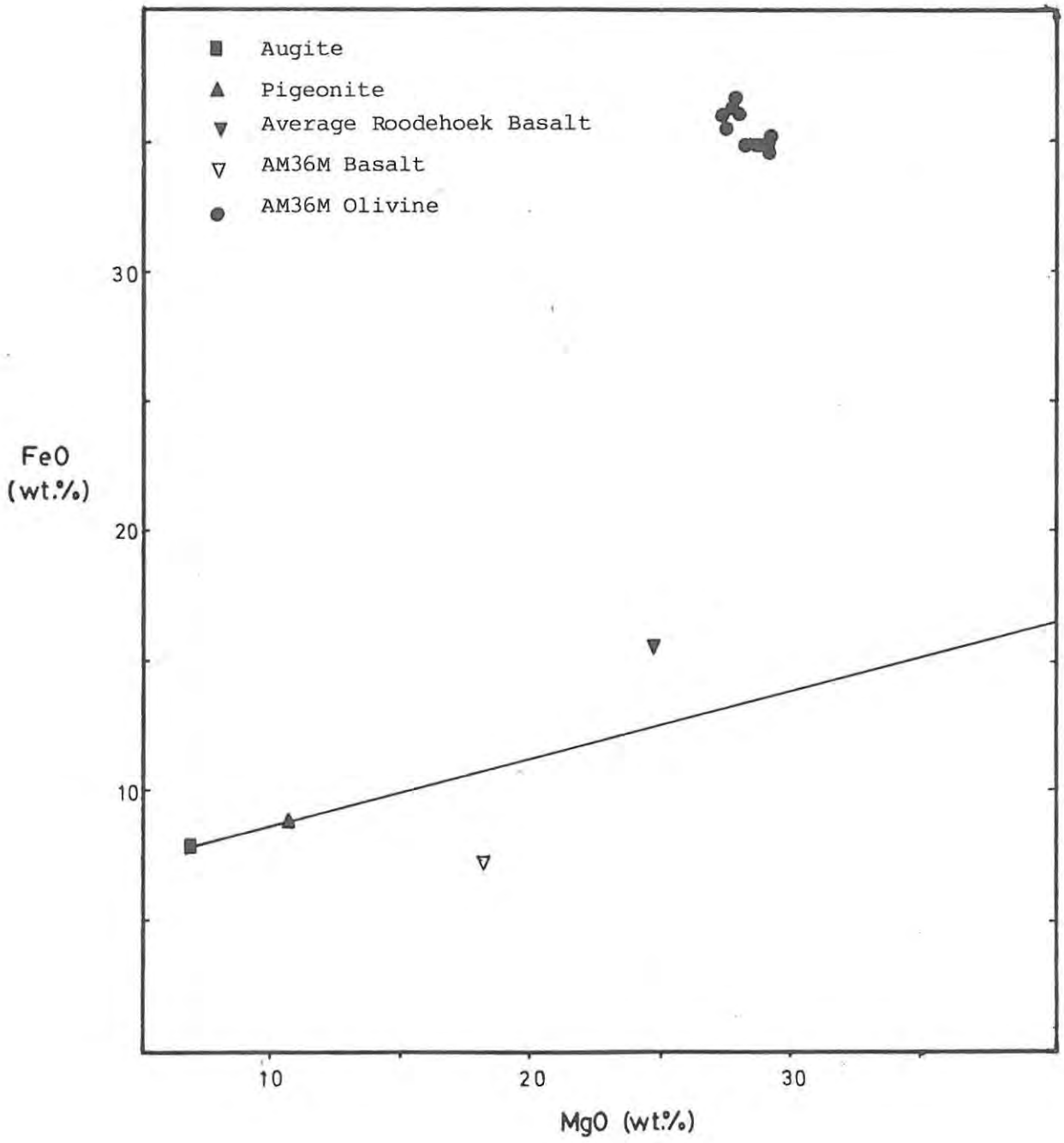
Augite
Pigeonite
Average Roodehoek Basalt
AM36M Basalt
AM36M Olivine
30
20
10
FeO
(wt.%)
10
20
30
MgO (wt.%)

Fig. 9

TABLE 1.1 OLIVINE ANALYSES BY MICROPROBE

1.1.a Brosterlea olivines

	AM36M/1 CORE	AM36M/1 MARGIN	AM36M/1 MARGIN	AM36M/2 MARGIN	AM36M/2 CORE	AM36M/3 CORE	AM36M/4 CORE	AM36M/4 MARGIN	AM36M/4 MARGIN	AM36M/4 MARGIN
SiO_2	36,69	36,69	36,72	36,49	36,85	37,68	36,61	36,06	36,82	36,64
FeO	36,12	35,23	36,82	36,32	35,09	35,61	34,84	36,13	35,11	35,04
MgO	28,38	29,48	28,07	28,07	29,34	27,83	29,43	27,58	29,10	28,94
NiO	0,13	0,13	0,10	0,08	0,12	0,06	0,12	0,09	0,13	0,14
TOTAL	101,32	101,53	101,71	101,96	101,40	101,18	101,00	99,86	101,16	100,76
Molecular %										
Fo	58,25	59,78	57,54	57,88	59,76	58,16	60,06	57,57	59,54	59,45
Fa	41,61	40,08	42,35	42,03	40,11	41,77	39,81	42,33	40,32	40,39
Ni-oliv.	0,14	0,14	0,11	0,09	0,13	0,07	0,13	0,10	0,14	0,16
TOTAL	100,00	100,00	100,00	100,00	100,00	100,00	100,00	100,00	100,00	100,00
Weight %										
Fo	49,50	49,95	48,96	48,96	51,17	48,54	51,44	48,10	50,75	50,48
Fa	51,20	51,42	52,20	51,49	49,74	50,48	49,39	51,22	49,77	49,67
Ni-oliv.	0,18	0,17	0,14	0,11	0,17	0,08	0,17	0,13	0,18	0,20
TOTAL	100,88	101,54	101,30	100,56	101,08	99,10	101,00	99,45	100,70	100,35
ppm Ni	1022	1022	786	629	943	472	943	707	1022	1100

TABLE 1.1 OLIVINE ANALYSES BY MICROPROBE

1.1.b Drumbo olivines

	JP17/1 MARGIN	JP17/2 MARGIN	JP17/2 CORE	JP17/2 MARGIN	JP17/3 MARGIN	JP17/3 MARGIN	JP17/4 CORE	JP17/4 CORE	JP61/1 CORE	JP61/2 CORE
SiO_2	34,37	37,50	34,62	37,15	35,64	35,03	38,13	38,72	38,50	36,56
FeO	51,80	33,80	49,37	33,63	41,38	45,75	25,77	25,74	28,56	39,07
MgO	14,37	29,74	18,28	30,60	23,87	20,57	36,29	33,71	33,52	25,34
NiO	0,01	0,06	0,02	0,09	0,04	0,02	0,12	0,07	0,09	0,04
TOTAL	100,55	101,10	102,29	101,47	100,93	101,37	100,31	98,24	100,67	101,01
Molecular %										
Fo	33,08	61,02	39,74	61,79	50,67	44,47	71,41	69,95	67,58	53,59
Fa	66,91	38,91	60,23	38,11	49,29	55,50	28,46	29,97	32,32	46,37
Ni-oliv.	0,01	0,07	0,03	0,10	0,04	0,03	0,13	0,08	0,10	0,04
TOTAL	100,00	100,00	100,00	100,00	100,00	100,00	100,00	100,00	100,00	100,00
Weight %										
Fo	25,06	51,87	31,88	53,37	41,63	35,88	63,29	58,79	58,46	44,19
Fa	73,42	47,91	69,98	47,67	58,66	64,85	36,53	36,49	40,48	55,38
Ni-oliv.	0,01	0,08	0,03	0,13	0,06	0,03	0,17	0,10	0,13	0,06
TOTAL	98,49	99,86	101,89	101,17	100,35	100,76	99,99	95,38	99,07	99,63
ppm Ni	79	472	157	707	314	157	943	550	707	314

6.3 Pyroxene

The general formula for pyroxenes, after Hess (1949), is :

$$(W)_{1-p}(X,Y)_{1+p}Z_2O_6$$

where W is filled by Ca and Na; X by Mg, Fe^{2+}, Mn and Ni; Y by Al, Fe^{3+}, Cr and Ti; Z by Si and Al. The value p = O for augites, approaching unity in the case of pigeonite and orthopyroxene. This expression of the structural formula, however, implies a too rigid partitioning of the various cations into the different sites, and the general formula used by Nielsen and Drake (1979) is perhaps more suitable in the light of more modern information on element partitioning within minerals. This latter formula is as follows :

$$(M1)(M2)T_2O_6$$

M1 is the smaller of the two octahedral M-sites, and is preferentially occupied by Mg, Fe, Al, Cr and Ti; M2 is preferentially occupied by Ca and Na and also contains Mg and Fe; T is a tetrahedrally co-ordinated site occupied primarily by Si and Al.

The Ca-Mg-Fe ternary diagrams for the pyroxenes of Am36M, AM23 and AM40 are displayed in Fig. 10 (a,b and c). The augites of AM40 (Perdekop Unit) show incipient development of a trend similar to that identified by Eales and Booth (1974) at Birds River. This is a typically tholeiitic trend, with Ca decreasing as Fe content of the pyroxenes increases. AM23 and AM36M, both members of the Roodehoek Unit, show more distinct trends of Ca depletion in augite than does AM40. This trend is similar to those identified by Fodor et al. (1975) in some Hawaiian tholeiites. The core zones of the AM36M pyroxenes are pigeonitic. This is by no means an isolated case, as pigeonite has been identified by optical means in a number of rocks of the Roodehoek Unit. Barberi et al. (1971) outline the differences between pyroxenes from alkalic and tholeiitic basalt types. Augites

from alkalic basalts display very little depletion in Ca content as Fe increases, whilst tholeiite-hosted augites show an initial trend of marked Ca depletion, followed by a trend of moderate Ca enrichment. This is the type of trend which characterises Skaergaard (Brown and Vincent, 1963) and Birds River (Eales and Booth, 1974). It is also characteristic, according to Barberi et al., for the tholeiitic suite to have a two-pyroxene assemblage - one Ca-rich and the other Ca-poor.

A shortcoming of the Ca-Mg-Fe ternary diagram is that it does not take into account the minor (non-stoichiometric) elements which substitute for Fe, Mg, Ca and Si in the pyroxene structure. The most important elements in this category are Mn, Cr, Ti, Na and Al.

Manganese (Mn^{2+}) partions between coexisting pyroxenes in favour of the Ca-poor variety, and both pyroxenes show a linear increase in Mn^{2+} content with decreasing enstatite content (Campbell and Borley, 1974). This is precisely the effect seen in the Brosterlea pyroxenes (Fig. 11d), with augites having MnO contents increasing from 0,11% to 0,30% as FeO content increases from 6,70% to 15,41%, and pigeonites increasing their MnO content from 0,37 to 0,42% as FeO increases from 15,87 to 21,47%. It is possibly noteworthy that the most Fe-rich augite analysed (AM40/4) shows a drop in Mn from the expected trend. This effect may be due to some of the Fe being present as ferric iron.

Chromium (Cr^{3+}) partitions strongly into early-formed pyroxenes (Fig. 11e), giving an inverse relation of Cr_2O_3 to FeO. Schweitzer et al. (1979) regard this type of trend as being characteristic of tholeiites, whereas alkalic basalts have consistently low Cr contents. The high partition coefficient of Cr^{3+} between pyroxene and melt (up to 40 in the Jimberlana intrusion : Campbell and Borley, op. cit.) can be explained in terms of Crystal Field Theory. The crystal field stabilisation energy (C.F.S.E.) of Cr in

octahedral sites is 37,6 Kcal. $mole^{-1}$ Burns (1970b), which is the highest C.F.S.E. value of any of the transition elements. The substitution of Cr^{3+} for divalent cations in the octahedral sites of pyroxenes is counterbalanced by the substitution of Al^{3+} for Si^{4+} in the tetrahedral sites (Campbell, 1977). On this basis, there should be a more or less linear correlation between Al_2O_3 and Cr_2O_3 in the pyroxenes. This holds for the clinopyroxenes in the Brosterlea basalts, but the pigeonites of AM36M are displaced from the linear trend (Fig. 11f). The displacement of the pigeonites is difficult to explain, unless substitution of small proportions of Fe^{3+} for Al is lowering the Al content of the pigeonites relative to the Cr contents. This, however, is a very tenuous suggestion, made with no supporting evidence.

Fleet (1974) shows that D_{Na} (the crystal/liquid distribution coefficient of Na for pyroxene) increases progressively with differentiation to a value near unity in the case of the Na-rich pyroxenes of the Skaergaard intrusion and the Bushveld Igneous Complex. This trend they ascribe to a coupled substitution of the type :

$$Ca,\ Mg \leftrightharpoons Na^{+},\ Fe^{3+}$$

At Na contents as low as those of the Brosterlea pyroxenes, however, valence balance does not depend on the above substitution effects, and no definite conclusions can be drawn as to the behaviour of Na under these circumstances. In their comparative study of pyroxenes from a variety of environments, Schweitzer et al. (1979) find that Na is generally very low in both tholeiites and alkali basalts, but tends to be slightly enriched in alkali basalts.

Titanium (Ti) content of the Brosterlea pyroxenes increases with differentiation (Fig. 11c) although this relationship is by no means linear. Two factors control the geochemistry of Ti : its zero C.F.S.E. (Burns, 1970b) and its 4+ valency. Ti can only enter the pyroxene structure

if its charge is balanced. This can be achieved by simultaneous substitution of two Al^{3+} ions in the tetrahedral site with substitution of one Ti^{4+} ion in the octahedral sites. The low concentration of Ti in the early-formed pyroxenes (Fig. 11c) is due to the fact that, with its relatively low C.F.S.E., Ti cannot compete with Cr for charge-deficient octahedral sites, and Ti only becomes an important constituent of pyroxene once Cr is significantly depleted in the melt (Campbell and Borley, 1974). This feature is verified by a comparison of Fig. 11c with Fig. 11e.

Fodor et al. (1975) and Nakamura and Coombs (1973) have used the variation of Al and Ti content in pyroxenes from a variety of volcanic rocks to characterise the magma type from which the minerals precipitated. Coish and Taylor (1979) however, are doubtful of the value of such exercises, because they believe that cooling rate of the magma has a decided effect on the composition of the co-existing pyroxenes. Enhancement of the Ti and Al contents of the pyroxenes is considered to be a direct function of cooling rate, which controls diffusion. Also, faster cooling results in a shorter crystallisation period for plagioclase, which has the effect of making more Al available for entry into the pyroxene structure. Barberi et al. (1971) point out that entry of Ti into clinopyroxenes is directly controlled by the Al and Si contents of the pyroxenes which, in turn, are related to the silica activity of the melt. Low silica activity favours entry of Al into the tetrahedral site which, as previously explained, is necessary in order to balance the entry of Ti into the octahedral sites. Kushiro et al. (1970) found that lunar basalts have a strong linear relationship between Ti and Al, which Ross et al. (1970) ascribe to substitution of the type :

$$M_y^{2+} + 2Si_z^{4+} \quad Ti_y^{4+} + 2Al_z^{3+}$$

where M is an octahedrally co-ordinated cation e.g. Fe or Mg, and the subscripts y and z imply octahedral and tetra-

hedral sites, respectively. The scatter of values in the case of the Brosterlea pyroxenes makes the linear Al/Ti trend indistinct. Gibb (1973) favours a substitution mechanism of the type described by Ross et al. (op. cit.) for balancing of Ti by Al. Gibb finds, in addition, that as the Al content of pyroxenes increases, so does the amount in excess of that required solely to fill the Si-deficient tetrahedral sites. This effect is also noted by Campbell and Borley (1974), and is the general case for the Brosterlea augites. Although excess Al may be related to the introduction of the jadeite molecule, Gibb (op. cit.) finds no corresponding variation in Na in pyroxenes from his studies of the Shiant Isles Sill, and regards as more likely a limited substitution effect of the type :

$$M_y^{2+} + Si_z^{4+} \rightleftharpoons Al_y^{3+} + Al_z^{3+}$$

No linear relationship between Na and Al is found for the Brosterlea pyroxenes, and the latter of Gibb's alternatives must be considered operative.

A problem arises in the recalculation of the Brosterlea pyroxenes on the basis of cations per six oxygens, in that Ti, and sometimes Fe^{3+}, have to be included in the tetrahedral site of the pigeonites, in order to make up the total of two cations. Kuno (1955) argued the case for inclusion of Ti and Fe^{3+} into the z-group to balance the structural formula, but this procedure is by no means accepted generally. In table 1.2, Fe and Ti have been included in the z-group, where necessary, to balance the Al and Si deficit, but this is merely an expedient, and does not imply agreement with the views of Kuno. In any event, the Si+Al deficit is only in the third decimal place, which hardly corresponds to the precision of microprobe analyses.

As mentioned earlier, a number of workers in the field have used the chemical composition of pyroxenes, especially their Ti and Al contents, to identify the nature of the parent rock. Nisbet and Pearce (1977) applied the statistical

technique of discriminant analysis to a large number of microprobe and chemical analyses of augites from a variety of environments. They were able, by this method, to predict the host rock of the pyroxenes with varying degrees of success. The Nisbet and Pearce technique was applied to the Brosterlea pyroxenes (Fig. 12), but the results are rather disappointing, in that they do not fall in the field of "Within-Plate Tholeiites", as defined. Nisbet and Pearce, however, only expect a 42% success rate in the case of "within-plate tholeiites", and many of their tholeiites plot in similar positions to the Brosterlea augites. The only really definite information to be gleaned from this diagram is that the Brosterlea pyroxenes have tholeiitic, rather than alkalic, affinities.

Fig. 10 a,b,c : Ca-Mg-Fe plots of clinopyroxenes

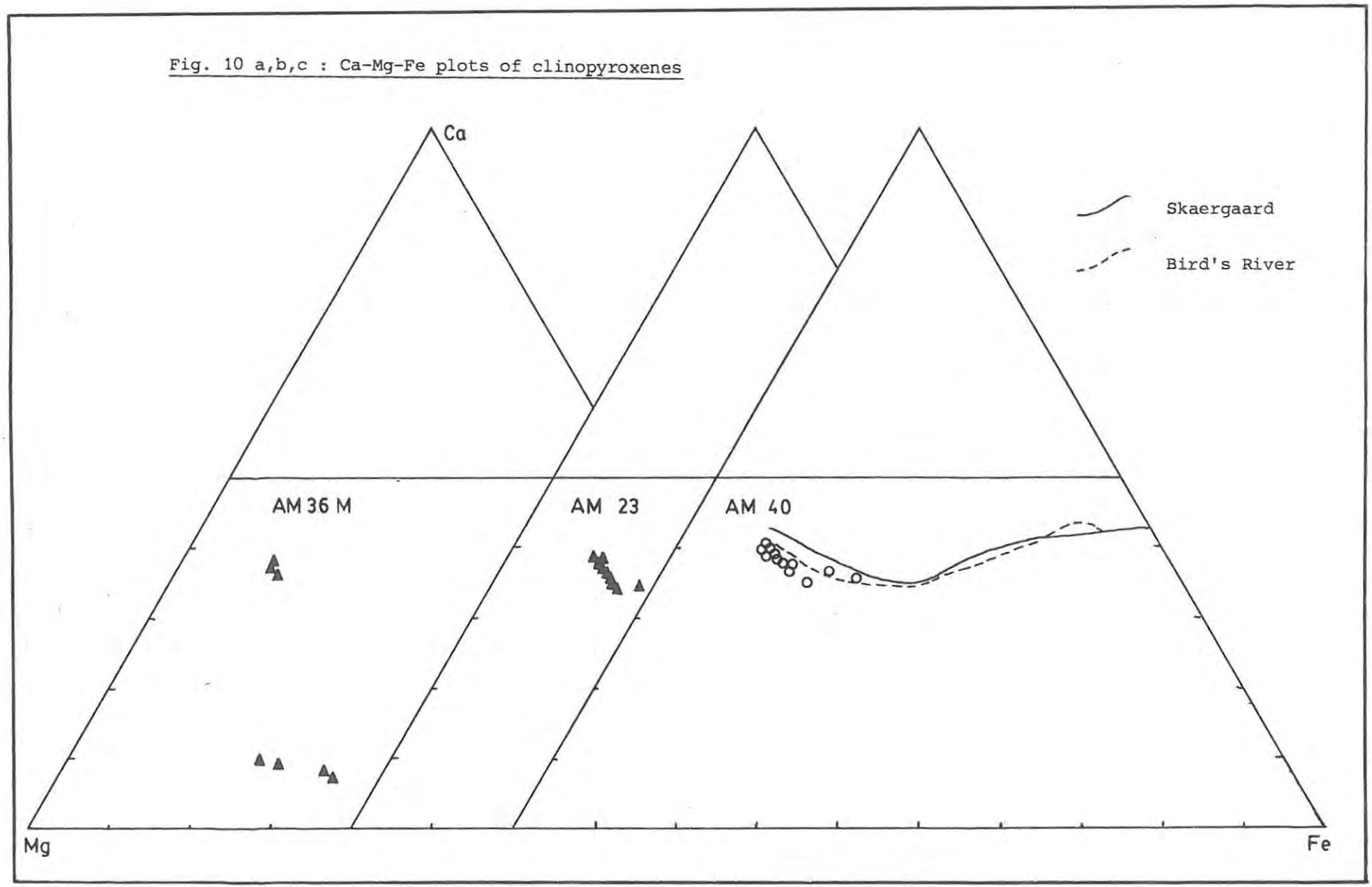

Fig. 11 a-f : VARIATION DIAGRAMS FOR BROSTERLEA PYROXENES

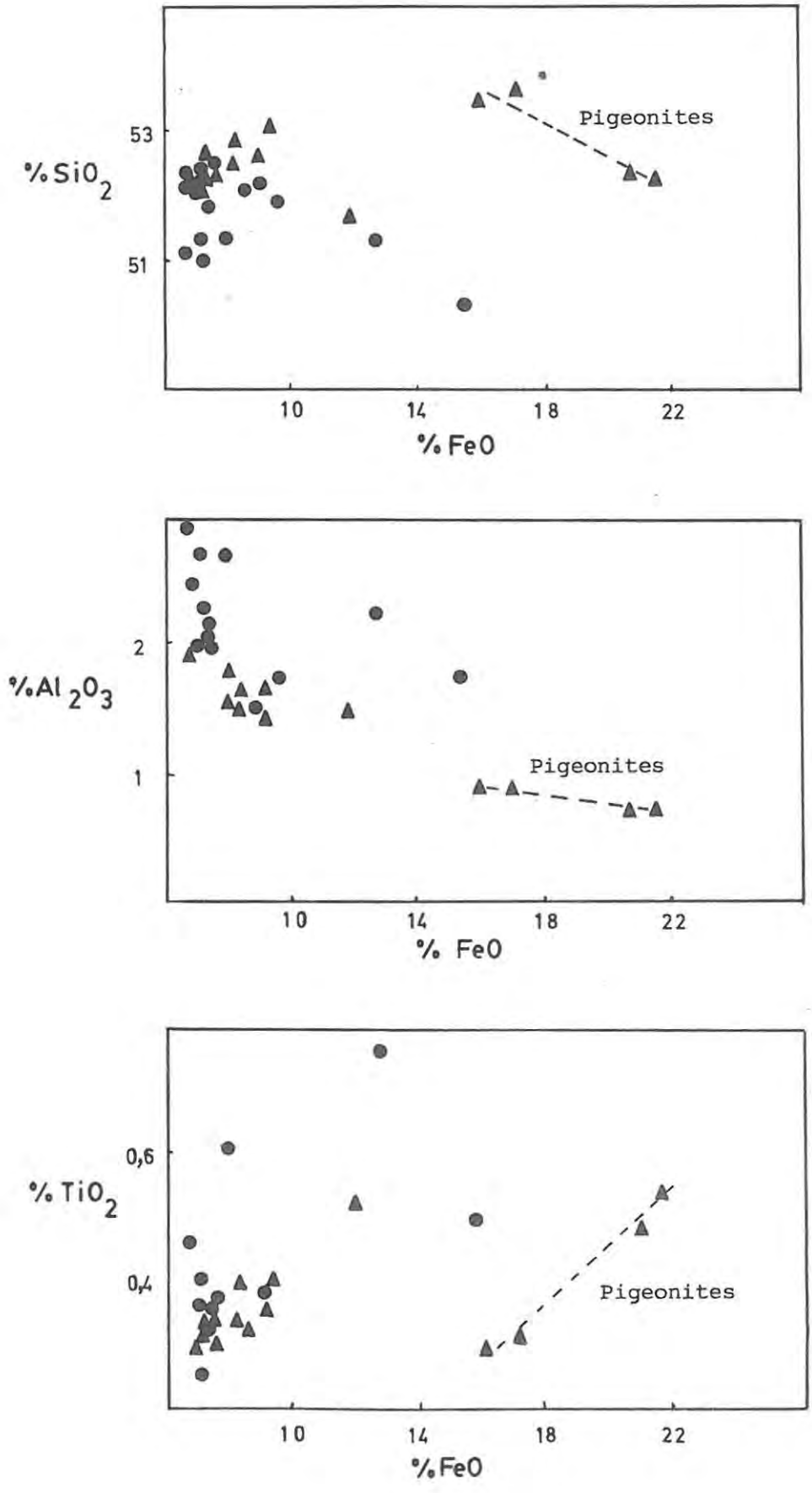

Fig. 11 a-f : VARIATION DIAGRAMS FOR BROSTERLEA PYROXENES

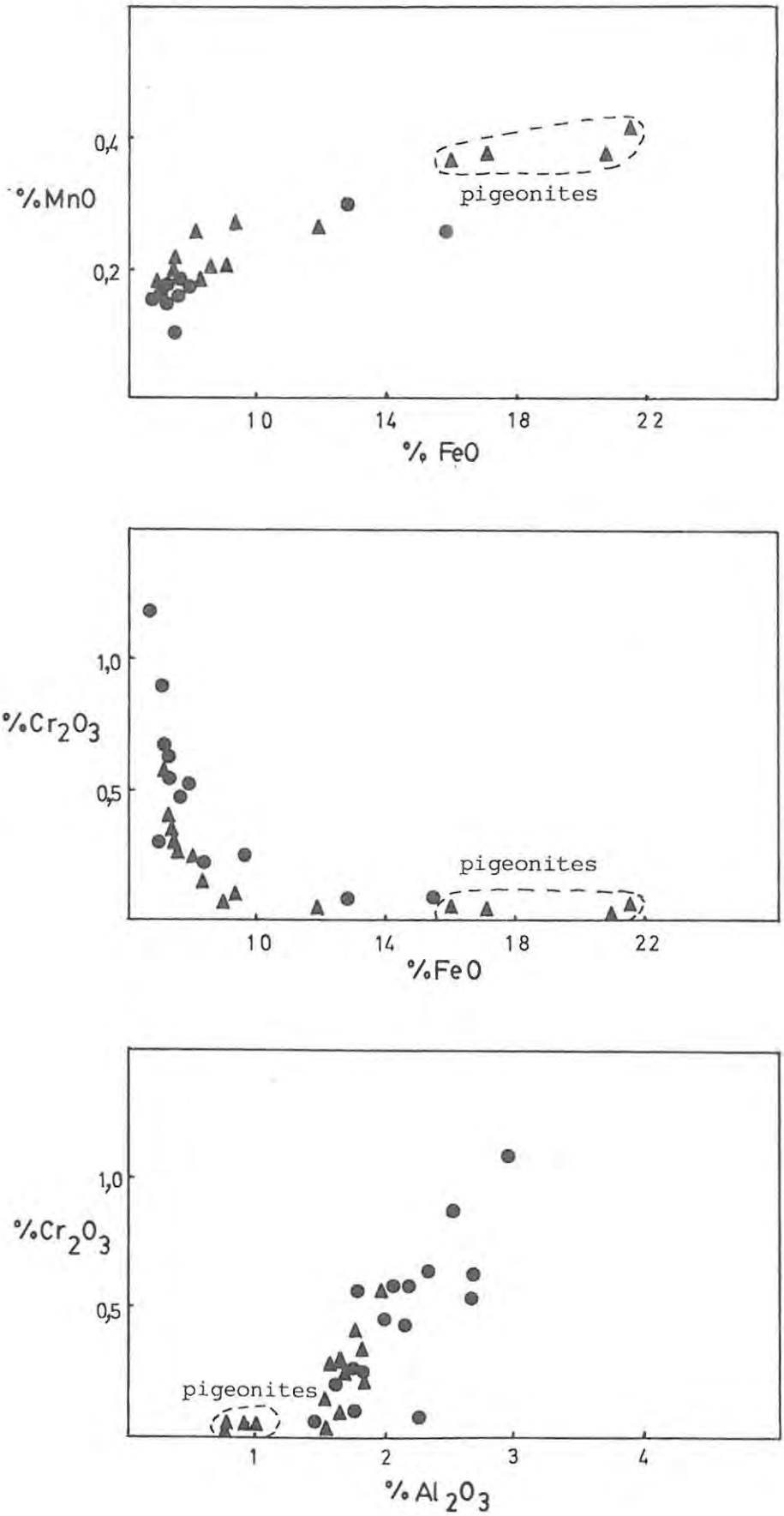

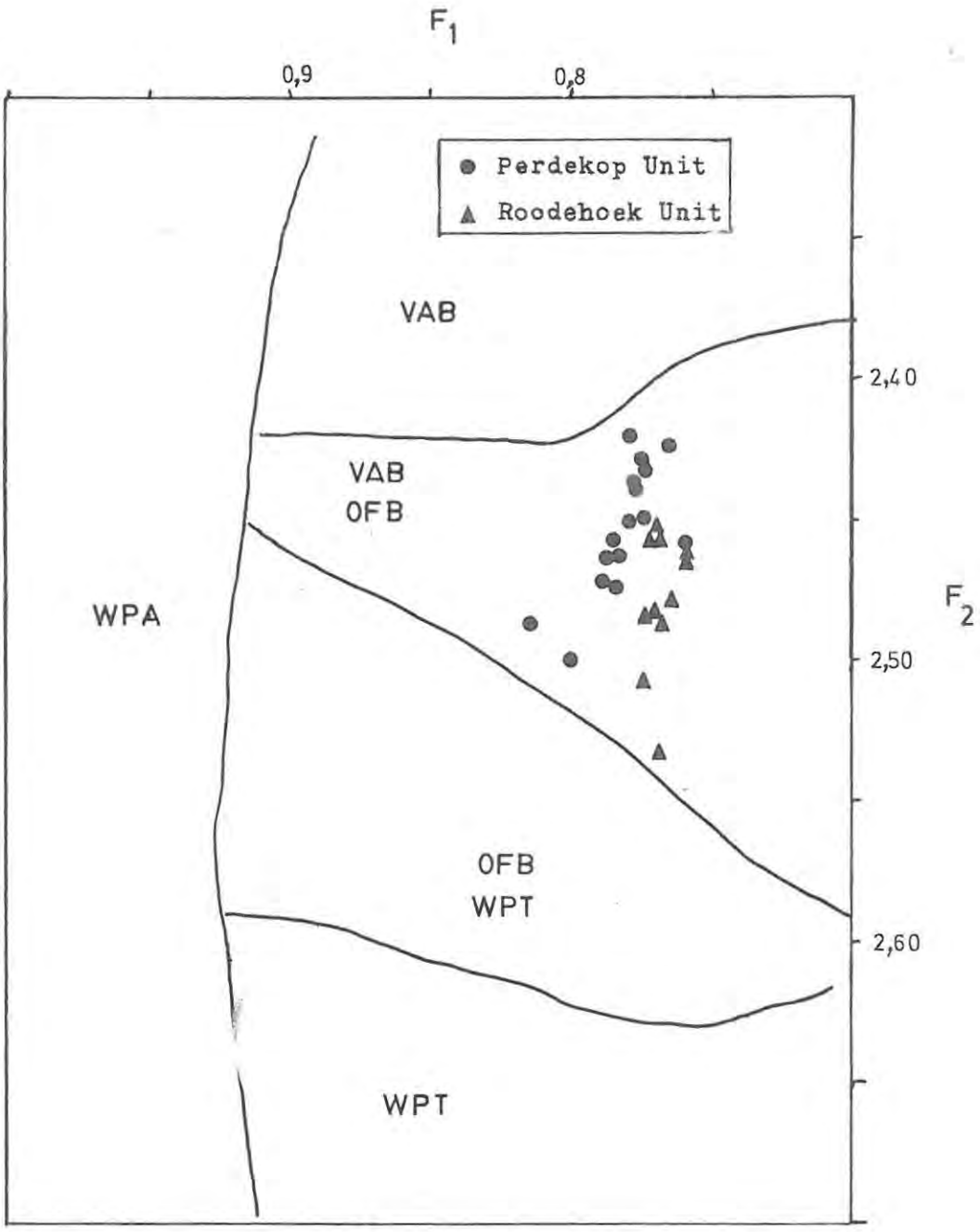

Fig. 12 : Plot of discriminant functions, F_1 against F_2, for the Brosterlea pyroxenes, where :

$F_1 = -0,012 \times SiO_2 - 0,0807 \times TiO_2 + 0,0026 \times Al_2O_3 - 0,0012 \times FeO - 0,0026 \times MnO + 0,0087 \times MgO - 0,0128 \times CaO - 0,0419 \times Na_2O$

$F_2 = -0,0469 \times SiO_2 - 0,0818 \times TiO_2 - 0,0212 \times Al_2O_3 - 0,0041 \times FeO - 0,1435 \times MnO - 0,0029 \times MgO + 0,0085 \times CaO + 0,0160 \times Na_2O$

and

VAB = Volcanic Arc Basalt

OFB = Ocean Floor Basalt

WPT = Within Plate Tholeiite

WPA = Within Plate Alkalic Basalt

TABLE 1.2 PYROXENE ANALYSES BY MICROPROBE

Lesotho Formation

	AM40/3 MARGIN	AM40/3 MARGIN	AM40/3 MARGIN	AM40/4 MARGIN	AM40/4 CORE	AM40/4 MARGIN
SiO_2	51,37	52,15	51,93	50,36	51,00	52,29
TiO_2	0,34	0,45	0,33	0,47	0,48	0,65
Al_2O_3	2,31	1,61	1,77	1,75	2,72	1,73
FeO	7,08	8,44	9,54	15,41	7,20	7,09
MnO	0,18	0,19	0,18	0,25	0,17	0,26
MgO	17,28	17,02	16,52	14,25	16,92	17,36
CaO	19,26	18,89	18,78	16,97	19,67	19,87
Na_2O	0,23	0,21	0,23	0,17	0,26	0,26
Cr_2O_3	0,66	0,22	0,27	0,10	0,64	0,28
TOTAL	98,71	99,18	99,55	99,73	99,06	99,79
Recalculated as cations per 6 oxygens (Z=2)						
Si	1,917	1,942	1,937	1,921	1,901	1,931
Al	0,083	0,058	0,063	0,079	0,099	0,069
Ti	0,010	0,013	0,009	0,014	0,013	0,018
Al	0,019	0,013	0,015	-	0,021	0,006
Fe	0,221	0,263	0,298	0,492	0,224	0,219
Mn	0,006	0,006	0,006	0,008	0,005	0,008
Mg	0,961	0,945	0,918	0,810	0,940	0,955
Ca	0,770	0,754	0,750	0,693	0,785	0,786
Na	0,017	0,015	0,017	0,012	0,019	0,019
Cr	0,019	0,006	0,008	0,003	0,019	0,008
X+Y	2,023	2,015	2,021	2,032	2,026	2,019
At% Mg	49,23	48,16	46,69	40,60	48,20	48,73
Fe	11,32	13,41	15,14	24,64	11,51	11,17
Ca	39,45	38,43	38,17	34,76	40,29	40,10

TABLE 1.2 PYROXENE ANALYSES BY MICROPROBE

Lesotho Formation

	AM40/1 MARGIN	AM40/1 CORE	AM40/1 MARGIN	AM40/2 MARGIN	AM40/2 CORE	AM40/2 MARGIN
SiO_2	52,34	51,14	52,08	52,52	51,37	51,18
TiO_2	0,40	0,46	0,36	0,37	0,61	0,76
Al_2O_3	2,51	2,95	2,02	1,98	2,73	2,24
FeO	6,88	6,70	6,91	7,48	7,97	12,66
MnO	0,17	0,16	0,18	0,19	0,18	0,30
MgO	17,51	17,20	17,75	17,26	17,04	15,81
CaO	19,70	19,56	19,63	19,64	19,18	17,28
Na_2O	0,24	0,29	0,25	0,27	0,17	0,24
Cr_2O_3	0,89	1,19	0,57	0,46	0,54	0,09
TOTAL	100,64	99,65	99,75	100,17	99,79	100,56
Recalculated as cations per 6 oxygens (Z=2)						
Si	1,913	1,892	1,922	1,924	1,900	1,911
Al	0,087	0,108	0,078	0,076	0,100	0,089
Ti	0,011	0,013	0,010	0,010	0,017	0,021
Al	0,022	0,020	0,010	0,009	0,019	0,010
Fe	0,211	0,207	0,213	0,229	0,246	0,395
Mn	0,005	0,005	0,006	0,006	0,006	0,009
Mg	0,954	0,948	0,976	0,942	0,939	0,880
Ca	0,772	0,775	0,776	0,771	0,760	0,691
Na	0,017	0,021	0,018	0,019	0,012	0,017
Cr	0,026	0,035	0,017	0,013	0,016	0,003
X+Y	2,018	2,024	2,026	1,999	2,015	2,016
At% Mg	49,27	49,11	49,66	48,51	48,27	44,74
Fe	10,87	10,73	10,85	11,80	12,67	20,10
Ca	39,86	40,16	39,49	39,69	39,06	35,16

TABLE 1.2 PYROXENE ANALYSES BY MICROPROBE

	Lesotho Formation				Roodehoek Unit		
	AM40/4 MARGIN	AM40/5 MARGIN	AM40/5 CORE	AM40/5 MARGIN	AM23/1 MARGIN	AM23/1 CORE	AM23/1 MARGIN
SiO_2	51,86	52,22	52,45	52,13	52,50	52,29	52,35
TiO_2	0,35	0,38	0,25	0,32	0,34	0,30	0,31
Al_2O_3	2,15	1,46	1,80	2,09	1,80	1,98	1,69
FeO	7,34	8,99	7,19	7,23	8,02	6,87	7,38
MnO	0,17	0,22	0,16	0,11	0,19	0,19	0,19
MgO	17,31	16,99	18,24	17,38	17,85	17,88	17,81
CaO	19,64	19,04	18,84	19,93	18,57	19,31	19,28
Na_2O	0,25	0,23	0,28	0,25	0,16	0,25	0,24
Cr_2O_3	0,59	0,06	0,57	0,42	0,24	0,58	0,28
TOTAL	99,66	99,59	99,78	99,86	99,67	99,65	99,53
Recalculated as cations per 6 oxygens (Z=2)							
Si	1,919	1,942	1,933	1,924	1,938	1,928	1,936
Al	0,081	0,058	0,067	0,076	0,062	0,072	0,064
Ti	0,010	0,011	0,007	0,009	0,010	0,008	0,009
Al	0,013	0,006	0,011	0,015	0,017	0,014	0,010
Fe	0,227	0,280	0,222	0,223	0,248	0,212	0,228
Mn	0,005	0,007	0,005	0,004	0,006	0,006	0,006
Mg	0,955	0,942	1,002	0,956	0,982	0,983	0,981
Ca	0,779	0,759	0,740	0,788	0,735	0,763	0,764
Na	0,018	0,017	0,020	0,018	0,012	0,018	0,017
Cr	0,017	0,002	0,017	0,012	0,007	0,017	0,008
X+Y	2,024	2,024	2,024	2,025	2,017	2,021	2,023
At% Mg	48,69	47,56	51,02	48,60	50,00	50,20	49,73
Fe	11,59	14,12	11,29	11,34	12,60	10,82	11,56
Ca	39,72	38,32	37,69	40,06	37,40	38,97	38,71

TABLE 1.2 PYROXENE ANALYSES BY MICROPROBE

Roodehoek Unit

	AM23/2 MARGIN	AM23/2 CORE	AM23/2 MARGIN	AM23/2 MARGIN	AM23/3 CORE
SiO_2	52,19	52,19	51,62	52,63	53,14
TiO_2	0,34	0,33	0,53	0,36	0,40
Al_2O_3	1,79	1,54	1,54	1,45	1,64
FeO	7,20	8,41	11,81	8,99	9,22
MnO	0,17	0,20	0,26	0,20	0,26
MgO	17,77	18,03	16,85	18,05	18,20
CaO	19,05	18,41	17,13	18,24	17,78
Na_2O	0,26	0,20	0,21	0,24	0,14
Cr_2O_3	0,34	0,15	0,04	0,07	0,09
TOTAL	99,11	99,46	99,99	100,23	100,87
Recalculated as cations per 6 oxygens (Z=2)					
Si	1,936	1,936	1,929	1,940	1,951
Al	0,064	0,064	0,068	0,060	0,049
Ti	-	-	0,003	-	-
Ti	0,010	0,009	0,012	0,010	0,011
Al	0,014	0,003	-	0,003	0,022
Fe	0,223	0,261	0,369	0,277	0,284
Mn	0,005	0,006	0,008	0,006	0,008
Mg	0,982	0,997	0,938	0,991	0,999
Ca	0,757	0,732	0,686	0,720	0,701
Na	0,019	0,014	0,015	0,017	0,010
Cr	0,010	0,004	0,001	0,002	0,003
X+Y	2,020	2,026	2,017	2,026	2,038
At% Mg	50,05	50,11	47,07	49,86	50,34
Fe	11,38	13,11	18,52	13,93	14,31
Ca	38,57	36,78	34,41	36,21	35,35

TABLE 1.2 PYROXENE ANALYSES BY MICROPROBE

Roodehoek Unit

	AM36M/1 CORE	AM36M/1 MARGIN	AM36M/1 MARGIN	AM36M/1 MARGIN	AM36M/2 CORE	AM36M/3 CORE	AM36M/3 CORE
SiO_2	53,65	52,31	52,24	52,33	53,50	52,73	52,87
TiO_2	0,32	0,32	0,55	0,49	0,30	0,34	0,40
Al_2O_3	0,88	1,73	0,72	0,72	0,92	1,65	1,57
FeO	17,05	7,18	21,47	20,71	15,87	7,34	8,04
MnO	0,38	0,20	0,42	0,38	0,37	0,22	0,25
MgO	23,98	18,01	21,22	21,59	24,90	18,10	18,35
CaO	4,85	18,43	3,93	4,19	5,23	19,01	18,35
Na_2O	0,07	0,21	0,09	0,10	0,08	0,23	0,25
Cr_2O_3	0,04	0,41	0,05	0,01	0,05	0,29	0,29
TOTAL	101,22	98,80	100,69	100,52	101,22	99,91	100,37
Recalculated as cations per 6 oxygens (Z=2)							
Si	1,951	1,942	1,948	1,949	1,939	1,939	1,938
Al	0,039	0,058	0,032	0,032	0,039	0,061	0,062
Ti	0,010	-	0,015	0,014	0,008	-	-
Fe^{3+}	-	-	0,005	0,005	0,014	-	-
Ti	-	0,009	-	-	-	0,010	0,011
Al	-	0,018	-	-	-	0,011	0,006
Fe	0,519	0,223	0,665	0,640	0,467	0,226	0,247
Mn	0,012	0,006	0,013	0,012	0,011	0,007	0,008
Mg	1,300	0,997	1,179	1,198	1,345	0,992	1,003
Ca	0,189	0,733	0,157	0,167	0,203	0,749	0,721
Na	0,005	0,015	0,007	0,007	0,006	0,016	0,018
Cr	0,001	0,012	0,001	-	0,001	0,008	0,030
X+Y	2,026	2,013	2,022	2,024	2,033	2,019	2,044
At% Mg	64,75	51,04	58,79	59,61	66,28	50,43	50,89
Fe	25,83	11,41	33,38	32,08	23,71	11,48	12,52
Ca	9,42	37,55	7,83	8,31	10,01	38,09	36,59

6.4 Feldspars

The minerals of the feldspar group are framework silicates, in which small, highly-charged cations in tetrahedral co-ordination with oxygen form the basic structure. Large, irregular cavities in the tetrahedral framework are filled by univalent or divalent cations of radius close to or greater than 1,0Å. The general formula is MT_4O_8, where the T site is filled primarily by Al and Si, with minor substitutions of B, Ga, Ge and Fe^{3+} (Smith, 1975). The stoichiometry of the tetrahedral group changes from $AlSi_3$ in the alkali feldspars (including albite) to Al_2Si_2 for calcic plagioclase (anorthite). The M group in the general formula is filled by Na, K, Ca, Rb, Sr, Pb, Ba and NH_4 (Smith, op. cit.), the most important being Na, K, and Ca. Other elements which might enter the feldspar structure are Fe^{2+}, Mg, Ti and P. This latter group of elements Smith regards as capable of entering either the M or the T sites.

Fifty microprobe analyses of plagioclase feldspars presented in table 1.3 span ten basalt samples, representing three of the basalt units at Brosterlea, namely the Perdekop Unit (AM28, AM40), the Vaalkop Unit (AM13, AM30 and AM44), and the Roodehoek Unit (AM21, AM22, AM23, AM25 and AM36M). Each of the plagioclase analyses has been recalculated in terms of cations per 32 oxygens, and also in terms of the end members albite, anorthite and orthoclase (molecular %). The plagioclase compositions in terms of the end members are plotted in Fig. 14.

The Brosterlea plagioclases are predominantly labradoritic, ranging into the field of sodic bytownite. The compositional range for each of the basalt units is as follows : Vaalkop Unit $An_{48,5-71,6}$; Roodehoek Unit An_{43-78}; Perdekop Unit An_{47-73}.

It would appear that in rocks where plagioclase occurs as a phenocryst phase (AM13, AM30, AM44, AM21 and AM22), the compositional range of the plagioclase is more restricted

than in cases where the analysed plagioclase is a groundmass phase. This effect may be a function of the limited number of analyses for certain of the rocks. If, however, it is a true reflection of the actual situation, the implication is that either the phenocrystic plagioclase was in continuous equilibrium with the melt up to the time the rock was quenched, or that the phenocrysts cooled too fast for zoning to be established (Evans and Moore, 1968). The groundmass plagioclase, on the other hand, is the product of non-equilibrium crystallisation and changing magma composition, which gave rise to zoning.

In Fig. 15, the Brosterlea plagioclases are plotted in terms of orthoclase vs. anorthite (molecular %). On the basis of this diagram, the various basalt units can be separated in terms of the orthoclase content of their plagioclases.

A very similar plot to Fig. 15, in this case for plagioclases of the Makaopuhi tholeiitic lava lake in Hawaii, is to be found in Evans and Moore (1968, Fig. 13). The most potassic of the Makaopuhi plagioclases are those found furthest from the chill zones of the lava lake, i.e. those expected to be most nearly in equilibrium with the coexisting melt phase. Comparison of the Makaopuhi plagioclase analyses with their host rock compositions (Moore and Evans, 1967) indicates no apparent compositional control by the parent melt on the K-content of the plagioclases. The K-content of the Brosterlea plagioclases, in contrast, is directly related to melt composition, in such a way that the Vaalkop Unit, with a relatively high bulk rock K_2O content, contains relatively potassic plagioclase, whilst the low-K basalts of the Roodehoek Unit contain potassium-poor plagioclase. The Perdekop Unit trend falls between these two extremes (Fig. 15). The average bulk rock K_2O content of the basalt units is tabulated in Fig. 13.

Unit	Bulk Rock		Feldspar	
	Average	Range	Average	Range
Roodehoek	0,42	0,27-0,76	0,14	0,07-0,39
Perdekop	0,69	0,67-0,71	0,22	0,06-0,38
Vaalkop	1,09	0,82-1,45	0,27	0,13-0,47

Fig. 13 : K_2O contents of feldspars and parent rock types (wt.% K_2O).

On the basis of available evidence, the orthoclase content of the Brosterlea plagioclases is a distribution coefficient effect, reflecting the K_2O content of the parent melts, assuming, that is, that the distribution coefficient is effectively the same for each of the basalt units. It should be noted that the high-K plagioclases of the Vaalkop Unit are the least zoned of the Brosterlea plagioclases, and might therefore be expected to be products of near-equilibrium crystallisation, which is in accord with the findings of Evans and Moore (op. cit.) in the Makaopuhi context. The plagioclases of sample AM36M are represented separately from the rest of the Roodehoek Unit on Fig. 15, because they do not tie in with the general pattern. This is a further manifestation of the unusual nature of the rock, as already displayed by the olivines.

Al_2O_3, SiO_2 and TiO_2 (weight percent) are plotted against molecular percent albite in Fig. 16. The SiO_2 values are more or less in accord with the values listed by Winchell (1961), but the Al contents are below the expected values by approximately 1%. The implication of this is that other elements are substituting for Al in the tetrahedral group. The strong correlation between the slopes of SiO_2 and TiO_2 indicates that Ti is entering the tetrahedral sites. Some labradorites analysed by Ribbe and Smith (1966) contained up to 0,06 weight % TiO_2, which is about the average value for the Brosterlea plagioclase, maximum TiO_2 contents of which reach 0,12%.

Although most of the Fe in alkali feldspar is probably present as Fe^{3+}, replacing Al, the situation is complicated in the case of plagioclase by a tendency for Fe^{2+} to enter the structure as well as Fe^{3+}. The terrestrial Fe^{2+}/Fe^{3+} ratio appears to vary about a mean value in the region of unity (Smith, 1975). On this evidence, the amount of Fe available for replacement of Al in the Brosterlea plagioclases is variable up to a value of something less than 1%.

Magnesium may enter either the M or the T sites in feldspar (Drake and Weill, 1970; Smith, 1975), but its distribution is uncertain. The MgO content of the Brosterlea plagioclases varies between 0,06 and 0,32%.

On the basis of available evidence, Fe and Mg must be considered the most important elements proxying for Al in the T sites of the Brosterlea plagioclases, with minor contributions from Ti and any other minor elements which might be present.

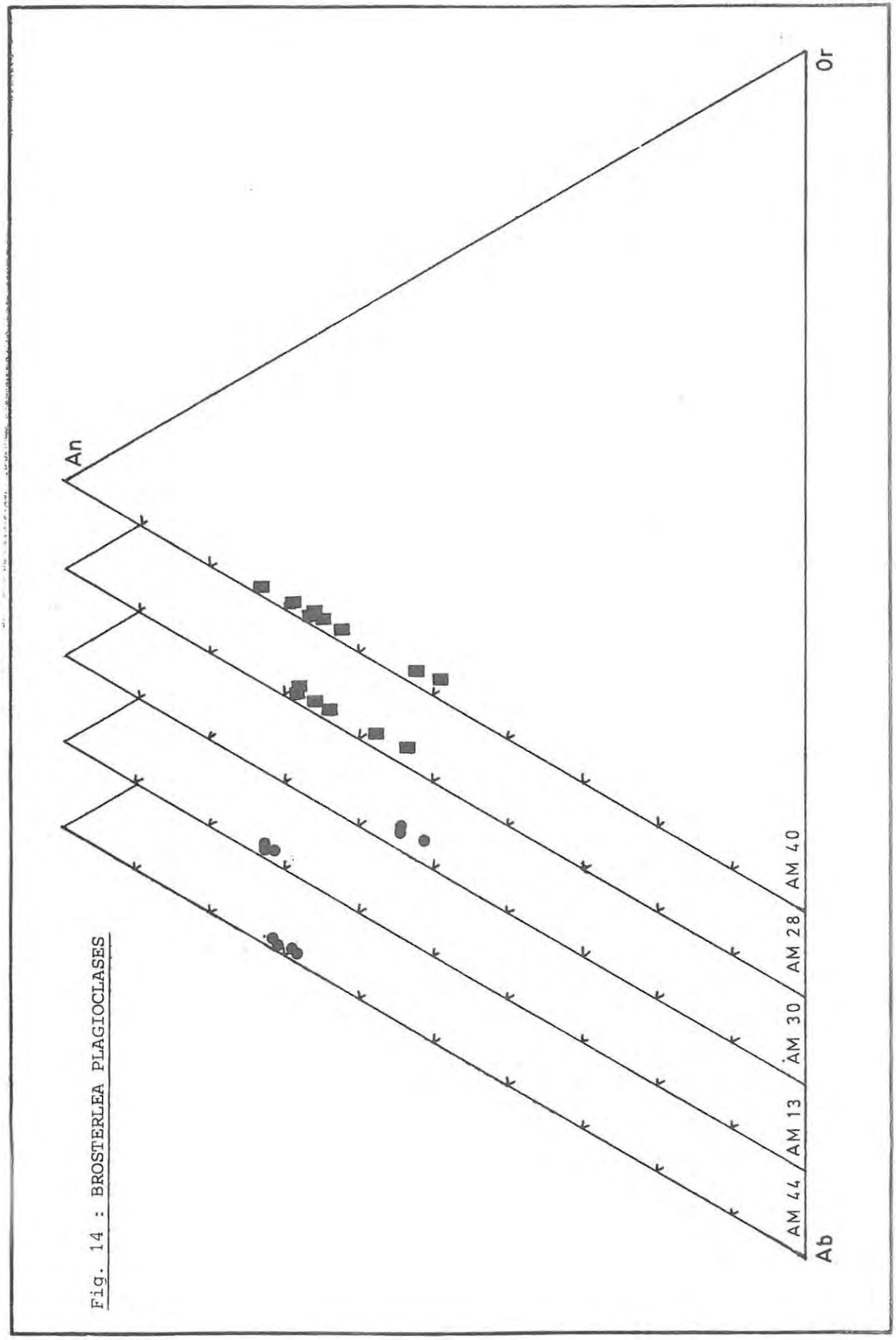

Fig. 14 : BROSTERLEA PLAGIOCLASES

Fig. 14 : BROSTERLEA PLAGIOCLASES

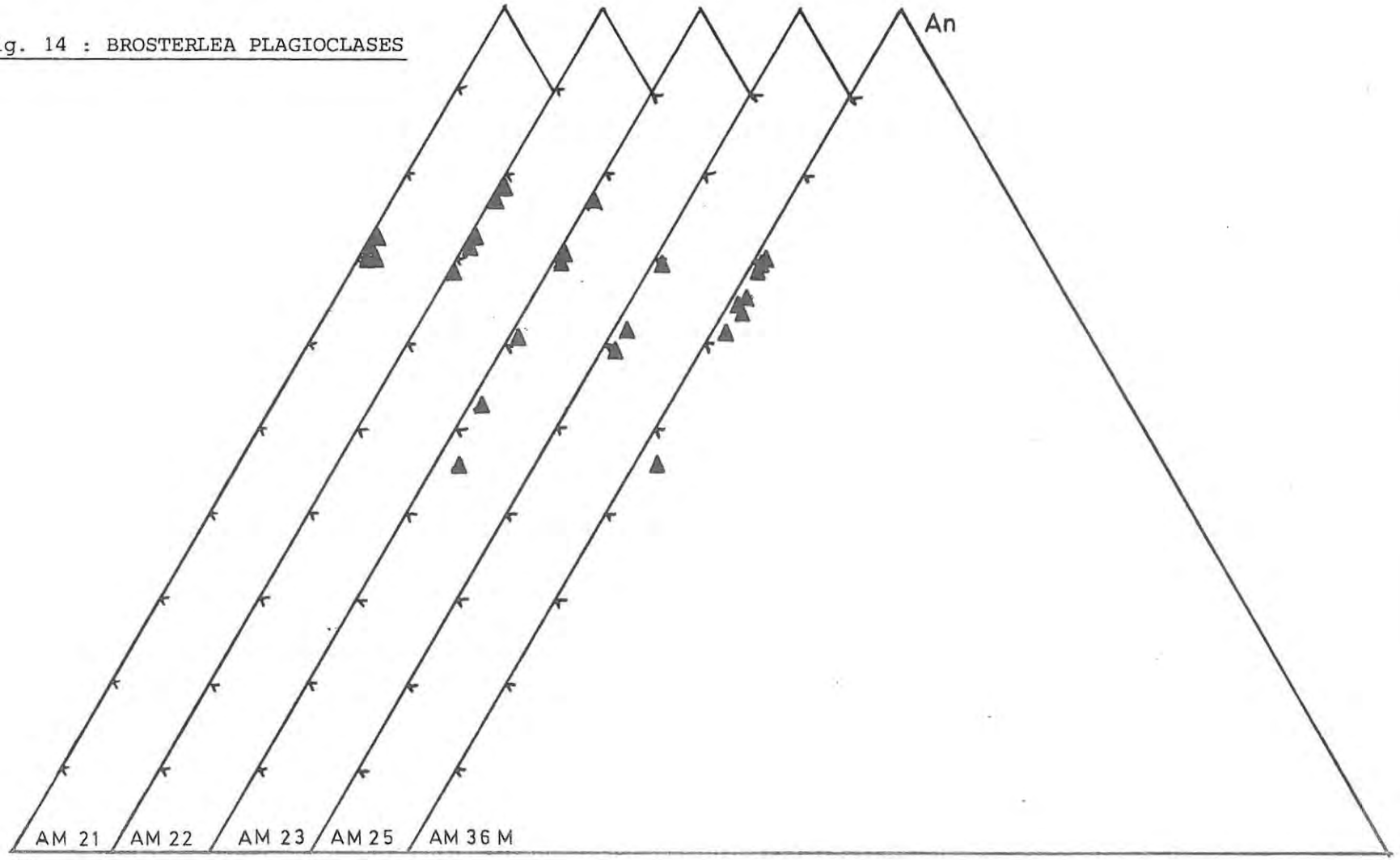

Fig. 15 : DIAGRAM SHOWING VARIATION OF MOLECULAR % ORTHOCLASE WITH MOLECULAR % ANORTHITE FOR THE BROSTERLEA PLAGIOCLASES

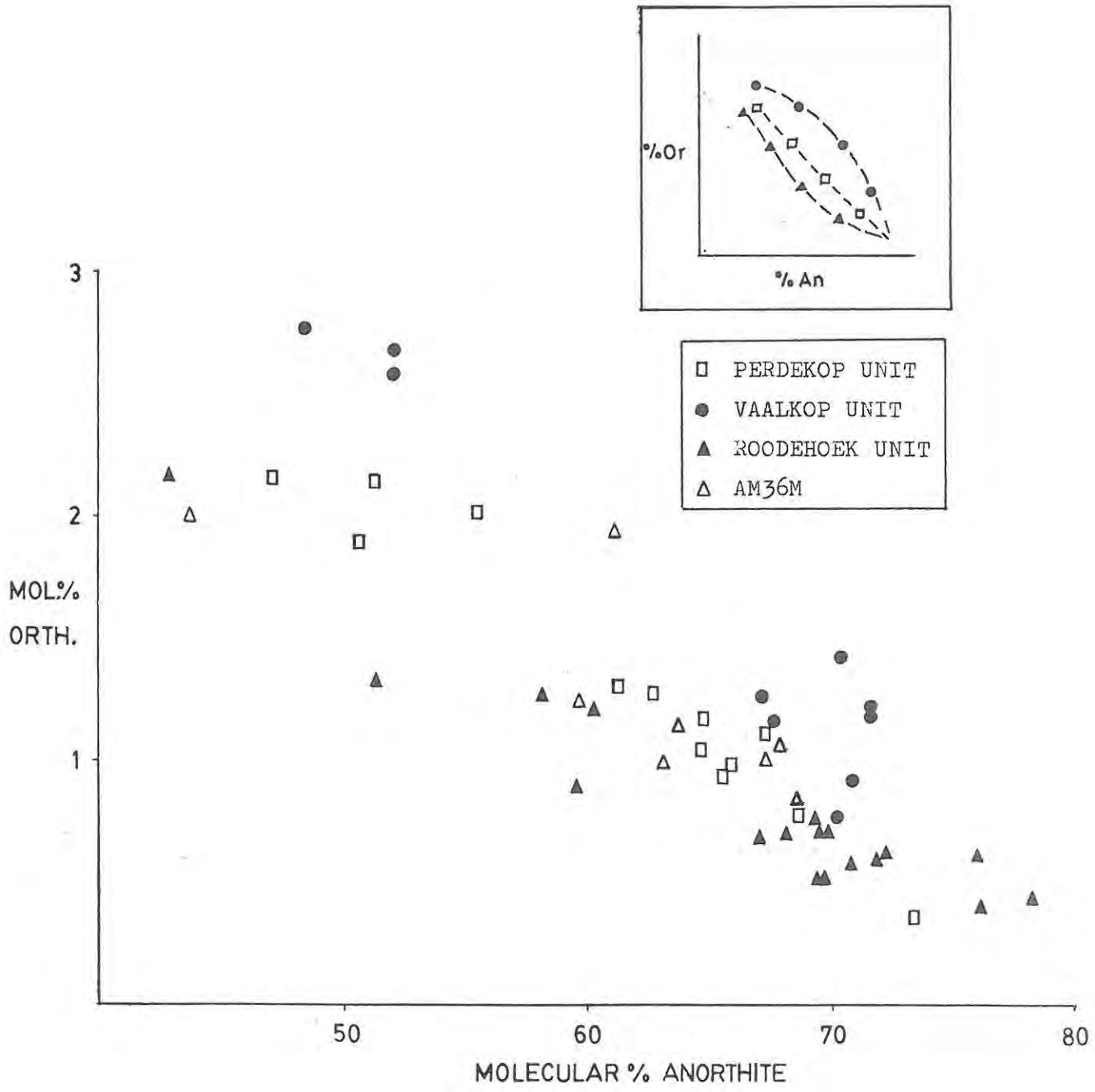

Fig. 16 : VARIATION OF WEIGHT % SiO_2, Al_2O_3 AND TiO_2 WITH INCREASING MOLECULAR % ALBITE

(Broken lines represent Winchell's (1961) values for SiO_2 and Al_2O_3 in plagioclase)

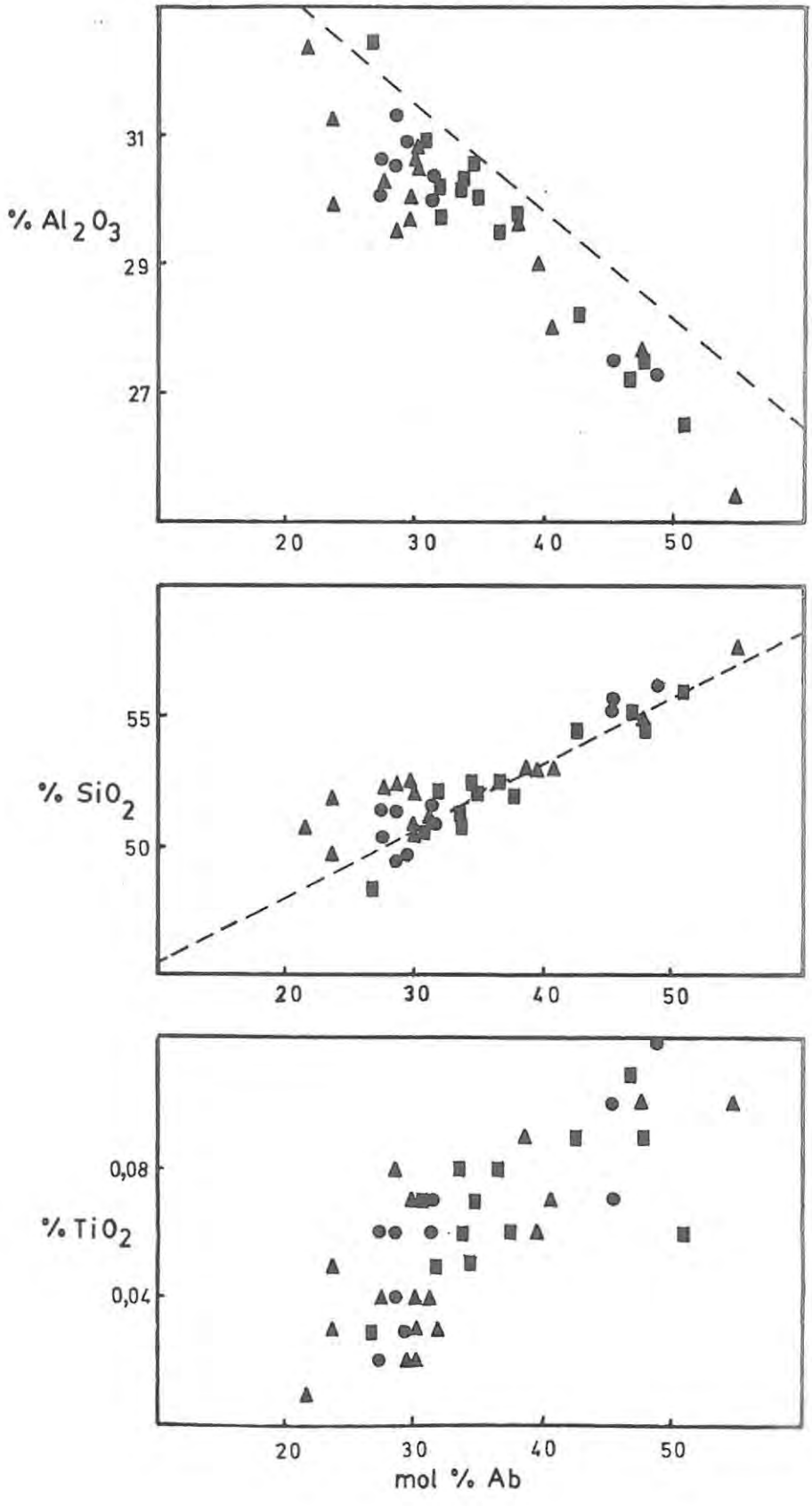

TABLE 1.3 PLAGIOCLASE ANALYSES BY MICROPROBE

Vaalkop Unit

	AM44/1 CORE	AM44/1 MARGIN	AM44/2 CORE	AM44/3 CORE	AM13/1 CORE	AM13/1 MARGIN
SiO_2	49,32	49,61	51,54	50,84	51,38	50,36
TiO_2	0,04	0,03	0,06	0,07	0,06	0,06
Al_2O_3	31,32	30,87	29,97	30,36	30,54	30,61
FeO	0,39	0,41	0,31	0,55	0,34	0,39
MgO	0,18	0,19	0,29	0,12	0,30	0,31
CaO	14,62	14,43	13,82	13,95	14,10	13,73
Na_2O	3,23	3,32	3,53	3,60	3,11	2,89
K_2O	0,16	0,13	0,20	0,22	0,24	0,19
TOTAL	99,26	98,99	99,72	99,71	100,07	98,54
Recalculated as cations per 32 oxygens						
Si	9,137	9,207	9,464	9,363	9,350	9,296
Al	6,840	6,753	6,486	6,591	6,550	6,660
Ti	0,006	0,004	0,009	0,010	0,009	0,009
Fe	0,060	0,064	0,047	0,085	0,052	0,060
Mg	0,050	0,052	0,079	0,033	0,081	0,085
Ca	2,902	2,869	2,719	2,753	2,749	2,715
Na	0,846	0,872	0,916	0,938	1,098	1,034
K	0,019	0,031	0,046	0,051	0,055	0,044
SUM	19,860	19,852	19,766	19,824	19,944	19,903
Mol% An	70,78	70,07	67,59	67,31	70,44	71,55
Ab	28,29	29,17	31,25	31,43	28,13	27,27
Or	0,93	0,76	1,16	1,26	1,43	1,18

TABLE 1.3 PLAGIOCLASE ANALYSES BY MICROPROBE

	Vaalkop Unit				Perdekop Unit	
	AM13/2 CORE	AM30/1 CORE	AM30/2 CORE	AM30/3 CORE	AM28/1 CORE	AM28/1 MARGIN
SiO_2	51,38	55,62	56,18	55,28	52,40	52,52
TiO_2	0,02	0,10	0,12	0,07	0,05	0,08
Al_2O_3	30,05	27,53	27,28	27,50	30,50	29,49
FeO	0,38	0,54	0,58	0,55	0,60	0,71
MgO	0,28	0,17	0,10	0,18	0,23	0,11
CaO	13,73	10,86	9,77	10,68	13,06	12,67
Na_2O	2,89	5,20	5,43	5,13	3,79	4,02
K_2O	0,20	0,45	0,47	0,46	0,20	0,22
TOTAL	98,93	100,47	99,93	99,85	100,83	99,82
Recalculated as cations per 32 oxygens						
Si	9,434	10,013	10,131	10,010	9,446	9,545
Al	6,502	5,842	5,800	5,869	6,491	6,331
Ti	0,003	0,014	0,016	0,010	0,007	0,011
Fe	0,059	0,081	0,088	0,084	0,091	0,108
Mg	0,076	0,045	0,027	0,049	0,062	0,030
Ca	2,701	2,096	1,888	2,072	2,523	2,473
Na	1,028	1,815	1,899	1,802	1,324	1,421
K	0,046	0,104	0,108	0,107	0,046	0,050
SUM	19,849	20,010	19,957	20,003	19,990	19,969
Mol% An	71,54	52,20	48,47	52,05	64,82	62,70
Ab	27,23	45,22	48,75	45,27	34,01	36,02
Or	1,23	2,58	2,78	2,68	1,17	1,28

TABLE 1.3 PLAGIOCLASE ANALYSES BY MICROPROBE

Perdekop Unit

	AM28/2 CORE	AM28/2 MARGIN	AM28/3 CORE	AM28/3 MARGIN	AM40/1 CORE	AM40/1 MARGIN
SiO_2	54,50	55,28	52,15	51,65	50,57	54,52
TiO_2	0,09	0,11	0,05	0,07	0,07	0,09
Al_2O_3	28,22	27,72	29,72	30,09	30,87	27,57
FeO	0,65	0,71	0,54	0,69	0,54	0,68
MgO	0,08	0,11	0,19	0,13	0,13	0,13
CaO	11,46	10,51	13,43	13,41	13,59	10,14
Na_2O	4,86	5,29	3,49	3,47	3,35	5,40
K_2O	0,35	0,37	0,19	0,16	0,13	0,33
TOTAL	100,21	100,10	99,76	99,67	99,25	98,86
Recalculated as cations per 32 oxygens						
Si	9,858	9,987	9,520	9,433	9,328	10,055
Al	6,017	5,903	6,395	6,478	6,712	5,993
Ti	0,012	0,015	0,007	0,010	0,010	0,012
Fe	0,098	0,108	0,082	0,105	0,083	0,105
Mg	0,022	0,029	0,052	0,035	0,035	0,024
Ca	2,222	2,034	2,627	2,624	2,686	2,004
Na	1,704	1,854	1,235	1,229	0,873	1,410
K	0,080	0,085	0,044	0,037	0,031	0,078
SUM	20,013	20,015	19,962	19,952	19,758	19,681
Mol% An	55,45	51,20	67,26	67,45	68,60	50,59
Ab	42,54	46,67	31,62	31,59	30,61	47,51
Or	2,01	2,13	1,12	0,96	0,79	1,90

TABLE 1.3 PLAGIOCLASE ANALYSES BY MICROPROBE

Perdekop Unit

	AM40/2 CORE	AM40/2 MARGIN	AM40/3 CORE	AM40/3 CORE	AM40/4 CORE	AM40/4 MARGIN
SiO_2	48,32	56,05	51,89	51,13	50,74	51,93
TiO_2	0,03	0,06	0,07	0,06	0,08	0,06
Al_2O_3	32,43	26,55	29,89	30,28	30,14	29,79
FeO	0,46	0,65	0,45	0,59	0,52	0,66
MgO	0,16	0,06	0,20	0,14	0,18	0,14
CaO	14,98	9,87	13,11	13,15	13,55	12,82
Na_2O	2,97	5,90	3,94	3,70	3,77	4,31
K_2O	0,06	0,38	0,18	0,16	0,17	0,23
TOTAL	99,41	99,52	99,73	99,21	99,15	99,94
Recalculated as cations per 32 oxygens						
Si	8,946	10,264	9,522	9,435	9,392	9,535
Al	7,078	5,700	6,468	6,587	6,576	6,446
Ti	0,004	0,009	0,010	0,009	0,011	0,009
Fe	0,071	0,099	0,069	0,091	0,050	0,039
Mg	0,045	0,017	0,055	0,039	0,050	0,039
Ca	2,971	1,937	2,578	2,600	2,687	2,522
Na	0,779	1,527	1,023	0,965	0,988	1,119
K	0,013	0,088	0,042	0,038	0,040	0,053
SUM	19,907	19,641	19,767	19,764	19,794	19,760
Mol% An	73,34	47,00	64,10	65,64	65,85	61,35
Ab	26,30	50,85	34,85	33,42	33,17	37,34
Or	0,36	2,15	1,05	0,94	0,98	1,31

TABLE 1.3 PLAGIOCLASE ANALYSES BY MICROPROBE

Roodehoek Unit

	AM23/1 CORE	AM23/1 MARGIN	AM23/2 CORE	AM23/2 MARGIN	AM23/3 CORE	AM23/3 MARGIN
SiO_2	51,01	52,95	54,90	57,61	49,61	50,58
TiO_2	0,04	0,06	0,10	0,10	0,03	0,07
Al_2O_3	30,60	29,04	27,64	25,40	31,19	30,47
FeO	0,50	0,74	0,55	0,66	0,55	0,62
MgO	0,20	0,14	0,11	0,09	0,19	0,18
CaO	14,14	12,64	10,98	9,21	15,40	14,07
Na_2O	3,35	4,60	5,58	6,50	2,64	3,36
K_2O	0,09	0,16	0,24	0,39	0,07	0,09
TOTAL	99,93	100,33	100,10	99,96	99,68	99,44
Recalculated as cations per 32 oxygens						
Si	9,356	9,679	10,021	10,494	9,146	9,332
Al	6,615	6,265	5,947	5,453	6,778	6,626
Ti	0,006	0,009	0,014	0,014	0,004	0,010
Fe	0,077	0,113	0,084	0,101	0,085	0,095
Mg	0,055	0,038	0,030	0,024	0,052	0,050
Ca	2,778	2,476	2,148	1,797	3,042	2,782
Na	0,868	1,188	1,441	1,675	0,689	0,876
K	0,022	0,037	0,055	0,090	0,016	0,020
SUM	19,777	19,805	19,740	19,648	19,812	19,791
Mol% An	69,62	59,75	51,39	42,96	76,05	69,46
Ab	29,85	39,34	47,27	54,87	23,54	30,01
Or	0,53	0,91	1,34	2,17	0,41	0,53

TABLE 1.3 PLAGIOCLASE ANALYSES BY MICROPROBE

Roodehoek Unit

	AM21/1 CORE	AM21/1 MARGIN	AM21/2 CORE	AM21/2 MARGIN	AM22/1 CORE	AM22/1 MARGIN
SiO_2	52,19	52,21	52,91	52,21	52,37	52,32
TiO_2	0,02	0,04	0,03	0,02	0,08	0,03
Al_2O_3	30,01	30,20	29,67	30,81	29,52	30,27
FeO	0,52	0,55	0,40	0,40	0,46	0,60
MgO	0,30	0,29	0,30	0,28	0,30	0,32
CaO	14,26	14,52	13,75	13,96	13,75	13,11
Na_2O	3,34	3,05	3,27	3,30	3,06	3,43
K_2O	0,12	0,10	0,13	0,12	0,09	0,11
TOTAL	100,76	100,96	100,46	101,10	99,63	100,19
Recalculated as cations per 32 oxygens						
Si	9,438	9,421	9,391	9,560	9,380	9,479
Al	6,397	6,423	6,532	6,319	6,232	6,464
Ti	0,003	0,005	0,003	0,004	0,011	0,004
Fe	0,078	0,084	0,061	0,061	0,069	0,089
Mg	0,080	0,078	0,075	0,080	0,080	0,086
Ca	2,764	2,807	2,690	2,662	2,639	2,545
Na	1,172	1,067	1,150	1,147	1,063	1,204
K	0,028	0,024	0,028	0,030	0,022	0,026
SUM	19,960	19,909	19,930	18,863	19,496	19,897
Mol% An	69,73	72,01	69,54	69,35	70,87	67,42
Ab	29,56	27,37	29,73	29,86	28,55	31,89
Or	0,71	0,62	0,73	0,79	0,58	0,69

TABLE 1.3 PLAGIOCLASE ANALYSES BY MICROPROBE

Roodehoek Unit

	AM22/2 CORE	AM22/2 MARGIN	AM22/3 CORE	AM25/1 CORE	AM25/2 CORE	AM25/3 CORE
SiO_2	51,93	51,44	50,70	51,10	52,95	53,01
TiO_2	0,05	0,04	0,01	0,04	0,07	0,09
Al_2O_3	29,87	30,99	32,35	30,16	27,98	29,60
FeO	0,50	0,48	0,40	0,70	0,68	1,02
MgO	0,25	0,27	0,27	0,23	0,13	0,14
CaO	15,09	14,49	15,73	13,85	11,71	12,15
Na_2O	2,57	3,08	2,40	3,51	4,51	4,28
K_2O	0,10	0,10	0,08	0,12	0,22	0,21
TOTAL	100,36	100,89	101,94	99,71	98,25	100,50
Recalculated as cations per 32 oxygens						
Si	9,427	9,294	9,085	9,353	9,778	9,592
Al	6,392	6,599	6,833	6,507	6,089	6,313
Ti	0,007	0,005	0,001	0,006	0,010	0,012
Fe	0,076	0,073	0,060	0,107	0,105	0,154
Mg	0,068	0,073	0,072	0,063	0,036	0,038
Ca	2,936	2,806	3,020	2,717	2,317	2,356
Na	0,905	1,079	0,833	1,245	1,616	1,503
K	0,024	0,024	0,017	0,029	0,051	0,048
SUM	19,835	19,887	19,921	20,027	20,002	20,016
Mol% An	75,95	71,78	78,03	68,08	58,16	60,32
Ab	23,43	27,61	21,53	31,20	40,56	38,46
Or	0,62	0,61	0,44	0,72	1,28	1,22

TABLE 1.3 PLAGIOCLASE ANALYSES BY MICROPROBE

Roodehoek Unit

	AM36M/1 CORE	AM36M/1 MARGIN	AM36M/2 CORE	AM36M/2 MARGIN	AM36M/3 CORE	AM36M/3 MARGIN	AM36M/4 CORE	AM36M/4 MARGIN
SiO_2	52,36	54,22	51,81	54,39	51,49	50,98	50,13	52,04
TiO_2	0,05	0,11	0,08	0,13	0,07	0,07	0,06	0,08
Al_2O_3	28,89	27,91	30,31	28,40	30,56	30,55	31,09	29,57
FeO	0,62	0,71	0,62	0,68	0,63	0,76	0,60	0,49
MgO	0,15	0,11	0,15	0,12	0,11	0,11	0,13	0,11
CaO	12,08	8,79	13,02	12,61	13,50	13,79	13,91	12,63
Na_2O	4,34	6,05	3,94	4,21	3,49	3,49	3,42	3,98
K_2O	0,21	0,34	0,20	0,34	0,17	0,18	0,14	0,17
TOTAL	98,70	98,24	100,13	100,88	100,02	99,93	99,48	99,07
Recalculated as cations per 32 oxygens								
Si	9,699	10,051	9,476	9,853	9,426	9,363	9,250	9,599
Al	6,301	5,949	6,524	6,064	6,574	6,613	6,750	6,401
Ti	0,007	0,016	0,011	0,017	0,010	0,010	0,009	0,011
Fe	0,096	0,110	0,095	0,103	0,088	0,117	0,093	0,075
Mg	0,041	0,030	0,041	0,033	0,030	0,030	0,035	0,030
Ca	2,398	1,746	2,555	2,448	2,648	2,714	2,750	2,496
Na	1,138	1,586	1,020	1,078	0,904	0,907	0,891	1,037
K	0,049	0,080	0,046	0,078	0,040	0,042	0,033	0,040
SUM	19,729	19,568	19,768	19,674	19,720	19,796	19,811	19,689
Mol% An	59,85	43,64	63,88	61,11	67,44	67,86	68,63	63,05
Ab	38,90	54,36	34,97	36,93	31,55	31,08	30,55	35,95
Or	1,25	2,00	1,15	1,96	1,01	1,06	0,82	1,00

7. MAJOR ELEMENT GEOCHEMISTRY

7.1 Introduction

Major element analyses are presented for 33 basalts and five associated dolerites from the Brosterlea and Modderfontein central vent complexes (Table 3). The analyses were performed by X-ray fluorescence spectrometry, analytical techniques and spectrometer settings for which are described in appendix 3.

All major element data used in the following discussion are anhydrous values, normalised to 100%. (H_2O^+ and L.O.I. inclusive analyses are provided in appendix 5.) Total Fe was determined as Fe_2O_3 in accordance with the rationale of Norrish and Chappel (1969). In the norm calculations, an Fe_2O_3/FeO ratio of 0,2 was used, in keeping with previous work in this department by Robey (1976), Pemberton (1978), and Rumble (1979). The normative chemistry is expressed as C.I.P.W. weight % norms.

7.2 The Classification of Basalts

Kennedy (1933) recognised the existence of two primary basalt magma types : "olivine basalt magma", which is the parent magma to an alkaline line of magmatic descent with trachyte and phonolite as the ultimate derivatives; and a "tholeiitic" magma type, which is parental to a more siliceous differentiation sequence, ending in rhyolite. This latter trend Kennedy equated with the calc-alkali series. Tilley (1950) agreed with Kennedy's concept of the calc-alkaline trend as a tholeiitic derivative. Tilley (op. cit.) altered the name of Kennedy's "olivine basalt" to "alkali olivine basalt". Kuno (1960) postulated the existence of a third primary basalt magma, which he termed "high alumina basalt". This third basalt type Kuno defined from analyses of Japanese, Korean and Manchurian basalts. Yoder and Tilley (1962) are not in agreement with Kuno as regards the existence of this third basalt type, and work by Pemberton (1978) and by the present writer casts

serious doubt on the existence of high alumina basalt, as such, in the Southern Karoo igneous province.

Yoder and Tilley (1962) provide a simple scheme of basalt classification, based on normative mineralogy. The five basalt types in this system of classification are as follows :

1. Tholeiite (oversaturated) - normative quartz and hypersthene.
2. Tholeiite (saturated; hypersthene basalt) - normative hypersthene.
3. Olivine tholeiite (undersaturated) - normative hypersthene and olivine.
4. Olivine basalt - normative olivine.
5. Alkali basalt - normative olivine and nepheline.

Within the framework of the Yoder and Tilley classification scheme, thirty-two of the Brosterlea and Modderfontein basalts and dolerites are oversaturated tholeiites, the remaining six being olivine tholeiites. Of the six olivine tholeiites, one, AA-21, is a dolerite, of particular note for its curious composition, having no potassium in the analysis, and yielding a value of 18% normative olivine. The case of AM36M, one of the olivine tholeiite basalts, has been discussed earlier in this thesis, in the chapter on mineralogy. The possibility has been mooted that this rock contains cumulus olivine, which would upset the bulk rock chemistry, and thus the normative calculations. Cox and Hornung (1966) consider the possibility that olivine-normative basalts within the Karoo province contain cumulus olivine, and a recent paper by Eales and Marsh (1979) indicates the probability that high-Mg basalts (which by their very nature generate normative olivine) are derivatives, by olivine enrichment, of "normal" Karoo magma. On the basis of these arguments, it is considered likely that the standard

Karoo basalt is an oversaturated tholeiite, and that the small percentage of olivine tholeiites in the Karoo province are the products of olivine enrichment.

Irvine and Baragar (1971) make use of a plot of weight percent $Na_2O + K_2O$ vs. SiO_2 for the purpose of chemical classification of basalts. This is the same diagram as is used by MacDonald (1968) and by Kuno (1968), except that Irvine and Baragar do not recognise the high-Al basalt field defined by Kuno (op. cit.). The dividing line between alkalic and tholeiitic rocks from Hawaii (MacDonald, op. cit.) is slightly lower down the $Na_2O + K_2O$ axis than the curved dividing line defined by Irvine and Baragar (op. cit.). Most of the Brosterlea basalts fall well within the subalkaline field, whichever of the two dividing lines is used (Fig. 17). This is further proof of the distinctly tholeiitic nature of the basalts in the present study.

7.3 The Basalt Tetrahedron

Compositional differences within the basalt series at Brosterlea and Modderfontein are reflected in their normative mineralogy. Approximate phase relations for these rocks may be inferred with the aid of the pseudoquaternary basalt tetrahedron of Yoder and Tilley (1962). Fig. 18 (a, b and c) shows the normative compositions of the Brosterlea and Modderfontein basalts and dolerites projected from the plagioclase and olivine coigns of the tetrahedron. The end-members of the quaternary system Pl - Di - Ol - Q were recalculated from the C.I.P.W. norms by the method of Cox and Hornung (1966). It is clear, as pointed out by Cox and Hornung, that the projections in Fig. 18 do not completely represent the bulk compositions of the basalts, since there is no provision for the representation of magnetite or apatite, which may quite reasonably be inferred to be cotectic phases with olivine and plagioclase, although they only occur in minor amounts.

The Roodehoek Unit basalts (Fig. 18a) trend along a very definite olivine-plagioclase control line, with a neg-

ligible component of diopside. AM36M, an olivine cumulate rock, is distinctive in being perceptibly closer to the olivine composition point than the balance of the Roodehoek rocks.

The Vaalkop Unit lavas show a separate trend compatible with the entry of clinopyroxene as a liquidus phase (Fig. 18b), and ultimately cross the divarient line Ol+Di+Pl+Liq. into the primary phase field of enstatite.

The paucity of data for the other units excludes the possibility of any further definite trends being identified, and only very general comments can be made about the balance of the Brosterlea and Modderfontein rocks. The Lesotho-type basalts of the Perdekop Unit, together with the uppermost basalt flow at Modderfontein, are displaced slightly to the left of the field defined by Cox and Hornung (1966) for the basalts of central Lesotho (Fig. 18c). The Modderfontein dolerites and the dolerite of the radial dyke system at Brosterlea plot very close to the Lesotho-type lavas. The lower lavas from the sequence at Modderfontein plot in a very similar position to the Kraai River Formation basalts (Pemberton, 1978) on the plagioclase projection of the basalt tetrahedron. The late-stage "Dragon's Back" intrusion also plots very close to the Kraai River Formation field. The dolerite from the Brosterlea ring dyke (AA-21) plots very close to the plagioclase and olivine composition points, and is uncommonly low in normative silica (Fig. 18c). The early lavas from Tafelkop in the Brosterlea complex show a wide scatter of normative compositions, and very little can be inferred about them.

The basalts and dolerites of this study straddle the diopside - enstatite join, regarded by Boyd and England (1961) as a thermal barrier operative at pressures greater than 10kb. The inference from this is that the Brosterlea and Modderfontein basalts achieved their present compositions by fractionation at pressures lower than 10 kb.

Of the various data included on the basalt tetrahedra (Fig. 18), the field of the Central Lesotho basalts is as defined by Cox and Hornung (1966), the Kraai River field is from Pemberton (1978), and the Ol+Di+Pl+Liq. devariant line is from Osborne and Tait (1952).

7.4 The AFM Diagrams

Working from analyses from Walker and Poldervaart (1949), Nockolds and Allen (1956) recognised three AFM trends in the Karoo dolerites :

(i) The Main trend, to which the majority of the rocks conform, characterised by slight absolute iron enrichment.

(ii) An iron-rich trend, best seen in the rocks of Elephant's Head and New Amalfi, with considerable iron enrichment.

(iii) A third trend, for which relatively few analyses are available. This trend shows no absolute iron enrichment.

From Fig. 19 it is clear that at least the Vaalkop Unit, and possibly also the Roodehoek Unit to a certain extent, follow the unusual "third trend" of Nockolds and Allen (op. cit.). The Roodehoek Unit, however, does seem to have some affinity for the "main trend" (Fig. 19a).

As far as the other units are concerned, the paucity of data restricts any definite interpretations. The same restrictions apply to the dolerites, except that AA-23 (the Dragon's Back) plots in a fairly advanced position along the iron-enrichment trend enjoyed by Elephant's Head and New Amalfi (Fig. 19c).

7.5 Discriminant Analysis

Using a stepwise discriminant analysis programme, Dr. A.R. Duncan of U.C.T. has determined two discriminant

functions, F_1 and F_2, which give the most satisfactory separation of the a priori groupings of the various groupings of the Karoo lavas of the north-eastern Cape, as originally determined by Robey (1976) and Pemberton (1978). The application of the discriminant functions derived from Robey's and Pemberton's data to the Brosterlea and Modderfontein suites yields the results represented diagrammatically in Fig. 20.

Although the significance of the variations between the groupings in Fig. 20 has not been determined quantitatively, a visual inspection of the emergent patterns offers some useful qualitative information : There is a very clear separation of the Roodehoek, Vaalkop and Strypoort Units. The separation of the Roodehoek and Perdekop Units, on the other hand, is not very definite, but this simply bears out similar conclusions to be drawn from an inspection of the SiO_2 variation diagrams. There appears to be some affinity between the Strypoort Unit and the Drumbo Basalt Member, although, as previously pointed out, no quantitative estimate of the significance of this affinity is available. Similarly, both the Roodehoek Unit and the Perdekop Unit plot close to the field of the Lesotho Formation, as do various basalts and dolerites of the Molteno district which have been tentatively correlated with the Lesotho Formation. It is encouraging that a plot of the average Omega Formation falls in the centre of the Roodehoek field, which tends to enhance the case for correlation of the two groups.

The discriminant analysis shows the affinity of the Vaalkop Unit for the Kraai River Formation. The major difference between these two units is in their SiO_2 contents, a factor not taken into account in the discriminant analysis. The Dragon's Back dyke (sample AA-23) plots very close to the Lesotho Formation in terms of the discriminant functions F_1 and F_2. This apparent similarity is, however, misleading, in that the Dragon's Back is distinct from the Lesotho Formation in certain aspects of its chemistry, most particularly its SiO_2 content, which is particularly high (55,92%).

Such artificial correlations as these arise from the fact that the discriminant coefficients, and thus the eigen vectors, have been derived from a matrix of values which does not correspond exactly to those of the Molteno basalts. For this reason, any conclusions drawn from this comparison must be treated with due caution.

7.6 Major Element Variation Diagrams

From the normative chemistry, AFM diagrams and discriminant analysis, it has been determined thus far that the Molteno basalts may be separated into chemically distinct units. Further, the normative basalt tetrahedron has given some idea of possible mineralogical controls on within-unit differentiation processes, particularly as regards the Roodehoek and Vaalkop Units.

Having ascertained that the Molteno lavas constitute a differentiated suite, two alternative possibilities must be explored. In the first instance, the units within the suite may be linked by fractional crystallisation or partial melting processes. A second alternative is that, as appears to be the case in the Barkly East district, the lava units are not related by any simple fractionation process, but are instead the products of an inhomogeneous mantle source.

Using SiO_2 as a simple index of differentiation, major element data are employed in this section in modelling possible controls on differentiation within the Brosterlea and Modderfontein basalt suites. This work differs from previous work by Cox et al. (1967), Wright (1974), Robey (1976) and Pemberton (1978) in using SiO_2, rather than MgO, as an index of differentiation in the Karoo lavas. The reason for this is that the Molteno basalts show an overall trend of SiO_2 enrichment, and very little variation in MgO content. Walker and Poldervaart (1949) point out that SiO_2 variation diagrams tend to emphasize variations in the late stages of differentiation more than those in the early to middle stages. Robey (1976) encountered similar problems in terms of MgO

variation diagrams. These problems, however, are negligible within the small SiO_2 ranges encountered in the Molteno basalts. Variations in the concentrations of the major elements with increasing SiO_2 may be summarised as follows :

TiO_2 enriches with differentiation (Fig. 21a), and clearly separates the lavas into distinct units. TiO_2 content increases from the Roodehoek Unit to the Vaalkop Unit in the Brosterlea suite. The Modderfontein suite, on the other hand, shows a depletion in TiO_2 with differentiation.

In the Brosterlea and Modderfontein suites, K_2O shows very indistinct trends (Fig. 21h), although the overall impression is one of slight enrichment with differentiation. The Roodehoek and Perdekop Units are relatively low-K types (below 1%), whereas the Vaalkop and Strypoort Units usually have K_2O contents in excess of 1%. The Modderfontein basalts are constant in K_2O content, all being below 1%. The dolerites from both Brosterlea and Modderfontein have concentrations of K_2O below 1%, except AA-23 (Dragon's Back), which has an exceptionally high K_2O content of 1,89%. Phosphorus mimmics almost exactly the behaviour of potassium (Fig. 21j). P_2O_5 contents are low and never exceed 0,25% in the Molteno basalts. Whilst the overall trends of Na behaviour are indistinct (Fig. 21g), both the Roodehoek and the Vaalkop Units display distinct within-unit Na-enrichment with differentiation.

Al_2O_3 depletion trends are quite distinct in both the Brosterlea and the Modderfontein suites (Fig. 21b), the majority of the rocks ranging between 15% and 17% Al_2O_3. Notable exceptions are AA-21 (18,21% Al_2O_3) and AA-23 (13,78% Al_2O_3). Fe_2O_3 variation trends are similar to those of Al, although somewhat subdued (Fig. 21c). The Fe_2O_3 content of the Molteno rocks ranges, generally speaking, between 10% and 12%. CaO is strongly depleted in the Brosterlea basalt suite, but remains fairly constant in the Modderfontein basalts and in the dolerites (Fig. 21f).

As mentioned previously, MgO displays only small variations within the range 6% - 8%, the exception being

sample AM-36M (10,32% MgO). The MnO data are imprecise, owing to mechanical defects in the Al filter mechanism, which result in imperfect exclusion of interference from the tube-derived Cr K_β peak on the Mn K_α peak of the sample.

In an attempt to determine possible mineralogical controls on differentiation in the Brosterlea basalt suite, mineralogical control lines have been incorporated into generalised representations of the major element variation diagrams (see Fig. 22). The inadequacy of the data precludes any detailed analysis of mineralogical controls on differentiation in the Modderfontein suite or in the dolerites. The interpretation of the available data is as follows :

In its progressive enrichment with differentiation, Ti displays incompatible tendencies, and has in fact often been used as an incompatible element in the literature (Kesson, 1973; Sun and Nesbitt, 1977). Duke (1976) calculated a D_{Ti}^{cpx} of the order of 0,29, which is reasonably close to the range of values from 0,3 to 0,5, as calculated from Brosterlea clinopyroxene data. Olivine and plagioclase virtually totally exclude Ti. From Fig. 22a it would appear that olivine is the dominant fractionating phase in the Ti-enrichment trend.

From Fig. 21, other major elements with incompatible tendencies are K and P. There is no mineralogical data available for P in the Brosterlea suite, but K_2O enrichment (Fig. 22b) appears to be dominated by olivine fractionation. Na_2O enrichment in the Brosterlea sequence is apparently controlled mainly by olivine fractionation, with a minor component of clinopyroxene and little or no plagioclase (Fig. 22c).

The constancy of MgO with differentiation can be resolved into the combined effects of olivine, clinopyroxene and plagioclase fractionation (Fig. 22d). Al_2O_3 depletion appears to be dominated by plagioclase fractionation, as does the depletion of CaO (Fig. 22e and f).

The inconsistency of the results obtained from analysis of the mineralogical controls on differentiation must be taken as an indication that there is no simple fractionation mechanism operative in the Brosterlea suite. Furthermore, the Roodehoek and Vaalkop Units only represent a part of the Brosterlea suite, and it must be remembered that the Strypoort Unit, the lowermost unit in the sequence, is relatively enriched in compatibles, whilst the uppermost Perdekop Unit reverts to a relatively primitive chemistry. In summary, the evidence thus far points to the existence of a series of units unrelated by fractionation or partial melting mechanisms. Final conclusions must, however, await the evaluation of the trace element data.

Fig. 17 : ALKALI-SILICA DIAGRAM FOR THE BROSTERLEA BASALTS

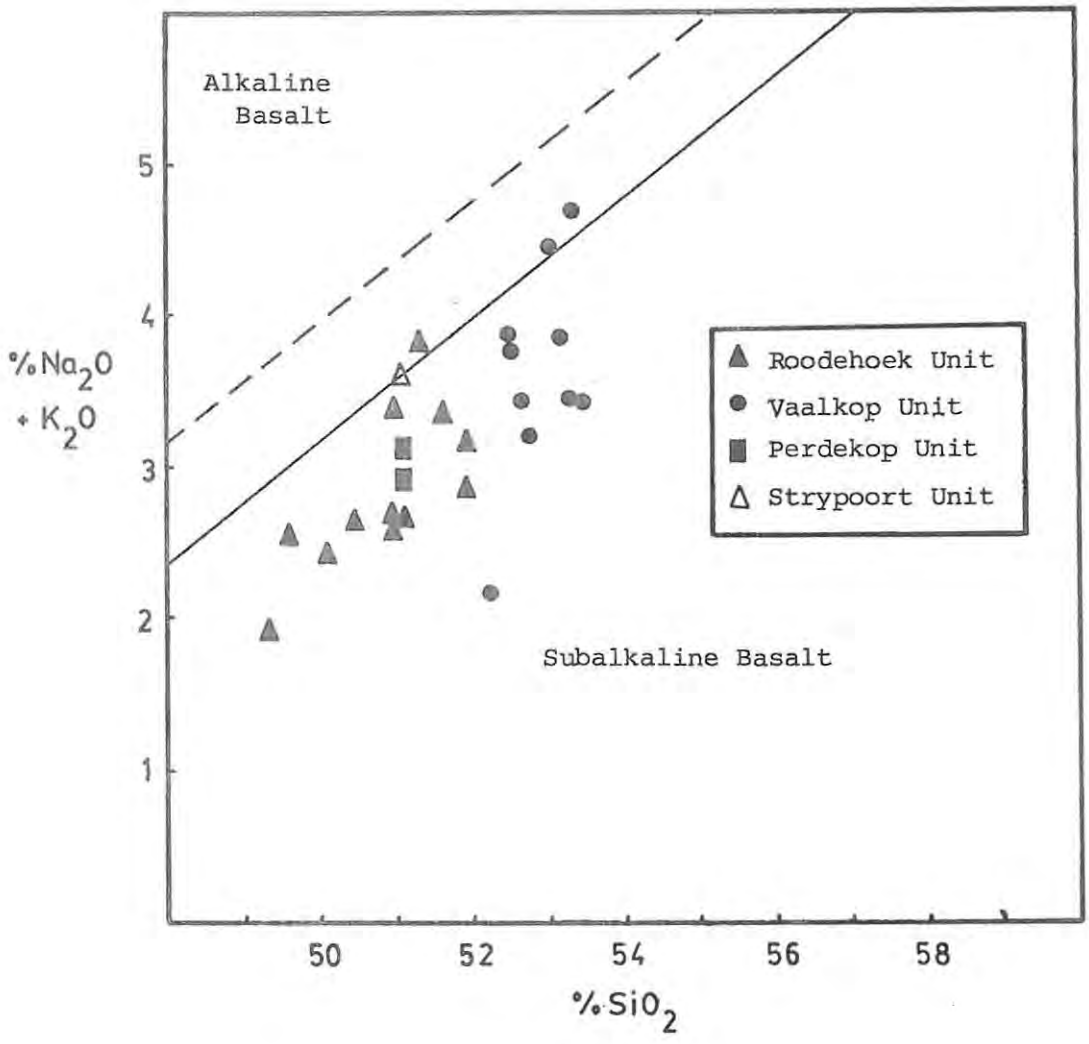

Fig. 18a : NORMATIVE BASALT TETRAHEDRON

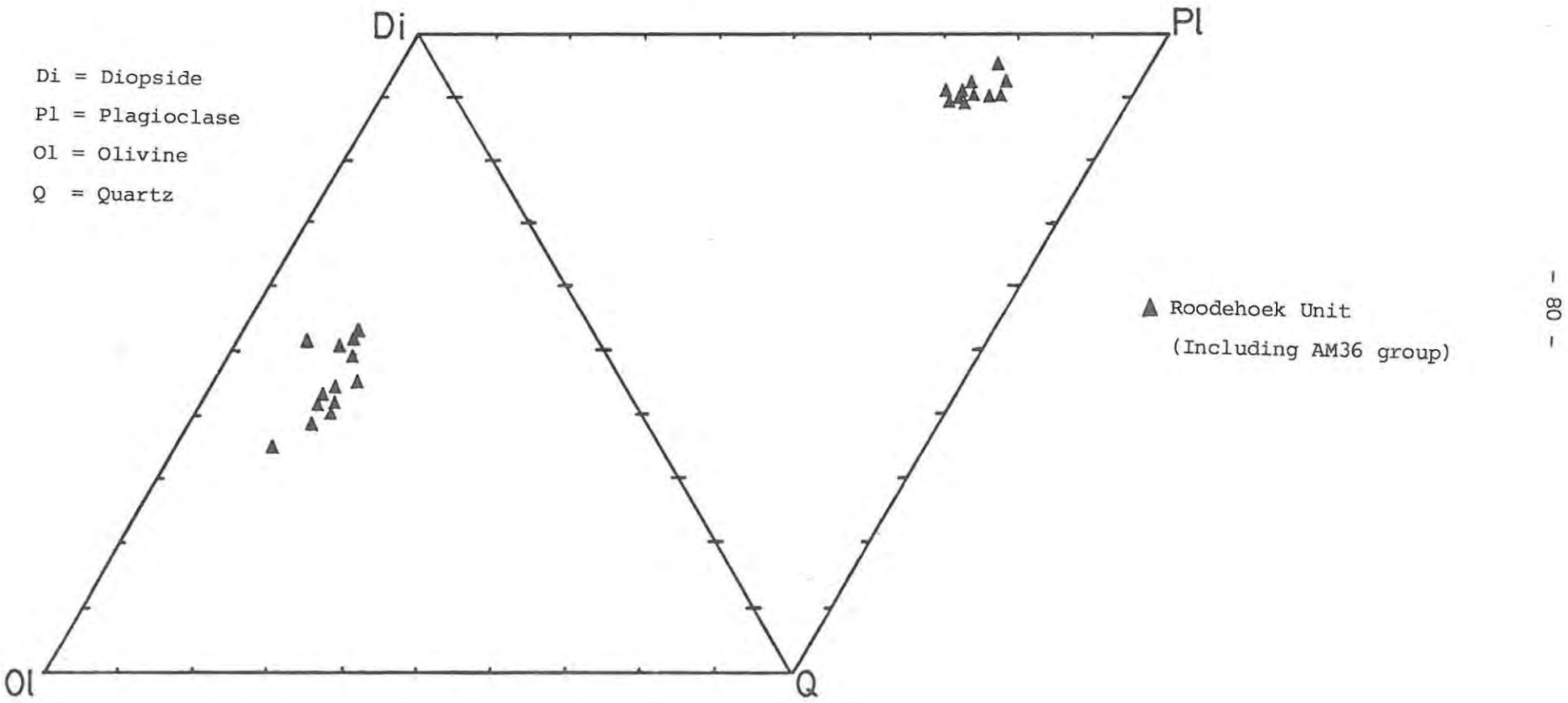

Fig. 18b : NORMATIVE BASALT TETRAHEDRON

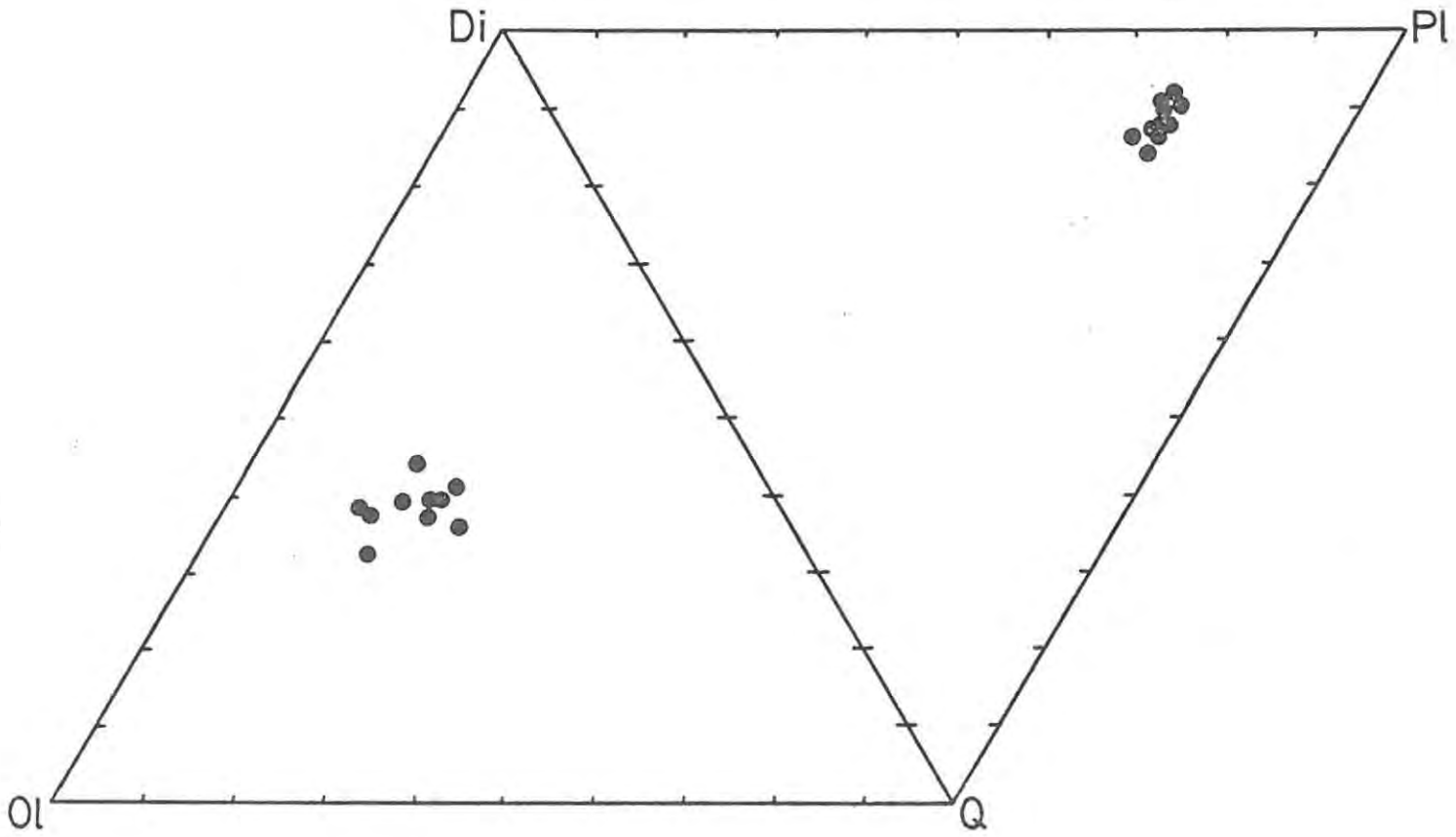

● Vaalkop Unit

Fig. 18c : THE NORMATIVE BASALT TETRAHEDRON

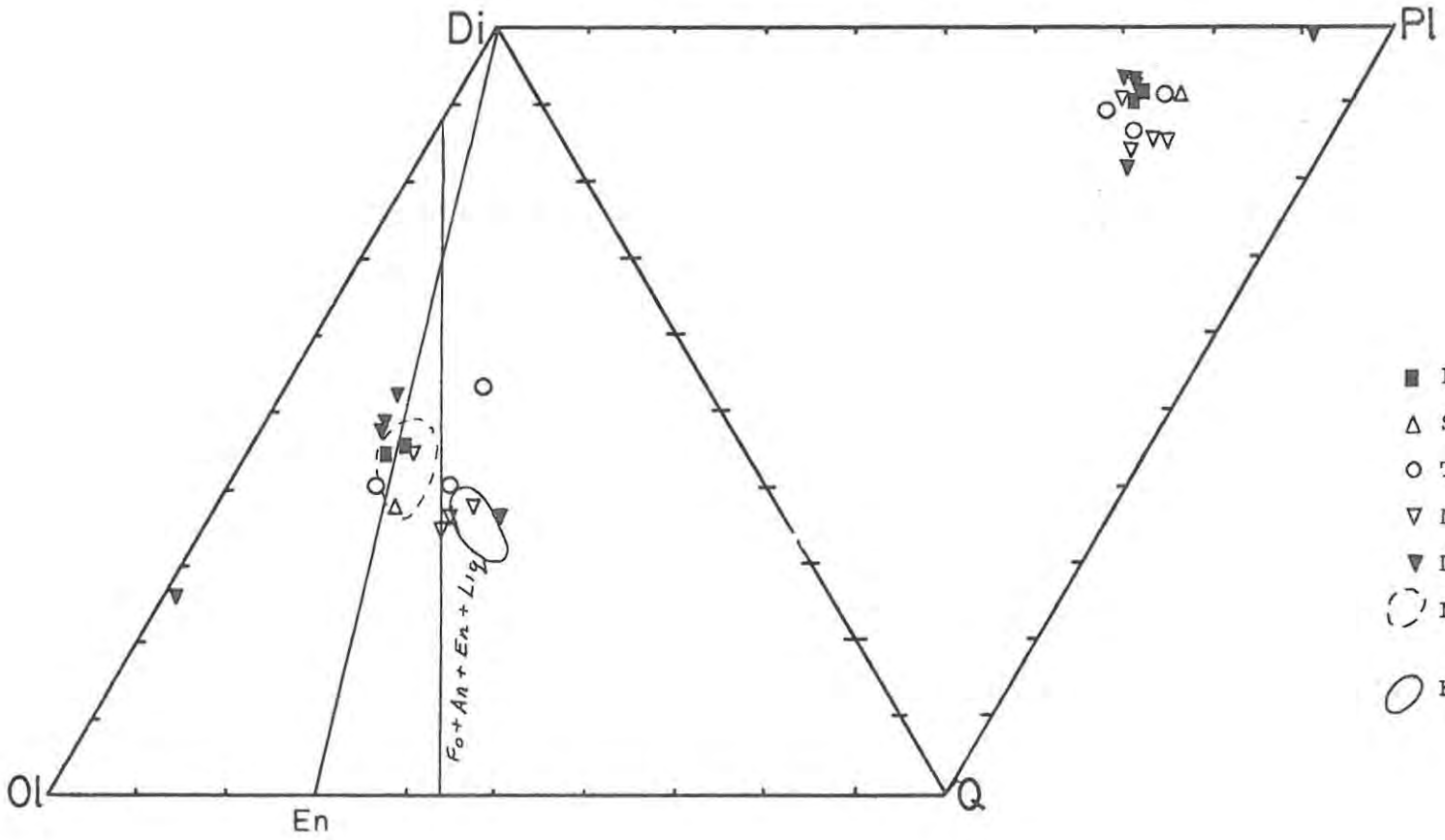

- Perdekop Unit
- Strypoort Unit
- Tafelkop Lavas
- Modderfontein Basalts
- Dolerites
- Lesotho Basalts (Cox & Hornung, 1976)
- Kraai River Basalts (Pemberton, 1978)

TABLE 2 C.I.P.W. WEIGHT PERCENT NORMS

Vaalkop Unit

		AM-11	AM-12	AM-13	AM-29	AM-30	AM-32	AM-34	AM-41	AM-43	AM-44
Ap		0,54	0,50	0,52	0,52	0,59	0,52	0,52	0,52	0,52	0,52
Il		2,14	2,05	2,10	2,08	2,23	2,10	2,07	2,20	2,12	2,08
Or		6,62	4,85	2,01	6,08	6,85	9,34	6,50	8,57	6,50	6,44
Ab		17,60	22,42	15,57	19,46	22,84	19,21	22,59	27,50	28,68	19,71
An		29,08	27,82	33,69	28,90	26,56	27,55	27,25	23,24	23,70	28,07
Mt		2,38	2,28	2,35	2,28	2,38	2,26	2,28	2,41	2,32	2,26
En	Di	4,58	4,34	4,15	4,40	4,07	3,98	4,82	3,11	3,72	4,35
Fs	Di	3,73	3,30	3,27	3,22	3,13	2,95	3,54	2,38	2,72	3,25
Wo	Di	8,59	7,93	7,69	7,92	7,47	7,20	8,69	5,69	6,70	7,90
En	Hy	10,53	11,23	12,03	11,67	11,94	11,76	11,04	12,95	12,74	11,29
Fs	Hy	8,57	8,54	9,48	8,54	9,19	8,72	8,09	9,91	9,30	8,43
Q		4,75	3,90	6,24	3,36	1,82	3,55	1,75	0,73	0,10	4,85

Ap - Apatite Il - Ilmenite Or - Orthoclase Ab - Albite

An - Anorthite Mt - Magnetite En - Enstatite Fs - Ferrosilite

Di - Diopside Wo - Wollastonite Hy - Hypersthene Q - Quartz

Fo - Forsterite Fa - Fayalite

TABLE 2 C.I.P.W. WEIGHT PERCENT NORMS*

Roodehoek Unit

	AM-14	AM-15	AM-21	AM-22	AM-23	AM-25	AM-31	AM36T	AM36M	AM36B
Ap	0,33	0,31	0,31	0,31	0,24	0,28	0,33	0,33	0,43	0,31
Il	1,76	1,52	1,67	1,69	1,56	1,58	1,69	1,99	1,69	2,20
Or	3,01	2,95	2,48	2,01	2,54	2,60	1,60	3,72	2,54	3,55
Ab	12,27	18,11	19,21	17,60	21,74	18,95	19,54	23,44	18,28	21,66
An	37,56	33,53	31,71	32,77	33,07	32,39	32,52	28,82	28,74	28,32
Mt	2,49	2,38	2,41	2,42	2,25	2,35	2,38	2,60	2,61	2,52
En (Di)	5,78	4,90	5,27	4,98	5,34	4,91	5,61	4,43	4,93	4,91
Fs (Di)	4,93	3,28	3,82	3,55	4,09	3,34	4,30	3,74	2,73	4,06
Wo (Di)	11,03	8,55	9,46	8,89	9,78	8,62	10,28	8,42	8,11	9,25
En (Hy)	9,88	14,06	12,61	13,27	10,24	13,67	10,96	11,23	13,74	10,78
Fs (Hy)	8,43	9,42	9,15	9,47	7,84	9,30	8,41	9,50	7,62	8,91
Q	1,58	-	0,98	1,12	0,45	1,11	1,49	-	-	2,47
Fo	-	0,05	-	-	-	-	-	0,41	4,77	-
Fa	-	0,04	-	-	-	-	-	0,38	2,91	-

* Oxidation ratio calculated as $Fe_2O_3/FeO = 0,2$

TABLE 2 : C.I.P.W. WEIGHT PERCENT NORMS

		Roodehoek Unit			Perdekop Unit		Tafelkop Lavas			Strypoort Unit
		AM-26	AM-27	AM-46	AM-28	AM-40	AM-37	AM38T	AM-38	AM-24
Ap		0,38	0,36	0,31	0,43	0,45	0,31	0,28	0,47	0,54
Il		1,80	1,80	1,67	1,99	1,91	1,61	1,75	2,05	2,12
Or		4,25	4,49	2,66	4,20	3,96	3,72	3,07	6,15	7,45
Ab		26,48	22,00	20,56	19,29	20,64	29,53	24,11	19,54	20,39
An		26,26	28,11	30,47	30,07	29,64	24,17	26,82	28,17	31,88
Mt		2,45	2,38	2,29	2,51	2,42	2,20	2,33	2,36	2,32
En	Di	5,38	4,96	6,12	5,13	5,09	4,51	6,50	4,44	3,56
Fs	Di	4,22	3,36	4,77	3,97	3,60	2,99	4,16	3,62	3,00
Wo	Di	9,94	8,69	11,28	9,43	9,06	7,84	11,18	8,32	6,76
En	Hy	7,25	13,67	9,52	11,73	12,89	13,15	8,32	10,50	10,64
Fs	Hy	5,69	9,26	7,41	9,08	9,12	8,72	5,32	8,55	8,96
Q		-	0,03	2,07	1,23	0,29	0,41	-	4,94	1,52
Fo		2,67	-	-	-	-	-	3,09	-	-
Fa		2,31	-	-	-	-	-	2,18	-	-

TABLE 2 : C.I.P.W. WEIGHT PERCENT NORMS

		Modderfontein Lavas				Dolerites				
		AM-50	AM-51	AM-52	AM-53	AA-21	AA-22	AA-23	AA-30	AA-31
Ap		0,33	0,36	0,47	0,52	0,28	0,40	0,57	0,26	0,26
Il		1,83	1,75	1,97	2,14	2,48	1,95	2,23	1,63	1,43
Or		3,66	2,25	3,25	1,42	-	3,96	11,17	1,95	1,95
Ab		19,88	19,80	19,88	16,16	37,40	23,52	22,51	19,71	19,71
An		29,53	28,82	30,59	34,76	29,85	27,18	20,08	32,53	32,25
Mt		2,42	2,23	2,28	2,33	2,75	2,64	2,75	2,39	2,23
En	Di	5,43	4,73	4,05	4,30	1,75	5,26	2,92	5,58	5,77
Fs	Di	3,69	3,35	2,89	3,13	1,62	4,93	4,31	3,88	3,77
Wo	Di	9,53	8,42	7,23	7,73	3,45	10,41	7,18	9,88	9,99
En	Hy	12,89	11,88	12,54	12,28	0,65	9,59	6,74	12,67	12,48
Fs	Hy	8,75	8,43	8,96	8,93	0,60	8,97	9,94	8,82	8,15
Q		1,00	7,16	5,02	5,40	-	0,19	8,55	0,05	0,15
Fo		-	-	-	-	8,98	-	-	-	-
Fa		-	-	-	-	9,14	-	-	-	-

Fig. 19 a-d : PARTIAL AFM DIAGRAMS FOR THE BASALTS AND DOLERITES OF BROSTERLEA AND MODDERFONTEIN

(Symbols as for other major element diagrams)

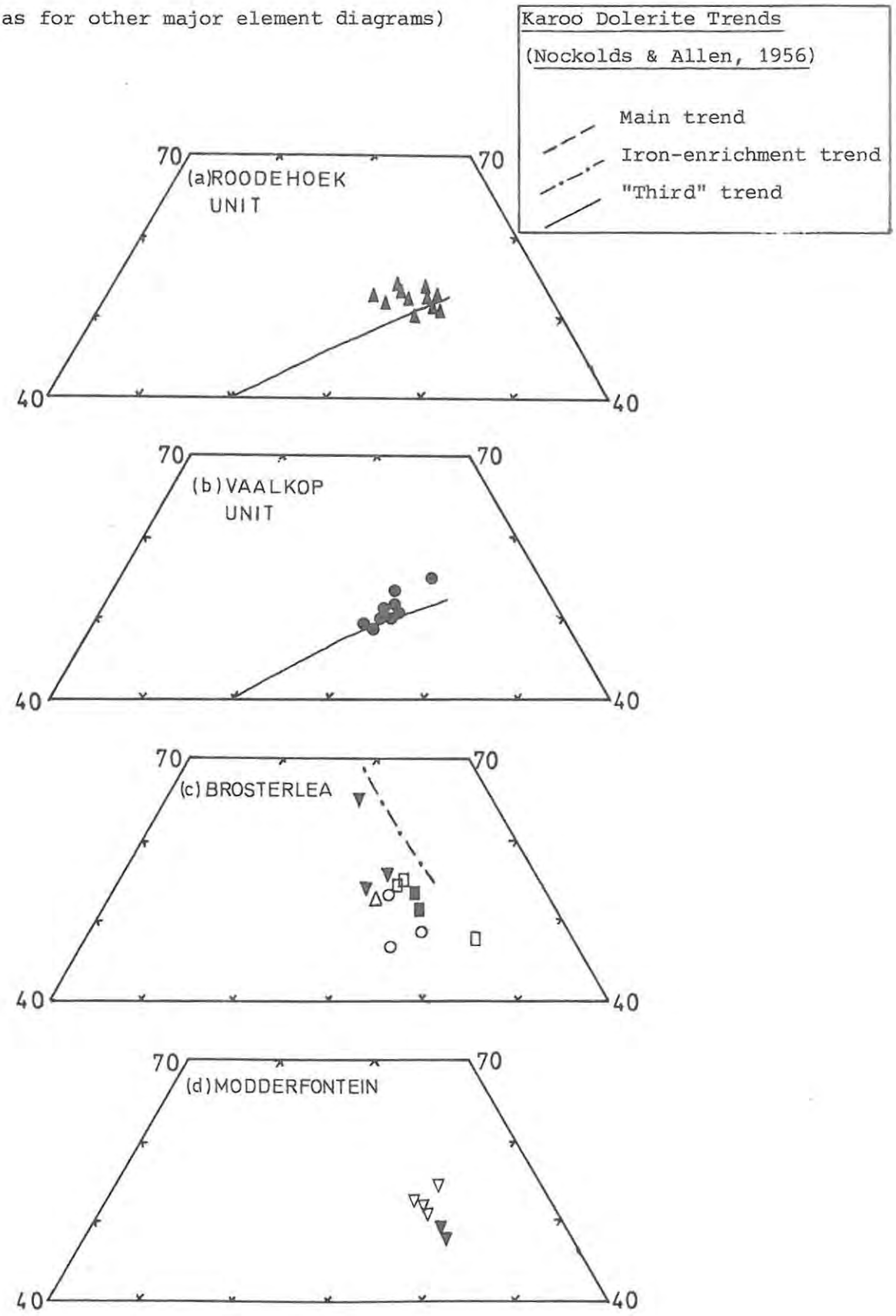

Fig. 20 ; DISCRIMINANT ANALYSIS OF BASALTIC ROCKS OF THE KAROO SUPERGROUP

F_1 = 1,0617-0,03917xFe_2O_3-0,32997xMgO-1,23122xNb-0,00778xNi +0,06901xZn+0,01242xCu+0,14195xY

F_2 = 18,13476-3,18309xFe_2O_3+1,76374xMgO-0,01790xNb-0,08480xNi +0,05511xZn-0,04958xCu+0,36057xY

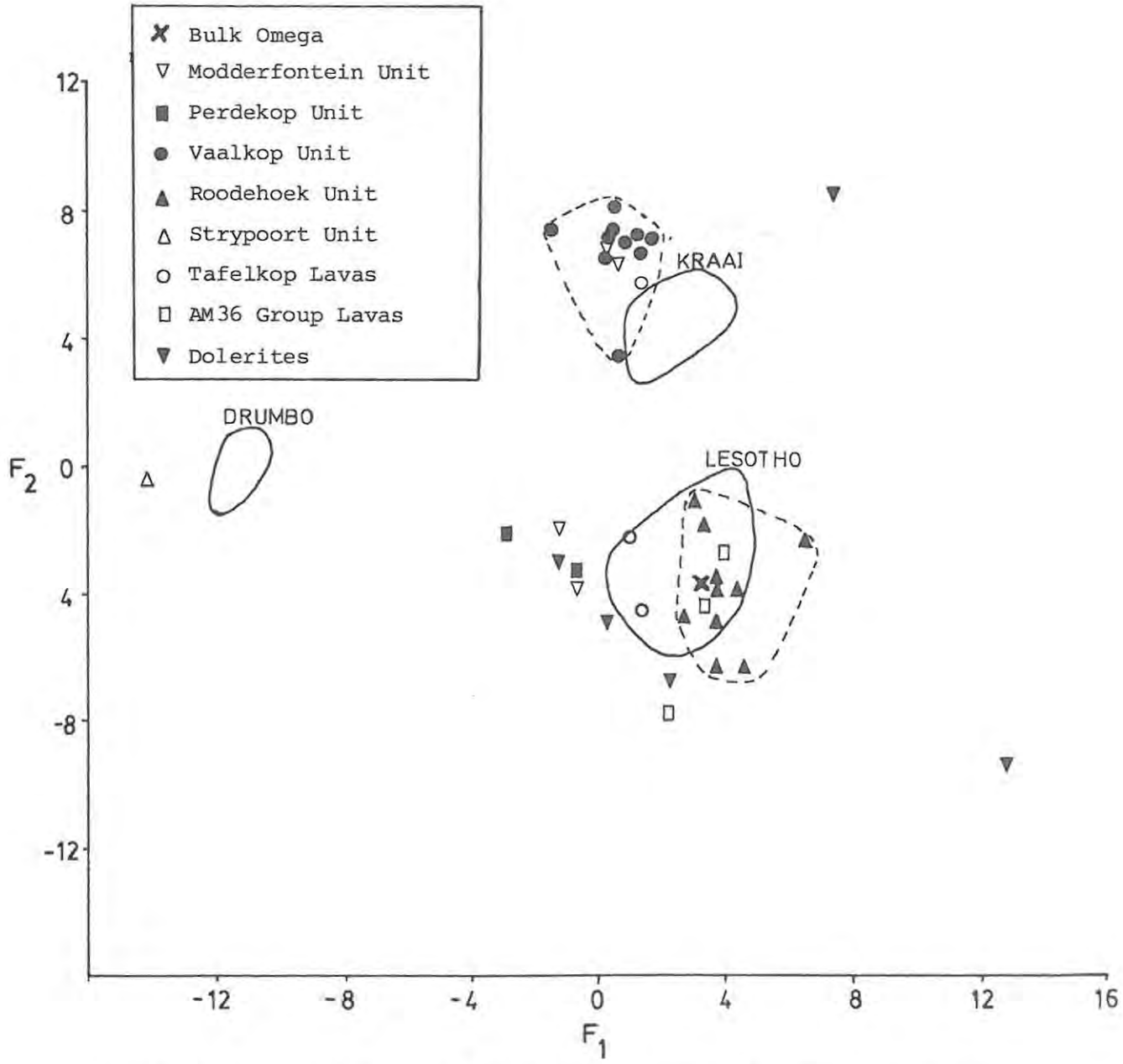

Solid lines donote limits of units from the work of Robey (1976) and Pemberton (1978). Dashed lines demarcate units from the present work.

Fig. 21a : MAJOR ELEMENT VARIATIONS (WEIGHT % OXIDES) USING SiO_2 AS THE ABSCISSA

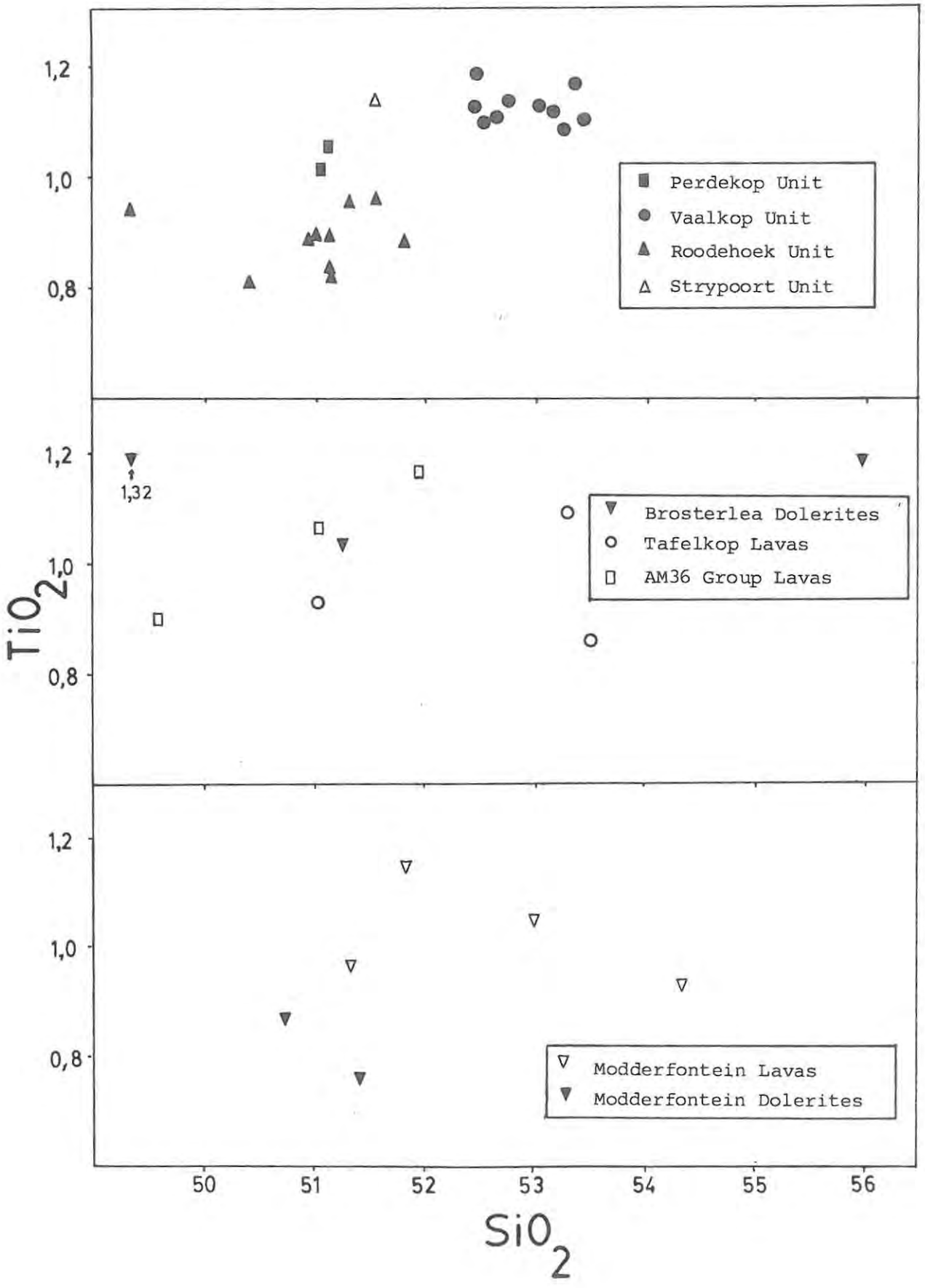

Fig. 21b : MAJOR ELEMENT VARIATIONS (WEIGHT % OXIDES) USING SiO_2 AS THE ABSCISSA

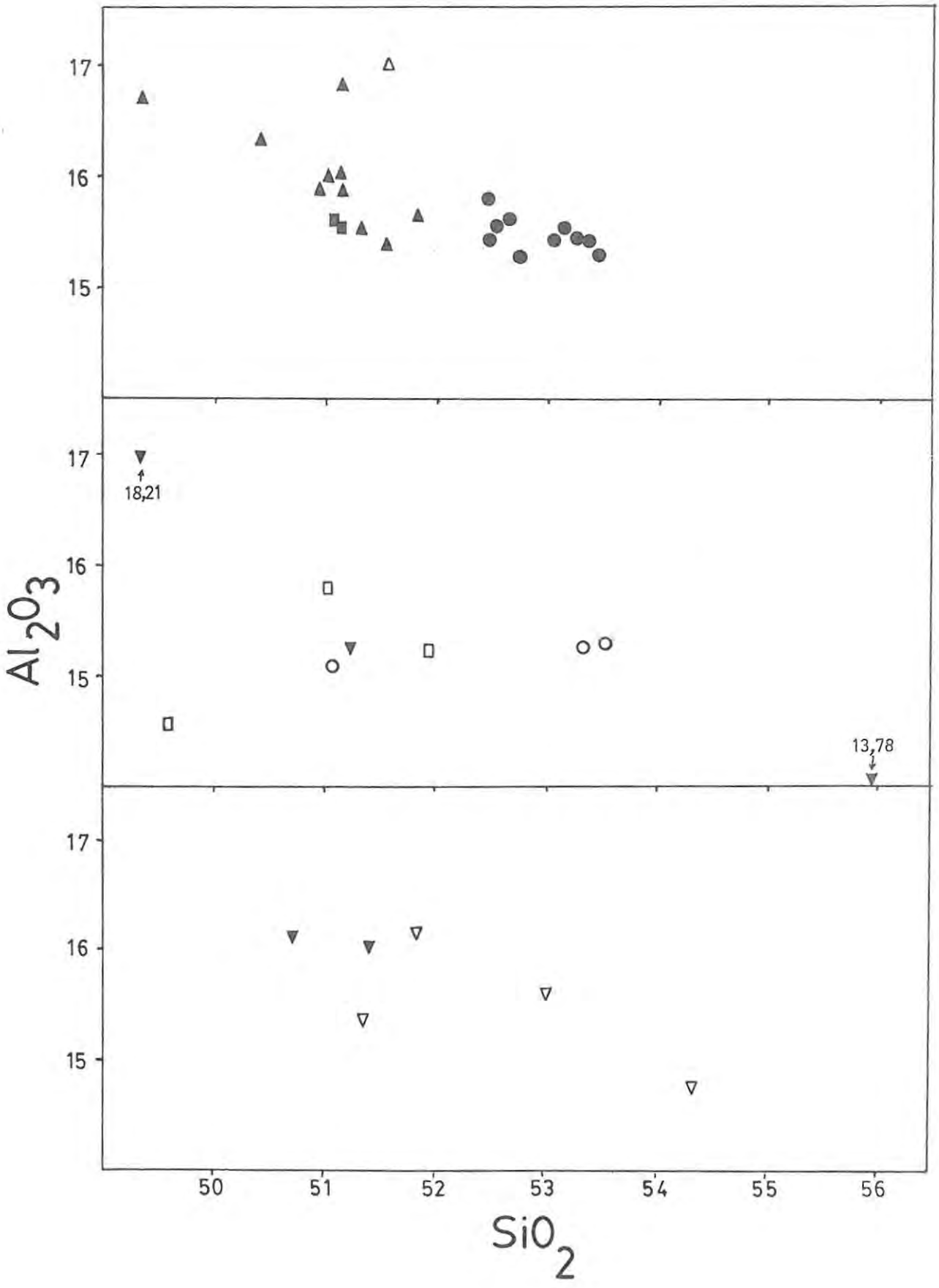

Fig. 21c : MAJOR ELEMENT VARIATIONS (WEIGHT % OXIDES) USING SiO_2 AS THE ABSCISSA

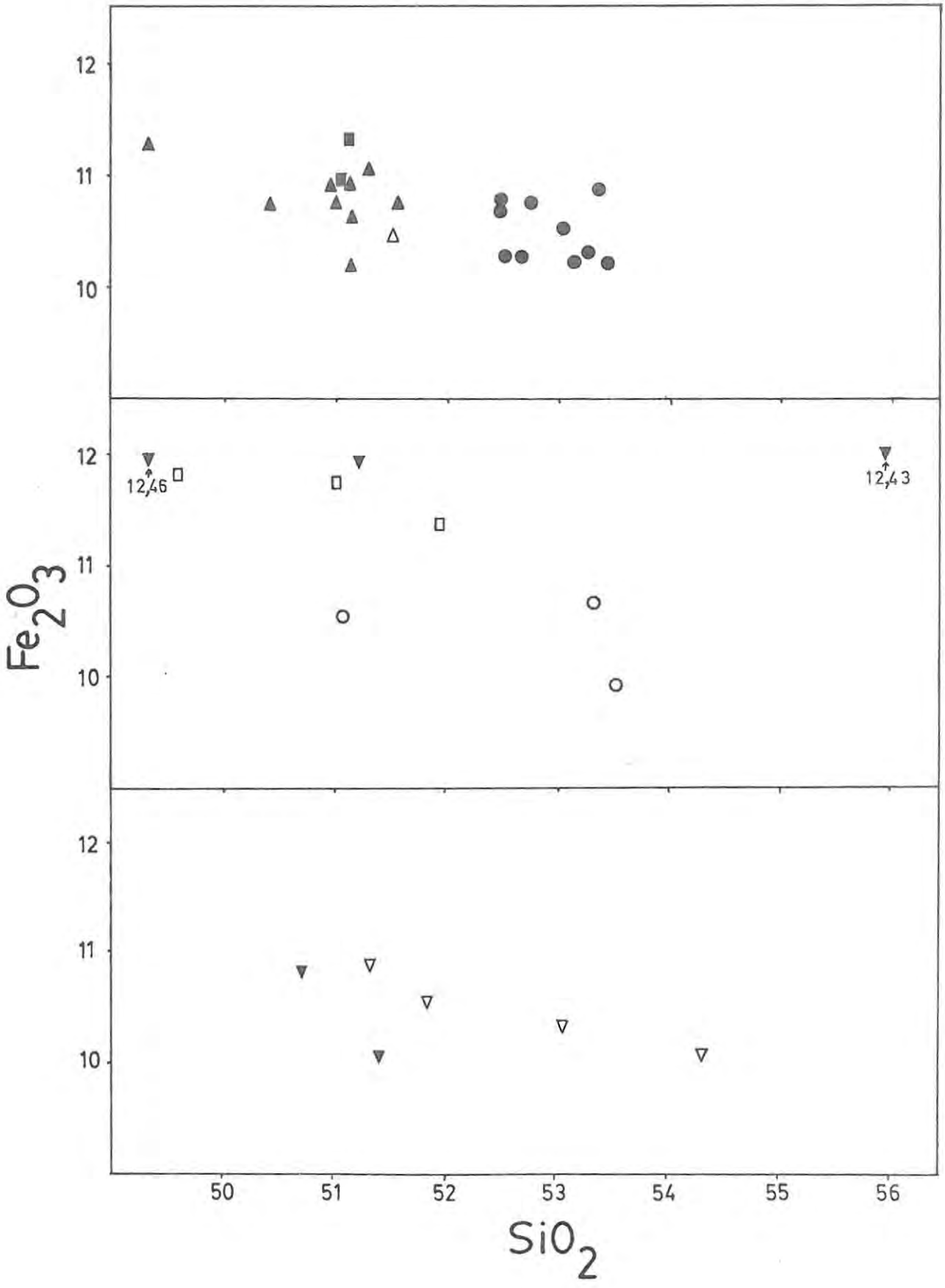

Fig. 21d : MAJOR ELEMENT VARIATIONS (WEIGHT % OXIDES) USING SiO_2 AS THE ABSCISSA

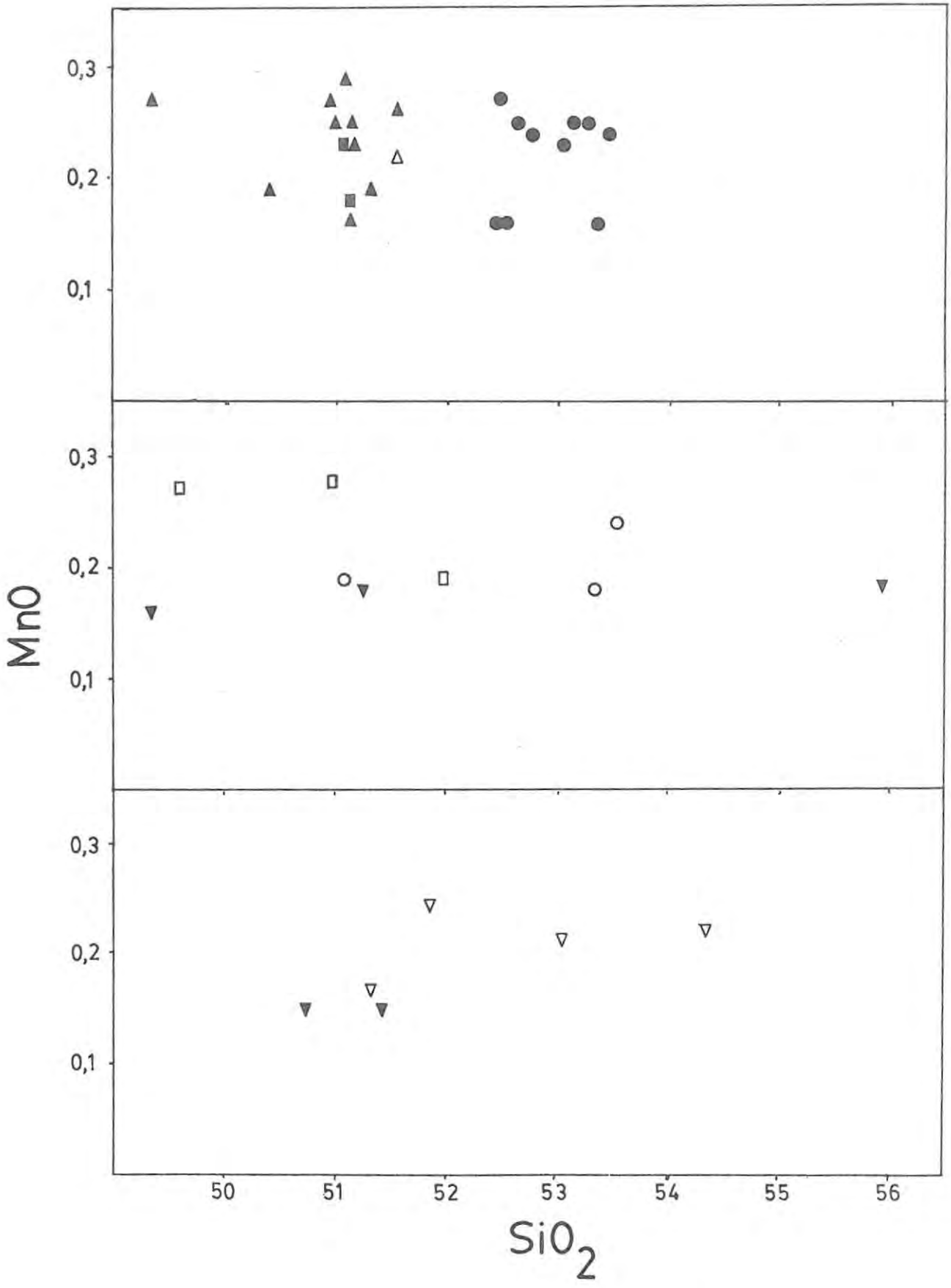

Fig. 21e ; MAJOR ELEMENT VARIATIONS (WEIGHT % OXIDES) USING SiO_2 AS THE ABSCISSA

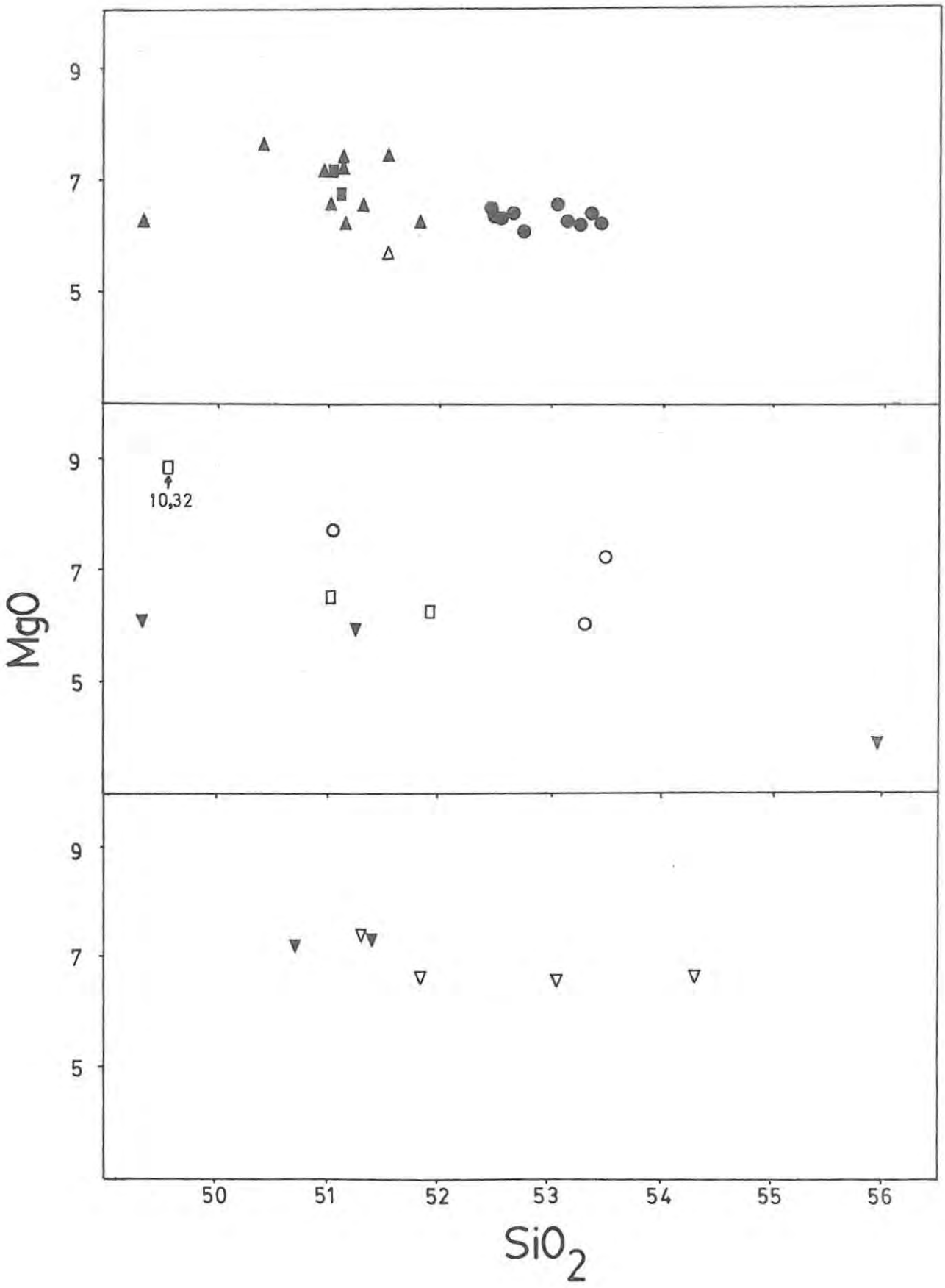

Fig. 21f : MAJOR ELEMENT VARIATIONS (WEIGHT % OXIDES) USING SiO_2 AS THE ABSCISSA

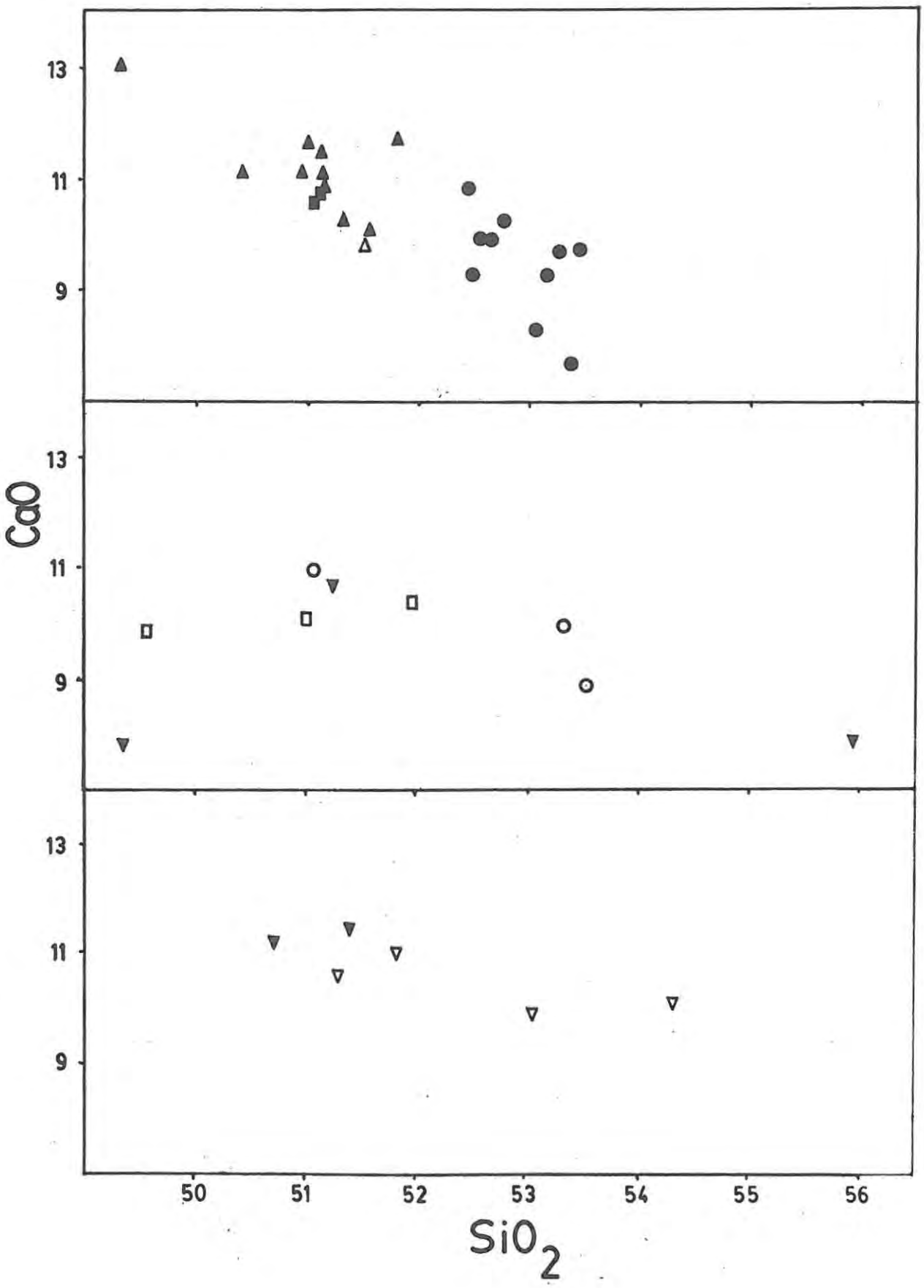

Fig. 21g : MAJOR ELEMENT VARIATIONS (WEIGHT % OXIDES) USING SiO_2 AS THE ABSCISSA

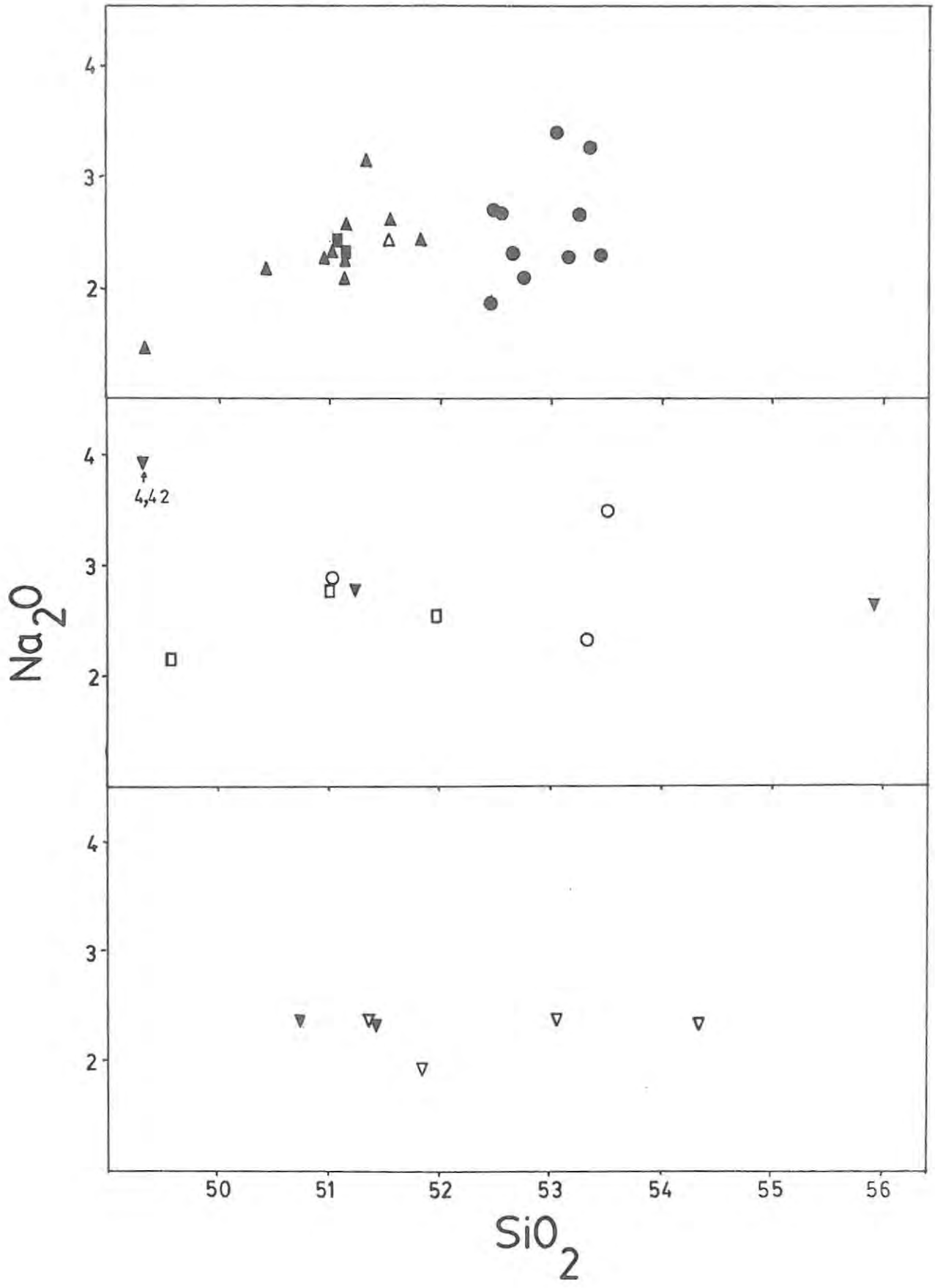

Fig. 21h : MAJOR ELEMENT VARIATIONS (WEIGHT % OXIDES) USING SiO_2 AS THE ABSCISSA

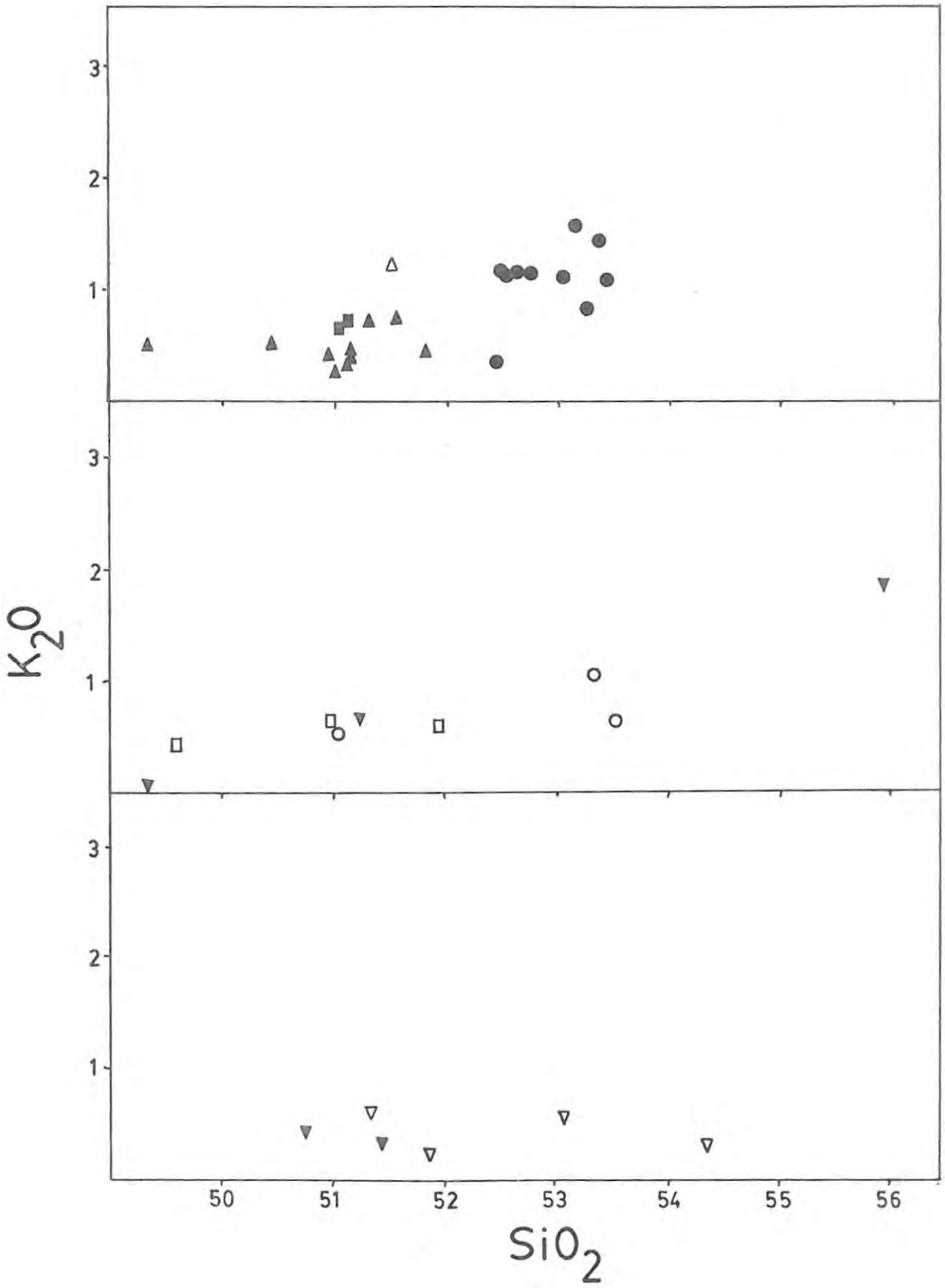

Fig. 21j : MAJOR ELEMENT VARIATIONS (WEIGHT % OXIDES) USING SiO_2 AS THE ABSCISSA

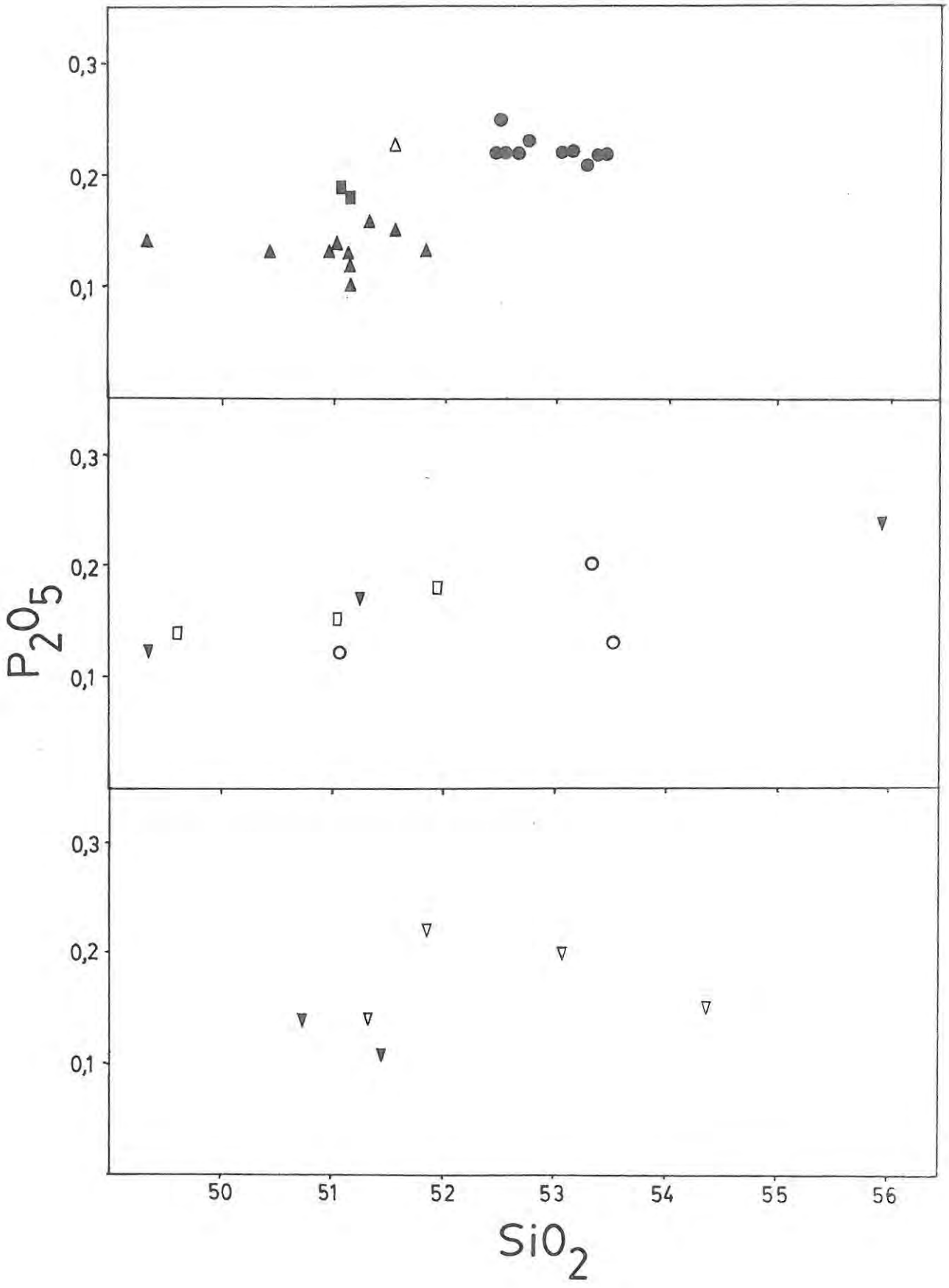

Fig. 22 a-f : MINERALOGICAL CONTROLS ON DIFFERENTIATION

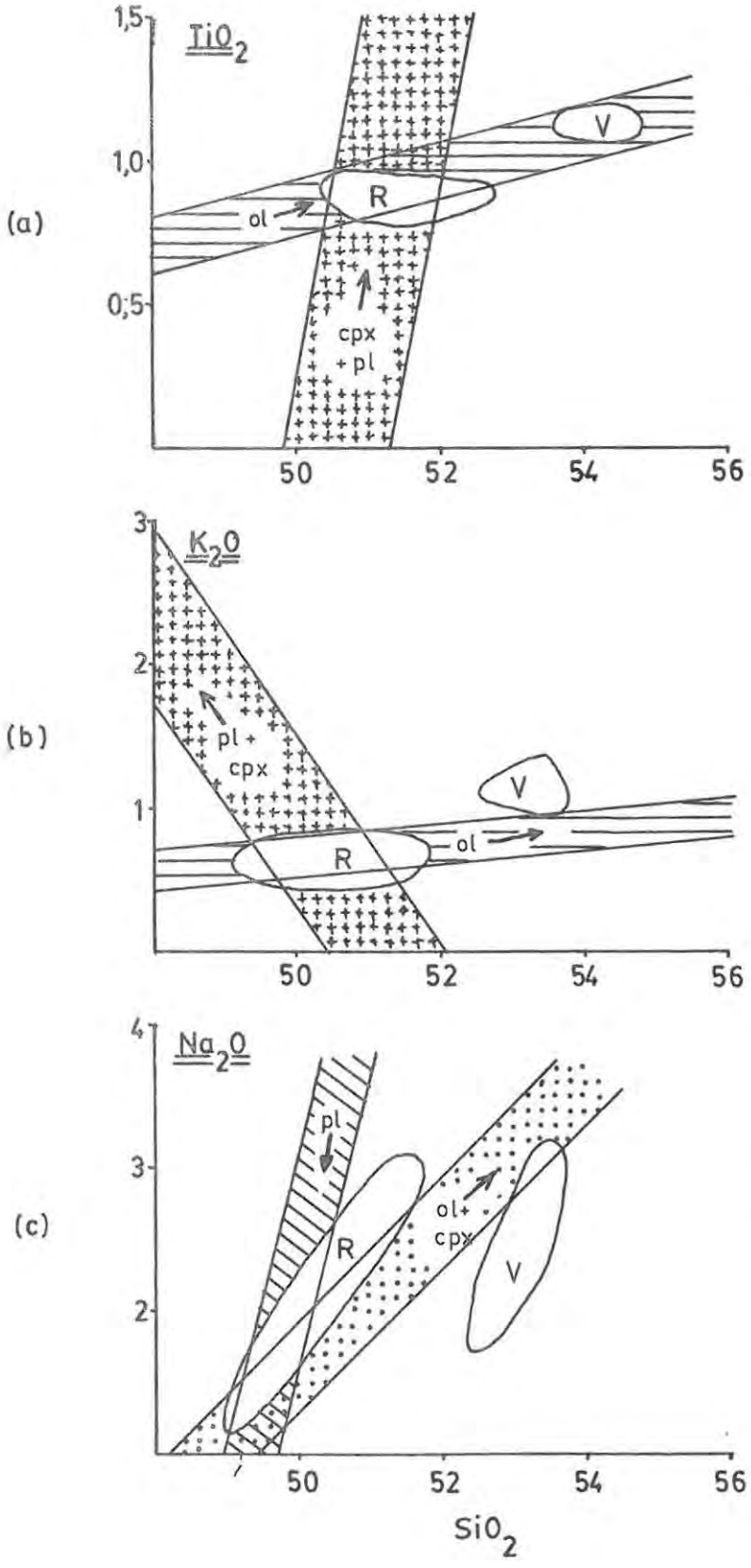

Fig. 22 a-f : MINERALOGICAL CONTROLS ON DIFFERENTIATION

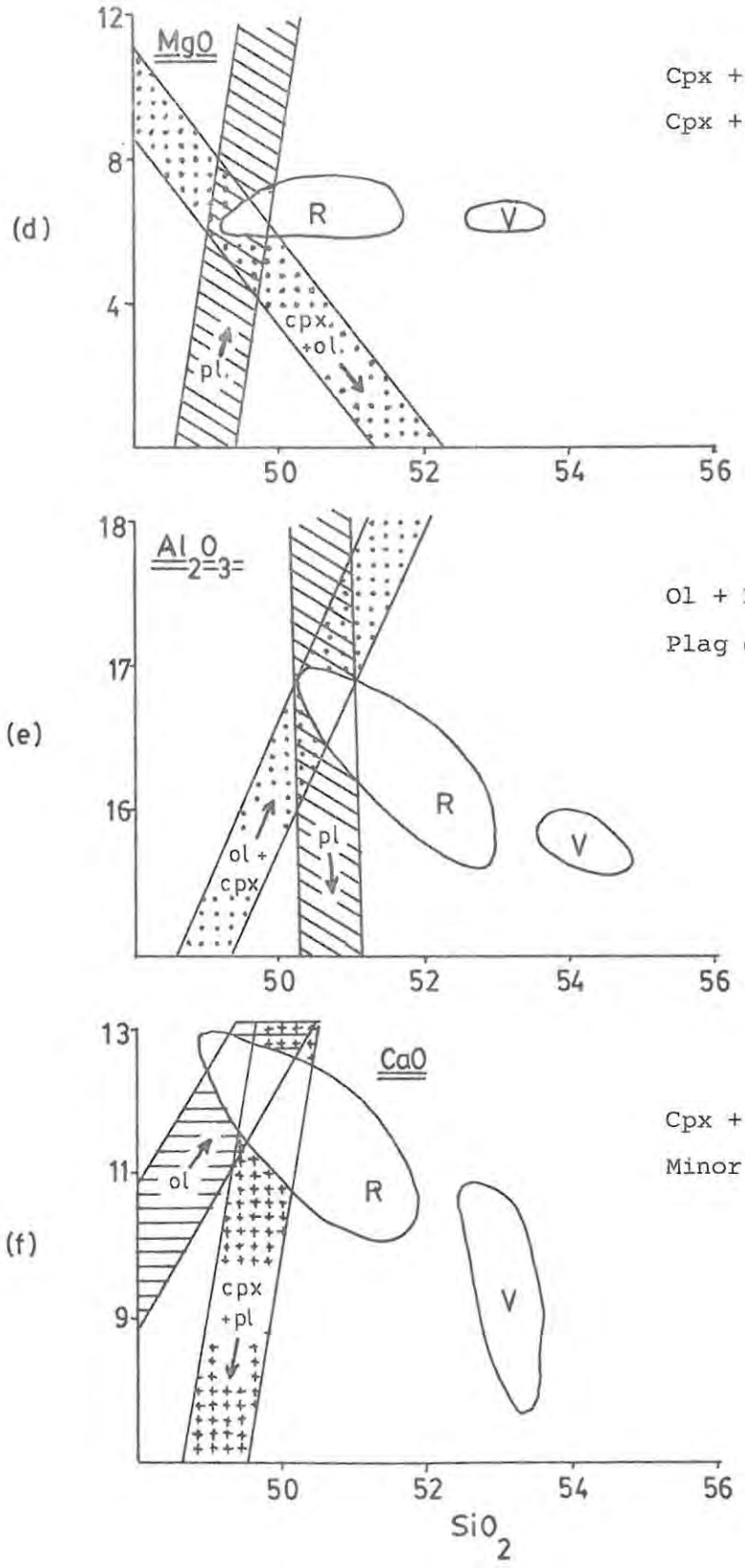

TABLE 3 : MAJOR ELEMENT ANALYSES (NORMALIZED TO 100%) AND TRACE ELEMENT ANALYSES

Vaalkop Unit

	AM-11	AM-12	AM-13	AM-29	AM-30	AM-32	AM-34
SiO_2	52,78	53,28	52,46	52,69	52,50	53,16	52,55
TiO_2	1,14	1,09	1,13	1,11	1,19	1,12	1,10
Al_2O_3	15,29	15,44	15,80	15,62	15,43	15,54	15,57
Fe_2O_3	10,74	10,30	10,69	10,27	10,78	10,22	10,28
MnO	0,24	0,25	0,16	0,25	0,27	0,25	0,16
MgO	6,07	6,25	6,52	6,45	6,43	6,32	6,37
CaO	10,31	9,71	10,83	9,94	9,29	9,32	9,98
Na_2O	2,08	2,65	1,85	2,30	2,70	2,27	2,67
K_2O	1,12	0,82	0,34	1,15	1,16	1,58	1,10
P_2O_5	0,23	0,21	0,22	0,22	0,25	0,22	0,22
TOTAL	100,00	100,00	100,00	100,00	100,00	100,00	100,00
Sr	167	318	307	222	279	206	226
Rb	32	23	5	28	25	48	25
Y	28	27	30	28	30	26	27
Zr	112	107	120	113	125	109	108
Nb	7	6	7	8	7	6	6
Co	44	42	43	43	45	43	43
V	242	239	245	256	253	248	247
Cr	352	353	335	370	310	129	373
Zn	86	86	87	92	92	88	93
Cu	80	36	37	39	40	42	39
Ni	24	21	22	22	22	23	26

TABLE 3 : MAJOR ELEMENT ANALYSES (NORMALIZED TO 100%) AND TRACE ELEMENT ANALYSES

	Vaalkop Unit			Tafelkop Lavas		
	AM-41	AM-43	AM-44	AM-37	AM38T	AM-38
SiO_2	53,37	53,05	53,46	53,52	51,08	53,31
TiO_2	1,17	1,13	1,11	0,86	0,93	1,09
Al_2O_3	15,43	15,45	15,30	15,28	15,08	15,25
Fe_2O_3	10,88	10,52	10,21	9,93	10,55	10,66
MnO	0,16	0,23	0,24	0,24	0,19	0,18
MgO	6,45	6,61	6,28	7,09	7,72	6,00
CaO	7,72	8,30	9,76	8,83	10,96	9,96
Na_2O	3,25	3,39	2,33	3,49	2,85	2,31
K_2O	1,45	1,10	1,09	0,63	0,52	1,04
P_2O_5	0,22	0,22	0,22	0,13	0,12	0,20
TOTAL	100,00	100,00	100,00	100,00	100,00	100,00
Sr	269	435	227	205	177	240
Rb	34	26	26	12	8	23
Y	30	28	28	21	24	29
Zr	120	114	118	72	78	115
Nb	8	7	8	4	4	6
Co	42	49	41	44	45	40
V	246	260	247	233	218	215
Cr	351	344	342	295	311	309
Zn	96	88	82	76	63	82
Cu	40	39	34	88	108	38
Ni	26	21	21	102	111	23

TABLE 3 : MAJOR ELEMENT ANALYSES (NORMALISED TO 100%) AND TRACE ELEMENT ANALYSES

Roodehoek Unit

	AM-14	AM-15	AM-21	AM-22	AM-23	AM-25	AM-26
SiO_2	49,34	50,43	50,99	50,13	51,15	51,15	51,33
TiO_2	0,94	0,81	0,89	0,90	0,83	0,84	0,96
Al_2O_3	16,70	16,35	15,81	15,80	16,81	16,03	15,55
Fe_2O_3	11,28	10,75	10,91	10,93	10,17	10,62	11,06
MnO	0,27	0,19	0,27	0,29	0,16	0,25	0,19
MgO	6,29	7,64	7,18	7,33	6,26	7,46	6,60
CaO	13,08	11,06	11,13	11,07	11,52	10,85	10,30
Na_2O	1,45	2,14	2,27	2,08	2,57	2,24	3,13
K_2O	0,51	0,50	0,42	0,34	0,43	0,44	0,72
P_2O_5	0,14	0,13	0,13	0,13	0,10	0,12	0,16
TOTAL	100,00	100,00	100,00	100,00	100,00	100,00	100,00
Sr	239	301	209	198	212	197	226
Rb	17	10	6	4	8	7	12
Y	23	22	26	25	22	23	28
Zr	68	59	76	75	74	72	94
Nb	3	2	3	3	3	3	4
Co	51	49	50	52	43	50	43
V	260	223	238	248	237	215	203
Cr	327	363	340	359	338	306	280
Zn	80	78	78	77	68	67	72
Cu	79	81	85	88	83	92	82
Ni	98	112	107	117	74	113	66

TABLE 3 : MAJOR ELEMENT ANALYSES (NORMALIZED TO 100%) AND TRACE ELEMENT ANALYSES

	Roodehoek Unit						Strypoort Unit
	AM-27	AM-31	AM36T	AM36M	AM36B	AM-46	AM-24
SiO_2	51,59	51,02	51,01	49,60	51,97	51,83	51,56
TiO_2	0,96	0,90	1,06	0,90	1,17	0,89	1,13
Al_2O_3	15,40	16,01	15,80	14,55	15,24	15,65	17,01
Fe_2O_3	10,74	10,75	11,71	11,83	11,38	10,35	10,49
MnO	0,26	0,25	0,28	0,27	0,19	0,23	0,22
MgO	7,48	6,65	6,52	10,32	6,30	6,28	5,70
CaO	10,06	11,70	10,07	9,89	10,41	11,76	9,99
Na_2O	2,60	2,31	2,77	2,16	2,56	2,43	2,41
K_2O	0,76	0,27	0,63	0,43	0,60	0,45	1,26
P_2O_5	0,15	0,14	0,15	0,14	0,18	0,13	0,23
TOTAL	100,00	100,00	100,00	100,00	100,00	100,00	100,00
Sr	231	206	205	167	177	179	296
Rb	26	4	12	8	11	4	18
Y	24	24	27	23	31	22	29
Zr	77	75	85	74	109	77	153
Nb	2	-	4	3	4	2	19
Co	49	47	46	60	44	49	48
V	219	239	229	210	214	272	255
Cr	324	333	310	402	264	370	303
Zn	61	73	87	85	72	76	85
Cu	94	94	88	74	91	83	79
Ni	97	70	60	186	92	124	70

TABLE 3 : MAJOR ELEMENT ANALYSES (NORMALIZED TO 100%) AND TRACE ELEMENT ANALYSES

	Perdekop Unit		Dolerites				
	AM-28	AM-40	AA-21	AA-22	AA-23	AA-30	AA-31
SiO_2	51,11	51,09	49,36	51,26	55,92	50,73	51,42
TiO_2	1,06	1,02	1,32	1,04	1,19	0,87	0,76
Al_2O_3	15,54	15,60	18,21	15,26	13,78	16,11	16,01
Fe_2O_3	11,32	10,94	12,46	11,95	12,43	10,84	10,09
MnO	0,18	0,23	0,16	0,18	0,18	0,15	0,15
MgO	6,77	7,22	6,11	5,96	3,88	7,24	7,33
CaO	10,85	10,60	7,84	10,73	7,83	11,12	11,47
Na_2O	2,28	2,44	4,42	2,78	2,66	2,36	2,33
K_2O	0,71	0,67	-	0,67	1,89	0,44	0,33
P_2O_5	0,18	0,19	0,12	0,17	0,24	0,14	0,11
TOTAL	100,00	100,00	100,00	100,00	100,00	100,00	100,00
Sr	244	245	359	189	279	205	205
Rb	12	12	1	14	48	6	5
Y	24	24	33	23	32	18	21
Zr	88	89	79	104	175	73	86
Nb	7	8	1	6	10	3	5
Co	47	47	69	43	38	44	43
V	209	213	495	247	206	226	209
Cr	222	233	136	260	28	391	390
Zn	82	69	126	83	100	73	72
Cu	78	69	216	102	52	77	87
Ni	78	82	82	68	33	117	130

TABLE 3 : MAJOR ELEMENT ANALYSES (NORMALIZED TO 100%) AND TRACE ELEMENT ANALYSES

Modderfontein Basalts

	AM-50	AM-51	AM-52	AM-53
SiO_2	51,36	54,33	53,07	51,86
TiO_2	0,97	0,93	1,05	1,14
Al_2O_3	15,36	14,82	15,67	16,14
Fe_2O_3	10,92	10,09	10,32	10,56
MnO	0,18	0,22	0,21	0,24
MgO	7,36	6,67	6,66	6,66
CaO	10,74	10,07	9,92	11,03
Na_2O	2,35	2,34	2,35	1,91
K_2O	0,62	0,38	0,55	0,24
P_2O_5	0,14	0,15	0,20	0,22
TOTAL	100,00	100,00	100,00	100,00
Sr	207	207	322	250
Rb	11	18	14	2
Y	24	23	26	26
Zr	84	104	106	107
Nb	6	7	6	6
Co	47	46	42	42
V	237	249	234	238
Cr	370	372	354	332
Zn	70	76	77	85
Cu	83	78	33	38
Ni	100	97	22	24

TABLE 4 : AVERAGE GEOCHEMISTRY OF THE BROSTERLEA BASALTS AND OTHER COMPARABLE KAROO IGNEOUS ROCKS

	Roodehoek (9 ANALYSES)		Vaalkop (10 ANALYSES)		Perdekop (2 ANALYSES)		Strypoort (1 ANALYSIS)	
	$\bar{x}$	$\frac{100\sigma}{x}$	$\bar{x}$	$\frac{100\sigma}{x}$	$\bar{x}$	$\frac{100\sigma}{x}$	$\bar{x}$	$\frac{100\sigma}{x}$
SiO_2	50,63	1,2	52,88	0,7	50,96	-	51,56	-
TiO_2	0,88	4,8	1,13	2,8	1,04	-	1,13	-
Al_2O_3	16,23	2,2	15,47	0,9	15,53	-	17,01	-
Fe_2O_3	10,78	3,0	10,48	2,4	11,10	-	10,49	-
MnO	0,24	-	0,22	-	0,21	-	0,22	-
MgO	6,98	7,6	6,37	2,3	6,98	-	5,70	-
CaO	11,49	6,1	9,51	9,2	10,95	-	9,99	-
Na_2O	2,15	14,9	2,55	18,2	2,35	-	2,41	-
K_2O	0,42	19,0	1,09	29,2	0,69	-	1,26	-
P_2O_5	0,13	-	0,22	-	0,19	-	0,23	-
TOTAL	100,00		100,00		100,00		100,00	
Sr	223	15,4	226	27,0	245	-	296	-
Rb	8	52,2	27	37,5	12	-	18	-
Y	24	5,9	28	4,7	24	-	29	-
Zr	71	7,9	115	4,9	89	-	153	-
Nb	3	16,7	7	11,1	8	-	19	-
Co	49	5,7	44	4,8	47	-	48	-
V	237	5,8	248	2,4	211	-	255	-
Cr	338	5,3	326	20,7	228	-	303	-
Zn	74	21,1	89	4,4	76	-	85	-
Cu	81	6,0	39	5,7	74	-	79	-
Ni	99	18,0	23	8,0	80	-	70	-

TABLE 4 : AVERAGE GEOCHEMISTRY OF THE BROSTERLEA BASALTS AND OTHER COMPARABLE KAROO IGNEOUS ROCKS

	Roodehoek[1] Andesites (7 ANALYSES)		Lesotho[2] (Naude's Nek) (32 ANALYSES)		Kraai River[3] (23 ANALYSES)		Drumbo[4] (9 ANALYSES)	
	$\bar{x}$	$\frac{100\sigma}{x}$	$\bar{x}$	$\frac{100\sigma}{x}$	$\bar{x}$	$\frac{100\sigma}{x}$	$\bar{x}$	$\frac{100\sigma}{x}$
SiO_2	66,36	0,5	51,52	2,5	54,15	2,3	51,91	1,6
TiO_2	0,78	1,8	0,95	6,2	0,87	3,2	1,02	3,6
Al_2O_3	16,02	0,5	15,68	3,1	15,22	1,2	15,51	1,3
Fe_2O_3	6,05	2,3	11,01	4,3	10,07	3,0	10,16	3,4
MnO	0,15	-	0,16	-	0,21	-	1,58	-
MgO	2,48	2,8	7,10	7,6	6,60	8,9	5,85	5,2
CaO	2,55	9,6	10,58	6,0	10,06	4,4	10,04	2,2
Na_2O	2,47	5,8	2,17	14,0	2,26	11,0	2,53	7,4
K_2O	2,96	4,2	0,67	39,0	0,39	70,0	1,20	5,1
P_2O_5	0,18	-	0,16	-	0,17	-	0,21	-
TOTAL	100,00		100,00		100,00		100,00	
Sr	246	6,2	183	16,0	202	7,7	306	6,2
Rb	118	3,7	13	72,0	20	57,0	21	7,7
Y	30	3,2	24	9,3	27	5,0	26	3,1
Zr	219	1,7	91	12,0	113	4,3	149	3,9
Nb	11	5,8	4	22,0	5	20,0	16	3,9
Co	20	4,5	46	4,4	37	7,6	40	3,6
V	87	5,4	234	7,7	235	7,1	218	4,6
Cr	82	6,1	271	18,0	261	7,4	295	6,9
Zn	83	4,0	85	7,5	81	5,9	83	6,7
Cu	21	8,7	83	11,7	61	8,2	71	8,4
Ni	22	7,6	89	16,0	50	16,0	67	10,0

[1] Rumble (1979)

[2] Pemberton (1979)

[3] Pemberton (1978), Barree (1977), Robey (1976)

[4] Pemberton (1978)

TABLE 4 : AVERAGE GEOCHEMISTRY OF THE BROSTERLEA BASALTS AND OTHER COMPARABLE KAROO IGNEOUS ROCKS

	Karoo[5] Dolerites (19 ANALYSES)	Omega Member[6] Massive Unit (7 ANALYSES)	Omega Member[7] Flow Unit (6 ANALYSES)
SiO_2	52,58	50,84	51,44
TiO_2	1,00	0,80	0,85
Al_2O_3	15,47	15,76	15,54
Fe_2O_3	11,37	10,41	10,57
MnO	0,18	0,16	0,16
MgO	6,63	7,84	7,21
CaO	10,69	11,22	11,38
Na_2O	2,27	2,36	2,32
K_2O	0,61	0,41	0,41
P_2O_5	0,17	0,20	0,12
Sr	206	192	186
Rb	13,6	6,2	6,6
Y	27,7	21,5	21,9
Zr	102	72	70
Nb	7,4	2,8	2,6
Co	41,7	44	46
V	239	213	242
Cr	243	442	409
Zn	84	71	77
Cu	93	80	85
Ni	78	119	113

[5] Robey (1976)

[6] J. Pemberton (1978) and M. Pemberton (1979)

[7] Bowen (1979

8. TRACE ELEMENT GEOCHEMISTRY

8.1 Introduction

Indications from major element chemistry are that the Brosterlea basalt suite constitutes a series of chemically unrelated basalt units. It remains, in this section, for this hypothesis to be tested against trace element data. In the following sections, the trace elements are dealt with individually in terms of simple, Harker-type diagrams. This is followed by a summary of the interelement ratio data. After a discussion of the theory behind trace element modelling, the significance of the trace element chemistry of the Brosterlea basalts and related rocks is evaluated. The trace elements analysed for are Sr, Rb, Y, Zr, Nb, Co, V, Cr, Zn, Cu and Ni.

8.2 Trace Element Variation Diagrams

Trace element variations are represented diagrammatically in a similar manner to the major elements, using SiO_2 as an index of differentiation (Fig. 24a-1). In this section, each separate element is briefly described.

8.2.a Strontium (Sr)

The Sr values of the Brosterlea basalts display a wide scatter (Fig. 23a), which tends to blur any differentiation pattern which might otherwise have been present. The Vaalkop Unit ranges between 167 and 435 ppm Sr, with an average value of 266 ppm, whilst the Roodehoek Unit has a range of 167-301 ppm (average 223 ppm). The lone sample of the Strypoort Unit has a Sr content of 296 ppm, which compares favourably with the values for the Drumbo Basalt Member (range 287 - 343 ppm, average 307 ppm : Pemberton, 1978). The Perdekop Unit of Brosterlea, with an average concentration of 244 ppm, exceeds the range of Sr values (185 - 233 ppm) quoted by Pemberton (op. cit.) for the Lesotho Formation of the Barkly East area. Of the dolerites, the two Modderfontein analyses (AA-30 and AA131) and the Brosterlea radial dyke (AA-22) fall within the range of 165 - 250 ppm quoted by

Robey (1976) for the dolerites of the north-eastern Cape, whilst AA-21 and AA-23, the two unusual dolerites from Brosterlea, fall well out of the said range.

8.2.b Rubidium (Rb)

The sympathetic behaviour of Rb and K is well illustrated by the rocks of the Brosterlea suite (compare Fig. 21h and Fig. 23b). The Roodehoek (average 8 ppm, range 4-26 ppm) has a lower Rb concentration than does the more differentiated Vaalkop Unit (average 27 ppm, range 5-48 ppm). AM-13, a member of the Vaalkop Unit, is noteworthy for its anomalously low Rb (5 ppm) relative to the other Vaalkop samples. The low Rb of AM-13 is mirrored in a relatively low K-content of 0,34 wt. %. The Strypoort Unit (18 ppm Rb) and the Perdekop Unit (12 ppm Rb) are intermediate between the Roodehoek and Vaalkop Units. A comparison of the Brosterlea Rb data with the data of Pemberton (1978), Pemberton (1979) and Bowen (1979) for the Barkly East district shows broad similarities between the Roodehoek Unit and the Omega Formation, the Vaalkop Unit and the Kraai River Formation, the Strypoort Unit and the Drumbo Basalt Member, and between the Perdekop Unit and the Lesotho Formation.

The Rb content of the Modderfontein lavas does not vary much with differentiation, and all these lavas have Rb concentrations below 20 ppm. The Modderfontein dolerites, together with the Brosterlea radial dyke (AA-22), have Rb values around 20 ppm, whereas the Brosterlea ring dyke (AA-21) is relatively low in Rb (1 ppm), and the Dragon's Back is strongly enriched (48 ppm).

8.2.c Yttrium (Y)

Yttrium contents are fairly constant throughout the Brosterlea and Modderfontein suites (Fig. 23c), with very few samples outside the range of 20 - 30 ppm Y. In the Brosterlea suite, the Strypoort and Vaalkop Units, lying between 25 and 30 ppm Y, are slightly enriched relative to the Roodehoek and Perdekop Units, which generally do not

exceed 25 ppm Y. A glance at the average Karoo yttrium values (Table 4) indicates that the majority of Karoo basalts fall within the range 20 - 30 ppm Y.

8.2.d Zirconium (Zr) and Niobium (Nb)

Zr and Nb, along with other incompatible elements, provide a good visual separation, on Harker diagrams, of the various basalt units at Brosterlea, each unit having distinctive Zr and Nb concentrations (Fig. 23d and e).

The average Zr and Nb values of the Strypoort Unit are relatively high (153 and 19 respectively), and agree closely with the data for the Drumbo Basalt Member (Pemberton, 1978). The Perdekop Unit has similar average Zr values to the Lesotho Formation (89 ppm, as compared with 91 ppm), but the Perdekop Nb values are somewhat higher than the Lesotho values (8 ppm as compared with 4 ppm). From Table 4, the Nb and Zr of the Roodehoek Unit are seen to compare favourably with the Omega Formation values, whilst the Vaalkop Unit values compare with those of the Kraai River Formation.

8.2.e Cobalt (Co)

In common with the Barkly East basalts, the Molteno basalts are generally constrained within the range 40 - 50 ppm Co. Notable exceptions are the Brosterlea ring dyke (69 ppm Co), and AM36M, from the Tafelkop sampling locality (60 ppm Co). The Vaalkop Unit appears to be slightly depleted in Co, the majority of these rocks having Co contents below 45 ppm, whereas most of the rocks of the other Brosterlea units have Co contents in the range 45 - 50 ppm.

8.2.f Vanadium (V)

Although there is some scatter of values, the mean value for almost all the basalts and dolerites of the Molteno district is in the region of 240 ppm, and there is very little variation of values from unit to unit, although the Vaalkop and Strypoort values are marginally higher than the majority of the Roodehoek and Perdekop vanadium values (Fig. 23g).

The only rock with a particularly unusual V-content is sample AA-21, the Brosterlea ring dyke. This rock has an extremely high V-content of 495 ppm, which ties in with its abnormal enrichment in the other transition metals.

The levels of vanadium in the Molteno basalts are typical of the concentrations encountered in most Karoo basalts (Table 4).

8.2.g Chromium (Cr)

The chromium values of most of the rocks of the Roodehoek, Vaalkop and Strypoort Units range between 280 and 370 ppm, and no discernible trends emerge. The Perdekop Unit, on the other hand, is substantially lower than the rest, with an average chromium content of 228 ppm (Fig. 23h). Sample AM-32, a member of the Vaalkop Unit, has an anomalously low Cr-content of 129 ppm.

The lavas of the Modderfontein suite have extremely constant Cr-contents, ranging from 330 ppm to 370 ppm, whilst the Modderfontein dolerites have somewhat higher Cr values of the order of 390 ppm. The Brosterlea dolerites display a scatter of values, the most "normal" being AA-22, with a value of 260 ppm. The Brosterlea ring dyke has a Cr-content of 126 ppm, and the Dragon's Back an even lower value of 28 ppm.

8.2.h Nickel (Ni)

The Roodehoek, Strypoort and Perdekop Units all have Ni values in the range 66 ppm to 124 ppm, considerably higher than the Vaalkop Unit, which has Ni values very tightly clustered within the range 20 - 26 ppm (Fig. 23j). The only really anomalous Ni value in the Brosterlea suite is that of AM36M (186 ppm), but this has already been explained in section 6.1 in terms of olivine enrichment.

The Modderfontein basalts display a wide scatter of Ni values in the range 22 - 100 ppm, whilst the Modder-

fontein ring dyke dolerites average 124 ppm Ni. Amongst the Brosterlea dolerites, AA-21 and AA-22 display fairly normal values of 82 ppm and 68 ppm, respectively, whereas the Dragon's Back (AA-23) has a somewhat lower Ni-content of 33 ppm.

From Table 4, there is reasonable agreement between the Lesotho Formation and the Perdekop Unit, the Drumbo and the Strypoort Unit, the Roodehoek Unit and the Omega Member, and between the Kraai River Formation and the Vaalkop Unit.

8.2.j Copper (Cu)

The trends in Cu values in the Molteno basalts and dolerites are very similar to the Ni trends, with the Vaalkop Unit having lower concentrations of Cu than are displayed by the other units in the Brosterlea suite. The Vaalkop Unit has copper concentrations in the range 36 - 42 ppm, with the exception of sample AM-11, which has an anomalously high Cu-content of 80 ppm. By contrast, the balance of the basalt units at Brosterlea have copper contents in the range 69 - 92 ppm (Fig. 23k).

As is the case with nickel, the Brosterlea units compare reasonably with their putative counterparts in Barkly East in terms of Cu-contents, with the exception of the Vaalkop Unit, which has discernibly lower Cu than does the Kraai River Formation (average values 39 ppm and 61 ppm, respectively).

The Brosterlea and Modderfontein dolerites fall within the same limits of Cu concentration as do the basalts, with the exception of AA-21, which has a very high Cu-content of 216 ppm.

8.2.k Zinc (Zn)

In terms of Zn, the Vaalkop Unit generally has higher contents than do the other Brosterlea basalt units. The Vaalkop Unit ranges from 82 - 96 ppm Zn, whereas the rest of the Brosterlea basalts range between 61 and 87 ppm zinc (Fig. 23l).

The Modderfontein Basalts, with Zn values in the range 70 - 85 ppm, display no discernible differentiation trend. The Modderfontein dolerites (72 - 73 ppm Zn) fall within the limits of the zinc contents of their associated basalts. Amongst the Brosterlea dolerites, AA-22 is comparable with the Brosterlea basalts in terms of Zn, but AA-21 and AA-23 have rather higher Zn-contents (126 ppm and 100 ppm, respectively).

The Barkly East basalts are consistent in having Zn contents in the range 80 - 85 ppm (average values; Table 4), with the exception of the Omega Member, which has an average Zn value of 71 ppm (data from the massive unit).

8.3 Interelement Ratios

A selection of the more significant interelement ratios for the Brosterlea and Modderfontein basaltic rocks is listed in Table 5, and interelement ratio trends are diagrammatically represented in Fig. 24 (a-e). Observed trends in interelement ratios are briefly described below. Their significance in terms of differentiation models will be discussed in a later section, together with data on the variation of the individual trace elements.

The K/Rb ratio varies widely for the Molteno basalts, with ranges of values from 242 to 934 for the Roodehoek Unit, 273 to 565 for the Vaalkop Unit, and 463 to 491 for the Perdekop Unit. The lone Strypoort Unit sample has a K/Rb value of 581. The Modderfontein basalt suite shows a wide variation, from 175 to 996.

The Cr/Ni ratio effectively distinguishes the Vaalkop Unit from the other basalt Units of the Brosterlea complex (Fig. 24a). Whereas the Cr/Ni ratios of the Roodehoek, Strypoort and Perdekop Units do not exceed a value of 6, the Vaalkop Unit gives ratios in the range 13 - 17, with the exception of AM-32 which, as previously noted, has an anomalously low Cr content.

The Ti/Al values of the Roodehoek Unit are widely scattered in the range 5,6 - 8,8, whereas the Vaalkop Ti/Al values are more tightly grouped between 8,0 and 8,8. There are not enough data available on the Perdekop and Strypoort Units for any meaningful trends to be drawn from them in terms of a ratio as complex as is Ti/Al. Pearce and Flower (1977) use both the Ti/Al ratio and the Cr/Ti ratio in an attempt to identify fractionation trends in basalts, but the results are equivocal, especially in the latter case. The Cr/Ti data included in Table 5 show that there is very little distinction between the different units at Brosterlea on the basis of this ratio, although some of the Roodehoek Unit rocks do have somewhat higher Cr/Ti values than does the average Vaalkop Unit basalt.

The Zr/Y ratio (Table 5; Fig. 24c) is one of the classic incompatible element ratios. In the Brosterlea suite, this ratio effectively distinguishes between the Roodehoek, Vaalkop, and Strypoort Units, with the Perdekop Unit having similar Zr/Y values to the Roodehoek Unit. The Roodehoek Unit values for Zr/Y range from 2,68 to 3,52, with the Perdekop Unit values marginally higher (3,67 - 3,71). The Vaalkop Unit displays values between 3,96 and 4,21, and AM-24, the sole representative of the Strypoort Unit, a value of 5,28.

Another significant incompatible element ratio is Zr/Nb (Fig. 24d). In terms of this ratio, all the Brosterlea units may be distinguished from one another. The Strypoort (8,05) has the lowest Zr/Nb ratio, followed by the Perdekop Unit (11,13 - 12,57). The Vaalkop Unit ranges in Zr/Nb values from 14,13 to 18,17, whilst at the top end of the scale, the Roodehoek Unit varies from 21,25 to 38,50.

A third ratio incorporating Zr is the Ti/Zr ratio (Fig. 24e). This ratio, similarly to the previous two, also provides a means of distinguishing one unit from another in the Brosterlea basalt suite. The lowest Ti/Zr value is that of the Strypoort Unit (44,28). Moving up the scale, the

Vaalkop Unit has values from 55,95 to 61,60. The Roodehoek Unit Ti/Zr values vary from 61,23 to 82,87, whilst the Perdekop Unit has Ti/Zr values of 68,71 and 72,21 for its two samples.

8.4 Theoretical Basis for Trace Element Modelling

Trace element modelling relies on the basic concept of the partition coefficient, which is an expression of the relative concentrations of any single element between two coexisting phases. In the case of most igneous systems, the two phases under consideration will be a crystalline phase and its coexisting parent liquid. In this case, a simple expression of the Partition Coefficient (K) will be :

$$K = \frac{[X]_{\text{crystal}}}{[X]_{\text{liquid}}} \qquad (1)$$

where [X] = concentration of the trace element X.

From K, Greenland (1970) derives a bulk distribution coefficient for fractional crystallisation :

$$D_s = W^a K^{a/l} + W^b K^{b/l} + \ldots\ldots \qquad (2)$$

where K is the solid-liquid partition coefficient for each of the precipitating phases, a, b etc., and W is the weight fraction of each precipitating phase.

Once D_s has been calculated, it may be incorporated into Greenland's (op. cit.) equation for fractional crystallisation :

$$\frac{C_L}{C_i} = F'^{(D_s - 1)} \qquad (3)$$

In this equation, F' is the fraction of liquid remaining, C_i is the concentration of a given trace element in the initial melt, C_L is the concentration of the element in the differentiated liquid.

Working from equation (3), when D_s approaches zero,

$$\frac{C_L}{C_i} \approx \frac{1}{F'} \qquad (4)$$

in which case the extent of crystallisation of the liquid is the only control on the concentration of the element in the residual melt. As D_s increases in magnitude above a value of $D_s = 1$, the residual liquid becomes progressively more depleted in the given element.

Greenland's (op. cit.) equations are applicable, in strict terms, only to the simplified case of phases crystallising in constant proportions with constant partition coefficients (Arth, 1976). Albarede and Bottinga (1972) show that variables such as crystal growth rate and trace element diffusion affect equilibrium crystallisation, resulting in deviations from ideal behaviour of the partition coefficient. Other factors affecting partition coefficients are temperature, pressure, and melt composition and structure (Irving, 1978). In addition, partition coefficient modelling requires that trace elements obey Henry's law for dilute solutions, which means that the upper limit of Henry's law behaviour must be determined for the element under consideration. This problem is discussed by Mysen (1978).

The case of batch partial melting, whereby a magma is generated from an original parent melt, is dealt with by Shaw (1970). Shaw's treatment is based on the equation :

$$C_L/C_O = 1/[D_o + F(1-P)] \qquad (5)$$

in which the concentration of a given trace element in a melt (C_L), relative to the concentration of the element in the residual parent (C_o), is controlled by D_O, the bulk distribution coefficient of the parent for a given trace element at the onset of melting, and by F, the weight fraction of melt relative to the residual parent, and also by P, the bulk distribution coefficient of the minerals making up the melt. By rearrangement of equation (5) :

$$C_L/C_O = 1/[(D_o - PF) + F] \quad (6)$$

it can be seen that D_o, the bulk distribution coefficient of the residual, changes with the extent of melting, the latter being represented by the factor PF. Equation (6) only applies while the main mineral phases involved in partial melting are still present in the residual fraction.

Hertogen and Gijbels (1976) have presented derivatives of Shaw's equations which overcome the restriction that no mineral phase in the residual may be used up, and allow melting proportions and mineral/melt distribution coefficients to vary during melting. These equations, however, require accurate estimates of the effect of temperature and mineral and melt compositions on mineral/melt distribution coefficients, and also require an understanding of the phase equilibria operational during partial melting. Since such information is poorly documented, Shaw's (op. cit.) equations are more useful in the general case than are those of Hertogen and Gijbels (1976).

Although there is a degree of consistency shown by trace element partition coefficient data, it is apparent, from such works as Albarede and Bottinga (1972) and Irving (1978) that it is impossible to construct a table of standard partition coefficients. Instead, as cautioned by Irving (op. cit.), reference works must be critically examined to ascertain the degree of applicability to the specific problem in hand. A list of partition coefficients used in this study is provided in Table 6.

Hanson (1978) introduces a semi-quantitative aspect to the treatment of interelement ratios (specifically, the K/Rb ratio) with the equation :

$$\frac{C_L K/Rb}{C_O K/Rb} = \frac{D_{Rb}(1 - F) + F}{D_K(1 - F) + F} \quad (7)$$

From this equation, the K/Rb ratio of the melt, relative to the K/Rb ratio of the parent, is a function of D (the distribution coefficient) and F (the fraction of melt relative to the parent). If D is smaller than F for both K and Rb, then the K/Rb of the melt (C_L K/Rb) approaches C_OK/Rb (the K/Rb of the parent). From equation (7), the relative values of D_K and D_{Rb} (D_K/D_{Rb}) can only affect the K/Rb of the melt for small degrees of partial melting i.e. when F is numerically much smaller than the D_K and D_{Rb} values.

8.5 Evaluation of Trace Element Data

Using the theoretical models discussed in section 8.4, the trace element variation trends described in sections 8.2 and 8.3 can now be used to test the hypotheses erected so far on the basis of major element geochemistry.

8.5a Rubidium and Strontium

Strontium has an ionic radius of 1,18 Å, intermediate between Ca (0,99 Å) and K (1,33 Å). Rubidium is very close to K in terms of electronegativity, ionization potential and ionic size and, indeed, in terms of its geochemical behaviour. Rubidium acts as an incompatible element, with D_{Rb} considerably less than unity for the main mineral constituents of the basaltic assemblage (Table 6). Strontium is rejected by olivine and clinopyroxene, but enters the plagioclase lattice fairly readily (Table 6). Korringa and Noble (1971) calculate a fairly wide range of D^{Sr}_{plag} values, up to a value of 7, and relate variations to plagioclase composition. Sun, Williams and Sun (1974) and Drake and Weill (1975), on the other hand, find a much smaller range in D^{Sr}_{plag} values, and relate any variations to temperature effects.

From available partition coefficient data, it may be concluded that Rb will enrich progressively in a differentiating system. Strontium, on the other hand, will enrich only as long as plagioclase is not a fractionating phase.

The Rb data from the Brosterlea suite show trends similar to those of the other incompatible elements, with the Vaalkop Unit enriched in Rb relative to the Roodehoek, Strypoort and Perdekop Units (Fig. 23b). The relative Rb-enrichment of the more highly differentiated Vaalkop Unit could conceivably be taken as evidence of a differentiation trend from the Roodehoek Unit through to the Vaalkop Unit. On the other hand, batch partial melting of an inhomogeneous mantle source would produce variation in [Rb] from unit to unit, assuming that each unit were a separate partial melt.

The Sr data, and to a lesser extent the Rb data, display a scatter of values within each separate unit, particularly in the case of the Vaalkop Unit. Variations displayed by Rb and Sr do not persist into the behaviour of other, more stable trace elements, such as Y, Nb and Zr, which suggests that Sr and Rb variations are not primary effects. From work at Amherst Siding, in the eastern Cape Province, J.S. Marsh (pers. comm.) finds variations of the order of 20% in Sr values from a sample sequence taken through a sill some ten meters thick. These variations are not mirrored by the behaviour of the more stable trace elements. Data collected by Pemberton (1978) show marked within-flow variations in Sr and Rb with, once again, very little corresponding variation in elements like Nb, Y and Zr. This evidence leads to the conclusion that Sr and Rb variations in the Karoo are often due to secondary processes.

Attempts have been made in the past to relate the ratio K/Rb to the tectonic setting of igneous rocks (Lessing, 1963; Jakes and White, 1972). There seems little merit in this approach when applied to the Karoo igneous province, due to the wide K/Rb range encountered.

Erlank and Hofmeyer (1966) calculate K/Rb in the range 303 - 609 for the Karoo dolerites, which compares favourably with the spread of values from 229 to 514 encountered by Robey (1976) for chilled dolerites from the N.E. Cape Province.

It would appear from Pemberton's (1978) data (K/Rb = 148 - 714) and the results of the present study (K/Rb = 175 - 996) that the basalts of the Karoo Central Province show an even greater K/Rb variation than do the dolerites. As indicated by Pemberton (op. cit.), the K/Rb ratio variation in the Karoo basalts is too large to be the result of mineralogical controls only, and it must be assumed that weathering is responsible to a large extent for the observed variation. Seen in this light, the K/Rb ratio is of no great practical use in the present study.

8.5.b Zirconium, Yttrium and Niobium

Zr, Y and Nb, in common with the major element Ti, are all elements with a high field strength, i.e. charge/radius ratio (Pearce and Norry, 1979). This property means, as previously mentioned, that these elements tend to remain unaffected by secondary processes.

The mineral/liquid partition coefficients listed in Table 6 for Zr, Nb, Y and Ti are those recommended by Pearce and Norry (1979) for use with basic rocks. Ti has been included along with the trace elements in Table 6 because it is an incompatible element, and as such, is used along with incompatible trace element data in discussing incompatible element ratios.

The value of the truly incompatible behaviour of Zr and Nb within the basaltic mineral assemblage, as an indicator of petrogenetic processes, has been illustrated in the Karoo Province by Eales and Robey (1976) and by Erlank and Kable (1976). Within the Brosterlea basalt suite, Zr and Nb have distinctive values for each of the units, as described in section 8.2.d.

To fit a crystal fractionation model, the Brosterlea basalt units would be expected to fit a differentiation trend for each of the incompatible elements. Although the Vaalkop Unit is enriched in Zr and Nb relative to the Roodehoek Unit, the two units may hardly be described as

representing a continuum (Fig. 23d and e). A further nail in the coffin of a crystal fractionation model for the Brosterlea suite is the divergence of the Strypoort and Perdekop Units from any differentiation trend which may possibly be imagined for the Roodehoek and Vaalkop Units. This statement is particularly true in the case of Nb (Fig. 23e).

Yttrium, with slightly higher partition coefficients for clinopyroxene and plagioclase than are shown by Zr and Nb, displays very much more diffuse trends on the Harker diagram than do the latter two elements, although the patterns are similar (Fig. 23c). The dispersion of the Y values within each unit is probably a function of different relative proportions of clinopyroxene crystallisation, because of the relatively high partition coefficient of clinopyroxene for Y (D^{Y}_{cpx} = 0,5 : Table 6).

Incompatible elements, by their very nature, should be rejected from the crystal lattices of most early-crystallising minerals. From this, it follows that during fractional crystallisation (or partial melting), two incompatible elements in a comagmatic suite of liquid compositions should maintain a constant ratio, right up to the most extreme phases of the process. Departures from constancy of incompatible element ratios within a suite of volcanic rocks are generally attributed to the influences other than simple fractionation or partial melting.

Wood et al. (1979) find it difficult to relate Ti, Zr, Y and REE variations to simple partial melting models, and resort to the probability that regional inhomogeneities exist in the mantle source feeding the mid-ocean ridge (MOR) basalts. Erlank and Kable (1976) have investigated MOR basalts with anomalously low Zr/Nb ratios. These they believe to be products of small degrees of partial melting of relatively undepleted mantle, whereas more "normal" MOR basalts are considered to have been derived by more extensive partial melting of depleted mantle. (The term depletion, as

employed by Erlank and Kable, implies earlier fractionation and/or partial melting of the original mantle.) McCallum and Charrete (1978) have attempted to quantify such processes as that suggested by Erlank and Kable in terms of experimentally derived Zr and Nb partition coefficients, used in conjunction with the mass balance equation.

Kesson (1973) believes that variations in incompatible element ratios are due to patchy distribution of such accessory minerals as amphibole, mica and apatite, all of which contain certain amounts of the incompatible elements, in the upper mantle. In support of his argument, Kesson cites experimental work by Green (1973), which indicates that accessory minerals may break down very close to the peridotite solidus, releasing incompatible elements into the initial partial melt.

Erlank et al. (1979) present data from a variety of sources which suggest that the mantle below southern Africa is horizontally heterogeneous, and that compositional variation of the Karoo basalts from one part of southern Africa to another cannot be explained by simple partial melting, fractional crystallisation or crustal contamination models. It is suggested (Erlank et al.) that mantle heterogeneity below southern Africa is due to pre-Karoo metasomatic processes. Data from Pemberton (1978) show variations in incompatible element ratios in successive basalt units from the same geographic location in the Barkly East area. These variations Erlank et al. (op. cit.) attribute to vertical inhomogeneities in the mantle source.

Pearce and Norry (1979) show that crystal fractionation and single stage partial melting processes have very little effect in altering the Zr/Y ratio, and that the only processes which can significantly affect this ratio are progressive partial melting or the creation of (mantle) source heterogeneities. Pearce and Norry point out that the mechanics of melt extraction and opportunity for variable mixing of increments will place considerable constraints on how much fractionation can be achieved, in reality, by

progressive partial melting processes, which leaves source heterogeneity as the only simple mechansim whereby differentiation of the Zr/Y ratio may be achieved.

Variation of the Zr/Y ratio of the Brosterlea suite from a minimum of 2,68 (Roodehoek Unit) to a maximum of 5,28 (Strypoort Unit) is fairly substantial, and it is believed probable that this range is the result of mantle heterogeneity. As indicated by Pearce and Norry (op. cit.), the Zr/Nb ratio is often more informative than the Zr/Y ratio, being less prone to variation by partial melting processes. As described in section 8.3, the Zr/Nb ratios of the Brosterlea basalts range between 8 and 39. This very definite variation in Zr/Nb gives added weight to the conclusion, already drawn from the Zr/Y ratio, that mantle inhomogeneity is a more likely mechanism than partial melting for producing chemical variations within the Brosterlea basalt suite.

The third incompatible element ratio examined is Ti/Zr (Fig. 24e). As shown in Table 6, this ratio may be strongly affected by crystallisation of magnetite, which has a partition coefficient of 7,5 for Ti. The trends of Fig. 21a (TiO_2 vs. SiO_2) however, are not compatible with fractionation of any significant amounts of magnetite, which would have led to a decrease in Ti with differentiation. The variations in Ti/Zr (Fig. 24e) bolster the argument already advanced on the strength of the Zr/Y and Zr/Nb ratios.

Each of the ratios, Zr/Y, Zr/Nb and Ti/Zr are effective in distinguishing the various basalt units from one another, but is is noticeable that the Roodehoek Unit shows a much wider range of values than does, for example, the Vaalkop Unit for each of the ratios. The ranges of 64 - 83 for Ti/Zr, and 21 - 38 for Zr/Nb, may be considered significant, and indicate that there were even chemical variations in the mantle source area of the basalts within the Roodehoek Unit, the earliest of the units at Brosterlea.

Although they are not described in detail, the incompatible element ratios of the Modderfontein basalts (Table 5) indicate that this basalt suite, too, derived from an inhomogeneous source.

8.5.c Cobalt, Chromium and Vanadium

Co, Cr and V are all members of the first transition series of the periodic table. The essentially compatible behaviour of these three elements within the basaltic system is well established, with Cr and V competing with one another for the Fe sites in mineral lattices, whilst Co generally substitutes for Mg (Burns, 1970b).

Co, Cr and V all substitute with great propensity in the magnetite structure, as indicated by the high partition coefficients listed in Table 6. These three elements also substitute fairly readily in the clinopyroxene lattice, whilst they are all rejected by plagioclase. Co is fairly readily accepted by olivine, but V is rejected by this mineral, due to charge imbalance restrictions set up by the substitution of V^{3+} for Fe^{3+} (Taylor, 1965). The D_{Cr}^{ol} figures of 3,1 - 10 quoted by Flower (1973) are probably unrealistically high, and are quite possibly brought about by the presence of tiny inclusions of Cr-spinel in the olivine (Gunn, 1971). In the light of Gunn's considerations, D_{Cr}^{ol} evaluations should be treated with due caution. Experimental data quoted by Irving (1978) indicate a D_{Cr}^{ol} in the region of unity.

Apart from a certain amount of scatter, Cr, Co and V contents within each of the units are fairly constant, indicating that fractionation of the transition metal-rejecting plagioclase phase is compensated by fractionation of clinopyroxene and, possibly, a certain amount of olivine. Slight Co depletion in the more differentiated members of the Vaalkop Unit probably signifies an increased proportion of clinopyroxene crystallisation, and possibly a small amount of magnetite fractionation.

8.5.d Zinc, Copper and Nickel

Although Zn, Cu and Ni are technically members of the first transition series, they are treated separately from Co, Cr and V because of their rather different behaviour. The distinctive behaviour of Cu and Ni is manifest in their partition coefficients (Table 6). The geochemistry of Zn is extremely complex (Neuman, 1949; Ahrens, 1964), and there is little or no information in the literature regarding partition coefficients for this element.

With its high octahedral site preference energy (O.S.P.E.) of 15,2 Kcal.mole^{-1} (Burns, 1970b), and similar ionic radius to Fe^{2+}, Cu^{2+} would be expected to behave as a compatible element within the basaltic assemblage. That this is not the case is explained by Burns (1970b) in terms of the Jahn-Teller distortion which Cu presumably sets up in its coordination polyhedra. Nickel, intermediate in size between Fe^{2+} and Mg^{2+}, is essentially a compatible element, substituting fairly readily in magnetite, olivine and pyroxene, but being rejected by plagioclase. Particular interest has been devoted, in the literature, to the behaviour of Ni in olivine, and this topic has received some attention in section 6.2 of the present work. Zinc displays some of the traits of incompatible elements, and this Ahrens (1964) relates to the relatively covalent nature of the Zn-O bond.

From Fig. 23 (j and k) the compatible nature of Cu and Ni can be seen graphically, with the Vaalkop Unit depleted in these two elements relative to the less differentiated units at Brosterlea. It is evident, however, that the Brosterlea suite does not form a true fractionation suite, the Vaalkop Unit being too radically depleted relative to the other units to be considered part of a continuous trend. The anomalously high Ni content of sample AM36M has already been discussed in section 6.2 in terms of olivine enrichment. The anomalously high Cu content of sample AM11, a member of the Vaalkop Unit, must be due to enrichment in one or more Cu-rich phases.

Zn values show trends of slight enrichment in the Brosterlea suite, whereas the Modderfontein suite displays a trend of essentially constant Zn content with differentiation.

Fig. 23a : TRACE ELEMENT VARIATIONS (IN PARTS PER MILLION) USING WEIGHT % SiO_2 AS THE ABSCISSA

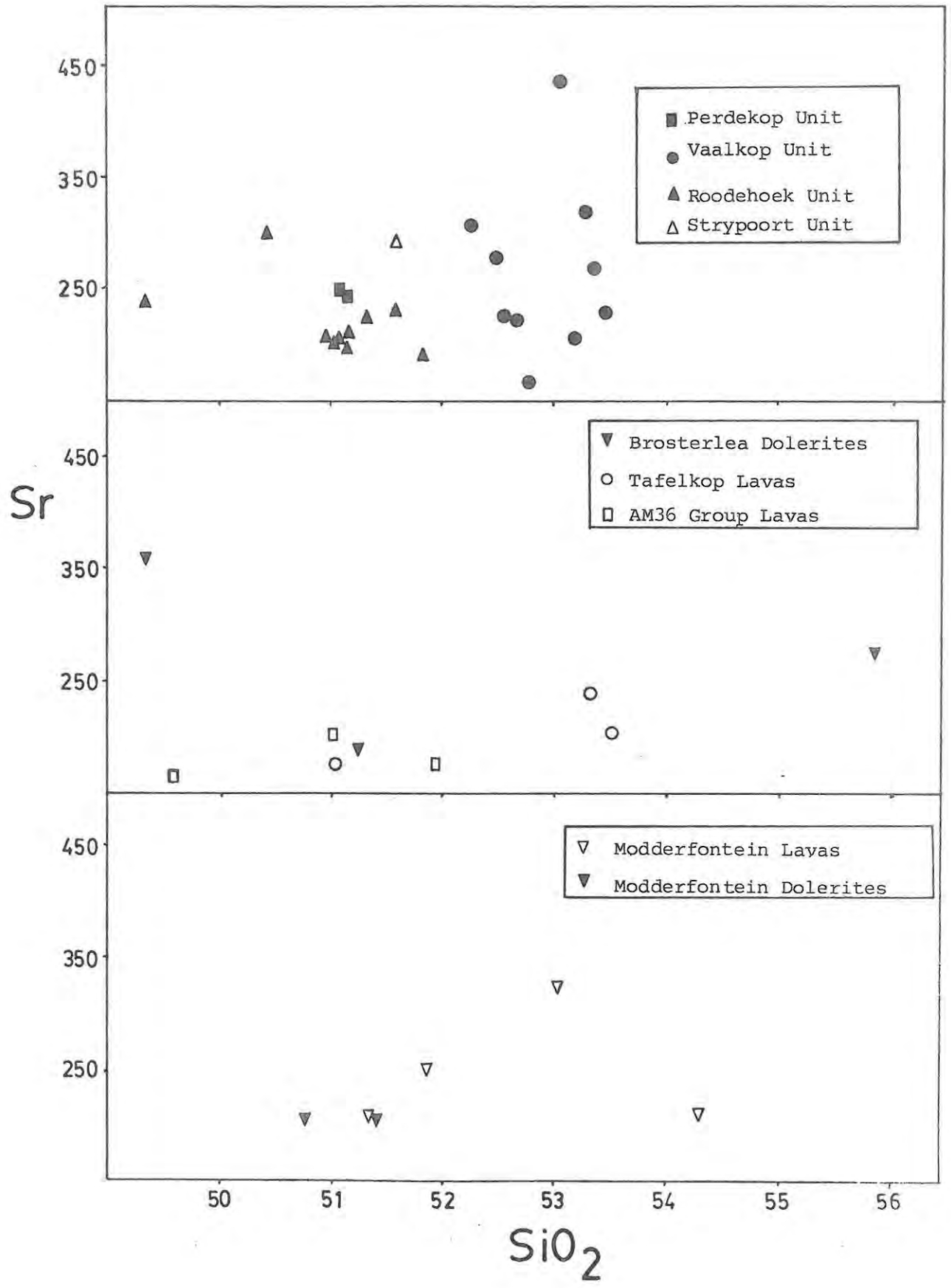

Fig. 29b : TRACE ELEMENT VARIATIONS (IN PARTS PER MILLION) USING WEIGHT % SiO_2 AS THE ABSCISSA

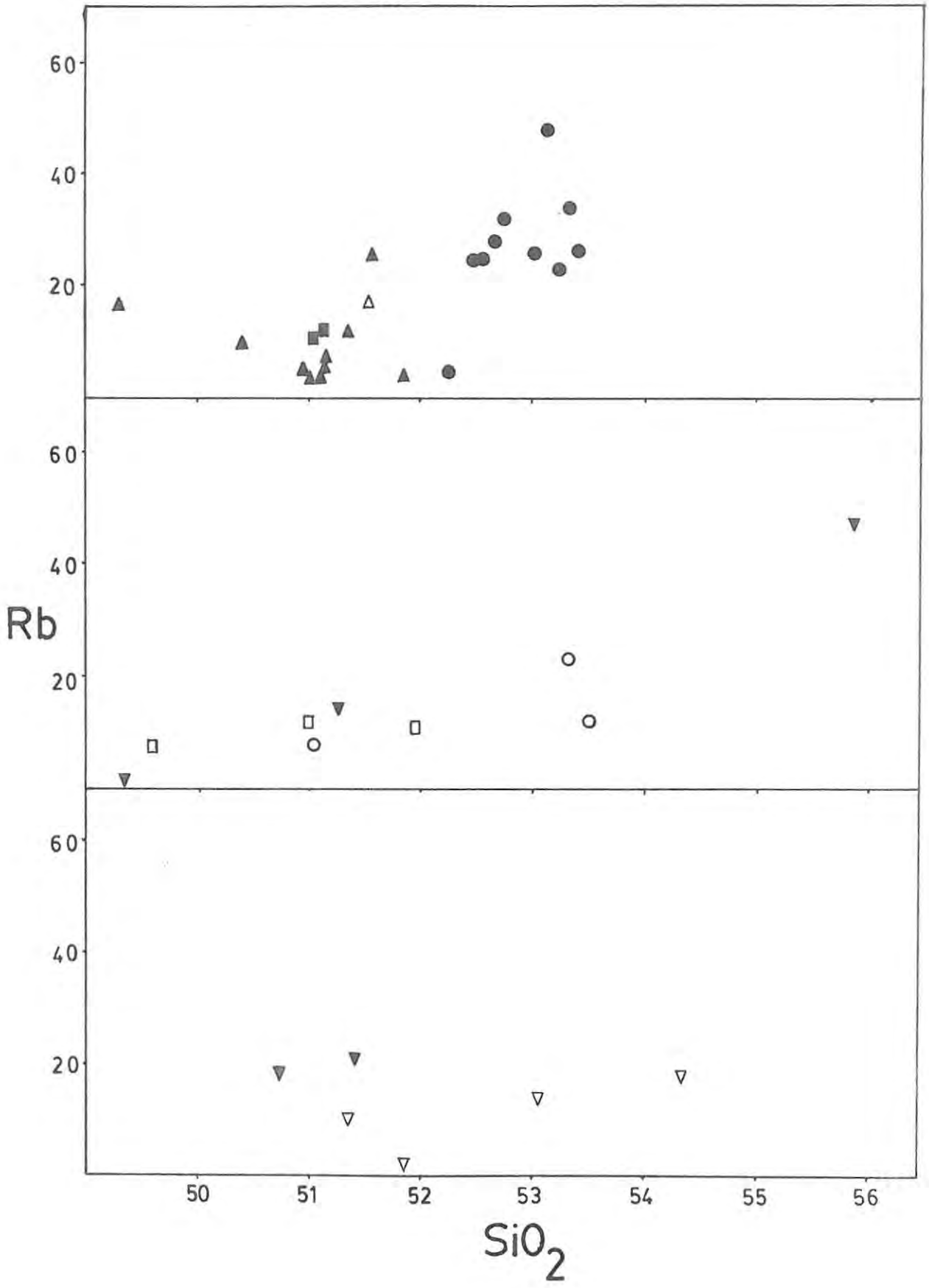

Fig. 23c : TRACE ELEMENT VARIATIONS (IN PARTS PER MILLION) USING WEIGHT % SiO_2 AS THE ABSCISSA

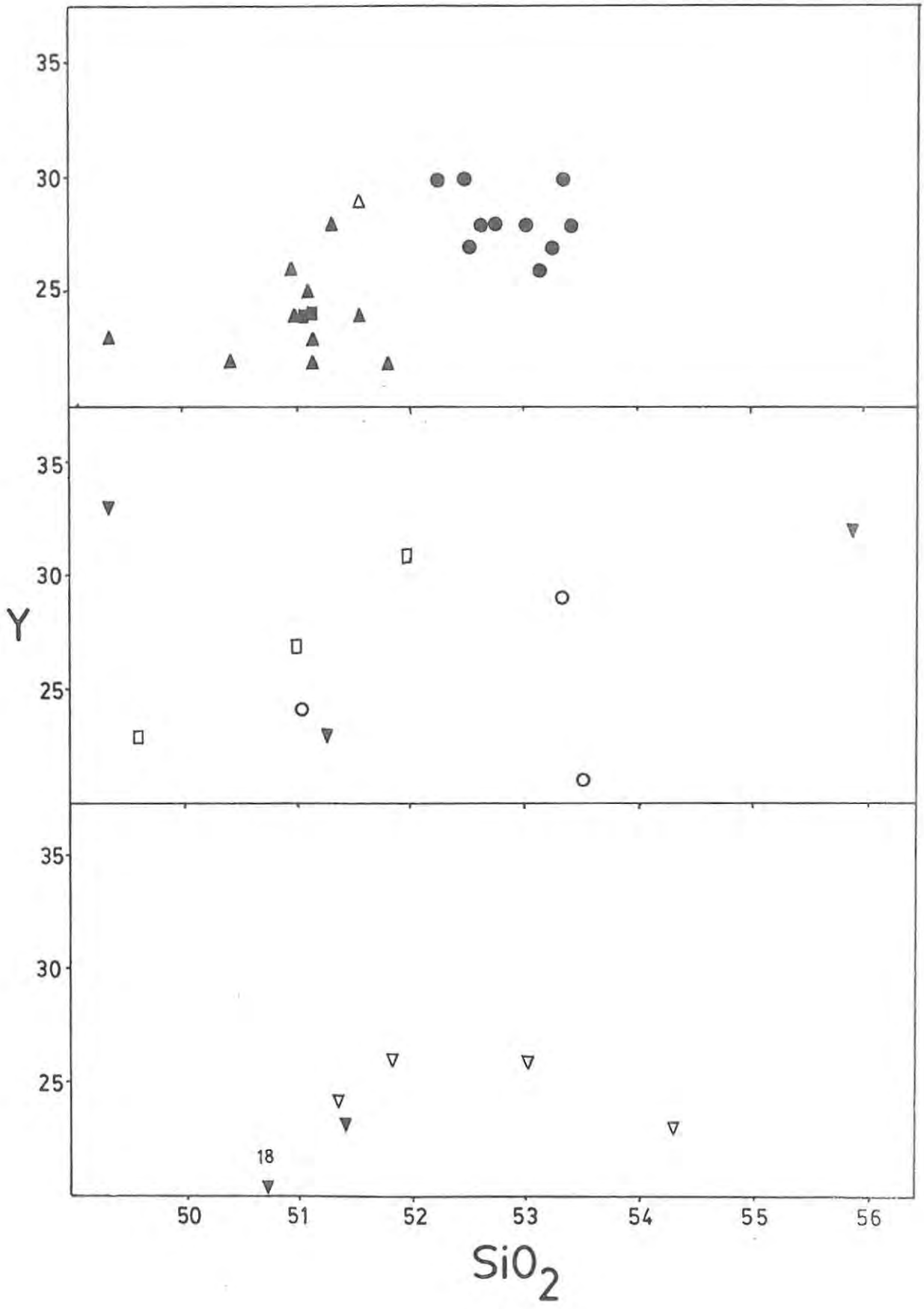

Fig. 23d : TRACE ELEMENT VARIATIONS (IN PARTS PER MILLION) USING WEIGHT % SiO_2 AS THE ABSCISSA

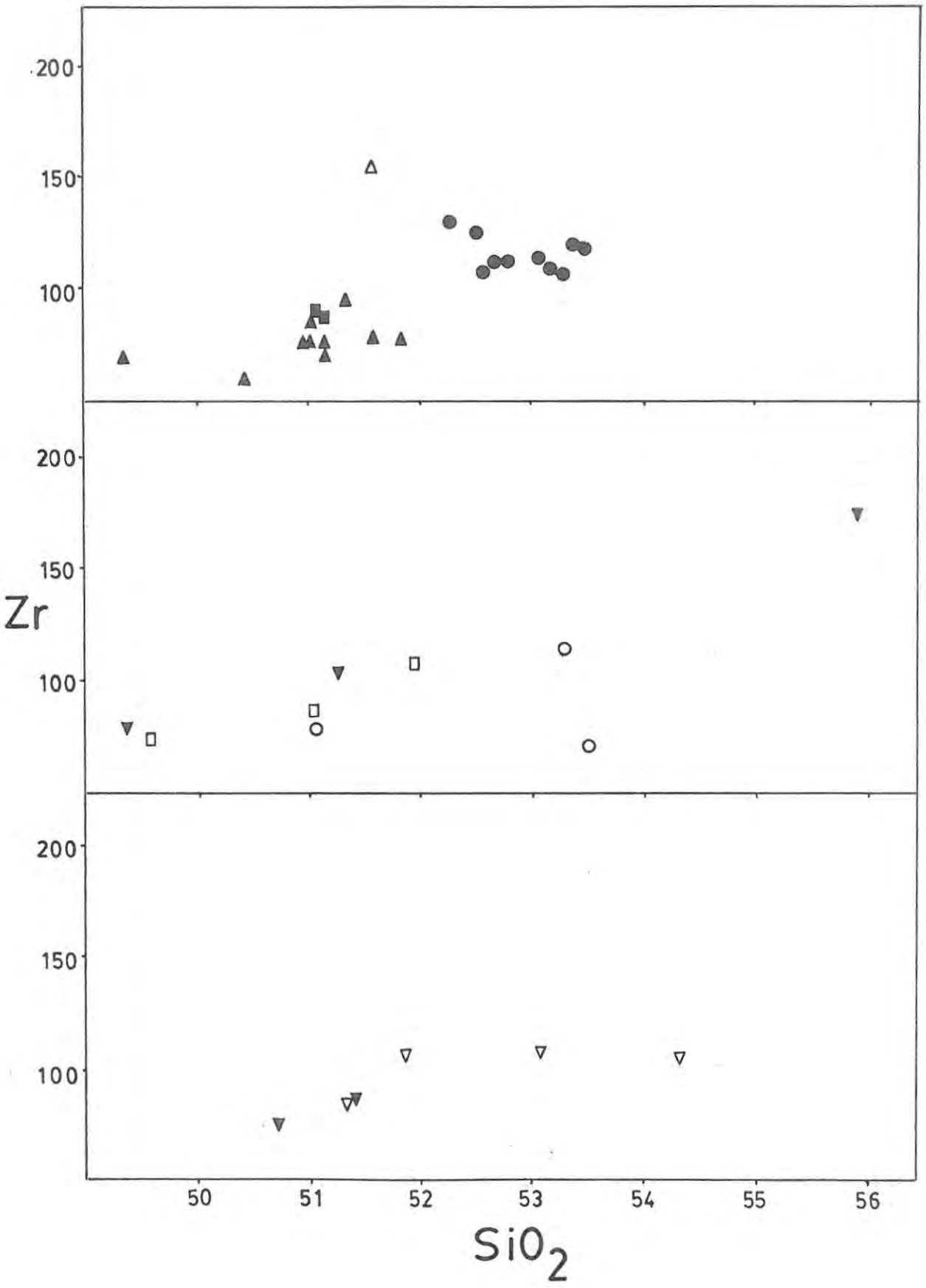

Fig. 23e : TRACE ELEMENT VARIATIONS (IN PARTS PER MILLION) USING WEIGHT % SiO_2 AS THE ABSCISSA

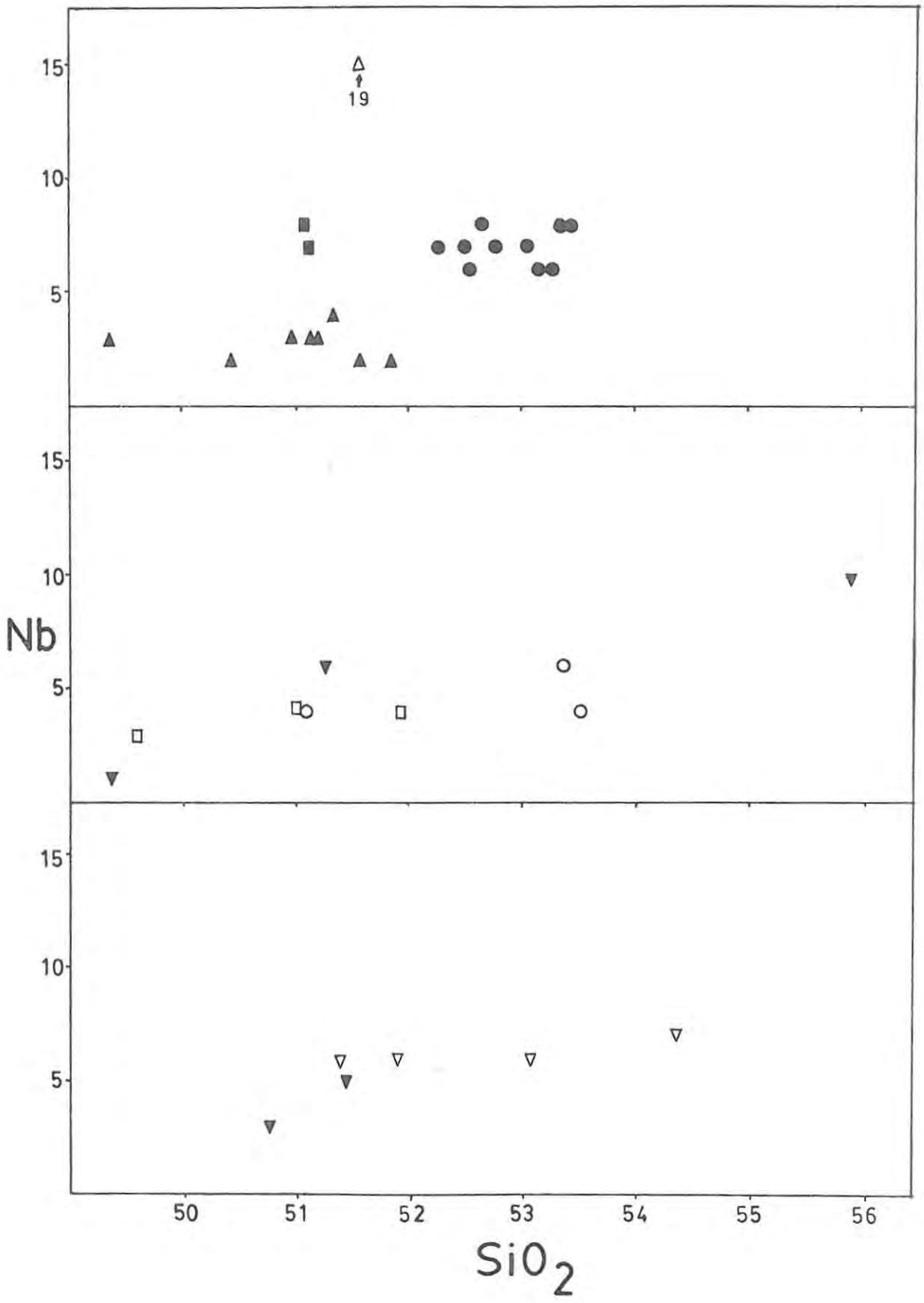

Fig. 23f : TRACE ELEMENT VARIATIONS (IN PARTS PER MILLION) USING WEIGHT % SiO_2 AS THE ABSCISSA

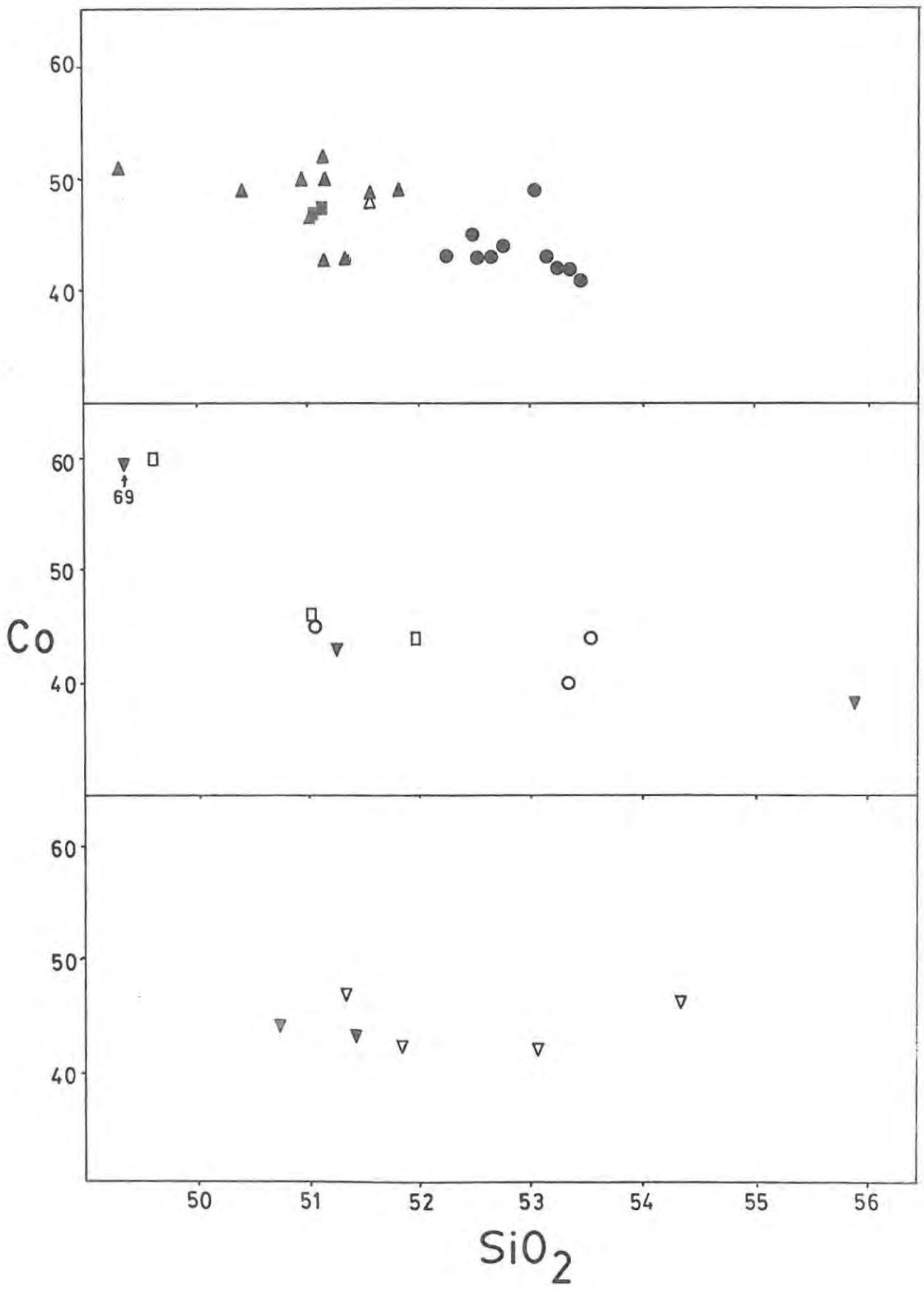

Fig. 23g : TRACE ELEMENT VARIATIONS (IN PARTS PER MILLION) USING WEIGHT % SiO_2 AS THE ABSCISSA

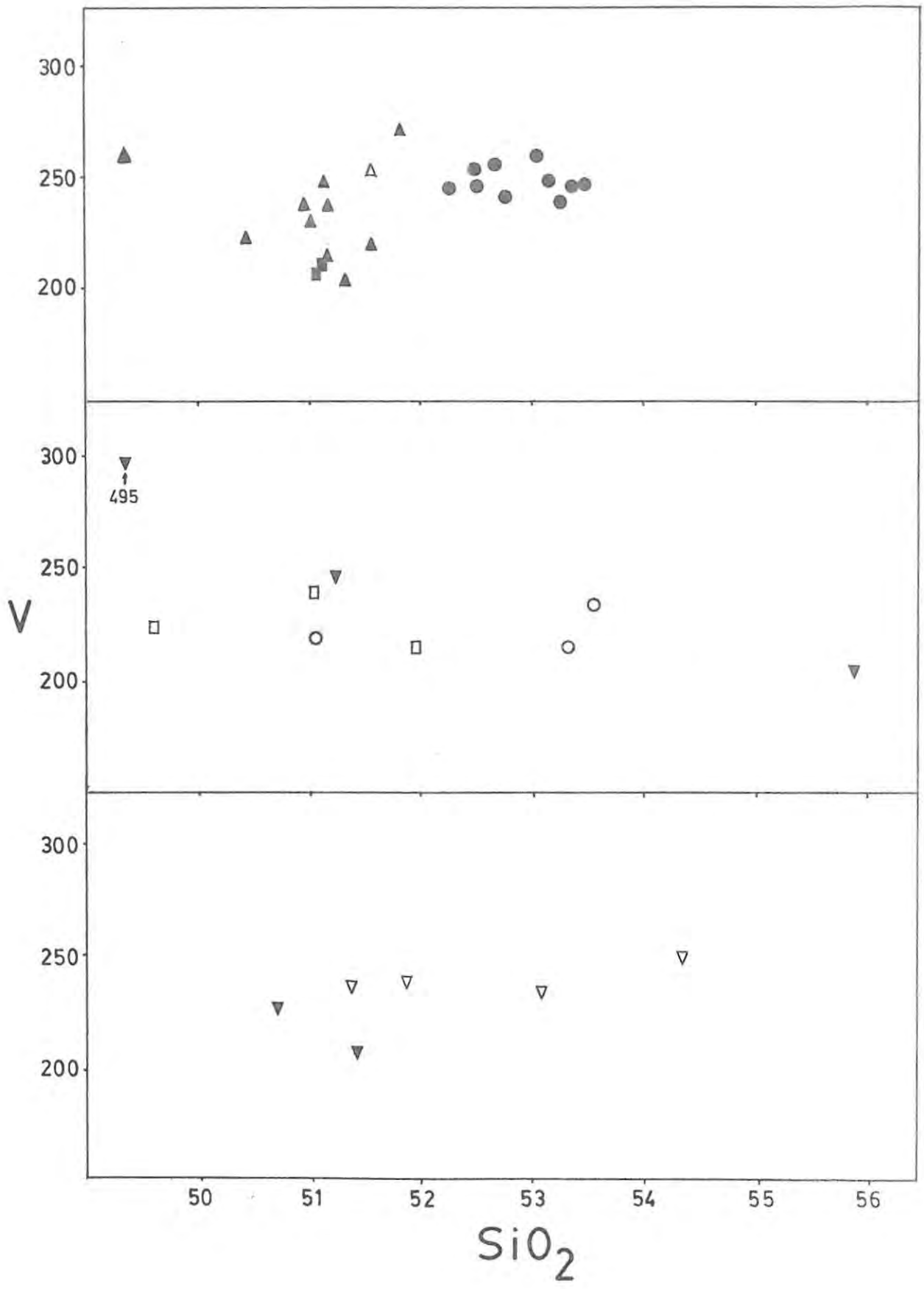

Fig. 23h : TRACE ELEMENT VARIATIONS (IN PARTS PER MILLION) USING WEIGHT % SiO_2 AS THE ABSCISSA

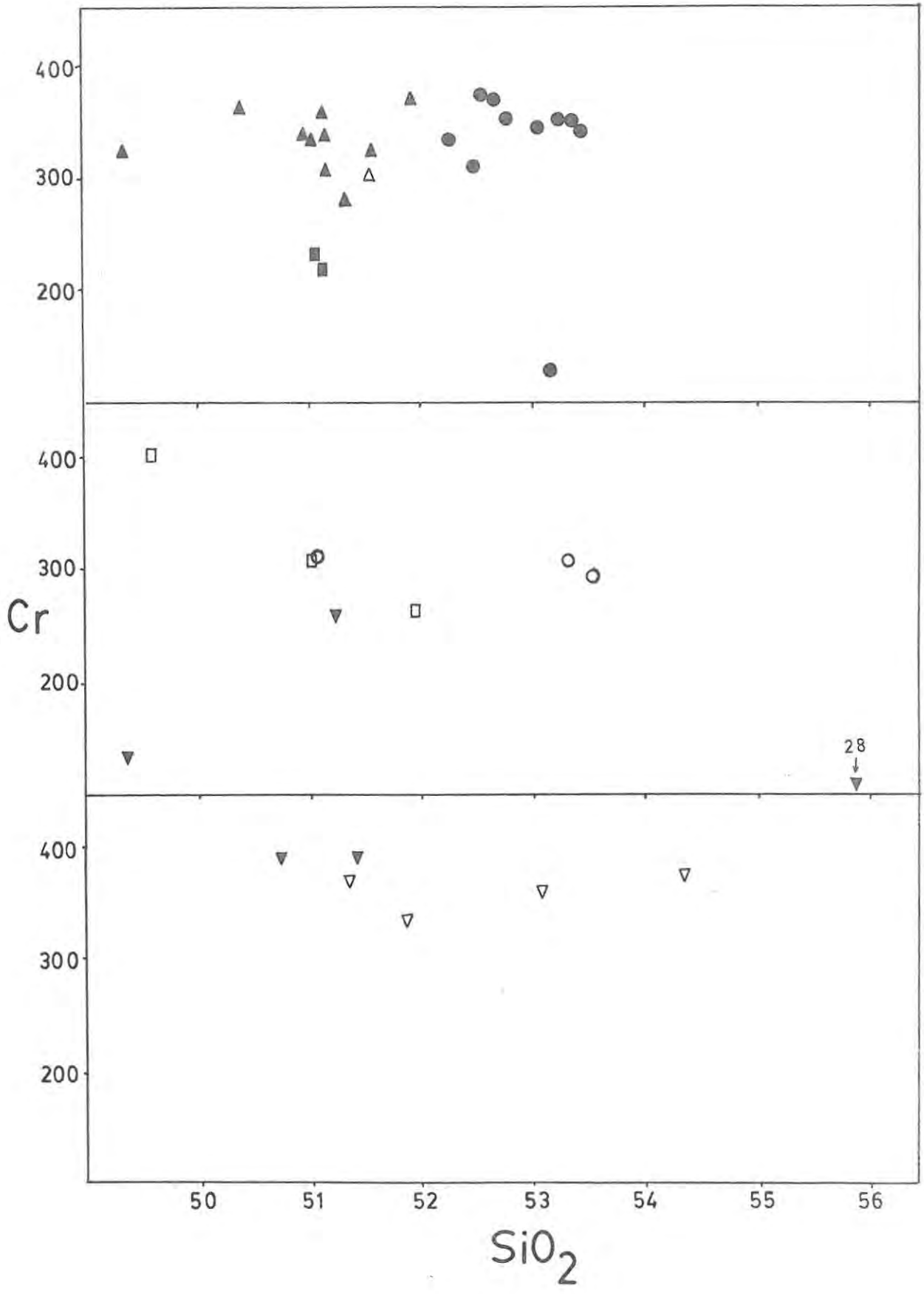

Fig. 23j : TRACE ELEMENT VARIATIONS (IN PARTS PER MILLION) USING WEIGHT % SiO_2 AS THE ABSCISSA

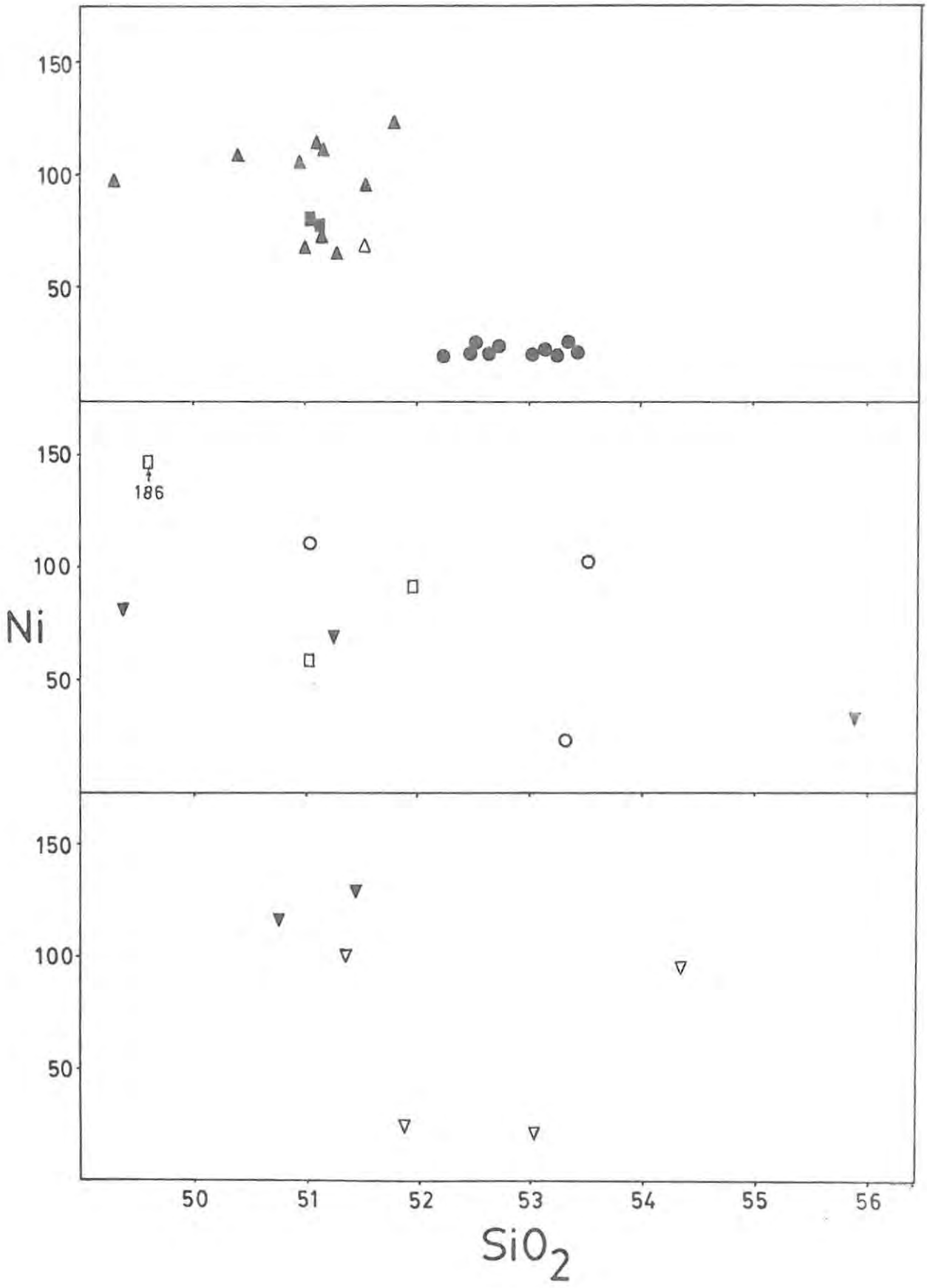

Fig. 23k : TRACE ELEMENT VARIATIONS (IN PARTS PER MILLION) USING WEIGHT % SiO_2 AS THE ABSCISSA

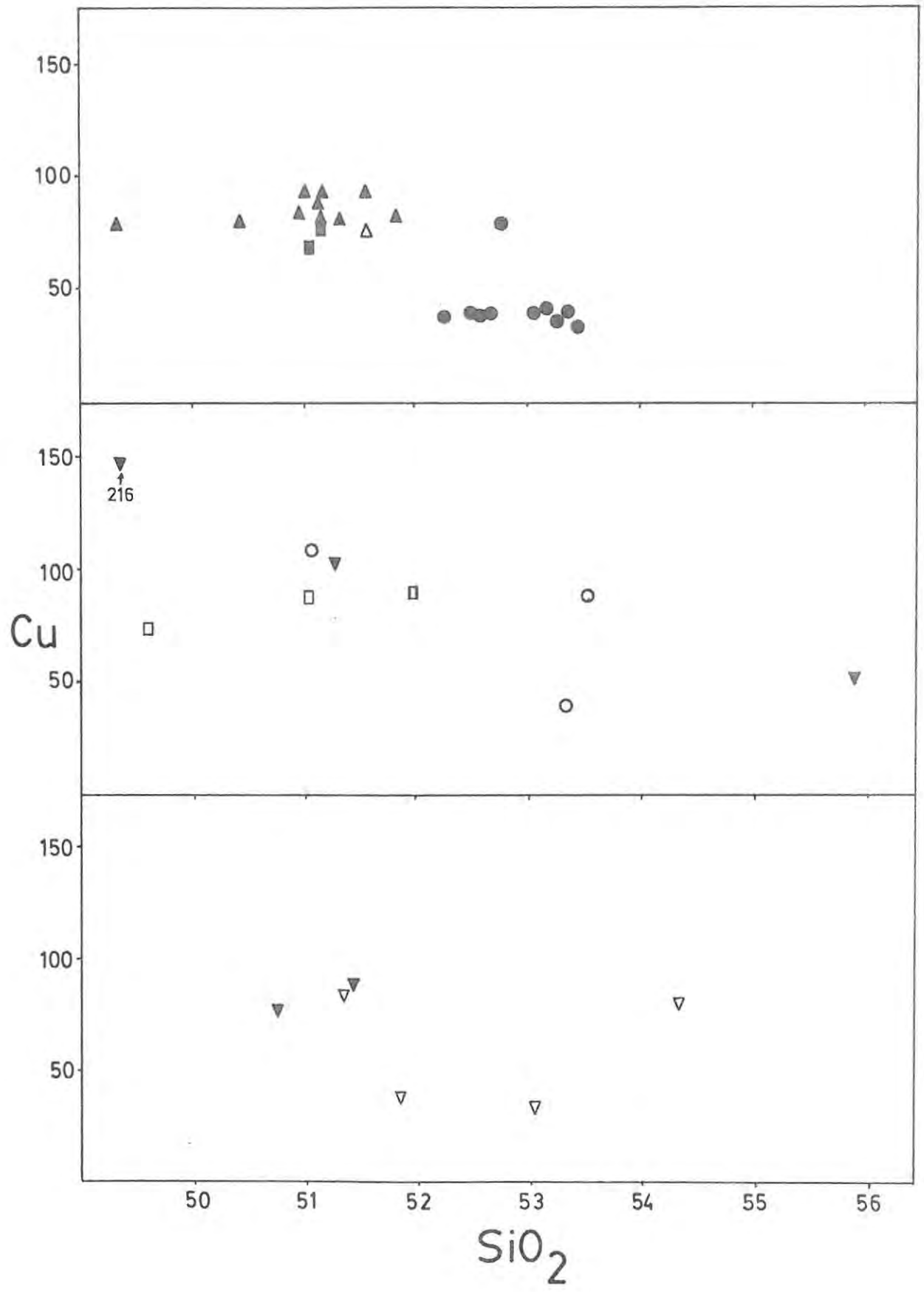

Fig. 231 : TRACE ELEMENT VARIATIONS (IN PARTS PER MILLION) USING WEIGHT % SiO_2 AS THE ABSCISSA

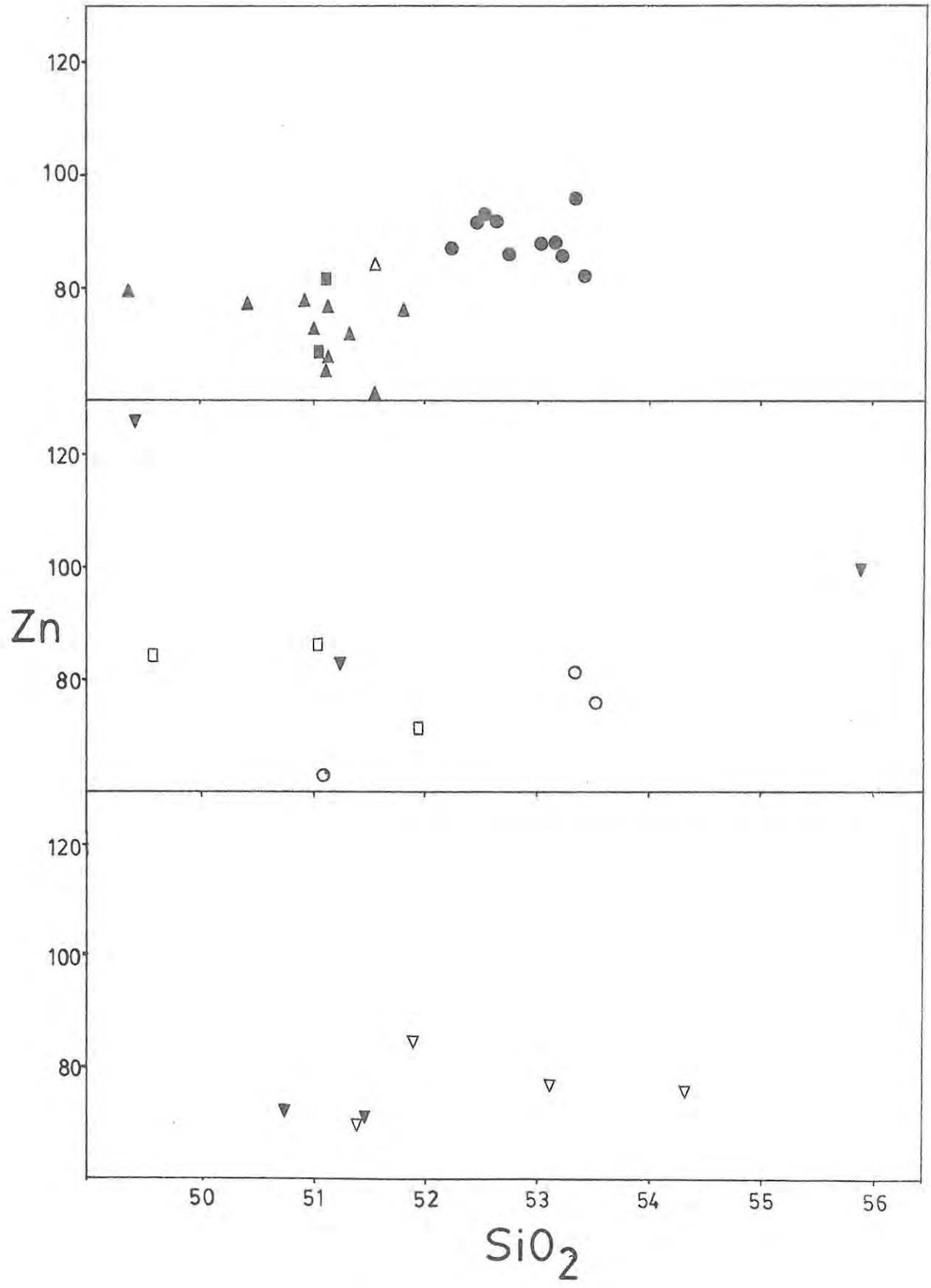

Fig. 24 a-e : INTERELEMENT RATIOS FOR THE BROSTERLEA BASALTS

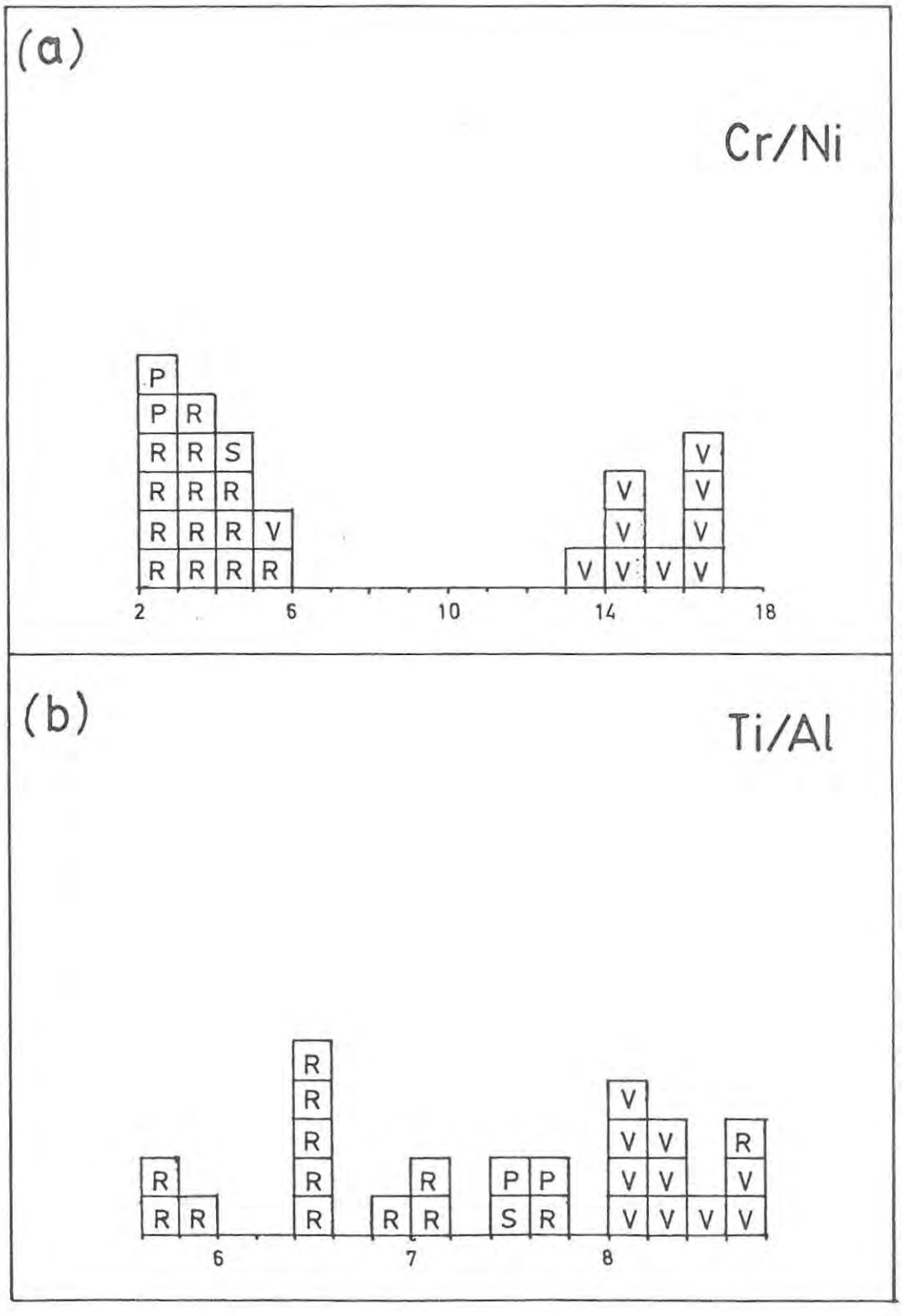

Fig. 24 a-e : INTERELEMENT RATIOS FOR THE BROSTERLEA BASALTS

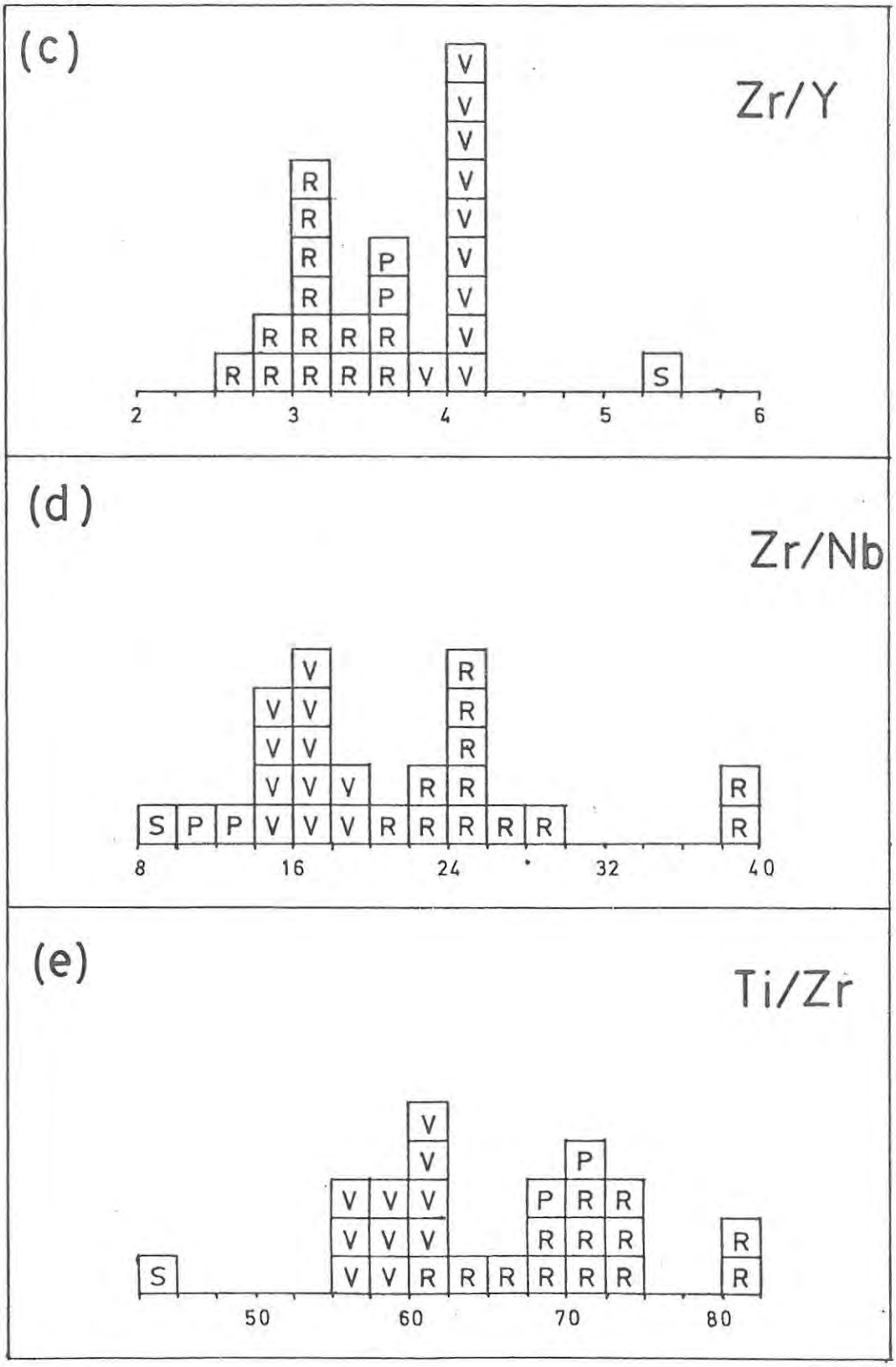

TABLE 5 : SELECTED INTERELEMENT RATIOS FOR THE BASALTS AND DOLERITES OF THE MOLTENO AREA

	Zr/Y	Sr/Nb	K/Rb	K/Zr	Ti/Zr
Roodehoek Unit					
AM-14	2,96	22,6	249	62,3	82,8
AM-15	2,68	29,5	415	70,4	82,3
AM-21	2,92	25,3	581	45,9	70,2
AM-22	3,00	25,0	705	37,6	71,9
AM-23	3,36	24,6	446	48,2	67,2
AM-25	3,13	24,0	521	50,7	69,9
AM-26	3,36	23,5	498	63,6	61,2
AM-27	3,21	38,5	242	81,9	74,7
AM-31	3,13	-	560	29,9	71,9
AM-36T	3,15	21,2	435	61,5	74,7
AM-36M	3,22	24,6	446	48,2	72,9
AM-36B	3,52	27,2	452	45,7	64,3
AM-46	3,50	38,5	933	48,5	69,2
Tafelkop Lavas					
AM-37	3,43	18,0	435	72,6	71,6
AM-38T	3,25	19,5	539	55,3	71,4
AM-38	3,97	19,1	375	75,1	56,8
Perdekop Unit					
AM-28	3,67	12,5	491	67,0	72,2
AM-40	3,71	11,1	463	62,5	68,7
Strypoort Unit					
AM-24	5,28	8,0	581	68,4	44,2

TABLE 5 : SELECTED INTERELEMENT RATIOS FOR THE BASALTS AND DOLERITES OF THE MOLTENO AREA

	Zr/Y	Zr/Nb	K/Rb	K/Zr	Ti/Zr
Vaalkop Unit					
AM-11	4,00	16,0	290	83,0	61,0
AM-12	3,96	17,8	296	63,6	61,0
AM-13	4,00	17,1	564	23,5	55,9
AM-29	4,04	14,1	341	84,5	58,8
AM-30	4,17	17,8	385	77,0	57,0
AM-32	4,19	18,1	273	120,3	61,6
AM-34	4,00	18,0	365	84,6	61,0
AM-41	4,00	15,0	354	100,3	58,4
AM-43	4,07	16,2	351	80,1	59,4
AM-44	4,21	14,7	348	76,7	56,3
Dolerites					
AA-21	2,39	79,0	-	-	100,1
AA-22	4,52	17,3	397	53,5	59,9
AA-23	5,47	17,5	326	89,7	40,7
AA-30	4,06	24,3	608	50,0	71,4
AA-31	4,10	17,2	547	31,9	52,9
Modderfontein Lavas					
AM-50	3,50	14,0	467	61,3	69,2
AM-51	4,52	14,8	175	30,3	53,6
AM-52	4,08	17,6	326	43,1	59,3
AM-53	4,12	17,8	996	18,6	63,8

TABLE 5 : SELECTED INTERELEMENT RATIOS FOR THE BASALTS AND DOLERITES OF THE MOLTENO AREA

	Cr/Ni	Ti/Al	Cr/Ti
Roodehoek Unit			
AM-14	3,34	0,06	0,05
AM-15	3,24	0,05	0,07
AM-21	3,18	0,06	0,06
AM-22	3,07	0,06	0,06
AM-23	4,57	0,05	0,06
AM-25	2,71	0,05	0,06
AM-26	4,24	0,06	0,04
AM-27	3,34	0,07	0,05
AM-31	4,76	0,06	0,06
AM-36T	5,17	0,07	0,04
AM-36M	2,16	0,07	0,07
AM-36B	2,87	0,08	0,03
AM-46	2,98	0,06	0,06
Tafelkop Lavas			
AM-37	2,89	0,06	0,05
AM-28T	3,80	0,07	0,05
AM-38	13,43	0,08	0,04
Perdekop Unit			
AM-28	2,85	0,07	0,03
AM-40	2,84	0,07	0,03
Strypoort Unit			
AM-24	4,33	0,07	0,04

TABLE 5 : SELECTED INTERELEMENT RATIOS FOR THE BASALTS AND DOLERITES OF THE MOLTENO AREA

	Cr/Ni	Ti/Al	Cr/Ti
Vaalkop Unit			
AM-11	14,6	0,08	0,05
AM-12	16,8	0,08	0,05
AM-13	15,2	0,08	0,04
AM-29	16,8	0,08	0,05
AM-30	14,0	0,08	0,04
AM-32	5,6	0,08	0,01
AM-34	14,3	0,08	0,05
AM-41	13,5	0,08	0,05
AM-43	16,3	0,08	0,05
AM-44	16,2	0,08	0,05
Dolerites			
AA-21	1,6	0,08	0,01
AA-22	3,8	0,07	0,04
AA-23	0,8	0,09	0,00
AA-30	3,3	0,06	0,07
AA-31	3,0	0,05	0,08
Modderfontein Lavas			
AM-50	3,7	0,07	0,06
AM-51	3,8	0,07	0,06
AM-52	16,0	0,07	0,05
AM-53	13,8	0,08	0,04

TABLE 6 : SELECTED PARTITION COEFFICIENTS FOR TRACE ELEMENTS IN THE BASALTIC ASSEMBLAGE

	Plagioclase	Augite	Olivine	Magnetite
D_{Sr}	1,5 - 2,2[1]	0,16 - 0,28[1]	0,01[2]	-
D_{Rb}	0,03[2]	0,1[3]	0,01[2]	-
D_{Zr}	0,01[4]	0,1[4]	0,01[4]	0,1[4]
D_{Y}	0,03[4]	0,5[4]	0,01[4]	0,2[4]
D_{Nb}	0,01[4]	0,1[4]	0,01[4]	0,4[4]
D_{Ti}	0,04[4]	0,3[4]	0,02[4]	7,5[4]
D_{Co}	0,1[5]	0,5 - 2,0[6] 1,7 - 4,9[7]	1 - 7[8]	6,3 - 11,1[7]
D_{Cr}	0,1[9]	up to 40[10]	3,1 - 10[11] $\pm$ 1[8]	up to 58[7]
D_{V}	0,1[9]	0,06 - 3,4[12]	0,05[13]	24 - 63[7]
D_{Cu}	0,24[7]	1,5 - 2,4[14]	0,3 - 0,5[8]	$\pm$ 1,3[7]
D_{Ni}	0,2[15]	6,5[7]	4,8 - 34[16]	12,2 - 19,4[8]

[1]Sun, Williams and Sun (1974). [2]Philpotts and Schnetzler (1970). [3]Hart and Brooks (1973). [4]Pearce and Norry (1979). [5]Jensen (1973). [6]Lindstrom and Weill (1978). [7]Ewart et al. (1973). [8]Irving (1978). [9]Walker (1970). [10]Campbell and Borley (1974). [11]Flower (1973). [12]Ringwood (1970). [13]Duke (1974). [14]Seward (1971). [15]de Long (1974). [16]Leeman and Lindstrom (1978).

9. A COMPARISON OF THREE CONTINENTAL FLOOD BASALT PROVINCES

9.1 Introduction

The salient features of three separate continental tholeiitic flood basalt provinces are compared. The three provinces, the Karoo Central Province, the Columbia River Plateau, and the Deccan Traps, are widely separated, both spatially and temporally, but there are certain common factors linking them. It is the aim in this chapter to outline and discuss the similarities and differences between the provinces.

9.2 The Karoo Central Province

Expanding on the postulate by Cox et al. (1967) of a twofold subdivision of the Karoo basalts of Southern Africa into Northern and Southern provinces, Eales and Marsh (1979b) identify six distinct provinces within the period of Mesozoic volcanism in Southern Africa. These six provinces they subdivide into three groups, on the basis of their tectonic setting :

(i) The Atlantic Province, the Northern Tectonic Province and the Lupata Province are associated with major rifting and/or continental separation involving the breakup of Gondwanaland.

(ii) The Northern Cratonic Province and the Southern Lebombo Province are less directly linked with major rifting, and may be regarded as regions where rift-controlled volcanism has extended onto cratonic areas.

(iii) The Karoo Central Province, outcropping mainly in the vicinity of Lesotho and the north-east Cape, is essentially atectonic, and is situated within a stable cratonic environment.

The location of the igneous provinces of southern Africa is shown in Fig. 25. Mesozoic volcanicity extended

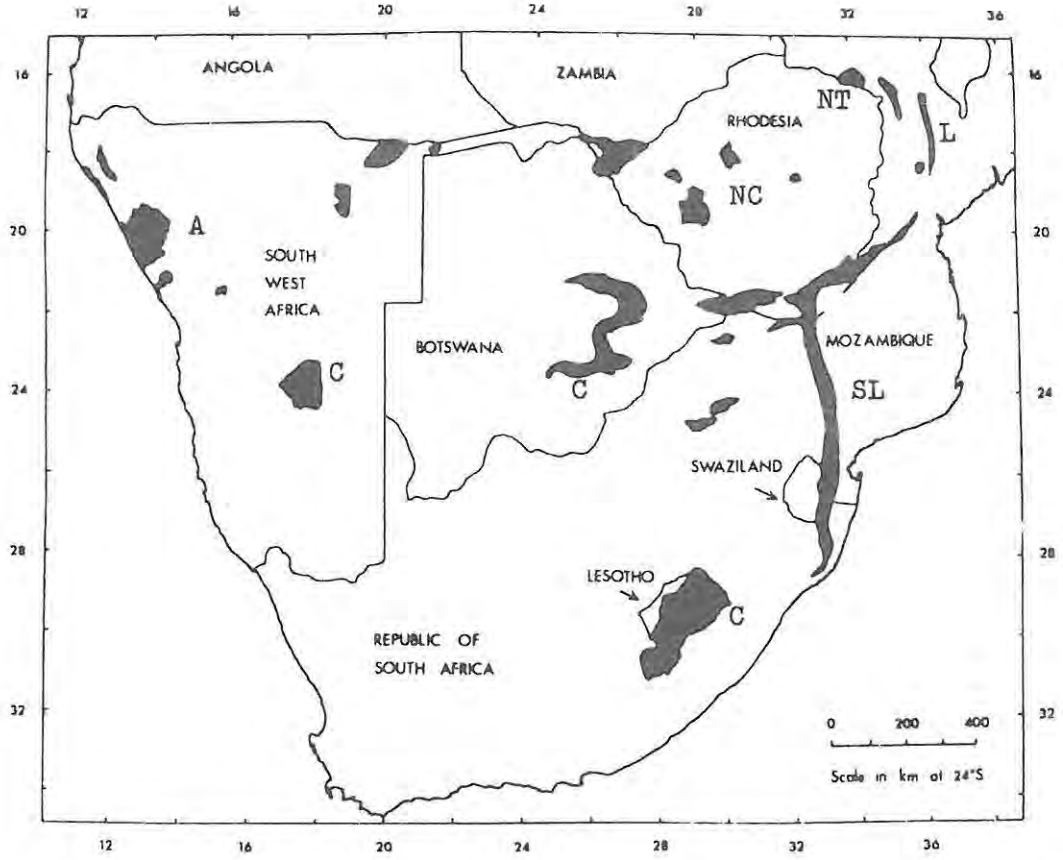

Fig. 25 : GENERALIZED MAP SHOWING DISTRIBUTION OF KAROO LAVA OUTCROPS IN SOUTHERN AFRICA (from The Geodynamics Project in South Africa, 1975).

A = Atlantic Province
C = Karoo Central Province
L = Lupata Province
NT = Northern Tectonic Province
NC = Northern Cratonic Province
SL = Southern Lebombo Province

in age from the late Triassic through to the Cretaceous, and volcanic material is estimated by Cox (1972) to have originally covered some 140 000 sq km of southern Africa. Eroded remnants of this vast expanse of lava today amount to little over one-tenth of the original extent of the volcanics, and the maximum preserved thickness is about 1400m, at Mont-aux-Sources in the Drakensberg Mountains.

The major concern of the present study is the infracratonic province of the Central Karoo. Volcanism in this province lasted from 187±7 my B.P. to at least 155 my B.P. (Fitch and Miller, 1971).

The earliest clear evidence of volcanism in the Central Province is the isolated tholeiitic basalt flow encountered in the Elliot Formation sediments on the farm Siberia, in the north-eastern Cape Province (Du Toit, 1904; Robey, 1976). The onset of widespread volcanism, however, began towards the closing phases of the deposition of the Clarens Formation sandstone.

The earliest expression of volcanism on a regional scale is the diatremes which dot the north-eastern Cape (Du Toit, 1904; Gevers, 1928). The diatremes are believed to be products of effusions of steam derived from superheated groundwaters, the heat engine apparently being the earliest phases of magmatic activity.

As the volcanic episode progressed, central vent complexes such as those described by Lock et al. (1974) and in the present study, came into being. The primary effusive products of the central complexes were of a pyroclastic nature, associated with a subordinate amount of magmatic material. It would appear that the pyroclastic phase often accompanied caldera collapse, as at Brosterlea and Kelvin Grove.

The central vent phase of eruption was terminated by effusion of flows of highly mobile tholeiitic lava from

the rapidly developing fissure system in the Karoo. Lock et al. (op. cit.) were able to subdivide the basalts of the Barkly East area into discrete formations on the basis of standard stratigraphic techniques. Geochemical work by Robey (1976) and Pemberton (1978) gave substance to the stratigraphic subdivisions proposed by Lock et al., whilst the present study shows that the basalt outliers west of Jamestown may also be subdivided into geochemically distinct units, most of which bear some resemblance to the formations of the Barkly East area.

The early phases of fissure eruption in the Central Province appear to have been erratic, both temporally and geochemically. That there were time intervals between successive pulses of igneous activity is indicated by the frequent intercalations of sandstone lenses and bands with the lavas in the lower part of the succession (e.g. Swart, 1979). These sandstone layers have been interpreted as playa lake deposits. From geochemical studies by Pemberton (op. cit.) and the present author, it is apparent that the early lava units of the Central Province are not related to a single parent magma by any simple fractionation process. Apart from the chemical inconsistency of the lower lava units, isolated occurrences of andesite are associated with the early basalts (Rumble, 1979). The chemical diversity of magmatic activity ended with the period of eruption of Lesotho Formation lavas, during which time great volumes of chemically consistent lavas were erupted (Pemberton, op. cit.).

The hypabyssal expression of the Karoo Province, i.e. the dolerites, forms a study in itself. A thorough summary of early work on the Karoo dolerites is to be found in the classic work of Walker and Poldervaart (1949), but more recent data, particularly of a geochemical nature, is to be found in Nockolds and Allen (1956), Erlank and Hofmeyer (1966), Le Roex and Reid (1978) and Robey (1976).

9.2.b Petrography

The petrography of the more important of the basalt types in the Central Province is discussed here by reference to Pemberton (1978) and to the present study. Data on the Karoo andesites is taken from Rumble (1979).

The Drumbo and Donnybrook Members of Barkly East and the Strypoort Unit of Brosterlea are hypocrystalline and phaneritic, with intergranular to intersertal texture. Plagioclase is zoned (An_{40}-An_{60}) and is generally less than 1 mm in length. Augite is ophitically related to plagioclase, and may have pigeonite cores. Olivine is present, but is generally highly altered. Microprobe studies show marked zoning of the olivine (Fa_{36}-Fa_{73}). The Drumbo and related basalts contain up to 15% glass, 5 - 10% olivine, $\pm$ 30% clinopyroxene and about 50% plagioclase.

The Kraai River Formation is hypocrystalline and porphyritic to glomeroporphyritic. Plagioclase (An_{50}-An_{60}) is the main phenocryst phase, but augite phenocrysts do occur. Large Bronzite phenocrysts have been identified by Pemberton in some of the Kraai River rocks. The groundmass is mainly clinopyroxene and plagioclase, and olivine, glass and oxide minerals make up a very small proportion of these rocks.

The Roodehoek Unit and Omega Formation vary from hypocrystalline phaneritic and equigranular to glomeroporphyritic in texture. In the equigranular variety, augite grains up to three millimeters in diameter are ophitically related to plagioclase laths (An_{50}-An_{80}). Pigeonite often forms a core to the augite. Augite makes up 30% to 40% of the rock, and plagioclase a similar proportion. The rest of the rock consists of glass, oxides and a small proportion of olivine. In the glomeroporphyritic type, clusters of labradorite are set in an intersertal groundmass of plagioclase and clinopyroxene.

The Vaalkop Unit of Brosterlea is hypocrystalline and porphyritic, tending towards glomeroporphyritic. Phenocryst phases are labradorite (An_{48}-An_{72}) and augite, occurring in a ratio of about 9:1. Olivine occurs only very rarely as a phenocryst phase. The groundmass is a microcrystalline intersertal network of plagioclase, augite and opaque oxides.

The Lesotho Formation, and the related Perdekop Unit of Brosterlea, is aphanitic to phaneritic, occasionally showing a glomeroporphyritic texture. Pigeonite cores to augite are common. Olivine, if present, is highly altered, and glass is present in all flows. The Lesotho Formation basalts are commonly amygdaloidal.

The andesites studied by Rumble (op. cit.) were taken from Belmore, Pronkberg and Roodehoek. The Belmore and Pronkberg andesites are similar to one another, and are hypocrystalline and porphyritic. Phenocrysts are plagioclase (An_{70}) and hypersthene. The groundmass is 50 - 60% glassy, containing crystallites of plagioclase, orthopyroxene, opaque oxides and quartz. The Roodehoek andesite differs from the other andesites in being intrusive, rather than extrusive. This rock is hypocrystalline, aphanitic to microcrystalline and seriate in texture. Dominant mineral phases are plagioclase (An_{40}-An_{60}), K-feldspar and quartz. No ferromagnesian minerals appear to be present in the rock. The groundmass is vitrophyric, and makes up approximately 60% of the rock.

9.2.c Geochemistry

Virtually all the basalts of the Central Province are quartz - normative, and it is only isolated rocks in a few of the units that show normative olivine. On this basis, the Central Province can be regarded as consisting predominantly of quartz tholeiites. The norms of the andesites (Rumble, 1979) are interesting in that they show normative corundum, an effect which Chayes (1970) relates to assimilation of Al-rich crustal material. The average normative

compositions of the Central Province basalt units are plotted on a Cox and Hornung (1966) type projection of the basalt tetrahedron (Fig. 26a).

On the generalised AFM diagram (Fig. 26b), the trends identified for the Karoo dolerites by Nockolds and Allen (1956) are plotted, as are data from a selection of basalt units from Pemberton (1978) and the present work. Some of the Karoo basalt units are also plotted in Fig. 28 for comparison with the Columbia data of MacDougall (1976).

As regards the trace element data, the Kraai, Drumbo and Vaalkop basalts are enriched in incompatible elements relative to the Lesotho and Roodehoek/Omega basalts. The K/Rb ratio is inconsistent, probably due to weathering, and is thus not of much diagnostic use. Incompatible element ratios are particularly important in that they differ from unit to unit in the Central Karoo Province. This inconsistency of ratios has been related to inhomogeneities in the mantle.

Compston et al. (1968) obtained average Sr^{87}/Sr^{86} values of 0,7057 for the Karoo dolerites. Data from Erlank et al. (1979) show a range of Sr isotope ratios from 0,7046 to 0,7083 for the mafic rocks of the Karoo Central Province. Data from Rumble (1979) for the Kraai River Formation and the Belmore andesite (0,70878 and 0,70981, respectively) are particularly high, and suggest a definite crustal component.

Fig. 26 : GENERALISED CHEMISTRY OF THE KAROO CENTRAL PROVINCE BASALTS

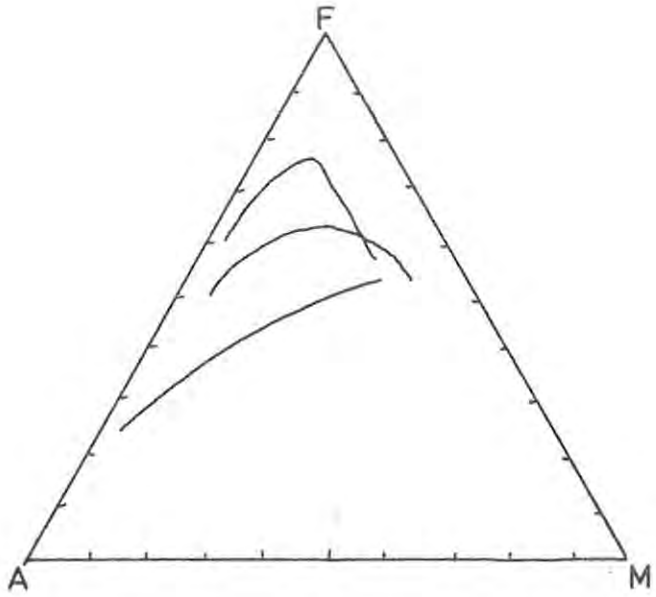

Fig. 26a : AFM diagram of the Karoo Central Province basalts showing the trends identified by Nockolds and Allen (1956).

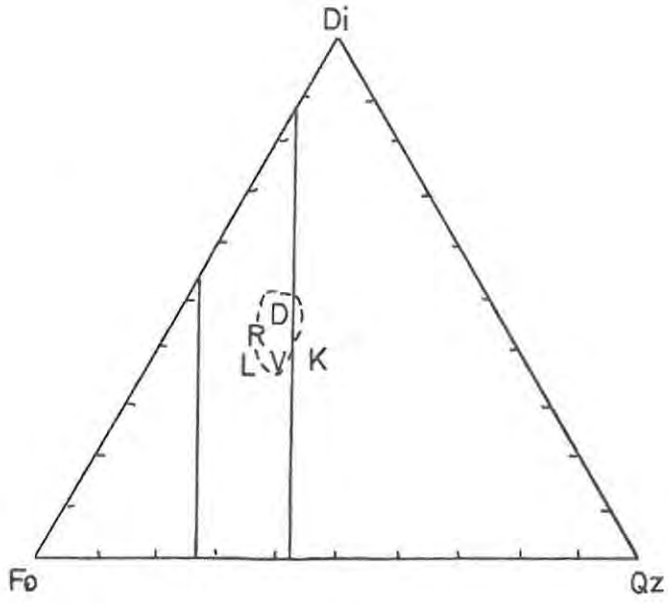

Fig. 26b : Normative basalt tetrahedron for the Karoo basalts

D = Drumbo Basalt Member (average)

K = Kraai River Formation (average)

L = Lesotho Formation (average)

V = Vaalkop Unit

R = Roodehoek Unit

= Lesotho Basalts (Cox and Hornung, 1966).

9.3 The Columbia River Plateau

9.3.a Geological Setting

Volcanism in the states of Washington, Oregon and Idaho in the U.S.A. started in the early Miocene (25 my B.P.), reaching a peak of activity around 16 to 13 my B.P. (Baksi and Watkins, 1973).

The tholeiitic basalts which constitute the Columbia River Province were poured into a sagging basin structure, filling it to a depth of 1 to 2 kilometers with horizontal flows of lava. The present-day extent of the province is about 500 000 km^2.

The basalts are fissure-erupted, and the extensive sub-volcanic network of dykes have been linked geochemically with the basalts.

The Columbia River basalts (Fig. 27) have been broadly subdivided into four units : (1) The lowermost basalts of the sequence in northern Oregon are the Picture Gorge basalts. In northeastern Oregon and Idaho, the lowermost basalts, although stratigraphically equivalent to the Picture Gorge basalts, show geochemical differences from the latter. These basalts, called the "lower" basalts by Wright et al. (1973), are referred to as the Imnaha basalts by MacDougall (1976), and as the Rock Creek basalts by Hooper (1974). (2) Overlying the Picture Gorge and Imnaha basalts is the Lower Yakima Basalt. (3) After a period of quiescence, represented by the Vantage Sandstone Member, the Lower Yakima was followed by the Middle Yakima Basalt. (4) The youngest basalts of the Columbia River Group, constituting the Upper Yakima Basalts, were studied by Schmincke (1967), who identified four flows, giving each flow member status and naming them the Umatilla, Pomona, Elephant Mountain and Ward Gap Basalt Members.

The Yakima Basalts are overwhelmingly dominant in the Columbia River Group. These basalts occur in flows

CHEMICAL VARIATION, COLUMBIA RIVER BASALT

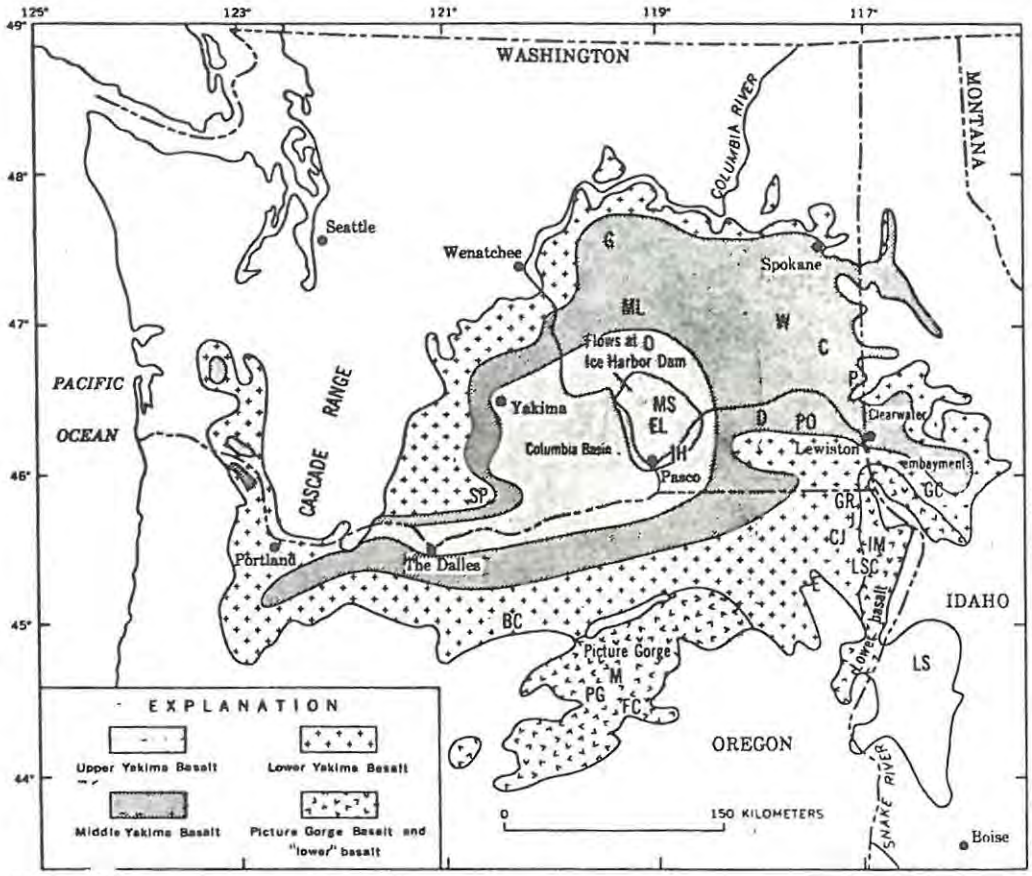

Fig 27 Highly generalized distribution map of stratigraphic units of the Columbia River basalt. Stratigraphic units are patterned as in Table 1.

The patterned areas represent the dominant stratigraphic unit present at the surface of the plateau. Older units may be exposed in the canyons of the Snake and Columbia Rivers and their tributaries, and in the cores of anticlinal ridges in the western part of the plateau. In northeastern Oregon and adjacent Idaho, the lower basalt is overlain by lower Yakima basalt and is exposed only in deep canyons; its outcrop area is exaggerated in order to emphasize its presence in this area. The blank area north of Boise is underlain by lower basalt and lower Yakima basalt whose relative distribution is poorly known. Near the crest of the Cascade Range, the Columbia River basalt is mostly covered by younger rocks.

BC = Butte Creek
C = Colfax
CJ = Chief Joseph dike swarm
D = Dodge
E = Enterprise
EL = Eltopia
FC = Flat Creek
G = Grand Coulee
GC = Grave Creek
GR = Grande Ronde River
IH = Ice Harbor Dam
IM = Imnaha River
J = Joseph Creek
LS = Little Salmon River
LSC = Little Sheep Creek
M = Monument dike swarm
ML = Moses Lake
MS = Mesa
O = Othello
P = Pullman
PG = Picture Gorge
PO = Pomeroy
SP = Satus Pass
W = Winona

Diagram after MacDougall (1976)

averaging 25m thick, and show characteristic collumnar jointing. In some places, pillow lavas indicate the presence of water during eruption. There are a number of thin intercalations of sandstone and dolomite with the basalts, particularly in the Middle Yakima Basalt (MacDougall, 1976).

Along the western coastal belts of Oregon and Washington, Snavely et al. (1973) report the association of volcanic vents with Miocene tholeiites and breccias. The vent-derived tholeiites show strong geochemical correlations with the Yakima Basalts (Snavely et al., op. cit.; MacDougall, op. cit.), and appear to be part of the same event.

MacDougall (loc. cit.) ascribes the Columbia River volcanic event to partial melting of upper mantle peridotite due to diapiric upwelling of mantle caused by tectonic extension in the Columbia Plateau area, possibly related to major readjustment involving plate movements in the Pacific north-west in mid-Miocene times.

9.3.b Petrography

The petrography of the Columbia River Basalts is summarised in table form by Wright et al. (1973). Detailed optical studies of the mineralogy of the Yakima Basalt are reported by Swanson (1967). The chemically diverse basalts of the Upper Yakima Basalt are discussed by Schmincke (1967).

The Imnaha Basalts are porphyritic, the only phenocryst phase being plagioclase. Olivine occurs in small amounts as a groundmass constituent. In contrast to the Imnaha Basalt, the Picture Gorge Basalt is non-porphyritic, and generally contains no olivine.

In general the Yakima Basalts are aphanitic. Porphyritic varieties are rare, except in the Lower Yakima Basalt, which typically contains a few percent of plagioclase microphenocrysts, and less often augite microphenocrysts.

The most common mineral phases in the Yakima Basalts are plagioclase (An_{65}-An_{50}. Swanson, op.cit.) and clinopyroxene. It is quite common for Augite grains to have pigeonite cores. Olivine may be encountered as a groundmass constituent, particularly in the Middle Yakima Basalt. Glass makes up as much as 10 - 15% of most of the Yakima rocks, and has associated with it apatite and opaque oxides.

9.3.c Geochemistry

Some of the most recent geochemical data for the Columbia River Group is contained in a paper by MacDougall (1976), on which this discussion is based.

In the Picture Gorge Basalts, five flows have been identified, the lowermost two of which are more mafic than the succeeding flows, as indicated by their higher MgO, Cr and Ni contents. Using a standard Fe_2O_3/FeO ratio of 0,2, MacDougall calculates that some of the Picture Gorge Basalts are quartz-normative, and others olivine-normative. The mean Sr^{87}/Sr^{86} ratio of these rocks is 0,7037 $\pm$ 0,0001.

The Imnaha Basalts appear to be geochemically similar to the Middle Yakima Basalts, and differ from the Picture Gorge Basalts, most especially in Sr isotope ratio, Sr abundances and K/Rb ratio. The Sr^{87}/Sr^{86} ratio of the Imnaha Basalts is 0,7043 (MacDougall), but this figure is based on a limited number of analyses.

The Lower Yakima Basalts are relatively high in SiO_2 (52,7 - 55,5%) and alkalis, but low in MgO. The trace element geochemistry is very constant, but Sr isotope ratios, on the other hand, are variable within the range 0,7049 - 0,7059. The variation in isotope ratios from flow to flow suggests to MacDougall that there are factors in operation other than simple fractional crystallisation from a homogeneous batch of magma. The Lower Yakima Basalts are all quartz-normative.

The Middle Yakima Basalts are remarkably uniform in composition. By comparison with the Lower Yakima, this group has high TiO_2 and Fe, and low SiO_2 content. K, Rb and Sr abundances all show a limited range, as does the Sr isotope ratio (0,7053 $\pm$ 0,0001).

The four Members of the Upper Yakima Basalt are geochemically distinct from one another, particularly with regard to their alkali contents. The Umatilla Member is strongly differentiated, with low MgO and high Fe and alkalis. The Pomona Member, on the other hand, has high MgO and CaO and low Fe. The Elephant Mountain and Ward Gap Members are similar in major element concentrations to the Middle Yakima. The Upper Yakima Basalts are distinguished from the Lower and Middle Yakima Basalts by their substantially higher Sr isotope values.

The major and trace element chemistry of the Columbia are represented diagrammatically in Fig. 28a and b (after MacDougall, 1976). Selected data from the Karoo are included, for comparison, on these diagrams.

Fig. 28a : COMPARATIVE MAJOR ELEMENT DIAGRAM OF THE COLUMBIA RIVER GROUP AND THE CENTRAL KAROO BASALTS (MODIFIED DIAGRAMS AFTER MACDOUGALL, 1976)

PG = Picture Gorge Basalt
LY = Lower Yakima Basalt
MY = Middle Yakima Basalt
K = Kraai River Formation
R = Roodehoek Unit
V = Vaalkop Unit

= Columbia River Group
= Central Karoo Province

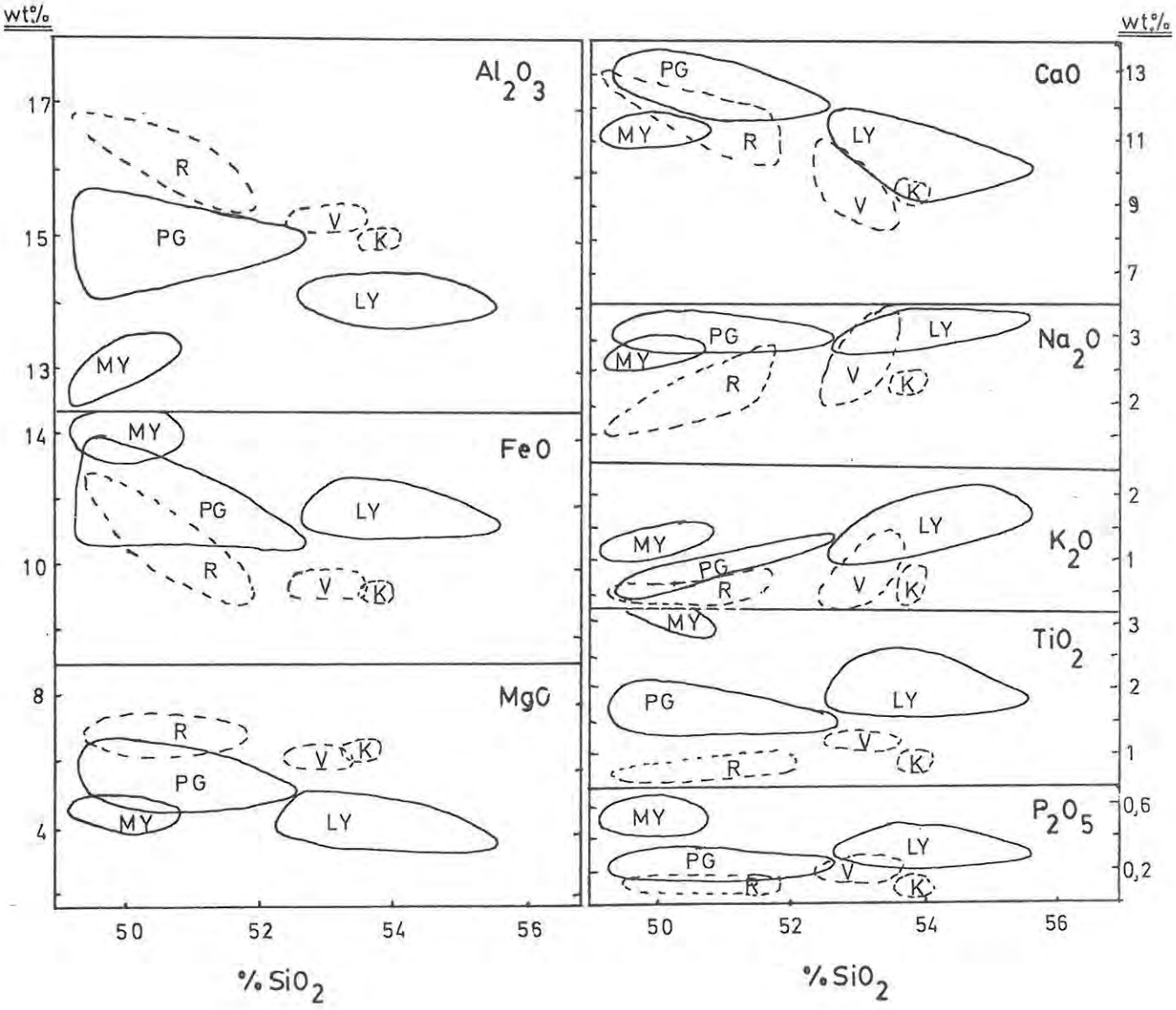

Fig. 28b : COMPARATIVE TRACE ELEMENT DIAGRAM OF THE COLUMBIA RIVER GROUP AND THE CENTRAL KAROO BASALTS
(MODIFIED DIAGRAMS AFTER MACDOUGALL, 1976)

PG = Picture Gorge Basalt
LY = Lower Yakima Basalt
MY = Middle Yakima Basalt

K = Kraai River Formation
R = Roodehoek Unit
V = Vaalkop Unit

= Columbia River Group

= Central Karoo Province

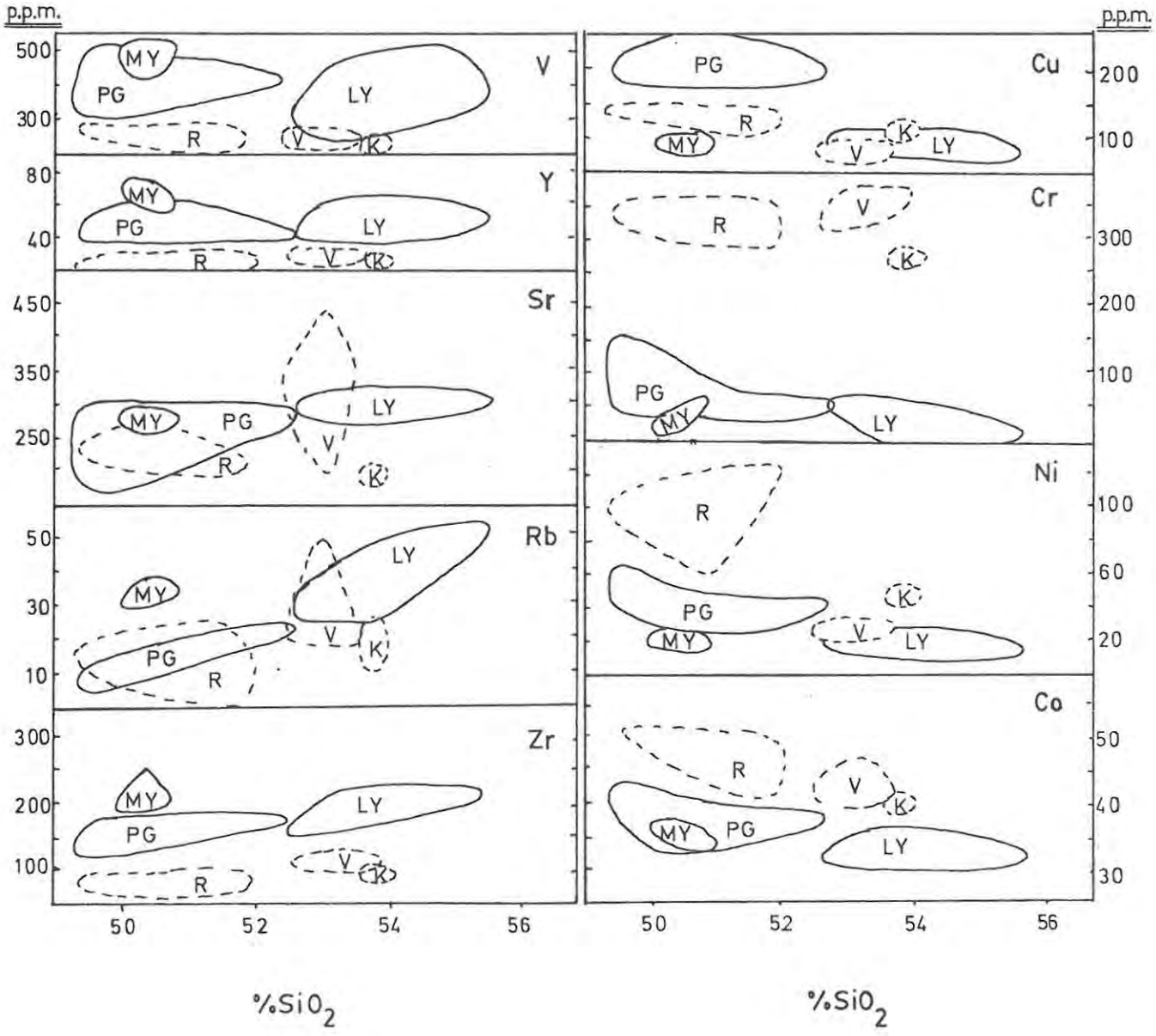

9.4 The Deccan Traps

9.4.a Geological Setting

The basalts of the Deccan Traps of India cover some 500 000 sq km (Fig. 29). The thickness of the volcanic pile varies from about 2000 meters along the western Indian coastline to 100 - 200 meters in the eastern extremities of the Traps.

The bulk of the Deccan basalts are of early Tertiary age, but early flows probably date back to the late Cretaceous (Bose, 1972).

The Deccan basalts have been subdivided into three groups (Wadia, 1926) :

(i) The Upper Group
(ii) The Middle Group
(iii) The Lower Group

Although Bose (op. cit.) feels that this subdivision is somewhat arbitrary, Alexander and Paul (1977) have identified the complete succession at Sagar, in the north-eastern part of the Traps. Borehole cores show that the groups are separated from one another by sedimentary bands.

The thin basalt pile in the east of the Traps is considered to consist of basalts of the Lower Group, while the type area of the Upper Group is the western seaboard, where the lava pile is much thicker. The lavas of the Upper Group have associated with them a fairly high proportion of pyroclastics.

Individual flows in the Deccan Traps average about 5 meters in thickness, reaching a maximum of about 15 meters (Turner and Verhoogen, 1960). In the west, the lavas are more complexly interbedded than they are in the east (Walker, 1972), and are more diversely chemically (Sukheswala and Poldervaart, 1958; Krishnamurthy and Cox, 1977), probably because of increased heat flow in the western part of the Traps (Bose, 1972).

Fig. 29 : SKETCH MAP OF INDIA, SHOWING THE EXTENT OF THE DECCAN TRAPS (SHADED AREA)

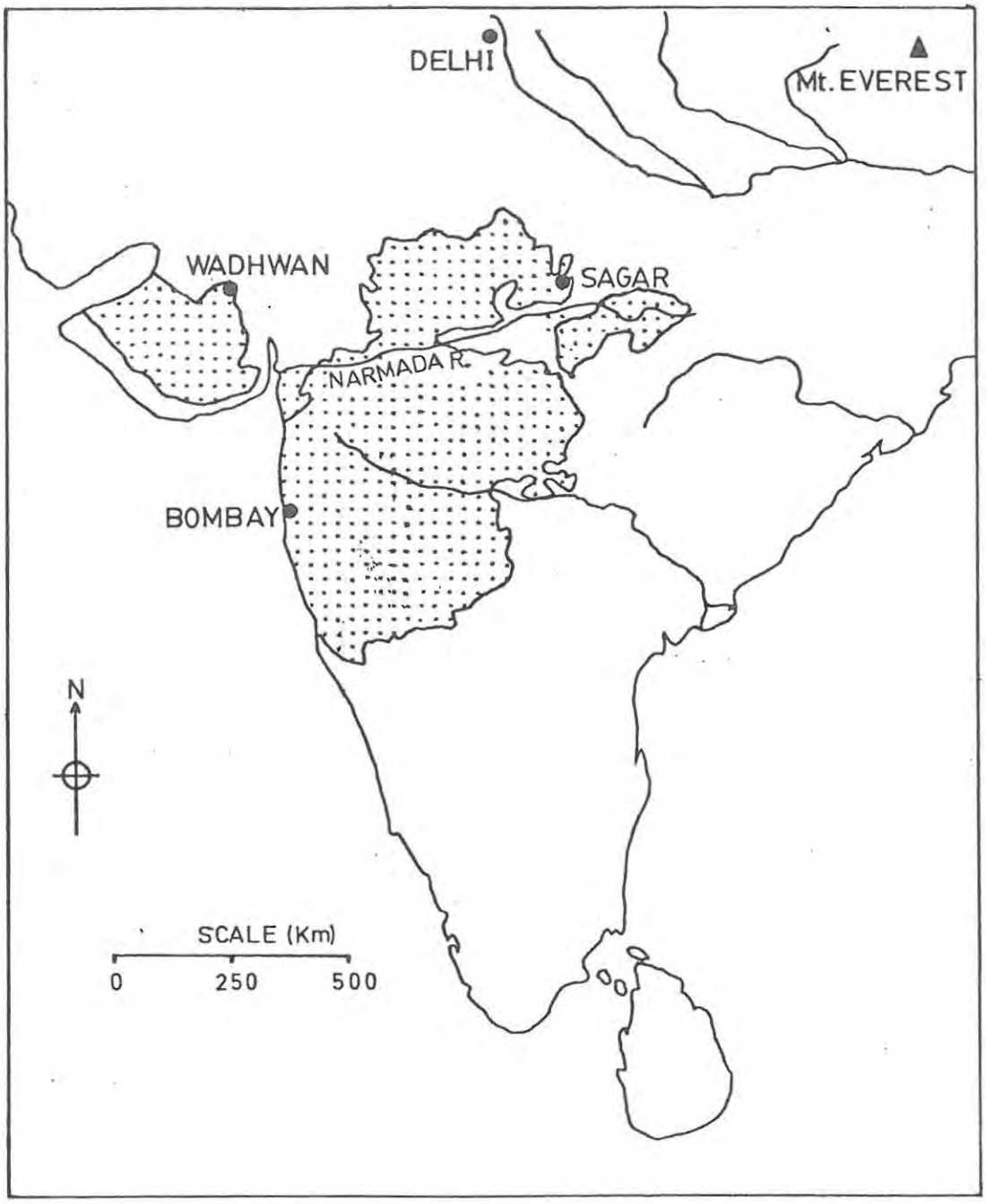

The Deccan lavas are known to be the products of fissure eruptions (Bose, op. cit.), but there has apparently been very little work done on the sub-volcanic expression of the province.

9.4.b Petrography

The basalts of the Deccan vary from a coarse, almost holocrystalline, ophitic type, to a fine-grained, hyalitic type (Bose, 1972).

Krishnamurthy and Cox (1977), working in the western part of the Traps, identify three types of basalt on the basis of petrography :

(i) Picrite basalt
(ii) Three-phenocryst basalt
(iii) "Ordinary" basalt

The work of Krishnamurthy and Cox (op. cit.) is valuable in that it supplies microprobe data on the mineral phases in the basalts.

Olivine is a minor phase in the ordinary and three-phenocryst basalts, where it is generally present only as altered remnants. In the picrites, on the other hand, olivine is an important phase, both as a phenocryst and in the groundmass. The picrite olivine phenocrysts range in composition from Fo_{90} to Fo_{87}, and have a size range 5 - 10 mm. Olivine phenocrysts from the three-phenocryst basalt, by comparison, vary from Fo_{88} to Fo_{84}.

Clinopyroxene is a dominant phenocryst, along with olivine, in the picrites. Clinopyroxene decreases in amount in the three-phenocryst basalts, and is almost absent from the phenocryst assemblage of the ordinary basalt. Average compositions vary from $Mg_{44-54}Ca_{43-46}Fe_{11-15}$ in the picrites to $Mg_{43-45}Ca_{40-44}Fe_{11-17}$ in the ordinary and three-phenocryst basalts. Zoning is not common in the pyroxenes, and the narrow range in clinopyroxene compositions, in comparison to

the wide range of bulk rock compositions, indicates to Krishnamurthy and Cox (op. cit.) that the rocks all erupted in a narrow temperature interval, not far below the temperature at which clinopyroxene began to crystallise.

Plagioclase is confined to the groundmass of the picrites, but is the dominant phenocryst of the ordinary and three-phenocryst basalts. Zoning in the plagioclases is not pronounced, but where encountered it is normal. The groundmass plagioclases of the picrites have a compositional range An_{88}-An_{74}. The three-phenocryst basalts show phenocryst plagioclases An_{88}-An_{72}, and groundmass plagioclases An_{76}-An_{62}. The ordinary basalts have phenocryst compositions in the range An_{66}-An_{57}.

Ore minerals are generally confined to the groundmass of all the basalt types, although they may occur as inclusions in the olivine phenocrysts of the picrites. Minor phases like apatite are present in small amounts, generally associated with the mesostasis.

9.4.c Geochemistry

The great majority of the Deccan basalts are low-Mg tholeiites, and it is only locally that other rock types are found (Krishnamurthy and Cox, 1977). Bose (1972) points out that, in addition to its low Mg and Al contents (average 12,79% Al_2O_3 and 5,40% MgO), the Deccan basalts are enriched in iron and (more particularly), in titanium (TiO_2 average 2,78 weight %). A generalised AFM diagram for the Deccan basalts (after Sukheswala and Poldervaart, 1958) is presented in Fig. 30a, and Bose's (1972) data are plotted on a projection of the normative basalt tetrahedron in Fig. 30b.

Krishnamurthy and Cox (op. cit.) present trace element, as well as major element data for the Deccan basalts, which are diagrammatically compared with selected

Karoo data in Fig. 31 (a and b). Sr isotope ratios for the Deccan basalts, as calculated by Alexander and Paul (1977), vary from 0,7039 to 0,7084.

9.5 General Discussion

Age-wise, the three provinces span, collectively, a period of some 170 million years. The Karoo Central Province is the oldest of the three (195 - 155 my B.P.), followed by the Deccan Traps (± 130 - 60 my B.P.) and, lastly, the Columbia River Group (25 - 13 my B.P.). The Deccan Traps and the Columbia River basalts are of similar areal extent (500 000 km^2), whereas the estimated original extent of the Karoo Province is much greater (1 400 000 km^2).

The early phase of Central Karoo volcanicity is marked by central vent-type eruptions. In the Columbia River Province, Snavely et al. (1972) present evidence for the association of central volcanic vents with the basalts in the western (coastal) part of the province, whilst in the Deccan, Krishnamurthy and Cox (1977) encounter agglomerate in the lava sequence of two of their three borehole cores, and make reference to the possibility of central vent eruptions having produced at least some of the volcanic material. In broad terms, however, the general consensus of opinion is that the greater proportion of the basalt in all three provinces is the product of fissure-type eruptions.

The major element chemistry of the three provinces, as broadly outlined in Figs 28a and 31a, shows the Deccan basalts to be relatively depleted in SiO_2, but otherwise fairly similar to the Columbia River basalts, whilst the Karoo basalts are relatively depleted in Ti and the alkalis, but enriched in Mg and Al. Ca and Fe appear fairly consistent for all three provinces.

As regards the trace elements, the Karoo basalts are strongly enriched in Cr, Ni and Co relative to the Deccan basalts, and enriched in Cr relative to the Columbia

River Group. The concentration of incompatibles in the Karoo is consistently lower than the incompatible element concentrations of either the Deccan or the Columbia River provinces. The Karoo basalts display a fairly wide spread of Sr and Rb values, which is attributed to weathering effects.

Fig. 30 : GENERALISED CHEMISTRY OF THE DECCAN BASALTS

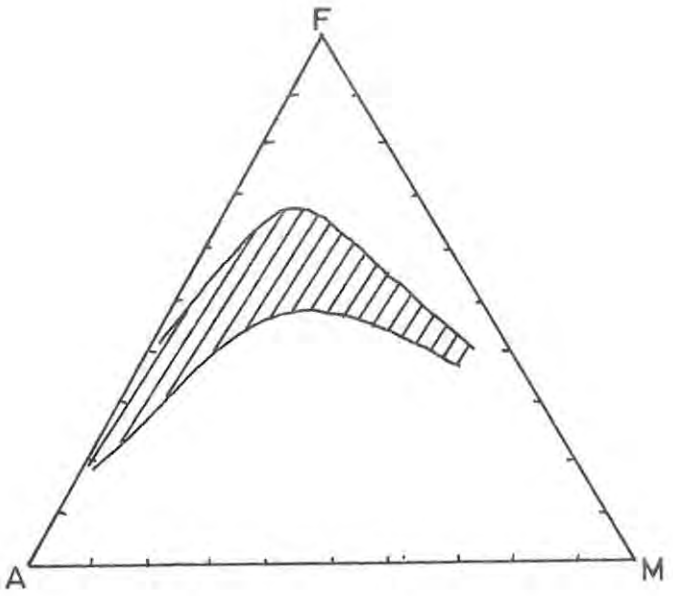

Fig. 30a : AFM diagram of the Deccan basalts (after Sukheswala and Poldervaart, 1958).

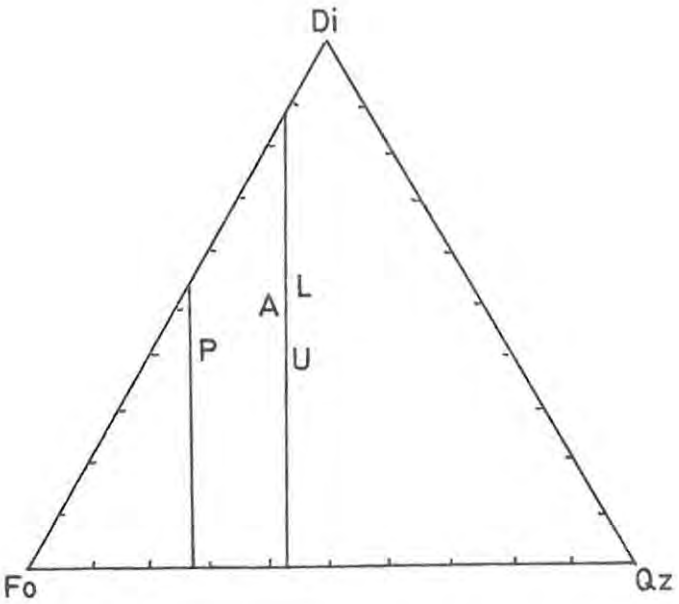

Fig. 30b : Normative basalt tetrahedron for the Deccan basalts (after Bose, 1972).

A = Average Deccan Basalt

L = Average Lower Deccan Basalt

U = Average Upper Deccan Basalt

P = Average Picrite Basalt

Fig. 31a : COMPARATIVE TRACE ELEMENT DIAGRAM OF THE DECCAN TRAPS BASALTS AND THE CENTRAL KAROO BASALTS

B = "Ordinary" Basalt

3P = Three-phenocryst Basalt

K = Kraai River Formation

R = Roodehoek Unit

V = Vaalkop Unit

⬭ = Deccan Traps Basalt

⬭ = Central Karoo Province

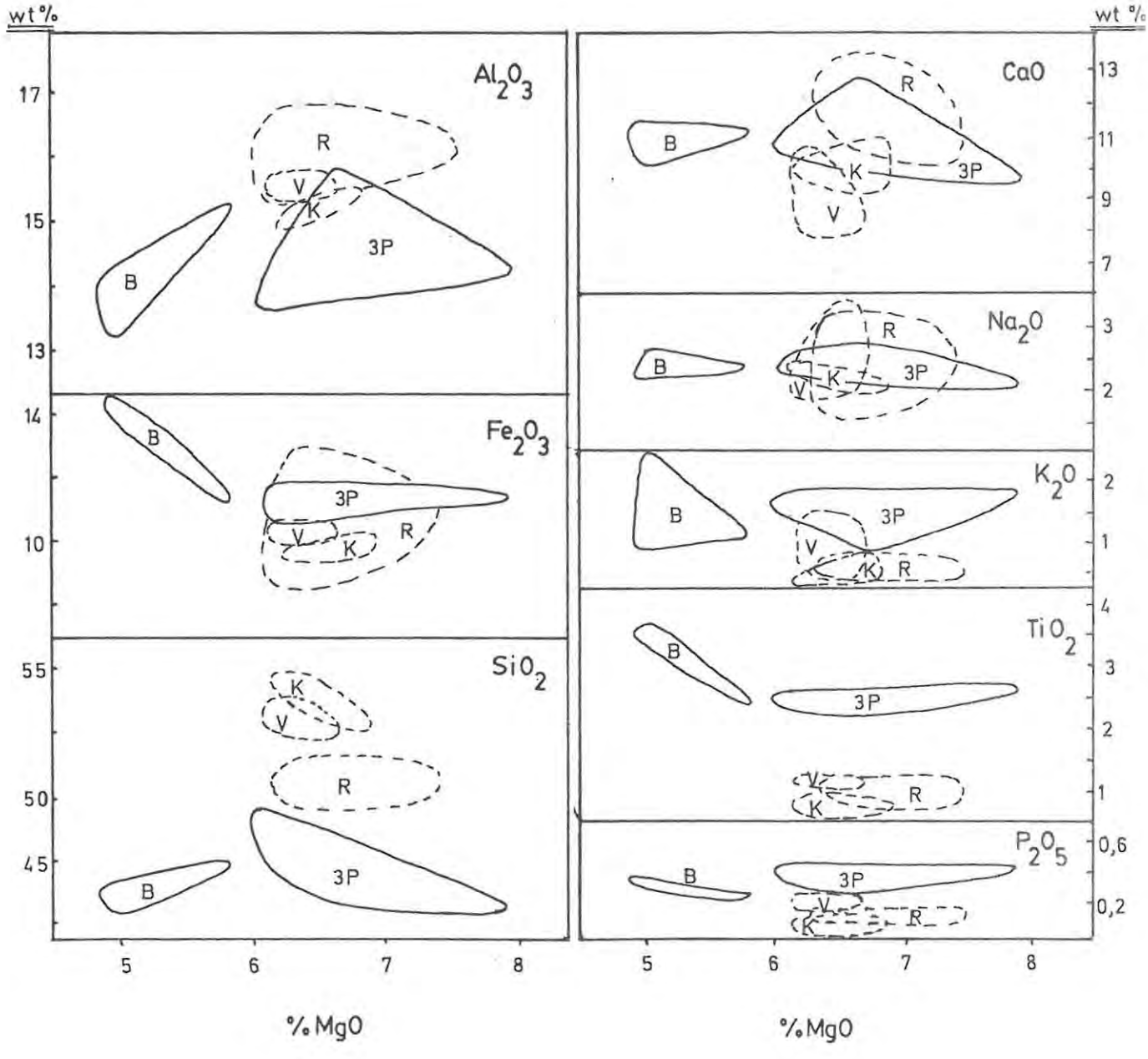

Fig. 31b : COMPARATIVE TRACE ELEMENT DIAGRAM OF THE DECCAN TRAP BASALTS AND THE CENTRAL KAROO BASALTS

B = "Ordinary" Basalt

3P = Three-phenocryst Basalt

K = Kraai River Formation

R = Roodehoek Unit

V = Vaalkop Unit

⬭ = Deccan Traps Basalt

⬭ = Central Karoo Province

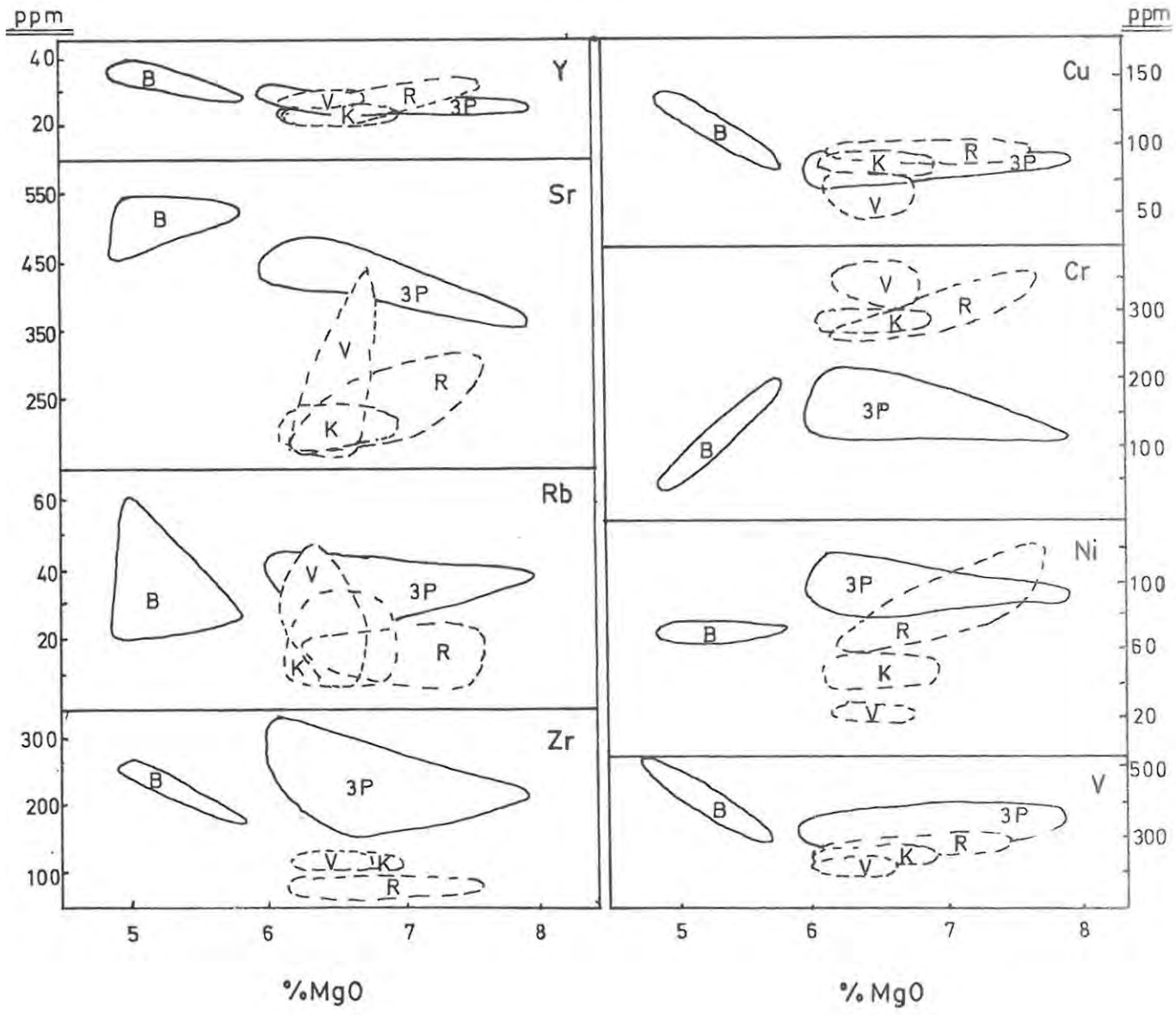

10. CONCLUSIONS

The dissected highland terrane lying between the towns of Molteno and Jamestown in the north-eastern Cape Province owes its rugged countenance to basalt cappings on the mountains, and to the complex network of dolerite intrusions which transect highlands and lowlands alike.

Mapping in the area, by Du Toit (1911) and by the present author, has brought to light the existence of two central volcanic vent complexes, with their associated radial and ring dyke structures (Fig. 2). The primary concern of this work is the southernmost of the two complexes, referred to in the text as the Brosterlea Complex. The structure of this complex is very involved, and postulates as to its evolutionary history can be regarded, at best, as only broad generalisations. A point of some interest in the geology of the complex is the occurrence, on the farm Roodehoek, of a body of andesite which, by its brecciated margins, is clearly intrusive. This is the only occurrence of clearly intrusive andesite mentioned by Rumble (1979), the andesites at Belmore, Pronksberg and Dikkop apparently being extrusive.

The dolerites of the Brosterlea complex, although only summarily dealt with in this study, are apparently of diverse and, in some cases, rather unusual composition, and warrant a more detailed study in the future.

The basalts covering the high ground in the area of study have been subdivided into a sequence of distinct units on the basis of their geochemistry. There appears to be some correlation between the units of the Brosterlea basalts, on one hand, and the various subdivisions of the Barkly East basalts (Pemberton, 1978) on the other. Some of the Brosterlea units are listed below, together with their postulated equivalents in the Barkly East area, the latter in brackets : Roodehoek Unit (Omega Formation); Strypoort

Unit (Drumbo Basalt Member); Perdekop Unit (Lesotho Formation). The remaining important unit of the Brosterlea sequence, the Vaalkop Unit, appears to have some affinities for the Kraai River Formation, but is probably more rightly considered transitional between the more primitive units (e.g. the Roodehoek Unit) and the Kraai River Formation per se. A generalised visual representation of the relationships between the various units is given in the text (Fig. 20) in terms of a discriminant analysis of the basalts.

Incompatible element ratios differ from unit to unit in the Brosterlea sequence, implying, as in the case of the Barkly East basalts (Pemberton op. cit.), that each separate basalt unit derives from a chemically distinct batch of magma, unrelated by fractional crystallisation or partial melting processes to its predecessors or successors. The ultimate implication of this is that the mantle source area of the basalts was inhomogeneous.

Routine analysis of four basalt samples associated with the Modderfontein central complex, to the north of Brosterlea, show that these basalts, too, can be separated into units with distinctive chemistry, particularly in terms of the incompatible elements.

In a comparison of the Karoo Central Province with the relatively younger Deccan Trap and Columbia River continental flood basalt provinces, the following points are of interest :

(i) The consensus is that all three provinces derive primarily from fissure-type eruptions, with central vents making only very minor contributions.

(ii) In each case, the overwhelming majority of the basalts are quartz-normative tholeiites.

(iii) Incompatible element concentrations are much lower in the Karoo basalts than in the two younger provinces.

Microprobe analyses of the silicate minerals in the Brosterlea basalts show that all the basalt units contain zoned plagioclase in the compositional range labradorite through to sodic bytownite. It is, however, interesting to note that there are systematic variations in K-content of the plagioclases from unit to unit. Pyroxene analyses from rocks of the Perdekop Unit define a fractionation trend which parallels the initial stages of the Birds River fractionation trend. In the Roodehoek Unit, on the other hand, pyroxenes show a trend of more rapid Ca-depletion with fractionation. It is also noteworthy that the Roodehoek Unit sample analysed has a two-pyroxene assemblage. Only one rock sample from the Brosterlea sequence contains olivines fresh enough for analysis, and these are probably a cumulus phase, as discussed in the text.

APPENDICES

APPENDIX 1

Sample Localities

Sampling localities, with corresponding sample numbers, are listed below. Samples from each locality are quoted starting from the top of the stratigraphic sequence, and working downward. A concise list of experimental work undertaken on each sample has been included in this appendix.

	Petrographic Investigation	X-Ray Fluorescence	Microprobe Analyses
1. VAALKOP			
AM-11	completed	completed	-
AM-12	completed	completed	-
AM-12B	completed	-	-
AM-13	completed	completed	plag
AM-14	completed	completed	-
AM-15	completed	completed	-
2. ROODEHOEK			
AM-23	completed	completed	plag, px
AM-22	completed	completed	plag
AM-21	completed	completed	plag
3. PERDEKOP			
AM-28	completed	completed	plag
AM-27	completed	completed	-
AM-26	completed	completed	-
AM-25	completed	completed	plag
AM-24	completed	completed	-
4. DRIEHOEK			
AM-29	completed	completed	-
AM-30	completed	completed	plag
AM-31	completed	completed	-

	Petrographic Investigation	X-Ray Fluorescence	Microprobe Analyses
5. TAFELKOP			
AM-34	completed	completed	-
AM-32	completed	completed	-
AM-33	completed	completed	-
AM-35	completed	-	-
AM-36T	completed	completed	-
AM-36M	completed	completed	plag, px, ol
AM-36B	completed	completed	-
AM-37	completed	completed	-
AM-38T	compelted	completed	-
AM-38	completed	completed	-
6. NOODHOEK			
AM-40	completed	completed	plag, px
AM-41	completed	completed	-
AM-42	completed	-	-
AM-43	completed	completed	-
AM-44	completed	completed	plag
AM-45	completed	completed	-
AM-46	completed	completed	-
7. WONDERPOORT			
AM-50	completed	completed	-
AM-51	completed	completed	-
AM-52	completed	completed	-
AM-53	completed	completed	-
AM-54	completed	-	-
8. KLIPFONTEIN			
AA-01	completed	-	-
AA-02	completed	-	-
AA-03	completed	-	-
AA-04	completed	-	-
AA-05	completed	-	-
AA-06	completed	-	-

	Petrographic Investigation	X-Ray Fluorescence	Microprobe Analyses
9. DOLERITES			
AA-21	completed	completed	-
AA-22	completed	completed	-
AA-23	completed	completed	-
AA-30	completed	completed	-
AA-31	completed	completed	-

The dolerite samples listed above are from various localities : AA-21 from the Brosterlea ring dyke; AA-22 from the Brosterlea radial dyke swarm; AA-23 from the "Dragon's Back" dyke; AA-30 and AA-31 from the Modderfontein ring dyke structure.

Abbreviations used in the tabulation above are as follows :

plag = plagioclase
px = pyroxene
ol = olivine

APPENDIX 2

X-Ray Fluorescence Spectrometry

All major elements, apart from sodium, were determined on duplicate fusion discs, prepared after the method of Norrish and Hutton (1969). Sodium was determined separately on pressed powder briquettes, as were all trace elements. All iron was determined on Fe_2O_3, and FeO was not separately determined.

Data were processed by computer, and corrections were made for position factors, dead-time, background, instrumental drift and spectral line interferences. Mass absorption coefficients, used in trace element data reduction, were derived from the major element data, using Heinrich's (1966) values.

H_2O^- was determined by heating samples overnight at 110°C and calculating the weight differential. L.O.I. (Loss on Ignition) was determined in a similar manner by calculating the weight differential after ignition overnight at a temperature of 950°C.

Working curves were calculated using the international rock standards AGV1, G-2, BCR-1, and GSP-1; the N.I.M. standards NIM-N, NIM-P, NIM-D and NIM-G; the U.C.T. in-house standards KL-11 and M-38.

Full details of analytical conditions for the major and trace element runs performed in this study are tabulated overleaf (Table A), and lower limits of determination and average absolute errors for the trace element runs are given in Table B.

TABLE A : X-RAY FLUORESCENCE ANALYTICAL CONDITIONS

Element	Emission line	Tube	kV	mA	Crystal	Time (secs)	Counter	Collimator	Specimen
Si	Kα	Cr	55	40	PET	40	flow	coarse	fusion disc
Ti	Kα	Cr	55	40	LiF(200)	10	flow	fine	fusion disc
Al	Kα	Cr	55	40	PET	40	flow	coarse	fusion disc
Fe	Kα	Cr	55	40	LiF(200)	20	flow	fine	fusion disc
Mn	Kα	Cr	55	40	LiF(200)	20	flow	coarse	fusion disc
Mg	Kα	Cr	55	40	TLAP	200	flow	fine	fusion disc
Ca	Kα	Cr	55	40	LiF(200)	10	flow	fine	fusion disc
Na	Kα	Cr	55	40	TLAP	100	flow	fine	powder pellet
K	Kα	Cr	55	40	LiF(200)	10	flow	fine	fusion disc
P	Kα	Cr	55	40	Ge	20	flow	coarse	fusion disc
Sr	Kα	W	55	40	LiF(220)	200	scint.	fine	powder pellet
Rb	Kα	W	55	40	LiF(220)	200	scint.	fine	powder pellet
Zr	Kα	W	55	40	LiF(220)	200	scint.	fine	powder pellet
Y	Kα	W	55	40	LiF(220)	200	scint.	fine	powder pellet
Nb	Kα	W	55	40	LiF(220)	200	scint.	fine	powder pellet
Co	Kα	W	55	40	LiF(220)	200	flow	fine	powder pellet
Cr	Kα	W	55	40	LiF(220)	200	flow	fine	powder pellet
V	Kα	W	55	40	LiF(220)	200	flow	fine	powder pellet
Zn	Kα	Mo	55	40	LiF(220)	200	flow+scint.	fine	powder pellet
Cu	Kα	Mo	55	40	LiF(220)	200	flow+scint.	fine	powder pellet
Ni	Kα	Mo	55	40	LiF(220)	200	flow+scint.	fine	powder pellet

TABLE B : AVERAGE LOWER LIMITS OF DETERMINATION (L.L.D.) AND ERRORS OF DETERMINATION FOR TRACE ELEMENT ANALYSES BY X-RAY FLUORESCENCE SPECTROMETRY

ELEMENT	L.L.D.	ABSOLUTE ERROR
Sr	1,27	0,50
Rb	1,27	0,71
Y	1,20	0,39
Zr	1,32	0,54
Nb	1,37	0,39
Zn	2,07	0,88
Cu	2,28	0,85
Ni	3,13	1,16
Co	4,30	1,35
Cr	2,80	1,34
V	4,00	1,30

APPENDIX 3

Electron Microprobe Analysis

Microprobe studies were carried out on Rhodes University's Cambridge Microscan V instrument. Polished specimen slides were vacuum-coated to a maximum thickness of 25nM with carbon. Specimen current was monitored at regular intervals by means of a Faraday Cage.

Nominal concentrations were corrected using a computer programme applying the Bence-Albee correction routine (Bence & Albee, 1968) using the α-factors of Albee and Ray (1970). The programme, HVE : MARK II, also makes corrections for dead-time counting losses.

Analytical conditions and standards employed are tabulated overleaf (Table A).

TABLE A : MICROPROBE ANALYTICAL CONDITIONS (OLIVINE)

Element	Crystal	Specimen Current	Accelerating Potential	Counter	Standard	Av. Std. Counts
Si	KAP	30nA	20kV	flow	St.J.Is.Ol	33303
Mg	KAP	30nA	20kV	flow	St.J.Is.Ol	29260
Fe	LiF(220)	30nA	20kV	flow	St.J.Is.Ol	7265
Ni	LiF(220)	30nA	20kV	flow	Ni-Magnetite	1026

TABLE B : MICROPROBE ANALYTICAL CONDITIONS (PYROXENE)

Element	Crystal	Specimen Current	Accelerating Potential	Counter	Standard	Av.Std. Counts
Si	KAP	30nA	20kV	flow	Px 5192	47500
Ti	LiF(220)	30nA	20kV	flow	Rutile	28293
Al	KAP	30nA	20kV	flow	Spinel	61480
Fe	LiF(220)	30nA	20kV	flow	Px 5182	21600
Mn	LiF(220)	30nA	20kV	flow	Rhodonite	32000
Mg	KAP	30nA	20kV	flow	Px 5182	19377
Ca	LiF(220)	30nA	20kV	flow	Px 5182	11566
Na	KAP	30nA	20kV	flow	Jadeite	3440
Cr	LiF(220)	30nA	20kV	flow	Chromite	37860

TABLE C : MICROPROBE ANALYTICAL CONDITIONS (PLAGIOCLASE)

Element	Crystal	Specimen Current	Accelerating Potential	Counter	Standard	Av. Std. Counts
Si	KAP	30nA	20kV	flow	Orth 1A	62430
Ti	Qtz	30nA	20kV	flow	Rutile	56371
Al	KAP	30nA	20kV	flow	Orth 1A	18602
Fe	Qtz	30nA	20kV	flow	Px 5182	17884
Mg	KAP	30nA	20kV	flow	Spinel	18150
Ca	Qtz	30nA	20kV	flow	Px 5182	11267
Na	KAP	30nA	20kV	flow	Jadeite	3450
K	Qtz	30nA	20kV	flow	Orth 1A	7045

APPENDIX 4

MAJOR ELEMENT ANALYSES (INCLUSIVE OF H_2O^- AND L.O.I.)

	AM-11	AM-12	AM-13	AM-29	AM-30	AM-32	AM-34	AM-41	AM-43	AM-44
SiO_2	50,37	51,58	51,11	52,30	50,88	51,97	52,32	51,44	51,45	52,77
TiO_2	1,09	1,05	1,10	1,10	1,15	1,09	1,09	1,13	1,10	1,09
Al_2O_3	14,59	14,95	15,39	15,50	14,96	15,19	15,50	14,87	14,98	15,10
Fe_2O_3	10,25	9,97	10,42	10,20	10,45	9,99	10,23	10,48	10,21	10,07
MnO	0,23	0,24	0,16	0,25	0,26	0,24	0,16	0,16	0,22	0,24
MgO	5,79	6,05	6,35	6,40	6,23	6,18	6,35	6,21	6,41	6,20
CaO	9,84	9,40	10,55	9,86	9,00	9,11	9,94	7,44	8,05	9,63
Na_2O	1,98	2,57	1,80	2,29	2,62	2,22	2,66	3,13	3,28	2,29
K_2O	1,07	0,79	0,34	1,15	1,12	1,55	1,10	1,39	1,07	1,08
P_2O_5	0,22	0,21	0,22	0,22	0,24	0,22	0,22	0,21	0,21	0,22
L.O.I.	3,54	3,36	1,44	0,23	1,63	2,09	0,71	1,96	2,24	0,51
H_2O^-	0,36	0,37	2,13	1,40	1,15	0,62	0,14	1,16	1,18	1,02
TOTAL	99,33	100,54	101,01	100,90	99,69	100,47	100,42	99,58	100,40	100,22

APPENDIX 4

MAJOR ELEMENT ANALYSES (INCLUSIVE OF H_2O^- AND L.O.I.)

	AM-14	AM-15	AM-21	AM-22	AM-23	AM-25	AM-31	AM36T	AM36M	AM36B
SiO_2	45,97	47,70	50,48	50,12	50,99	50,12	50,07	50,16	48,84	51,31
TiO_2	0,88	0,77	0,89	0,90	0,83	0,83	0,88	1,04	0,88	1,15
Al_2O_3	15,56	15,47	15,65	15,80	16,76	15,68	15,71	15,54	14,32	15,05
Fe_2O_3	10,51	10,17	10,80	10,93	10,14	10,38	10,55	11,51	11,65	11,23
MnO	0,25	0,18	0,27	0,29	0,16	0,24	0,25	0,27	0,27	0,19
MgO	5,87	7,22	7,11	7,33	6,25	7,30	6,52	6,41	10,07	6,22
CaO	12,19	10,46	11,01	11,07	11,48	10,61	11,48	9,91	9,73	10,28
Na_2O	1,35	2,03	2,24	2,09	2,55	2,18	2,28	2,72	2,14	2,53
K_2O	0,47	0,47	0,42	0,34	0,43	0,43	0,27	0,62	0,43	0,59
P_2O_5	0,13	0,12	0,13	0,13	0,10	0,12	0,13	0,15	0,14	0,18
L.O.I.	6,66	4,38	1,11	0,84	0,19	0,18	0,87	1,71	1,18	0,19
H_2O^-	0,54	0,91	0,39	1,04	0,54	0,95	1,00	0,48	0,57	0,71
TOTAL	100,38	99,88	100,50	100,88	100,42	99,02	100,01	100,52	100,22	99,63

APPENDIX 4

MAJOR ELEMENT ANALYSES (INCLUSIVE OF H_2O^- AND L.O.I.)

	AM-26	AM-27	AM-28	AM-40	AM-37	AM38T	AM-38	AM-24	AM-46
SiO_2	49,98	50,26	49,99	51,09	52,21	50,04	52,22	50,18	49,32
TiO_2	0,93	0,94	1,04	1,02	0,84	0,91	1,07	1,10	0,85
Al_2O_3	15,14	15,00	15,20	15,60	14,91	14,77	14,94	16,56	14,89
Fe_2O_3	10,77	10,46	11,07	10,94	9,69	10,34	10,44	10,21	9,85
MnO	0,18	0,26	0,18	0,23	0,24	0,19	0,17	0,22	0,22
MgO	6,43	7,28	6,62	7,22	6,92	7,56	5,87	5,54	5,98
CaO	10,03	9,81	10,61	10,60	8,62	10,74	9,76	9,73	11,19
Na_2O	3,06	2,54	2,22	2,44	3,40	2,79	2,27	2,35	2,32
K_2O	0,70	0,74	0,69	0,67	0,61	0,51	1,02	1,22	0,43
P_2O_5	0,16	0,15	0,18	0,19	0,13	0,12	0,20	0,22	0,13
L.O.I.	0,93	2,26	0,93	0,67	2,97	0,53	0,97	2,50	2,55
H_2O^-	0,71	1,15	1,36	0,32	0,53	1,15	0,95	0,54	1,03
TOTAL	99,02	100,85	100,09	100,99	101,07	99,65	99,88	100,37	98,76

APPENDIX 4

MAJOR ELEMENT ANALYSES (INCLUSIVE OF H_2O AND L.O.I.)

	AM-50	AM-51	AM-52	AM-53	AA-21	AA-22	AA-23	AA-30	AA-31
SiO_2	50,84	54,05	50,10	49,75	48,26	50,93	55,15	49,31	51,72
TiO_2	0,96	0,93	1,00	1,09	1,30	1,03	1,17	0,84	0,77
Al_2O_3	15,20	14,74	14,80	15,48	17,80	15,17	13,59	15,66	16,10
Fe_2O_3	10,80	10,04	9,75	10,13	12,18	11,87	12,26	10,54	10,15
MnO	0,18	0,22	0,20	0,23	0,15	0,18	0,17	0,15	0,15
MgO	7,29	6,63	6,29	6,39	5,97	5,92	3,83	7,04	7,37
CaO	10,63	10,02	9,37	10,58	7,67	10,66	7,72	10,81	11,54
Na_2O	2,31	2,33	2,23	1,84	4,32	2,77	2,63	2,29	2,35
K_2O	0,61	0,38	0,52	0,23	0,00	0,66	1,87	0,43	0,33
P_2O_5	0,14	0,15	0,20	0,21	0,11	0,17	0,24	0,14	0,11
L.O.I.	0,56	0,92	4,40	2,36	1,77	0,39	0,76	0,43	0,47
H_2O^-	0,70	0,07	1,14	1,64	0,98	0,40	1,14	0,71	0,68
TOTAL	100,22	100,48	100,00	99,93	100,51	100,15	100,53	98,35	101,74

ACKNOWLEDGEMENTS

This project was financed by the Council for Scientific and Industrial Research, within the framework of the South African contribution to the International Geodynamics Program, Working Group 4 "GEODYNAMICS OF CONTINENTAL AND OCEANIC RIFTS (b) Comparative Geochemical Studies of Oceanic and Continental Volcanic Rocks".

My supervisors, Prof. H.V. Eales and Dr. J.S. Marsh, have provided guidance and assistance throughout the course of this study. Amongst other members of the Geology Department at Rhodes University whose aid and advice were gratefully accepted are Mr. D.A. Gouws (Senior Technical Officer in charge of the electron microprobe), Mr. D.S. Cawood, who supervised preparation of thin sections, and Mr. K.C. Rumble, a fellow research student in this department.

The hospitality of the farmers in my field area, particularly Mr. & Mrs. Sandy Stretton and Mr. & Mrs. John Broster, is greatly appreciated.

Typing was undertaken by Mrs. M. Jackson.

REFERENCES

Albarede, F., and Bottinga, Y., 1972, Kinetic disequilibrium in trace element partitioning between phenocrysts and host lava : Geochim. et Cosmochim., v.36, p. 141-156.

Albee, A.L., and Ray, L., 1970, Correction factors for electron probe microanalysis : Analyt. Chem., v. 42, p. 1408-1414.

Ahrens, L.H., 1964, The significance of the chemical bond for controlling the chemical distribution of the elements. Part I : Phys. Chem. Earth, v. 5, p. 1-54.

Alexander, P.O., and Paul, D.K., 1977, Geochemistry and strontium isotopic composition of basalts from the eastern Deccan volcanic province, India : Min. Mag. v. 41, p. 165-171.

Arth, J.G., 1976, Behaviour of trace elements during magmatic processes - A summary of theoretical models and their applications : Journ. Research U.S. Geol. Survey, v. 4, No. 1, p. 41-47.

Baksi, A.K., and Watkins, N.D., 1973, Volcanic production rates : Comparison of ocean ridges, islands and the Columbia Plateau basalts : Science, v. 180, p. 493-496.

Barberi, F., Bizouard, H., and Varet, J., 1971, Nature of the clinopyroxene and iron enrichment in alkalic and transitional basaltic magmas : Contrib. Miner. Petrol., v. 33, p. 93-107.

Baree, P.D., 1977, The Kraai River Formation : A petrographical and geochemical study of an occurrence in the vicinity of Barkly East : Unpubl. Honours Project, Rhodes University.

Bence, A.E. and Albee, A.L., 1968, Empirical correction factors for the electron microanalysis of silicates and oxides : J. Geology, v. 76, p. 382-403.

Birle, J.D., Gibbs, G.V., Moore, P.B. and Smith, J.V., 1968, Crystal structure of natural olivines : Amer. Min., v. 47, p. 383-394.

Bose, M.K., 1972, Deccan basalts : Lithos, v. 5, p. 131-145.

Bowen, M.P., 1979, Some petrological aspects of the Omega Member near Barkly East : Unpubl. Honours Project, Rhodes University.

Boyd, F.R. and England, J.L., 1961, Melting of silicates at high pressure : Carnegie Inst. Wash. Yb., v. 60, p. 113-125.

Brown, G.M. and Vincent, E.A., 1963, Pyroxenes from the late stages of fractionation of the Skaergaard intrusion, East Greenland : J. Petrology, v. 4, p. 175-197.

Burns, R.G., 1970a, Crystal Field Spectra and evidence of cation disordering in olivine minerals. : Amer. Min., v. 55, p. 1608-1632.

Burns, R.G., 1970b, Mineralogical applications of Crystal Field Theory : Cambridge University Press, 224p.

Campbell, I.H., 1977, A study of macro-rythmic layering and cumulate processes in the Jimberlana intrusion, Western Australia. Part I : The Upper Layered Series : J. Petrology, v. 18, p. 183-215.

Cambbell, I.H. and Borley, G.D., 1974, The geochemistry of pyroxenes from the lower layered series of the Jimberlana Intrusion, Western Australia : Contrib. Miner. Petrol., v. 47, p. 281-297.

Chayes, F., 1970, On the amounts of silica and normative quartz in analyses of andesite, dacite and rhyodacite : Carnegie Inst. Wash. Yb., v. 68, p. 177-179.

Coish, R.A. and Taylor, L.A., 1979, The effects of cooling rate on texture and pyroxene chemistry in DSDP LEG 34 Basalt : A microprobe study : Earth Planet. Sci. Lett., v. 42, p. 389-398.

Compston, W., McDougall, I. and Heier, H.S., 1968, Geochemical comparison of the Mesozoic basaltic rocks of Antarctica, South Africa, South America and Tasmania : Geochim. et Cosmochim., v. 32, p. 129-149.

Cox, K.G., 1972, The Karoo volcanic cycle : J. Geol. Soc. Lond., v. 128, p. 311-336.

Cox, K.G. and Hornung, G., 1966, The petrology of the Karoo Basalts of Basutoland : Amer. Min., v. 51, p. 1414-1432.

Cox, K.G., MacDonald, R. and Hornung, G., 1967, Geochemical and petrographic provinces in the Karoo basalts of southern Africa : Amer. Min., v. 52, p. 1451-1474.

de Long, S.E., 1974, Distribution of Rb, Sr and Ni in igneous rocks, central and western Aleutian islands, Alaska : Geochim. et Cosmochim., v. 38, p. 245-266.

Drake, M.J. and Weill, D.F., 1971, Petrology of Apollo 11 sample 10071. A differentiated mini-igneous complex : Earth Planet. Sci. Lett., v. 13, p. 61-70.

Duke, J.M., 1976, Distribution of the period four transition elements among olivine, calcic pyroxene and mafic silicate liquid : Experimental results : J. Petrology, v. 17, p. 499-521.

Du Toit, A.L., 1904, Geological survey of the divisions of Aliwal North, Herschel, Barkly East and part of Wodehouse : 9th Ann. Rpt. Geol. Commission, Colony of Cape of Good Hope, p 69-110.

Du Toit, A.L., 1911, Geological survey of parts of the Stormbergen : 16th Ann. Rpt. Geol. Commission, Colony of Cape of Good Hope, p. 113-136.

Du Toit, A.L., 1954, The geology of South Africa (3rd Edn.) : Oliver and Boyd, Edinburgh.

Eales, H.V. and Booth, P.W.K., 1974, The Birds River gabbro complex, Dordrecht district : Trans. Geol. Soc. South Africa, v. 77, p. 1-15.

Eales, H.V. and Marsh, J.S. 1979a, High-Mg tholeiitic rocks and their significance in the Karoo Central Province : South African Journ. Sci., v. 75, p. 400-404.

Eales, H.V. and Marsh, J.S. 1979b, A review of Mesozoic volcanism in southern Africa : International Committee on Geohydrology : "The geohydrology of volcanic terranes" : In press.

Eales, H.V. and Robey, J. v.A., 1976, Differentiation of tholeiitic Karoo magma at Birds River, South Africa : Contrib. Miner. Petrol., v. 56, p. 101-117.

Erlank, A.J. and Hofmeyer, P.K., 1966, K/Rb and K/Cs ratios in Karoo dolerites from South Africa : J. Geophys. Res., v. 71, p. 5439-5445.

Erlank, A.J. and Kable, E.J.D., 1976, The significance of incompatible elements in Mid-Atlantic Ridge basalts from 45°N with particular reference to Zr/Nb : Contrib. Miner. Petrol., v. 54, p. 281-291.

Erlank, A.J., Allsop, H.L., Duncan, A.R. and Bristow, J.W., 1979, Mantle heterogeneity beneath southern Africa : Evidence from the volcanic record : South African contribution No. 44 to the International Geodynamics Project.

Evans, B.W. and Moore, J.G., 1968, Mineralogy as a function of depth in the prehistoric Makaopuhi tholeiitic lava lake, Hawaii : Contrib. Miner. Petrol., v. 17, p. 85-115.

Ewart, A., Bryan, W.B. and Gill, J.B., 1973, Mineralogy and geochemistry of the Younger Volcanic islands of Tonga, S.W. Pacific : J. Petrology, v. 14, p. 429-465.

Fitch, F.J. and Miller, J.A., 1971, Potassium-argon radioages of Karoo volcanic rocks from Lesotho : Bull Volcan., v. 35, p. 64-84.

Fleet, M.E., 1974, Partition of major and minor elements and equilibrium in coexisting pyroxenes : Contrib. Miner. Petrol., v. 44, p. 259-274.

Flower, M.J., 1973, Trace element distribution in lava flows from Anjouan and Grande Comore, Western Indian Ocean : Chem. Geol., v. 12, p. 81-98.

Fodor, R.V., Keil, K. and Bunch, T.E., 1975, Contributions to the mineral chemistry of Hawaiian rocks : IV. Pyroxenes in rocks from Haleakala and West Maui volcanoes, Maui, Hawaii : Contrib. Miner. Petrol., v. 50, p. 173-195.

Gevers, T.W., 1928, The volcanic vents of the western Stromberg : Trans. Geol. Soc. South Africa, v. 31, p. 43-62.

Gibb, F.G.F., 1973, The zoned pyroxenes of the Shiant Isles sill, Scotland : J. Petrology, v. 14, p. 203-230.

Gunn, B.M., 1971, Trace element partition during fractionation of Hawaiian basalts : Chem. Geol., v. 8, p. 1-13.

Green, D.H., 1973, Experimental melting studies on a model upper mantle composition at high pressures under water-saturated and water-undersaturated conditions : Earth Planet. Sci. Lett., v. 19, p. 37-53.

Greenland, L.P., 1970, An equation for trace element distribution during magmatic crystallization : Amer. Min., v. 55, p. 455-465.

Hanson, G.H., 1978, The application of trace elements to the petrogenesis of igneous rocks of granitic composition : Earth Planet. Sci. Lett., v. 38, p. 26-43.

Hart, S.R. and Brooks, C., 1974, Clinopyroxene-matrix partitioning of K, Rb, Cs, Sr and Ba : Geochem. et Cosmochim., v. 38, p. 1799-1806.

Hart, S.R. and Davis, K.E., 1978, Nickel partitioning between olivine and silicate melt : Earth Planet. Sci. Lett., v. 40, p. 203-219.

Heinrich, K.F.J., 1966, X-ray absorption uncertainty : In McKinley, T.D., Heinrich, K.F.J. and Wittry, D.B. (eds.) : The Electron Microprobe, Wiley, New York.

Henderson, P., and Dale, I.M., 1969, The partitioning of selected transition ions between olivine and groundmass of oceanic basalts : Chem. Geol., v. 5, p. 267-274.

Hertogen, J. and Gijbels, R., 1976, Calculations of trace element fractionation during partial melting : Geochim. et Cosmochim., v. 40, p. 313-322.

Hess, H.H., 1949, Chemical composition and optical properties of common clinopyroxenes : Amer. Min., v. 34, p. 621-666.

Hooper, P.R., 1974, Petrology and chemistry of the Rock Creek flow, Columbia River Basalt, Idaho : Geol. Soc. Amer. Bull., v. 84, p. 371-386.

Irvine, T.R. and Baragar, W.R.A., 1971, A guide to the chemical classification of the common volcanic rocks : Canad. Jour. Earth Sci., v. 8, p. 523-548.

Irving, A.J., 1978, A review of experimental studies of crystal/liquid trace element partitioning : Geochim. et Cosmochim., v. 42, p. 743-770.

Jakes, P. and White, A.J.R., 1972, Major and trace element abundances in volcanic rocks from orogenic areas : Geol. Soc. Amer. Bull., v. 83, p. 29-40.

Jensen, B.B., 1973, Patterns of trace element partitioning : Geochim. et Cosmochim., v. 37, p. 2227-2242.

Johnson, M.R., Botha, B.J.V., Hugo, P.J., Keyser, A.W., Turner, B.R. and de la Winter, H., 1975, Preliminary report on lithostratigraphic nomenclature in the Karoo sequence : Unpubl. Internal. Report, S.A.C.S.

Kennedy, W.Q., 1933, Trends of differentiation in basaltic magmas : Amer. J. Sci., v. 25, p. 239-256.

Kesson, S.E., 1973, The primary geochemistry of the Monaro Alkaline volcanics, south-eastern Australia - Evidence for upper mantle heterogeneity : Contrib. Miner. Petrol., v. 42, p. 93-108.

Korringa, M.K. and Noble, D.C., 1971, Distribution of Sr and Ba between natural feldspar and igneous melt : Earth Planet. Sci. Lett., v. 11, p. 147-151.

Krishnamurthy, P. and Cox, K.G., 1977, Picrite basalts and related lavas from the Deccan Traps of western India : Contrib. Miner. Petrol., v. 62, p. 53-75.

Kuno, H., 1955, Ion substitution in the diopside-ferropigeonite series of clinopyroxenes : Amer. Min., v. 40, p. 70-93.

Kuno, H., 1960, High-alumino basalt : J. Petrology, v. 1, p. 121-145.

Kuno, H., 1968, Differentiation of basalt magmas : In : Hess, H.H., and Poldervaart, A. (eds.), Basalts, v.1&2, p. 623-689, Wiley, New York.

Kushiro, I., Nakamura, Y., Harumura, H. and Akimoto, S., 1970, Crystallisation of some lunar mafic magmas and generation of rhyolitic liquid : Science, v. 167, p. 610-612.

Leeman, W.P. and Lindstrom, D.J., 1978, Partitioning of Ni^{2+} between basaltic and synthetic melts and olivines - an experimental study : Geochim. et Cosmochim., v. 42, p. 801-816.

Le Roex, A.P. and Reid, D.L., 1978, Geochemistry of Karoo dolerite sills in the Calvinia district, western Cape Province, South Africa : Contrib. Miner. Petrol., v. 66, p. 351-360.

Lessing, P., Decker, R.W. and Reynolds, R.C., 1963, Potassium and rubidium distributions in Hawaiian lavas : J. Geophys. Res., v. 68, p. 5851-5855

Lindstrom, D.J. and Weill, D.F., 1978, Partitioning of transition metals between diopside and coexisting silicate liquids - 1. Nickel, cobalt, and maganese : Geochim. et Cosmochim., v. 42, p. 817-832.

Lock, B.E., Paverd, A.L. and Broderick, T.J., 1974, Stratigraphy of the Karoo volcanic rocks of the Barkly East district : Trans. Geol. Soc. South Africa, v. 77, p. 117-129.

McCallum, I.S. and Charette, M.P., 1978, Zr and Nb partition coefficients : Implications for the genesis of Mare basalts, KREEP and sea floor basalts : Geochim et Cosmochim., v. 42, p. 859-869.

MacDonald, G.A., 1968, Composition and origin of Hawaiian lavas : Mem. Geol. Soc. Amer., v. 116, p. 477-522.

McDougall, I., 1976, Geochemistry and origin of basalt of the Columbia River Group, Oregon and Washington : Geol. Soc. Amer. Bull., v. 87, p. 777-792.

Moore, J.G. and Evans, B.W., 1967, The role of olivine in the crystallisation of the prehistoric Makaopuhi lava lake, Hawaii : Contrib. Miner. Petrol., v. 15, p. 202-223.

Mysen, B.O., 1978, Limits of solution of trace elements in minerals according to Henry's Law : Review of experimental data : Geochim. et Cosmochim, v. 42, p. 871-886.

Nakamura, Y., and Coombs, D.S., 1973, Clinopyroxenes in the Tawhiroko tholeiitic dolerite at Moeraki, north-eastern Otago, New Zealand : Contrib. Miner. Petrol., v. 42, p. 213-228.

Neumann, H., 1949, Notes on the mineralogy and geochemistry of zinc : Min. Mag., v. 28, p. 575-581.

Nielsen, R.L. and Drake, M.J., 1979, Pyroxene-melt equilibria : Geochim. et Cosmochim., v. 43, p. 1259-1273.

Nisbet, E.G. and Pearce, J.A., 1977, Clinopyrocene composition in mafic lavas from different tectonic settings : Contrib. Miner. Petrol., v. 63, p. 149-160.

Nockolds, S.R. and Allen, R., 1956, The geochemistry of some igneous rock series : Part III : Geochim. et Cosmochim., v. 9, p. 34-77.

Norrish, K. and Chappel, B.W., 1967, Physical methods in Determinative mineralogy (ed. J. Zussman) : Academic Press.

Norrish, K. and Hutton, J.T., 1969, An accurate X-ray spectrographic method for the analysis of a wide range of geologic samples : Geochim. et Cosmochim., v. 33, p. 431-453.

Osborn, E.F. and Tait, D.B., 1952, The system diopside-forsterite-anorthite : Amer. J. Sci., Bowen volume, p. 413-433.

Pearce, J.A. and Flower, M.F.J., 1977, The relative importance of petrogenetic variables in magma genesis at accreting plate margins : J. Geol. Soc., v. 134, p. 103-127.

Pearce, J.A. and Norry, M.J., 1979, Petrogenetic implications of Ti, Zr, Y and Nb variations in volcanic rocks : Contrib. Miner. Petrol., v. 69, p. 33-47.

Pemberton, J., 1978, The geochemistry and petrology of Karoo basalts of the Barkly East area, north-eastern Cape : Unpubl. M.Sc. Thesis, Rhodes University.

Pemberton, M., 1979, A study of the massive unit of the Omega Member near Barkly East. Unpubl. Honours Project, Rhodes University.

Philpotts, J.A. and Schnetzler, C.C., 1970, Phenocryst-matrix partition coefficients for K, Rb, Sr and Ba, with applications to anorthosite and basalt genesis : Geochim. et Cosmochim., v. 34, p. 307-322.

Ribbe, P.H. and Smith, J.V., 1966, X-ray-emission microanalysis of rock-forming minerals IV. Plagioclase feldspars : J. Geology, v. 74, p. 217-233.

Ringwood, A.E., 1970, Petrogenesis of Apollo 11 basalts and implications for lunar origin : J. Geophys. Res., v. 75, p. 6453-6479.

Robey, J. v.A., 1976, Aspects of the geochemistry of the dolerites and basalts of the north-eastern Cape Province, South Africa : Unpubl. M.Sc. Thesis, Rhodes University.

Roeder, P.L. and Emslie, R.F., 1970, Olivine-liquid equilibrium : Contrib. Miner. Petrol., v. 29, p. 275-289.

Ross, M., Bence, A.E., Dwornik, E.J., Clark, J.R. and Papike, J.J., 1970, Lunar clinopyroxenes : chemical composition, structural state, and texture : Science, v. 167, p. 628-630.

Rumble, K.C., 1979, The geochemistry and petrology of the Karoo andesites and associated basalts of the north-eastern Cape Province : Unpubl. M.Sc. Thesis, Rhodes University.

Sato, H., 1977, Nickel content of basaltic magmas : identification of primary magmas and a measure of the degree of olivine fractionation : Lithos, v. 10, p. 113-120.

Seward, T.M., 1971, The distribution of transition elements in the system $CaMgSi_2O_6$ - $Na_2Si_2O_5$ - H_2O at 1000 bars pressure : Chem. Geol., v. 7, p. 73-95.

Schmincke, H-U., 1967, Stratigraphy of four upper Yakima basalt flows in south-central Washington : Geol. Soc. Amer. Bull., v. 78, p. 1385-1422.

Schweitzer, E.L., Papike, J.J. and Bence, A.E., 1979, Statistical analysis of clinopyroxenes from deep-sea basalts : Amer. Min. v. 64, p. 501-513.

Shaw, D.M., 1970, Trace element fractionation during anatexis : Geochim. et Cosmochim., v. 34, p 237-248.

Shimizu, N., 1974, An isotope detection technique for analysis of the R.E.E. : Carnegie Inst. Wash. Yb., v. 73, p. 964-967.

Smith, J.V., 1975, Some chemical properties of feldspars. In : P.H. Ribbe (ed.), Feldspar mineralogy, v. 2, Min. Soc. Amer.

Snavely, P.D., MacLead, N.S. and Wagner, H.C., 1968, Tholeiitic and alkalic basalts of the Eocene Siletz River volcanics, Oregon Coast Range : Amer. J. Sci., v. 266, p. 454-481.

Swanson, D.A., 1967, Yakima basalt of the Tieton River area, south-central Washington : Geol. Soc. Amer. Bull., v. 78, p. 1107-1110.

Swart, R., 1979, The geology and environment of deposition of the Heuningneskloof Sandstone, Barkly East : Unpubl. Honours Project, Rhodes University.

Sukheswala, R.N. and Poldervaart, A., 1958, Deccan basalts of Bombay area, India : Bull Geol. Soc. Amer., v. 69, p. 1475-1494.

Sun, S.S. and Nesbitt, R.W., 1977, Chemical heterogeneity of the Archean mantle, composition of the Earth and mantle evolution : Earth Planet. Sci. Lett., v. 35, p. 429-448.

Sun, C-O, Williams, R.J., and Sun, S-S, 1974, Distribution coefficients of Eu and Sr for plagioclase-liquid and clinopyroxene-liquid equilibria in ocean ridge basalt : an experimental study : Geochim. et Cosmochim., v. 38, p. 1415-1433.

Taylor, S.R., 1965, The application of trace element data to problems in petrology : Phys. Chem. Earth, v. 6, p. 133-214.

Tilley, C.E., 1950, Some aspects of magmatic evolution : Quart. J. Geol. Soc. Lond., v. 106, p. 37-61.

Turner, F.J. and Verhoogen, J., 1960, Igneous and Metamorphic Petrology, McGraw-Hill, New York.

Wadia, D.N., 1926, Geology of India, MacMillan and Co., London.

Walker, F. and Poldervaart, A., 1949, Karroo dolerites of the Union of South Africa : Bull Geol. Soc. Amer., v. 60, p. 591-706.

Walker, G.P.L., 1972, Compound and simple lava flows and flood basalts : In : International symposium on Deccan Trap and other flood eruptions, Proceedings Part 1 : Bull. Volcanol., v. 35, p. 579-590.

Winchell, A.N. and Winchell, H., 1961, Elements of optical mineralogy (4th Edn.), Wiley, New York.

Wood, D.A., Tarney, J., Varet, J., Saunders, A.D., Bougaut, H., Joron, J.I., Treuil, M. and Cann, J.R., 1979, Geochemistry of basalts drilled in the North Atlantic by IPOD LEG 49 : Implications for mantle heterogeneity : Earth Planet. Sci. Lett., v. 42, p. 77-97.

Wright, T.L., 1974, Presentation and interpretation of chemical data for igneous rocks : Contrib. Miner. Petrol., v. 48, p. 233-248.

Wright, T.L., Grolier, M.J. and Swanson, D.A., 1973, Chemical variation related to the stratigraphy of the Columbia River Basalt : Geol. Soc. Amer. Bull., v. 84, p. 371-386.

Yoder, H.S. Jnr. and Tilley, C.E., 1962, Origin of basaltic magma : An experimental study of natural and synthetic rock systems : J. Petrology, v. 3, p. 342-532.